Author:
Volders, Filip Denis Maria

Title:
Biomarker hydrocarbon molecularand deuterium isotope stratigraphic records from ombrotrophic mires for palaeoclimate reconstruction

BIOMARKER HYDROCARBON MOLECULAR AND DEUTERIUM ISOTOPE STRATIGRAPHIC RECORDS FROM OMBROTROPHIC MIRES FOR PALAEOCLIMATE RECONSTRUCTION

Filip Denis Maria Volders

A dissertation submitted to the University of Bristol in accordance with the requirements of the degree of Doctor of Philosophy in the Faculty of Science, School of Chemistry.

September 2003

Word Count *ca*. 46,000

Abstract

The exploitation of biomarker stratigraphic records as climate proxies is well established in ocean and lake sediments, but not as yet in peat deposits. Peat bog vegetation and hydrology are strongly influenced by climate and are unique amongst terrestrial ecosystems in their preservation of stratigraphic records of climate change. Biomarkers and their isotopic compositions can be used to access that record, but there have been relatively few studies of peat deposits and useful biomarker and isotopic proxies have yet to be fully developed and tested. The aim of this thesis was to build on preliminary investigations of biomarker hydrocarbons performed at Bolton Fell Moss and develop molecular and deuterium isotope records extending to longer timescales (present to 5,500 y B.P.) and provide parallel records from the adjacent bog of Walton Moss. A dating model was established based on a combination of ^{210}Pb and ^{14}C dates. Variations in *n*-alkane and triterpene hydrocarbon abundances provide records of vegetation change during bog development (*n*-alkane average chain length; ACL) and microbial activity (hopane abundances). The ACL record showed strong correlation with known climatic events, detected in earlier macrofossil analyses. The synchronicity of hydrocarbon abundances with macrofossil changes is still unresolved and this work shows the potential for species-specific biomarker abundances to qualitatively identify climatic induced vegetation changes.

Recent analytical developments were used to determine compound-specific δD values for individual biomarker hydrocarbons after optimising of the instrument operational parameters, in order to develop reliable down-core δD profiles of lipid biomarkers. It was hypothesized that compound-specific δD values would reflect temperature and evaporation induced changes in the δD values of the bog water. The observed correlations of *n*-alkane δD records with recent meteorological records suggest compound-specific δD values have potential utility as a new climate proxy. δD values determined for higher plant biomarkers (*n*-alkanes and triterpenoids) suggest that the biochemical incorporation of hydrogen during lipid biosynthesis is complex but offers the potential for the development of new palaeoclimate proxies.

Acknowledgements

First of all my thanks goes to my supervisor Professor R.P. Evershed, who provided me with the opportunity and support for undertaking the research presented in this thesis. I am also grateful to him for his help and support in preparing this manuscript as well as for the discussions regarding the finer points of this work.

Secondly, I would like to thank Dr. Jim Carter whose help and experience in IRMS were greatly appreciated, and invaluable for obtaining the isotope data and getting a completely new technique of the ground.

Thanks also to Dr. R.P. Pancost, who helped by providing a discussion forum and guidance to this work.

I would also like to thank Dr. Paul Hughes, Dr. Dmitri Mauquoy, Dr. Darrel Maddy and Professor Frank Chambers for their original help with coring Bolton Fell Moss and Walton Moss as well as providing expert palaeoecological help and advice. I also would like to thank Professor Keith Barber for invaluable help with accessing the sample sites.

To everybody in the Organic Geochemistry Unit by providing a place where doing research was enjoyable and making a foreigner feel genuinely welcome.

And lastly, my biggest thanks goes to my parents Robert and Philomena Volders-Aerts without whose support this thesis would probably never have been written. Also thanks to my brother Bart whose frequent visits made home feel a lot closer.

Author's Declaration

I declare that the work in this thesis dissertation was carried out in accordance with the Regulations of the University of Bristol. The work is original except where indicated by the special reference in the text and no part of the dissertation has been submitted for any other degree.

Any views expressed in the dissertation are those of the author and in no way represent those of the University of Bristol.

The dissertation has not been presented to any other University for examination either in the United Kingdom or overseas.

SIGNED: 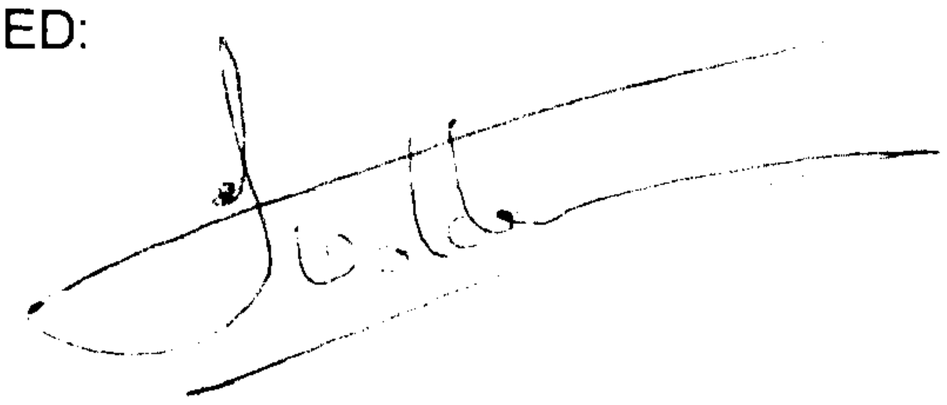

DATE: 12/2/[illegible]

Contents

List of Tables

List of Figures

Abbreviations

ACL	Average Chain Length
AD	Anno Domini
AMS	Accelerator Mass Spectrometry
ATP	Adinosine TriPhosphate
BC	Before Christ
BFM	Bolton Fell Moss
BFX	Bolton Fell Moss Monolith (Xie, 2000)
BP	Before Present (present = 1950)
°C	Degrees Celsius
Cal. Yr.	Calendar Year
CIC	Constant Initial Concentration
CRS	Constant Rate of Supply
CO_2	carbon dioxide
CH_4	methane
CPI	Carbon Preference Index
DCA	Detrended Correspondence Analysis
DOC	Dissolved Organic Matter
GC	Gas chromatography
GC/MS	Gas chromatography/Mass Spectrometry
GC/TC	Gas chromatography/Thermal Conversion
HPLC	High Performance Liquid Chromatography
IPP	Isopentyl Diphosphate
IRMS	Isotope Ratio Mass Spectrometry
MEP	Methylerythiol Phosphate
MVA	Mevalonic Acid
NADPH	Nicotinamide Adenine Dinucleotide Phosphate
PGA	Phosphoglycerate
SMOW	Standard Mean Ocean Water
TC/EA	Thermal Conversion / Elemental Analyser
UOM	Unidentified Organic Matter
V	Volt
V-SMOW	Vienna Standard Mean Ocean Water
WM	Walton Moss

1 Introduction

1.1 Introduction

The Quaternary is the most recent major subdivision (period) of the geological record, and it extends up to, and includes, the present day (Figure 1.1). Together with the Tertiary it forms the Cenozoic, the fourth of the geological eras. In the geological timescale, periods are conventionally divided into epochs, and the Quaternary includes two formally designated intervals (Hedberg, 1976): the Pleistocene, which ended about 10 ky BP, and the Holocene, which is the present warm interval within which we live.

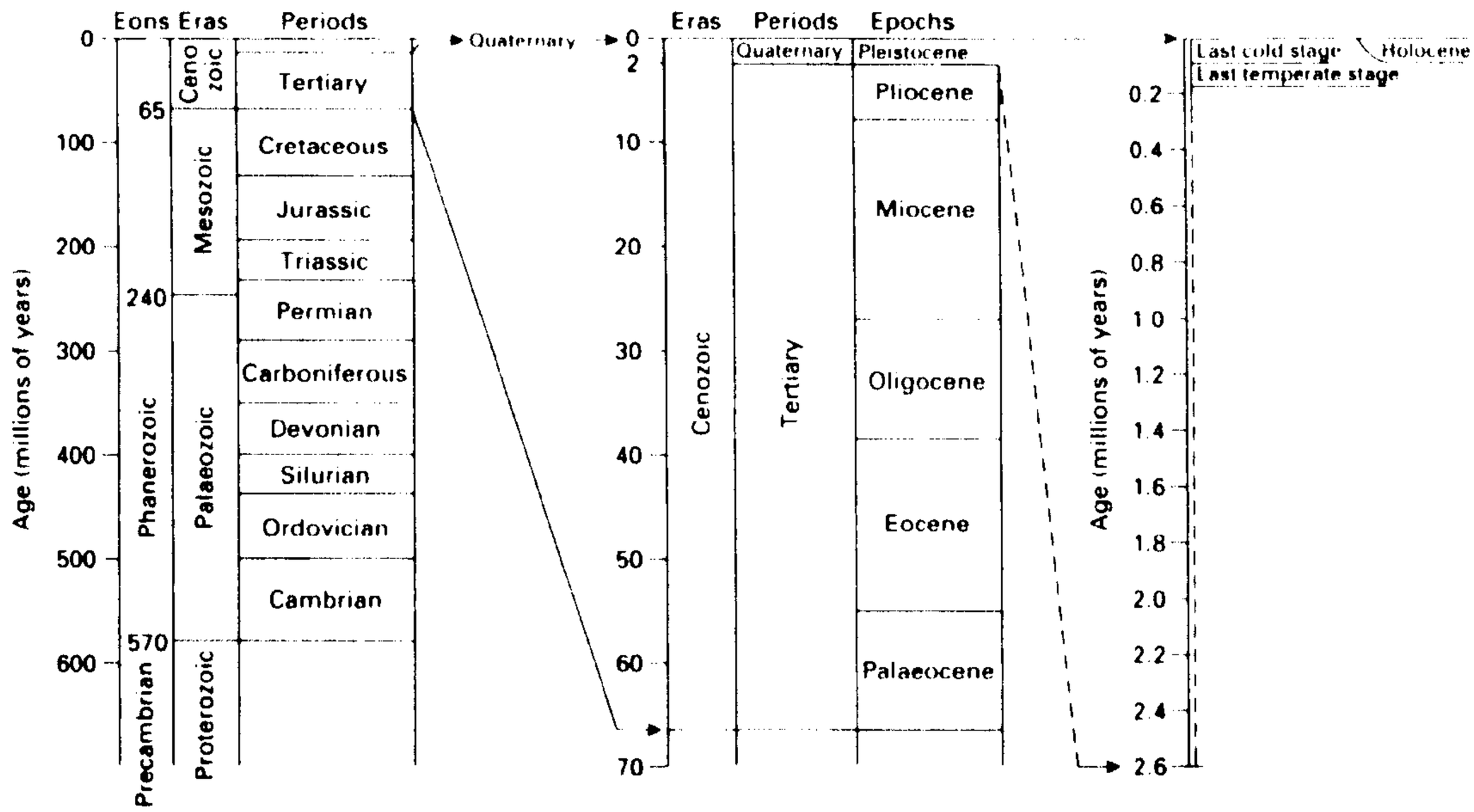

Figure 1.1. The Quaternary relative to the geological timescale (after Shackleton and Hall, 1990).

Although our perspective on the past is somewhat short-sighted, the Quaternary has been nonetheless a period of major change, possibly greater than any other time. An understanding of our present climate can, amongst others, be achieved through the study of past climatic systems. The changes, which have occurred in the landscape over the last 20,000 years, have been dramatic. Evidence for these past environmental and climatic changes comes from a variety of sources. For the relatively recent past, instrumental data on temperature and precipitation are available for some areas of the world, although the timescale seldom exceeds 300 years. Historical records also provide snapshots of former climatic conditions in the

form of ship's logs, harvest dates, pictures and diaries, but they seldom constitute a continuous time-series. By far the most widely used bases for environmental and climatic reconstruction are proxy records. The term proxy is used to refer to any line of evidence that provides an indirect measure of former climates or environments (Ingram et al., 1981). It can include materials as diverse as pollen grains, isotope records, glacial sediments, tree rings or animal bones (Bell and Walker, 1992). Therefore, proxy records originating from different sources will differ in age, longevity, sensitivity, resolution and completeness. In the next section an overview of the different palaeoclimate proxies will be given with the aim of placing the major focus of this thesis, namely ombrotrophic mires, into the larger picture.

1.2 Sources of palaeoclimate information

There has been an 'information explosion' in the field of palaeoclimate research in the last 20 years. This explosion is mainly the result of a growing concern over the effects of anthropogenically-induced changes to our environment. In order to estimate the anthropogenic component to our present day climate, the need arose to know the natural climate variability and its different forcing factors. Since historical records are extremely limited in time (less then three hundred years) different proxy techniques have been developed to reconstruct past climate variability. In Table 1.1 an overview of the different palaeoclimate proxies is given. Although these are useful general categories within which to describe particular techniques and approaches, they are to some extent artificial and there are considerable overlaps between them. Hence, in the next section only the major categories will be briefly discussed and the basis for this discussion will be their source, namely: glacial, marine or terrestrial.

1.2.1 Glacial records

The accumulation of past snowfall in the polar ice caps and ice sheets of the world provides an extraordinary record of palaeoclimate and palaeo-environmental conditions. These conditions are studied by detailed physical and chemical analyses of ice cores recovered from all over the globe. Palaeoclimatic information has been obtained from ice cores by four main approaches. These involve the analyses of: (i) stable isotopes of water and atmospheric O_2; (ii) other gases from air bubbles trapped within the ice; (iii) dissolved and particulate matter, and (iv) the physical characteristics of the ice (Bradley, 1999).

Table 1.1. Principle sources of proxy data for palaeoclimate reconstructions (Bradley, 1999).

(1) Glaciological (ice cores)

(a) geochemistry (major ions and isotopes of oxygen and hydrogen)
(b) gas content in air bubbles
(c) trace element and microparticle concentrations
(d) physical properties (e.g., ice fabric)

(2) Geological

(A) Marine (ocean sediment cores)
(i) Biogenic sediments (planktonic and benthic fossils)
(a) oxygen isotopic composition
(b) faunal and floral abundance
(c) morphological variations
(d) alkenones (from diatoms)
(ii) Inorganic sediments
(a) terrestrial dust and ice-rafted debris
(b) clay mineralogy
(B) Terrestrial
(a) glacial deposits and features of glacial erosion
(b) periglacial features
(c) shorelines
(d) aeolian deposits
(e) lacustrine sediments
(f) pedological features
(g) speleothems (age and stable isotope composition)

(3) Biological

(a) tree rings (density, width, stable isotope composition)
(b) pollen (type, relative abundance, and/or absolute concentrations)
(c) plant macrofossils (age and distribution)
(d) insects (assemblage characteristics)
(e) corals (geochemistry)
(f) diatoms, ostracods and other biota in lake sediments (assemblage, abundance, and/or geochemistry)
(g) modern population distribution (refugia and relict populations of plants and animals)

(4) Historical

(a) written records of environmental indicators (parameteorological phenomena)
(b) phenological records

The oxygen isotopic composition of ice is measured by mass spectrometry and is expressed as deviations ($\delta^{18}O$) per mil from a standard (SMOW; standard mean ocean water). During evaporation from the ocean surface, atmospheric water becomes depleted in the heavier ^{18}O isotope by, on average, 10‰ (Robin, 1983). However, there is seasonal variability in this value, so that the range of $\delta^{18}O$ values between summer and winter precipitation over the ice sheets is commonly about 15‰. Thus, seasonal changes can be detected in ice cores by precise measurements of oxygen isotope variations. Although the amplitude of the $\delta^{18}O$

signal decreases with depth due to diffusion effects, significant variations are still detectable over the last 160 ky, and these predominantly reflect changes in global climate. Hydrogen isotopes behave much in the same way as oxygen isotopes. The deuterium profile from the Vostok record shows long-term variations that match those from the Greenland oxygen isotope record (Figure 1.2; Jouzel et al., 1990). As the fractionation of isotopes is temperature dependant, the variations in these profiles broadly reflect global temperature changes.

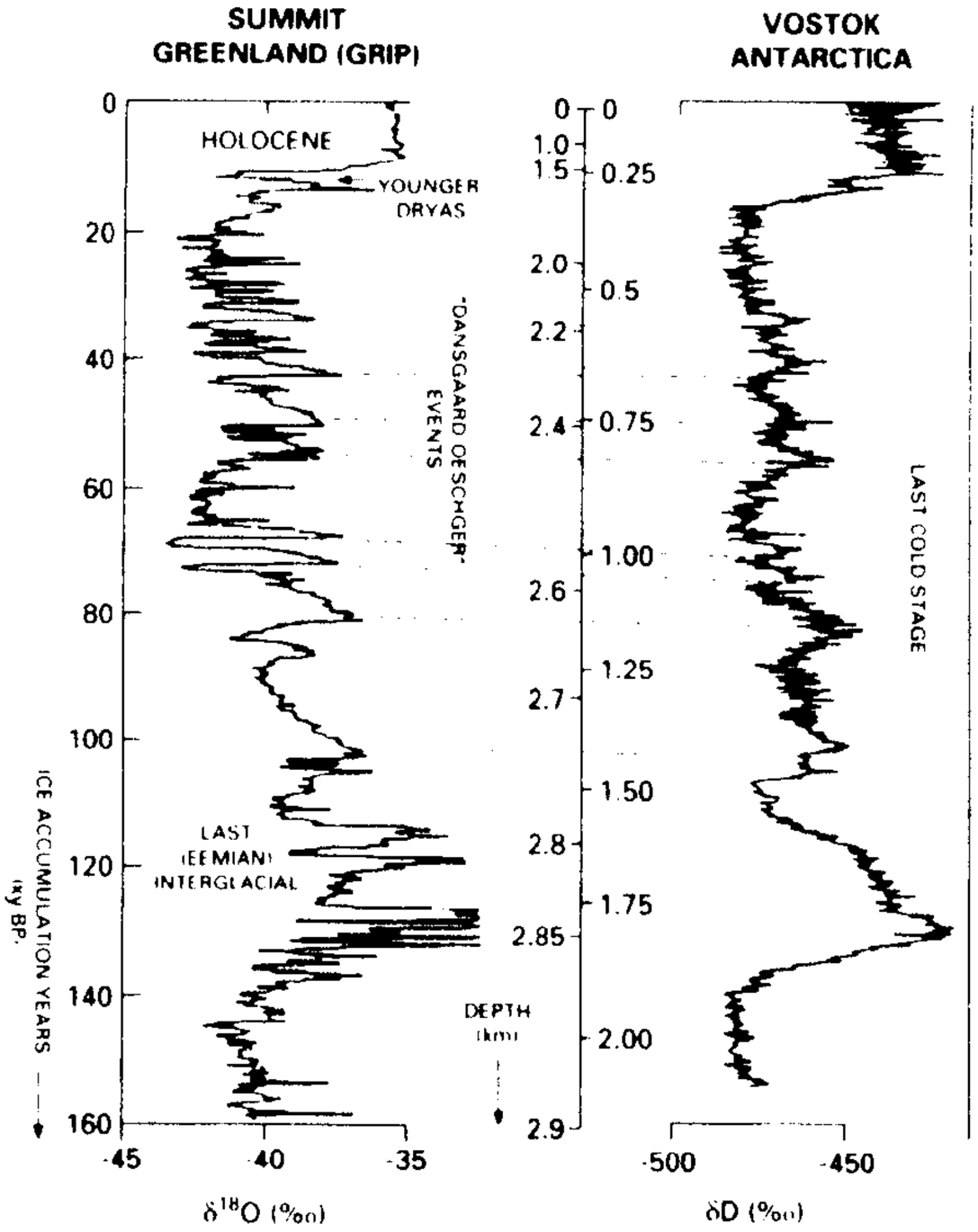

Figure 1.2. Stable isotope variations during the last 160 ky recorded in the GRIP Greenland summit core (oxygen isotope ratios) and the Vostok core from Antarctica (deuterium isotope ratio).

Ice core records also provide evidence of long- and short-term changes in atmospheric gas content. Measurements of the composition of ancient air in bubbles trapped in the ice reveal concentrations of the various atmospheric gases. For example, data from the Vostok core show that over the course of the past 160 ky, similar variations have occurred in CO_2 and CH_4 concentrations; moreover, these parallel very closely the oxygen derived temperature records for the same time period. This apparent relationship between atmospheric gas content and global temperatures has led to the suggestion that fluctuations in these 'greenhouse gases' may have exerted an influence on global temperatures (Chappellaz et al., 1990). Over shorter timescales, the gas content in the upper layers of ice constitutes an important record of recent human activity. The gradual increase in CO_2 in Greenland

ice from the mid-eighteen century onwards, and the more rapid increase over the last 50 years, provide clear evidence of the extent of human impact on the atmosphere (Neftel et al., 1985). Measurements of the carbon isotopic composition of atmospheric CO_2 over the last two centuries mirror this effect, values becoming more depleted over time, consistent with CO_2 released from fossil fuel combustion and biomass destruction (Friedli et al., 1986). The use of carbon isotope ratios has been extended to the last glacial period to derive information about the driving force behind CO_2 fluctuations (Leuenberger et al., 1992).

1.2.2 Marine records

Occupying more than 70% of the Earth's surface, the oceans are a very important source of palaeoclimatic information. Between 6 and 11 billion metric tons of sediment accumulate in the ocean basins annually, and this provides an archive of climatic conditions near the ocean surface or on the adjacent continents. Sediments are composed of both biogenic and terrigenous materials. The biogenic component includes the remains of planktonic (near surface-dwelling) and benthic (bottom dwelling) organisms, which provide records of past climate and oceanic circulation (in terms of surface-water temperature and salinity, dissolved oxygen in deep water, nutrient or trace element concentrations, etc.). By contrast, the nature and abundance of terrigenous material mainly provides records of: humidity-aridity variations on the continents; the intensity and direction of winds blowing from land areas to the oceans; and other modes of sediment transport to, and within, the oceans (fluvial erosion, ice-rafting, turbidity currents, etc.).

Perhaps the simplest of these proxies is the morphological evidence derived from sediments and the landforms they comprise. For example, former episodes of low sea level are indicated by submerged landforms in present offshore areas and evidence for higher than present sea levels by erosional features (Bell and Walker, 1992). In many ocean sediment sequences a broad correlation can be detected between the deposition of terrigenous material and former glacial episodes. This is most clearly reflected in the large volumes of ice-rafted debris that are found in the ocean sediments. In the North Atlantic, for example, the debris deposition appears to have been by far the most important mechanism for supplying terrigenous material to the ocean floor (Robinson et al., 1995). In the deeper oceans, the sediments tend to be finer grained and are often dominated by biogenic material consisting of the accumulation of the carbonaceous and siliceous remains of micro-organisms that formerly lived in the ocean waters. They contain recognisable fossil remains, which provide a record of ocean circulation, ocean water temperature, and

by implication, atmospheric temperature. One example is the use of fossil remains from phytoplankton to reconstruct past ocean water temperatures using the U^{K}_{37} index (Brassell et al., 1986). Certain marine phytoplanktons respond to changes in water temperature by altering their molecular composition. Specifically, as water temperature decreases, they increase the production of unsaturated alkenones. Cells contain a mixture of long-chain alkenones with 37, 38 or 39 carbon atoms, which are either di- or tri-unsaturated, with the ratio of these biomarkers changing with temperature. The importance of these organic biomarkers is that they do not appear to significantly degrade (e.g. their relative rates of decay are comparable) in marine sediments, nor is it thought they are influenced by changes in salinity. Thus, they provide a crucial complement to $\delta^{18}O$ and faunal composition studies.

Further evidence for environmental change in the oceans comes from the chemical and isotope content of the marine organisms contained within them. It is the application of oxygen isotope analysis to ocean sediments that has by far had the greatest impact on palaeoclimate research. The method provides one of the principal indices of global environmental change. The variations in the isotopic composition of ocean waters over time can be reconstructed from $\delta^{18}O$ values of carbonate shells and skeletons preserved in sediments. Many marine organisms secrete (or build) carbonate structures and oxygen is abstracted from seawaters for this purpose. Thus, the oxygen isotope ratios in fossil carbonates buried in sediments should reflect the ratios prevailing in the oceans at the time of their secretion. However, the $\delta^{18}O$ ratio is also dependent upon the temperature of seawater during secretion. Oxygen isotope profiles from marine deposits are mostly interpreted as a record of global palaeoglaciation, instead of palaeotemperature (Shackleton and Opdyke, 1977). This is due to the fact that during glaciations large amounts of the lighter isotope are sequestered in the growing ice sheets.

The analysis of carbon isotopes in marine sediments can also provide valuable data on oceanographic changes. $\delta^{13}C$ profiles in marine sediment sequences show cyclic variations, very similar to those in oxygen isotope traces, and it appears, therefore, that these also reflect important environmental changes. Carbon isotope data from micro-organisms provide information on productivity changes in the upper layers of the oceans and on the flux of ^{12}C in surface waters. This evidence also offers insight into former atmospheric variations in CO_2 (Shackleton et al., 1992), and therefore, forms a complementary source of information to the ice cores.

1.2.3 Terrestrial records

The range of terrestrial settings providing information to palaeoclimatology is vast. Indeed, one could argue that virtually all continental sedimentary deposits contain a palaeoclimatic signal to some degree. Commonly, climatic inferences drawn from such evidence are qualitative and even dating the features may be very difficult. Nevertheless, such evidence of past changes in climate is ubiquitous, and many innovative approaches have been developed. The main sources of palaeoclimatic records are lake sediments, caves, tree rings and peat bogs.

Lakes accumulate sediments from their surrounding environment and sediment cores recovered from lakes provide a record of environmental change. Accumulation rates for lakes are often high, so lake sediments offer the potential for high-resolution records of past climatic change. Lake sediments are made up of two basic components: allochthonous material, originating from outside the lake basin, and autochthonous material, produced within the lake itself. The most widely studied component of lake sediments is their pollen content. Pollen grains and spores provide a record of past vegetation changes that may be due to changes of climate. Pollen are dispersed over a wide area and therefore reflect regional vegetation patterns (Bell and Walker, 1992). Other techniques used in the analysis of lake sediments include macrofossils (which can supplement the pollen analysis; Hannon and Gaillard, 1997), isotope analysis, varve counting (the visible seasonal layers of deposition) and distributions of diatoms (microscopic unicellar algae), which are found in lakes and reflect water chemistry. Diatom distribution is controlled by a range of environmental variables (e.g. pH, mineral and nutrient concentration, degree of oxygenation, water temperature); thus, their abundances have been related to water temperatures (Pienitz et al., 1995), and oxygen isotopes in their silica have been used to estimate palaeotemperature (Shemesh and Peteet, 1998).

A second terrestrial setting is cave sediments. Caves form natural sediment traps in which the deposits are largely protected from the effects of sub-aerial weathering agencies and erosions. Thus, detailed physical and chemical analysis of cave sediments can provide valuable data concerning climate change. The most important of all cave settings are the so-called speleothems, $CaCO_3$ formations occurring in limestone caves, most commonly as stalagmites and stalactites. Speleothems are the longest and most detailed palaeoenvironmental records from a cave context (Gascoyne, 1992). Isotopic analysis has been used to reconstruct past air temperature (Atkinson et al., 1986) through the relationship between the isotopes

in the precipitate and the waters from which they grew, a relationship closely controlled by temperature (Lowe and Walker, 1984).

A third setting used for palaeoclimate data is tree rings. Valuable information can be obtained from the actual physical properties of the rings. The width of a ring in any one tree is a function of many variables, including species, age, nutrients in the soil, but also climate. Favourable environmental conditions lead to the formation of wide growth rings, while adverse conditions result in narrow rings, producing a sequence of broad and narrow rings. Hence ring width can be indicative of climate, for example a narrow ring could be the result of cold summer and/or low rainfall (Roberts, 1998). Another use of tree rings is the isotope content of them. Many studies have demonstrated empirically that variations in the isotopic content of tree rings ($\delta^{13}C$, $\delta^{18}O$ and δD) are related to climate. To avoid the difficulties of chemical heterogeneity in wood samples, a single component, 5α-cellulose is extracted for isotopic analysis. The variations in the isotopic content of the cellulose reflect the variations in the isotopic content of precipitation, which are largely determined by past temperatures. As a consequence, correlations can be made between $\delta^{18}O$ or δD and air temperature and relative humidity (Burk and Stuiver, 1981). Fluctuations in the global carbon cycle have also been inferred from $\delta^{13}C$ records in tree rings ranging from the post-industrial revolution anthropogenic effect (Epstein and Krishnamurthy, 1990) to the major changes that appear to have occurred in the composition of the global carbon reservoir at the last glacial-interglacial transition (Krishnamurthy and Epstein, 1990). The most-widely used application to come from tree ring research is the calibration curve for the ^{14}C timescale (Stuiver et al., 1998).

The fourth setting from which continuous records of terrestrial climate change can be deduced are peat bogs, chosen for study in this thesis. A more detailed review of peat as palaeoclimate and palaeovegetation indicator is given in the next section.

1.3 Ombrotrophic mires

1.3.1 Peat bog development and characteristics

There may be more carbon incorporated in *Sphagnum* (the main peat forming plant), dead and alive, than in any other genus of plants. It is estimated that about 3.4% of the Earth's surface is covered by peat deposits, containing around 240 Gt of carbon (Matthews and Fung, 1987). This is a little less then four times the amount of carbon fixed on the Earth's surface (Clymo, 1991). Whilst these figures

are estimates they emphasise that peatlands are numerous and may have a significant effect on the Earth's carbon budget.

Peat deposits are classed as a wetland ecosystem. Wetlands include non-peat forming, intermittently flooded marshes, and peat-forming, permanently wet mires. Mires (peatlands) are usually classified as:

(i) Fens - which are fed by groundwater (minerotrophic) and therefore usually rich in nutrients. They are often an early stage in the formation of raised bogs.

(ii) Bogs - which are fed by rainwater (ombrotrophic) and therefore poor in nutrients.

Two types of bogs exist: Raised bogs (or ombrotrophic bogs) have a dome-shaped surface of waterlogged peat above the original watersurface and require the annual precipitation to exceed the evapotranspiration. Raised bogs only receive nutrients in the form of rainwater or wind-borne dust. In temperate climates, raised bogs are rarely higher then 6 m and more then a few kilometres across. A more extensive second type of bog is the blanket bog. Blanket bogs form in wet climates (annual rainfall >1600 mm, with a low summer precipitation deficit), and form a blanket-like layer of peat over the surface of the underlying mineral soil.

The most common form of bog development is the classic hydrosere, also known as lake in-fill (Figure 1.3). The last glaciation or ice age ended about 13,000 years ago. The retreating glaciers left behind an undulating landscape, with basins and deep hollows. These depressions filled with water due to the poor drainage characteristics from the basin soils creating a lake environment. In this successional model, small lakes become filled in from the edges towards the middle over a period of several thousand years. A mat of reed, sedges and grasses forms a pioneer community and floating mat upon which other herbaceous plants develop. When these plants died they only partially decay and their remains accumulate on the bottom of the lake. The gradual in-fill of these lakes created a fen peat environment and when the surface vegetation is no longer influenced by mineral-rich ground waters, *Sphagnum* colonizes the mat and the surface layer becomes increasingly isolated from mineral water. This is driven by the tolerance of *Sphagnum* for the nutrient poor conditions present in rain waters. In the absence of disturbance, such as changes in climate and hydrology, this sequence from open water to aquatic bed-dominated plant communities, to sedge peat to *Sphagnum* lawn flats to a lens shaped dome is typical for the formation of ombrotrophic mires.

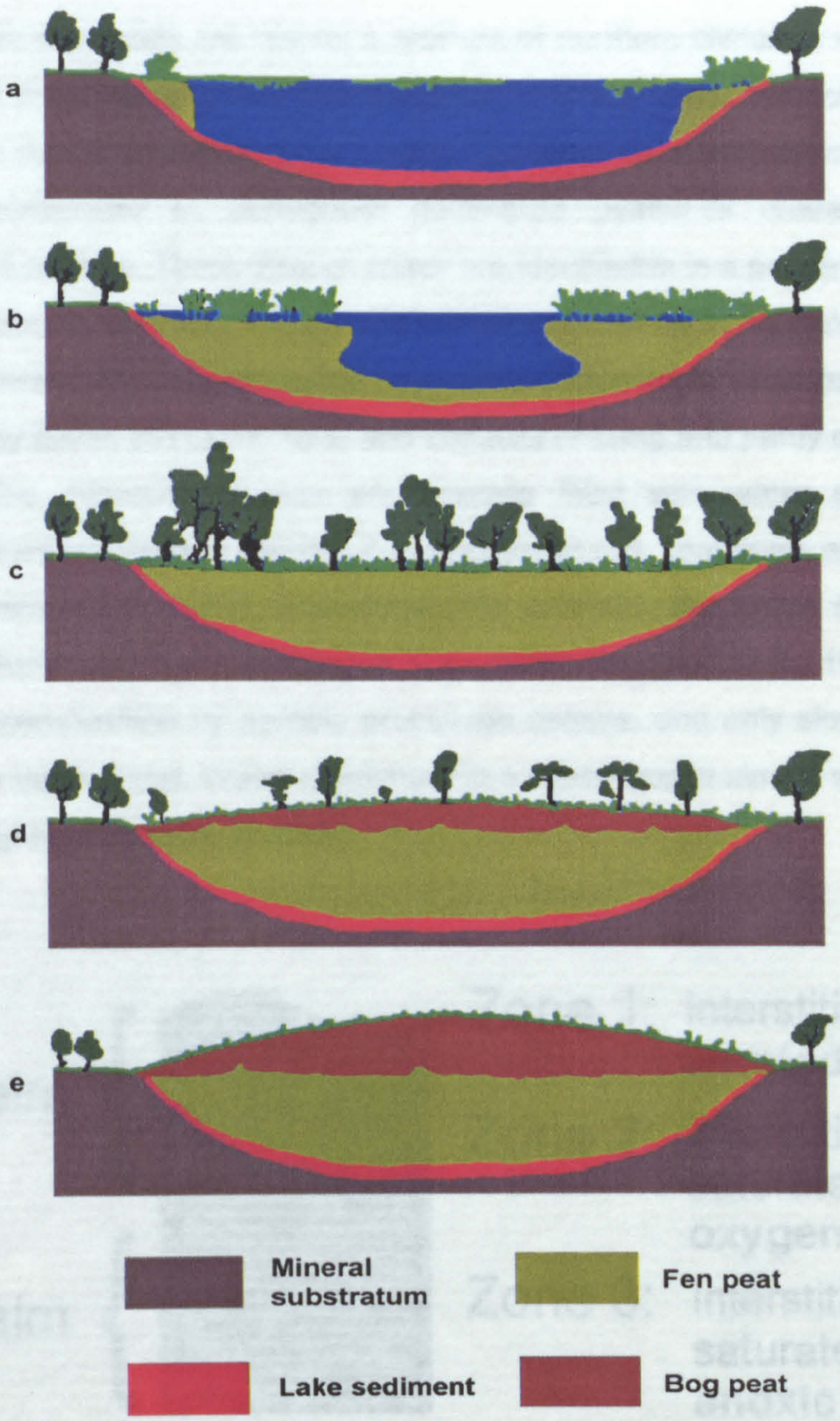

Figure 1.3. Development of a raised bog: (a) lake sediment; (b)-(c) fen; (d)-(e) bog.

Peat itself is a heterogeneous mixture of more or less decomposed plant (humus) material that has accumulated in a water-saturated environment in the absence of oxygen. Peatlands occur when the rate of production of organic material exceeds the rate of decomposition (Moore and Bellamy, 1974), causing partially decomposed organic matter to accumulate. It is not so much that the production of organic matter is unusually high in peatlands, but that the rate of decomposition is unusually low (Craft and Richardson, 1993). This slowed rate of decomposition is typically due to a combination of water-logging, acidity, and anoxic conditions (Clymo, 1984). Gignac and Vitt (1990) state that the two most important factors maintaining slowed decomposition rates are cold temperatures and high water

levels. As such, peatlands are largely a product of northern climates, with a water balance where precipitation exceeds evapotranspiration. An important characteristic of a peatland is the presence of a vertical gradient of dissolved oxygen. It is particularly pronounced in *Sphagnum* dominated peatlands characterized by hummocks and hollows. Three distinct zones are identifiable in a profile (Figure 1.4) through a hummock. The uppermost zone is characterized by living *Sphagnum*, and the spaces between the *Sphagnum* stems are not permanently saturated. Zone two lies immediately below the upper zone and consists of living and partly decomposed *Sphagnum*. The interstitial spaces are typically filled with water and have a measurable dissolved oxygen content. Zones one and two, combined, are called the acrotelm (Ingram, 1978; 1982). Zone three, the catotelm, lies below the acrotelm and begins where the dissolved oxygen is depleted (Ingram, 1978; 1982). In this zone, peat decomposition by aerobic processes ceases, and only slow anaerobic decomposition takes place. Water movement in a raised bog is almost wholly lateral through the highly permeable acrotelm.

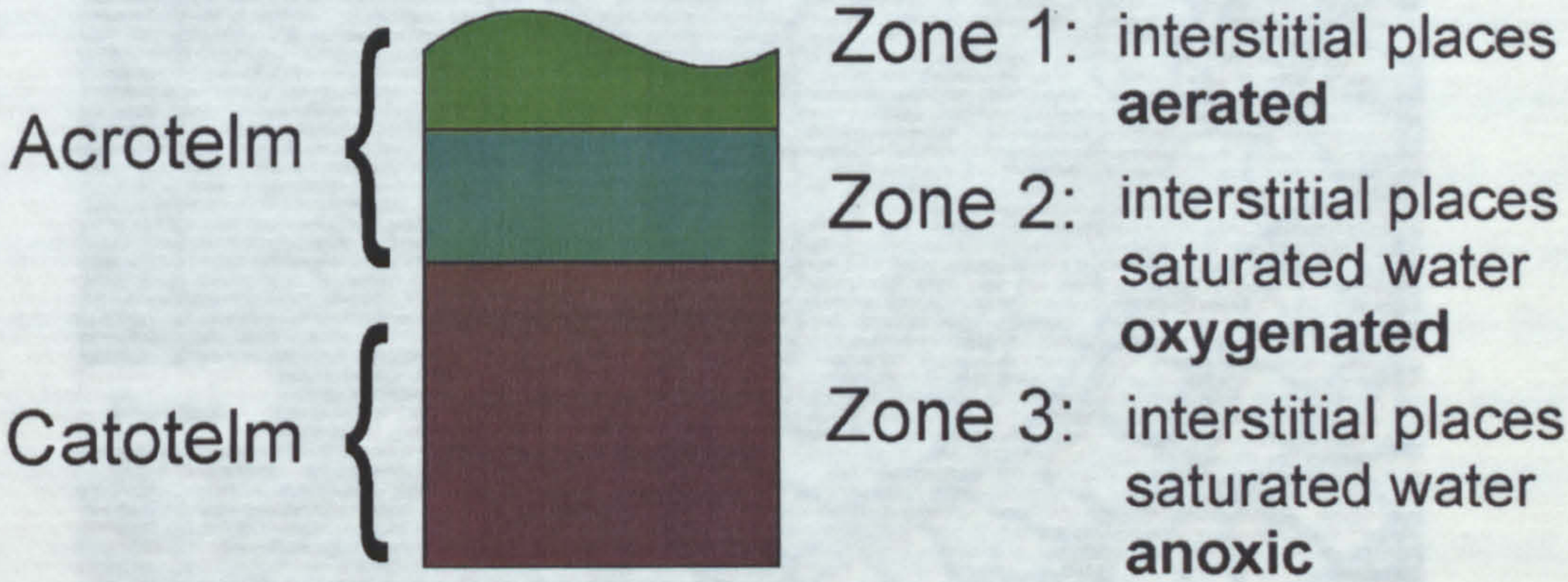

Figure 1.4. The acrotelm and catotelm zones within a typical peat bog.

One plant family dominates most ombrotrophic mires, namely: *Sphagnaceae*. The success of *Sphagnum* is due to its ability to create a habitat in which very few other plants can flourish and for which *Sphagnum* is ideally adapted (van Breemen, 1995). Nutrients enter bogs mainly by wet and dry atmospheric deposition. *Sphagnum* lacks rhizoids and internal water-conducting tissue, and some species are very susceptible to desiccation. Therefore, the *Sphagnum* plants depend on water from rain or from the water table in the acrotelm, drawn up through capillary spaces formed by overlapping branches (Clymo and Hayward, 1982). The

Sphagnum morphology makes them capable of surviving these conditions. The main stem of the *Sphagnum* plant is composed of a central region surrounded by one to five layers of hyaline cells. The leaves are arranged with the large dead, hollow hyaline cells (making up about 80% of the plant's volume) interspersed with smaller live photosynthetic or green cells (Figure 1.5). The morphology of these hyaline cells enables them to retain large amounts of water. They die at maturity and are frequently perforated by pores. These hollow spherical cells hold water like a vase. Some species of *Sphagnum* have been shown to hold 16 to 26 times their dry weight in water. Water will wick up both the stem and pendant branches, filling each hyaline cell and then wicking up the cell wall of the next hyaline cell and spilling into and filling it (McQueen, 1990). In this way, *Sphagnum* wicks and stores water and remains moist even feet above the water table. This is unlike vascular plants that regulate carbon and water exchange by controlling stomatal apertures on leaf surfaces; *Sphagnum* lacks stomata and possess little short-term control over these processes.

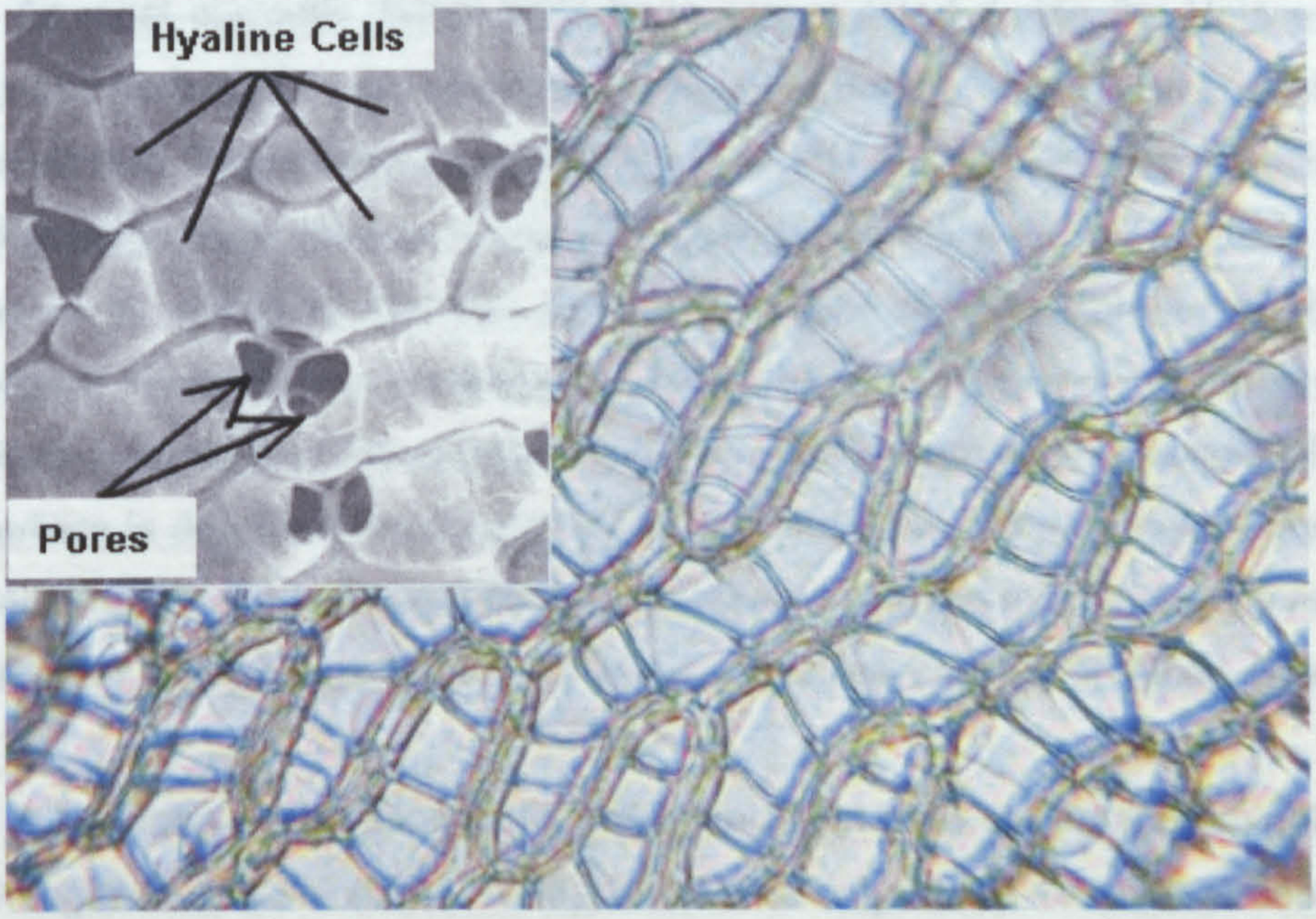

Figure 1.5. The large hollow hyaline cells (with pores for uptake of water), interspersed with photosynthetic cells, giving the *Sphagnum* plant its water holding properties (Linne von Berg, 2001; Webb, 2003).

Since nutrients enter the bogs by wet and dry atmospheric deposition *Sphagnum* efficiently intercepts these. *Sphagnum* plants use cation exchange (by uronic acid) to obtain macro- and micronutrients that are often in low concentrations (Clymo, 1982). They acidify the area by exchanging hydrogen ions for base cations (K^+, Na^+, Ca^{++}, Mg^{++}). Many other plants do not tolerate the low mineral nutrient and

acidic environment that results, so there is very little competition for resources. This acidic, cold, constantly saturated and mineral-poor environment impedes decomposition of the older portions of the plant below the growing tip. Growth and reproduction of bacteria and fungi that normally mediate decomposition are limited or prevented under these conditions. The lack of decomposition results in the accumulation of peat.

In this section, the presence of peatlands and the special conditions that govern their occurrence have been explored. It is clear that these nutrient poor habitats are closely linked with climate. With the only source of nutrients being wet and dry deposition and a water table maintained by an excess of rain over evapotranspiration, peat bogs form an ideal setting to study climate, especially since changes in the surface wetness of a bog can influence which species of plants thrive there.

1.3.2 Palaeo-records in peat

As most currently 'living' bogs have accumulated during the Holocene, the records that they contain are especially relevant to understanding and predicting the present climate. Assumptions underpinning peat-based climate studies include: (i) mire vegetation assemblages respond to changes in the watertable, which is itself responsive to changing climate; (ii) the subfossil remains (preserved but not mineralised) of vegetation, preserved in mires are an accurate record of the original vegetation cover at the time of deposition; (iii) more decomposition occurs when the mire surface is dry, thus resulting in more humified peat, a darker colour and fewer identifiable remains than in peat that accumulates when the mire surface is relatively wet; and (iv) reliable age estimates of peat profiles can be obtained (Blackford, 2000).

It has long been recognized that changes in peat stratigraphy might reflect past changes in climate (Blytt, 1876), but it was only in the 1970s that continuous proxy-climate records began to be sought from peat deposits. The peat bog archive includes macrofossil analysis (Barber et al., 1994; Mauquoy and Barber, 1999; Mauquoy et al., 2000b; Hughes et al., 2000), humification (Aaby, 1976; Blackford and Chambers, 1995), biomarker abundance data (Nott, 2000; Nott et al., 2000; Avsejs, 2001; Avsejs et al., 2002, Pancost et al., 2002) and stable isotope data (Nott, 2000; Xie et al., 2000; Pancost et al., 2003; Xie et al., in press).

Identification and quantification of the species in subfossil samples have been used to show changes in mire conditions. The proportion of peat composed of *Sphagnum* and the relative abundance of different species have been used to show

wetter and drier phases. Barber and co-workers (1994) developed a method with which individual macrofossil abundances could be converted into a wet shift profile through a peat bog. They obtained wet shift data that was found to correlate with data from locations over large areas (Mauquoy and Barber, 1999; Barber et al., 2000; Mauquoy et al., 2002a; Mauquoy et al., 2002b; Barber et al., 2003). Synchronicity between distant bogs is usually explained by changes in climate (Blackford, 2000). However, there are times when *Sphagnum* remains are either absent or unidentifiable because of decomposition and where competition between species, rather then climatic factors, causes the assemblage to change. The degree of peat humification (the decomposition of plant material into amorphous humus) has been widely used to infer changes in peat surface wetness, either by recording the field stratigraphy in terms of colour and preservation, or by a laboratory based colorimetric method (Aaby, 1976; Blackford and Chambers, 1993). Colorimetric analyses have been shown to be replicable, applicable to all peat types and show more variation than detectable in the visible stratigraphic record, although problems remain regarding the effect of species change on the rate of decomposition and the optical density of the humic extract (Blackford and Chambers, 1993). In theory, humification data indicate changes in the time elapsed between the death of plant matter and their remains reaching the anaerobic catotelm. Thus the humification data represent a proxy for the position of the water table at the time of deposition. A possible link between solar variability (number of sunspots) and changes in the humification data has been found (Blackford and Chambers, 1995) and indicates the potential for peat profiles in identifying some of the stronger forcing factors of the climate system. The range of palaeoenvironmental indicators used has broadened to include an expanded range of micro- and macrofossils and peat chemical properties. These include fungal remains, shown to have palaeohydrological affinities (van Geel et al., 1995), and abundances of testate amoebae (Woodland et al., 1998; Charman et al., 1999), unicellar organisms partially enclosed in a shell and shown to occupy distinct ranges of watertable positions. A multi-proxy approach in combination with ^{14}C wiggle-matching enables changes in each proxy reconstruction to be validated against each other, producing more reliable and replicable palaeoclimatic reconstructions and strengthening the plausibility of correlations with other climatic reconstructions (Mauquoy et al., 2002b; Langdon et al., 2003).

A newly developing field is the use of organic geochemical tools to deduce palaeoenvironmental information from peats. Studies using this molecular stratigraphic approach are limited. Farrimond and Flanagan (1995) attempted to

compare the lipid records of changing vegetation/environment of a peat bed from Northumberland with the pollen record. This comparison revealed that similar pollen profiles could have very different lipid distributions and vice versa. However, a general trend was established. Another attempt was made by Ficken and co-workers (1998) who also found problems with relating lipid abundances to macrofossil-reconstructed plant inputs on a Scottish montane bog. More success was obtained using plant-specific lipid biomarkers (Nott et al., 2000; Avsejs et al., 2002; Xie et al., in press). The latter studies correlated plant-specific biomarkers (*n*-tricosane and 5-*n*-alkylresorcinols) to their respective plant inputs. The plant-specific lipid biomarkers (*n*-tricosane and the resorcinols) were even found to correlate to the recorded lower temperatures at the time of deposition. However, the signals are sometimes found to be ambiguous and only qualitatively indicative of the possible plant inputs (Pancost et al., 2002). In general, it can be stated that the controls on the lipid abundances go well beyond just simple plant input and climate (see also Chapter 3 for a further discussion).

Values of δD, $\delta^{13}C$ and $\delta^{18}O$ have been measured from different peat components, resulting in climatic reconstructions of the Holocene. Bulk $\delta^{13}C$ values from peat cores have been used to reconstruct periods of dry and wetter climate (Sukumar et al., 1993) and can be correlated with temperature (Nott, 2000). The main emphasis of $\delta^{13}C$ research has been the reconstruction of past atmospheric CO_2 concentrations (White et al., 1994). The $\delta^{13}C$ values of peat macrofossil components (sedge and moss species) can be determined and used to provide CO_2 concentrations for both atmosphere and peat water. Unlike sedges, mosses do not posses stomata and therefore their $\delta^{13}C$ value depends on atmospheric CO_2 and available water. The $\delta^{13}C$ values of sedges from the same peat can be used to remove the water signal. As peat has a high accumulation rate the CO_2 concentrations can be determined to a higher resolution then from other settings, and peat $\delta^{13}C$ values have been used to identify a possible link with thermohaline circulation (Figge and White, 1995). Compound-specific $\delta^{13}C$ values have been correlated with temperature and plant input (Nott, 2000; Xie et al., in press) and parallels between the $\delta^{13}C$ values in peat and the anthropogenic changes in atmospheric $\delta^{13}C$ values have been observed (Ficken, 1998; Nott, 2000; Pancost et al., 2003; Xie et al., in press). Carbon isotopes in peat bogs have also been used in the tracing of carbon cycling in peat bogs using the $\delta^{13}C$ values of lipids (Pancost et al., 2000; Pancost and Sinninghe Damsté, 2003).

$\delta^{18}O$ Values of 5α-cellulose have, beside their use in tree ring reconstructions, also been used to identify solar forcing in Chinese peat, where the

$\delta^{18}O$ record tracked the known climatic (warm/cold) cycles (Hong et al., 2000). A combination of $\delta^{18}O$ and δD values from cellulose extracted from a peat bog (Brenninkmeijer et al., 1982) showed potential as palaeoclimate indicators by correlation with pollen evidence for the climatic deterioration of the Subboreal/Subatlantic transition. Although differences between the bog mosses and other vascular plants were large (25‰ for δD and 5‰ for $\delta^{18}O$ values) not all of the variations in the profile could be attributed to changing plant abundances. A further study by Dupont and Mook (1987) revealed that under identical climatic conditions the deuterium content of various plants differed. However, after correction of the data for species variation, a correlation between cellulose $\delta^{18}O$ values and palaeotemperature was identified. Work on Carbury Bog (van Geel and Middeldorp, 1988) proved less conclusive, and in non-taxa specific isotope data (as in the case of peat cellulose) the species-induced signal was found to be inseparable from the climatic signal. As such, no correlation with Lambs climate index could be established (Lamb, 1977).

A further step in the development of stable isotopes to climate reconstruction using peat bog archives was the development of a compound-specific isotope approach (see Chapter 4), using taxa-specific biomarkers. A first application of this new technique published by Xie et al. (2000) showed the *n*-C_{23} alkane δD to be correlated with recorded growing season temperatures.

1.3.3 Organic geochemistry of peat

As seen in previous sections, peat deposits record climate through a variety of different physical and chemical properties. Most of these properties are the result of microbial decomposition of the raw plant material under aerobic conditions prevalent in the upper part of the peat deposits (acrotelm); during diagenesis a proportion of organic matter disappears completely and is lost from the molecular fossil record (Huang et al., 1997). Most decomposition is due to diagenetic processes associated with aerobic organisms, which are depleted in peat as there is limited access to oxygen. Under anaerobic conditions present in the permanently waterlogged catotelm the decomposition of organic compounds is dramatically slowed.

During the formation of peat, organic matter classified under the general term 'humic substances' is formed. These humic substances are composed of: (1) humic acids, (2) fulvic acids, and (3) humans, classified by their solubility in various solvents: humic acids are soluble in alkali; fulvic acids remain in solution after precipitation of the humic acids with acid; and Humins are the organic residues that

remain in the peat afterwards (Oden, 1919), although this classification is falling out of use. Another class of organic compounds found in abundance in peat are lipids. These are compounds that are soluble in organic solvents and insoluble in water. Previous studies involving the analysis of peat have revealed that dry peat contains about 5-20% lipidic matter (Ketola et al., 1987). However, the lipids present in peat can vary widely depending on such factors as the type of peat-forming plant communities, bacterial and fungal populations and the level of preservation. Lehtonen and Ketola examined the total lipid fraction of different peat cores. The total lipid fraction contains four major groups of compounds: long-chain fatty acids (C_{12}-C_{34}), ω-hydroxy acids (C_{12}-C_{28}), long-chain 1-alkanols (C_{12}-C_{34}) and a group of phytosterols and their microbial metabolites. Of these, *n*-fatty and ω-hydroxy acids are the major groups comprising 60-90% of the lipids. The combined contribution of 1-alkanols and sterols range up to 25% of the total lipid fraction. Long-chain alkanes (C_{16}-C_{35}) and α,ω-alkanedioic acids (even-carbon C_{14}-C_{28} and C_9) as well as acyclic methyl ketones (C_{17}-C_{35}) and triterpenoids and phenolic acids exist as minor components (Lehtonen and Ketola, 1993). Compositional changes occur gradually when peat is formed through decomposition of the present plant material. The relative content of longer-chain aliphatic components increased during humification, thereby providing a strong indication, together with changes in average chain length and fraction sizes, for the decay resistance of *Sphagnum* mosses. Several variables control the final lipid composition of humified peat and this will be discussed in greater detail in Chapter 3.

1.4 Deuterium isotope ratios in the natural environment

In the previous section (1.3) the close relationship between raised or ombrotrophic peat bogs and climate has been demonstrated. Especially noteworthy was the relationship with precipitation because rainfall is the sole provider of nutrients and water to this type of peat forming ecosystem. In the next sections a close relationship between climate and the isotopic composition of rainfall will be established.

1.4.1 Delta notation (relative units)

Water is the most abundant compound on Earth and the primary compound in all forms of life. In common with most other elements, the constituents of water, oxygen and hydrogen may exist in the form of different isotopes. Isotopes result from variations in mass of the atom of each element as a result of different numbers

of neutrons in the nucleus. Hydrogen has two stable isotopes, ^{1}H and ^{2}H (D; deuterium) with relative proportions of 99.984% and 0.016%, while oxygen exists in three forms (^{16}O, ^{17}O and ^{18}O). Consequently, water molecules may exist as any one of nine possible combinations. However, as water with more then one "heavy" isotope is very rare only three combinations are common. The average occurrences of the most important isotopical compositions of water ($H_2{}^{16}O$, $HD^{16}O$ and $H_2{}^{18}O$) are related as approximately 997680:320:200 ppm (parts per million; Dansgaard, 1964). Due to the very low abundances of the minor isotopes (D, ^{18}O) it is much easier to measure relative differences between two samples than the absolute values for one sample. Fortunately, greatest interest is attached to the variations in isotopic composition, and thus in variation between samples. Variations in natural abundances are quoted in relative units, per mil (‰), on the delta (δ) scale. Delta values for deuterium isotopes are defined as (Preston, 1992):

$$\delta D(‰) = \left[\frac{(D/H)_{sample}}{(D/H)_{standard}} - 1 \right] * 1000$$

The standard used is Vienna standard mean ocean water (V-SMOW; Gonfiantini, 1978), whose composition is very close to that of the World's oceans; by definition, for ocean water δD = 0‰.

1.4.2 Isotope fractionation factors in precipitation

The isotopic composition of natural waters covers a wide per mil range, more then 400‰ for δD, the largest of any natural isotope. The basis for most variations in the stable isotope content of water molecules is that the vapour pressure of $H_2{}^{16}O$ is higher than that of $HD^{16}O$ and $H_2{}^{18}O$ (10% higher than HDO, 1% higher than $H_2{}^{18}O$; Bradley, 1999). This causes fractionation in all condensation processes and evaporation processes of water.

The fractionation factors for such processes depend upon the temperature and the rate of reaction. If the process proceeds so slowly that the equilibrium conditions are practically realized at the boundary between the phases, no kinetic isotope effects will come into play. All fractionation effects can be divided into four categories: condensation, evaporation, temperature and amount of rainfall (Dansgaard, 1964). In a non-equilibrium state the fractionation is dependant on the rate of exchange, with the lightest component being the fastest ($H_2{}^{16}O$ > $HD^{16}O$ > $H_2{}^{18}O$). Since evaporation of water in nature takes place in environments already

containing some vapour, the influence of equilibrium exchange of isotopically distinct molecules between vapour and the evaporating water must also be considered.

(i) *Condensation*

Most important for the isotopic composition of precipitation is the condensation process, e.g. the formation of droplets (rainfall) from atmospheric vapour. Condensing the vapour results in preferential loss of the isotopically heavy molecules, such that δD values for the remaining vapour and, consequently, for newly formed condensate become increasingly negative as the vapour becomes depleted in deuterium. Hence, compared to the vapour, the condensation will be enriched in the heavy isotopes. Condensate is usually the result of cooling of the vapour phase and with increasing cooling this process proceeds more rapidly depleting the vapour phase, volumetrically and isotopically. Most condensation does not happen under equilibrium conditions, but are the result of so called Rayleigh processes involving immediate removal of the condensate from the vapour phase after formation. Rayleigh processes lead to higher isotopic variability than processes in which the two phases are allowed to equilibrate by exchange.

(ii) *Evaporation*

During their fall from the cloud to the ground raindrops are subjected to evaporation and exchange with the environmental vapour. These processes are especially important for the final isotopic composition of the liquid precipitation when it reaches the ground. The degree of evaporation is relatively high in dry air; however, where humidity is high the exchange process will possibly become the dominating factor. By analogy with the condensation effect, the water droplets will preferentially lose the lighter isotope (due to its higher vapour pressure) and become isotopically enriched during in deuterium evaporation.

(iii) *Temperature effect*

Isothermal condensation never happens in the atmosphere. Any formation of precipitation is caused by some kind of cooling process. Cooling processes responsible for the formation of droplets occur at different temperatures, called condensation temperatures. The lower the condensation temperature the higher the degree of fractionation between the vapour phase and the condensate and this is a direct consequence from the difference in vapour pressure, which is temperature related. In general, at higher temperatures less deuterium will condense, resulting in more negative δD values for the precipitation, while lower temperatures result in

more deuterium condensing causing the vapour to be more depleted in deuterium (more negative).

(iv) *Amount effect*

A negative correlation can be demonstrated between δD values and the amount of monthly rainfall, i.e. low δD values in rainy months and high δD values in dry months. The explanation lies in the degree of evaporation and exchange between a droplet and the surrounding vapour phase. The fractionation by isotopic exchange between the falling raindrops and the environmental vapour is most pronounced for less intense rains resulting in relatively high δD values. This arises because the vapour below the cloud has not yet been exposed to cooling processes (in heavy rain the vapour composition is more or less determined by the liquid phase); the same effect occurs due to evaporation from falling drops. The low humidity of low altitude air causes considerable relative loss of lighter molecules, thereby considerably enriching the rain in deuterium (high δD values). Thus, both evaporation and exchange tend to enrich small amounts of rain in heavy isotopes. Low δD values of tropical rain must, therefore, be due to deep cooling of the air followed by relatively little enrichment due to other processes, e.g. in case of heavy and/or long lasting rain. At higher latitudes the amount effect becomes less pronounced, partly because of the lower degree of evaporation from falling drops. The "amount effect" is observed all year round at most tropical locations, and in the summer time at mid latitudes, but never at polar locations, where the temperature effect is the dominating factor.

These different effects, all controlling the isotopic composition of the precipitation are virtually indistinguishable at mid-latitudes (like the sample sites in this study). This is demonstrated in Figure 1.6 for a mid-latitude weather station.

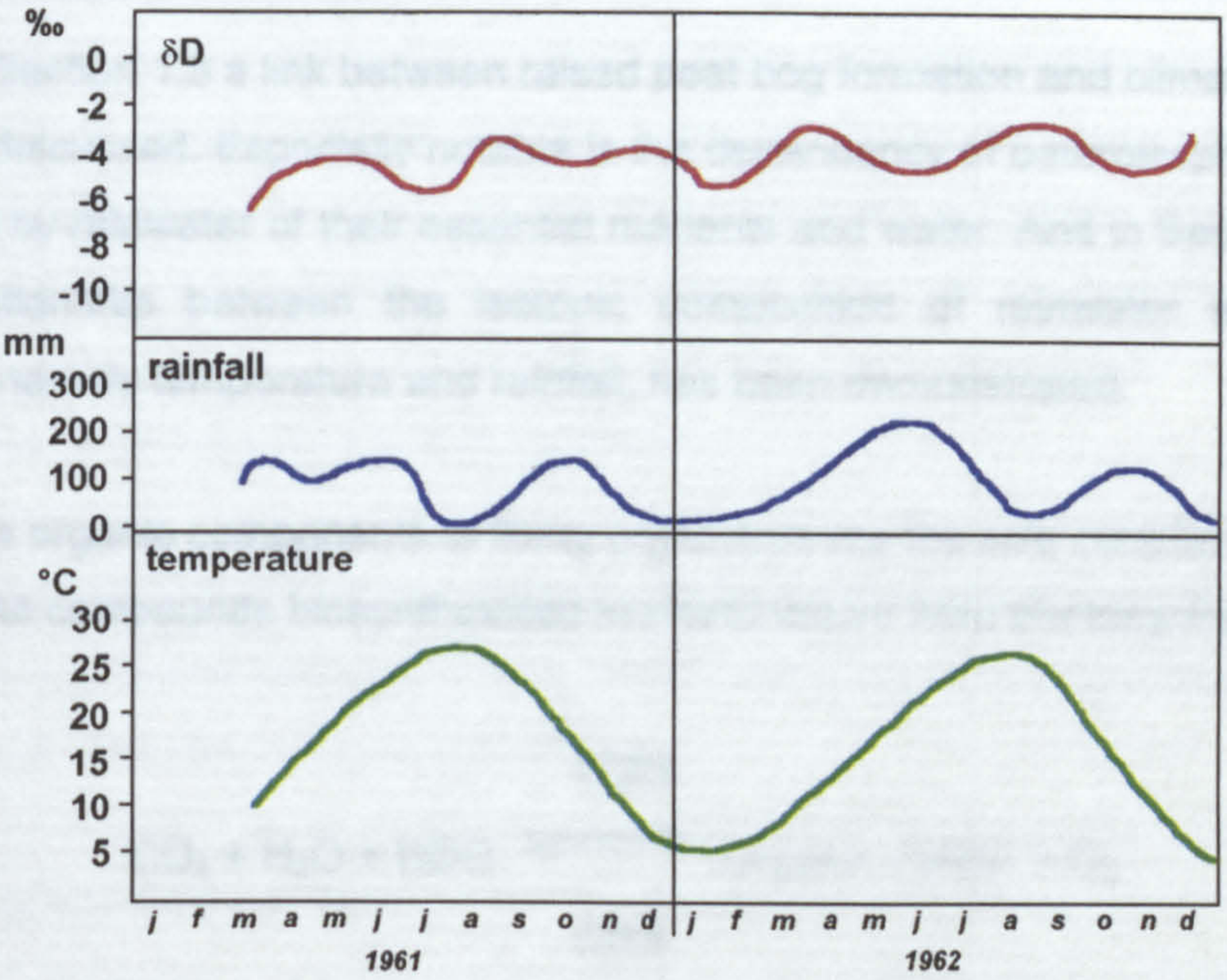

Figure 1.6. Combined temperature effect and amount effect at mid-latitudes (Tokyo), showing the correlation with δD values (after Dansgaard, 1964).

As a result of these basic controls on the isotopic composition of rainfall, Schiegl (1970) distinguished the following effects on the deuterium content of precipitation and consequently bog water:

(i) Latitude effect: With increasing geographical latitude, the deuterium content of precipitation decreases, following the temperature gradient between the equator and the poles.

(ii) Altitude effect. With increasing altitude, the deuterium content of precipitation will gradually decrease, again following a temperature gradient.

(iii) Seasonal effects: The deuterium content of precipitation at higher latitudes (>30°) varies seasonally with a maximum in the summer and a minimum in the winter.

(iv) Continental effect: Precipitation will contain less deuterium the further the air mass moves from the coast into the interior of a continent. This is due to the condensation effect preferentially removing heavier isotopes.

It has been demonstrated that both temperature and rainfall amounts influence the isotopic composition of the precipitation that peat bogs require for the growth of their vegetation. Several other fractionations, linked with the special conditions governing peat bogs and their dominating *Sphagnum* taxa, will be discussed in Chapter 5.

1.5 Hypothesis and aims

In Section 1.3 a link between raised peat bog formation and climate variables has been discussed. Especially notable is the dependency of ombrotrophic mires on the supply by rainwater of their essential nutrients and water. And in Section 1.4 the close relationship between the isotopic composition of rainwater and climate variables, namely temperature and rainfall, has been demonstrated.

The organic components of living organisms are the sole contributors to peat deposits. All compounds biosynthesised in plants derive from photosynthesis:

$$CO_2 + H_2O + HDO \underset{\text{Dark}}{\overset{\text{Light}}{\rightleftharpoons}} \text{Organic matter} + O_2$$

The forward reaction is driven by light, whereas the reverse respiratory reaction occurs in darkness. Under the conditions present in the bog ecosystem the only source of deuterium and hydrogen for growing organisms is the bog water. Since *Sphagnum* plants lack stomata, they take up bog water without any discrimination or fractionation (Aravena and Warner, 1992). Thus, the organically bound hydrogen and deuterium should be correlated to the isotopic composition of the bog water. Schiegl (1972) was the first to recognize that the deuterium content of peat could be used as a palaeoclimate indicator. However, subsequent studies on the link between bulk hydrogen isotopic composition of peat and climate variables have been hampered by factors unrelated to climate, e.g. vegetation (for further discussion see Chapter 5).

With the development of the analytical capability of measuring δD values of nanogram quantities of individual compounds (compound-specific deuterium ratio mass spectrometry; see Chapter 4 & 7), new possibilities exist for investigating the relation between isotope values in peat and climate. If species-specific lipid biomarkers can be identified, than their individual δD values should reflect changes in climate, since species-specific fractionation effects during the biosynthesis of compounds can be minimised or even eliminated. The research presented in this thesis focuses on the hydrocarbon lipid components in ombrotrophic peat. The main reason for focusing on this group of components is their relatively high resistance to post-depositional microbial degradation, and the absence of exchangeable

hydrogens, which could complicate interpretations. As noted in Section 1.3.3, the hydrocarbon fraction is only a minor fraction of the total lipid content of peat forming plants; however they are linked with the major biochemical fractions through their biosynthesis (Kolattukudy, 1976), hence the trends in the δD values of hydrocarbons through the cores, if linked with climate, will reflect those of the other fractions.

The hypothesis of this thesis is then as follows:

δD Values of individual lipid biomarkers will reflect the isotopic composition of the source water, which in itself will reflect climatic conditions during growth and can be used to reconstruct past climatic conditions.

The aims of this thesis are to:

(i) Date a set of peat cores, thereby providing a framework for correlation with known climate records, documentary and previously developed proxies (Chapter 2).

(ii) Investigate the hydrocarbon lipid composition and identify specific lipid biomarkers for use as palaeoclimate proxies (Chapter 3).

(iii) Establish the instrumental parameters for a down-core compound-specific δD study of lipids in terms of sample size, linearity, precision and accuracy of the measurements (Chapter 4).

(iv) Determine compound-specific δD-values of the identified biomarkers, establishing a down-core profile for correlation with known climate records using a synchronous set of cores from two neighbouring bogs spanning the same time period (Chapter 5).

2 Sample Set Description and Dating

2.1 Introduction

Among all the systems presently used in the reconstruction of past climate, peat bogs occupy a special position. Peat bogs are formed by unique plant communities, which are not only strongly influenced by climatic variations, but also preserve a record of these variations. Peat bogs are especially interesting since many have developed during the Holocene period (last 11,200 years). Now that human influence is contributing to the changes in the climate system, it is important that scientists learn how to distinguish between natural and human factors. Ice cores and marine and lake sediments are widely used in such research. We now aim to add peat bogs as an additional setting from which to derive palaeoclimate records.

Peat is predominantly the remains of plants that once grew on the surface, but that have decayed incompletely due to the anoxic preservation conditions prevailing within the mire. Peat consists mainly of the remains of *Sphagnum* mosses and *Sedge* plants. These species continuously grow on top of one another, slowly dying off and being buried by new shoots. As a consequence of this burying process, the plant remains gradually accumulate in thick layers, and changes within their stratigraphy reflect past changes in vegetation cover. The replacement of species is mainly due to the sensitivity of all plants to their growth environment, and in particular the humidity. Such changes will be reflected in the changing plant communities on the peat bog surface and the changes in plant communities recorded by their macrofossil stratigraphic records with depth. This study hopes to extend the techniques used for studying these changes by adding compound-specific δD records as a new tool for palaeoclimate reconstruction.

The bogs chosen for this study (Bolton Fell Moss and Walton Moss) are ombrotrophic mires. The growth of their plant communities are closely coupled to atmospheric climate variables as they receive all their nutrients through deposition by precipitation (Chapter 1). The results of previous studies discussed in section 2.3, have indicated that the plant communities of both peat bogs exhibit a known relation with past climate. It is therefore logical that this study uses the same sites for which such correlations are known to exist.

In this chapter a detailed review will be given of the changing plant communities as analysed through their macrofossils and of the synchronicity of the records between both bogs. Besides these, dating of the cores was undertaken, so

that cores from both bogs could be matched with one another and correlated with previous studies. Later on in the thesis, discussions will be based on calibrated ages instead of burial depth.

2.2 Geographical setting of sample sites

2.2.1 Bolton Fell Moss

Bolton Fell Moss (BFM; National grid reference NY 495 695) is a large ombrotrophic mire located in Cumbria, Northern England (Figure 2.1). The bog covers an area of almost 365 ha and has a maximum depth in excess of 10 m. It forms part of the 'Border Mires', which comprise a collection of 48 mires located on the Scottish-English border, which collectively have a total of 955 ha of open bog vegetation (Mauquoy and Barber, 1999). Bolton Fell Moss is an example of a typical peat bog, having a raised central dome and an average depth of 6 meters. Presently, the bog is dominated by *Sphagnum* moss and its stratigraphy consists of horizontal swathes of peat of varying humification. There is a relatively low frequency of the high hummocks that represent climatically insensitive parts of the bog surface. Bolton Fell Moss exhibits a variety of taxa and niches, which are fundamental to recording climatic changes. Bolton Fell Moss is now subject to

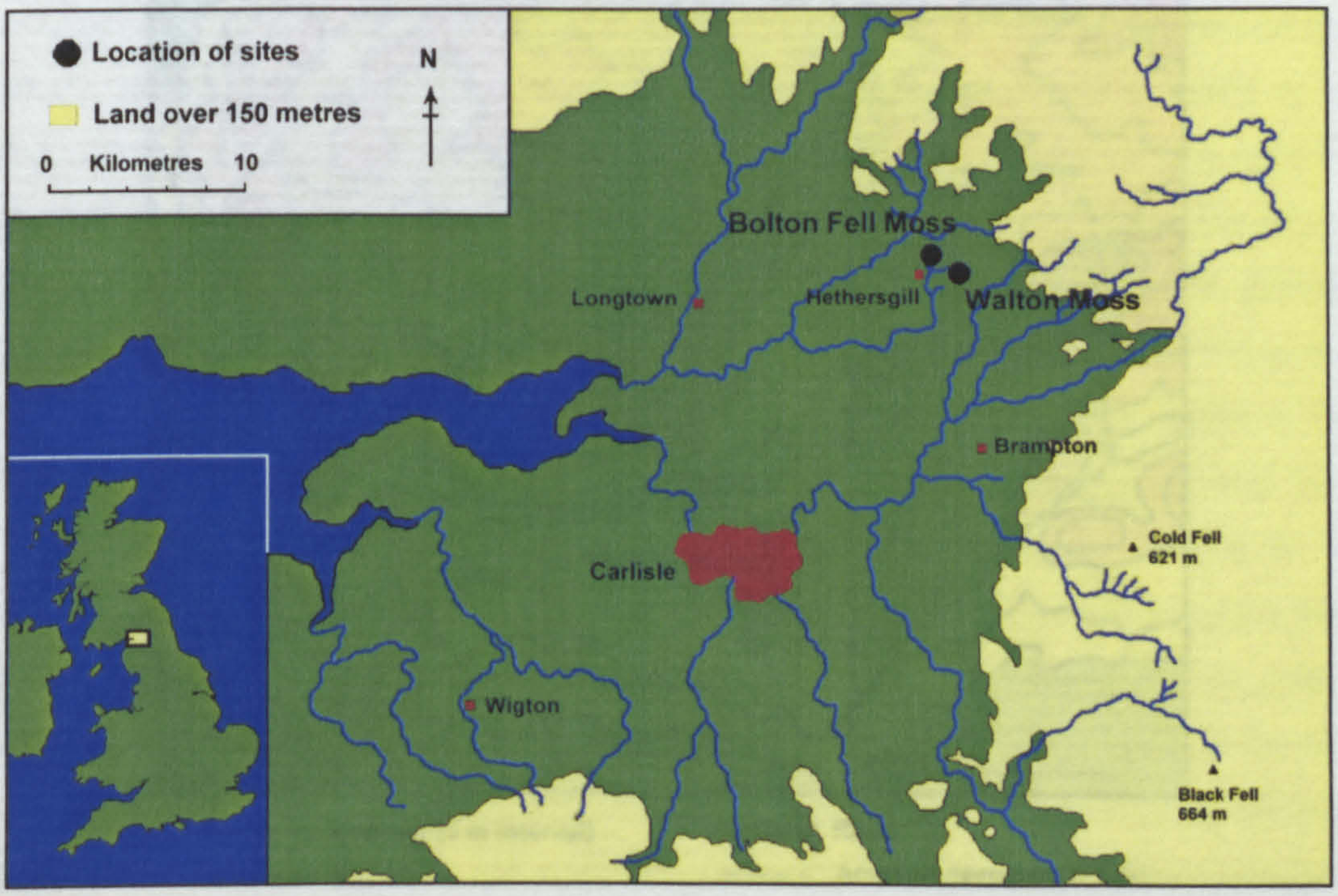

Figure 2.1. Location of Bolton Fell Moss and Walton Moss (Cumbria, UK).

extensive peat cutting and milling, but there remains a reserve area of bog (ca. 30 ha) over the deepest peat. This still has flourishing flora, but its surface is considerably more hummocky than when the bog was largely untouched in 1960 (Barber, 1981).

2.2.2 Walton Moss

Walton Moss (WM; NY 504667) is approximately 150 ha in area and is about 2.5 km south west of Bolton Fell Moss. They are separated from each other by a small valley and stream (Barber et al., 1998). The locations of both bogs are shown in detail in Figure 2.2. In contrast to Bolton Fell Moss, Walton Moss has only suffered very minor peripheral hand-cutting dating from the nineteenth century. It possesses a virtually intact rand, such that this bog is possibly the most intact ombrotrophic bog in the UK (declared a national nature reserve in 1997; Hughes et al., 2000). Both bogs have similar vegetation and both are classified as wet raised mire communities rich in *Sphagna*. Just like Bolton Fell Moss, the microtopography of the bog is very subdued. It has a range of only 30 cm or so on the occasional hummock and large lawn areas have relief differences of no more then 10 cm.

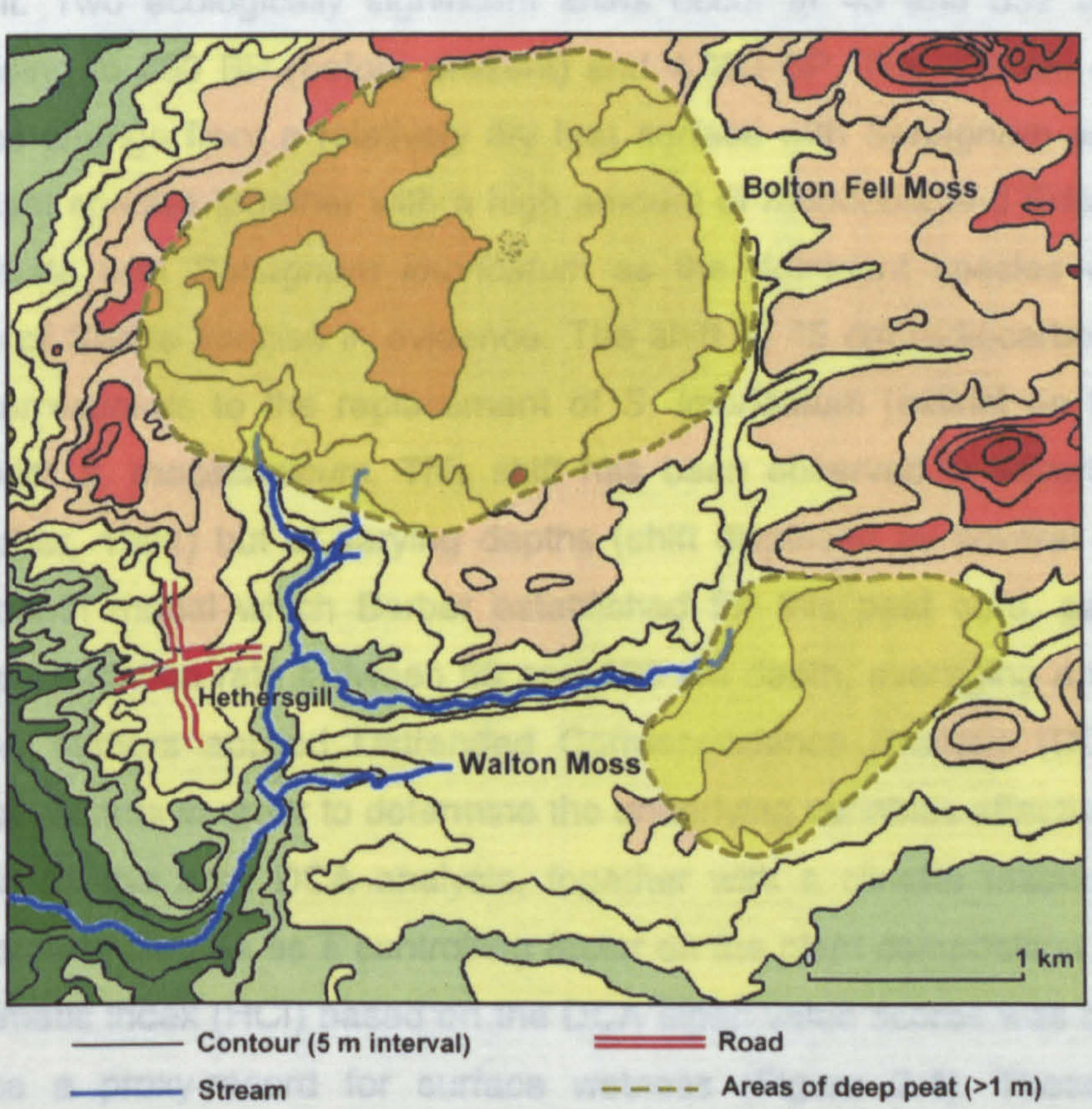

Figure 2.2. Local map of Walton Moss and Bolton Fell Moss (Hughes et al., 2000).

2.3 Previous studies

2.3.1 Bolton Fell Moss

Since the original study of Barber (1981) in which a full description of Bolton Fell Moss was given, several studies have used Bolton Fell Moss as a site from which to derive detailed climatic records. Two major techniques have been applied: (i) macrofossil analysis and the study of transects through the bog, and (ii) studies of the lipid composition of the peat bog, relating their abundance and isotope ratios to climatic events. In this section an overview of the results of these investigations will be given.

Macrofossil analyses have been successfully applied to the study of Bolton Fell Moss (Barber, 1994). In this study, a 5 m core was extracted from the bog and macrofossil analysis of the profile was undertaken every 4 cm on a 1 cm subsection (4 cm^3). Plant remains were identified using a ten-fold magnification and individual *Sphagna* taxa identified using a 400-fold magnification. The resulting macrofossil profile is given in Figure 2.3. The diagram is arranged as a hydrophilous sequence, with the unidentified organic matter (UOM) as the driest indicator.

These macrofossil profiles show changes in the relative proportions of each component. Two ecologically significant shifts occur at 45 and 332 cm depths, corresponding to 880 BP (before present) and 4,000 BP. The 332 cm depth shift records the change from a relatively dry bog surface with *Sphagnum acutifolia* as the dominant species together with a high amount of *monocots* and *Ericaceae* to a wetter climate with *Sphagnum imbricatum* as the dominant species with a low proportion of *Sedge* species in evidence. The shift at 45 cm radiocarbon dated to 880 BP corresponds to the replacement of *S. imbricatum* (extinct on the bog at present) with *S. magellanicum*. This shift has been observed in several different cores (Barber, 1981) but at varying depths (shift displaced by several centuries). The age-depth model which Barber established for this peat core, gave a very uniform accumulation rate between 50 and 500 cm depth, averaging around 12 yr cm^{-1}. The authors applied Detrended Correspondence Analysis (DCA) to the macrofossil records in order to determine the underlying variables affecting the plant succession on the bog. DCA analysis, together with a climate response model, revealed climate change as a controlling factor on the plant composition in the bog. A hydroclimatic index (HCI) based on the DCA eigen value scores was constructed to produce a proxy-record for surface wetness (Figure 2.4). These analyses demonstrated BFM to be particularly responsive to climatic change.

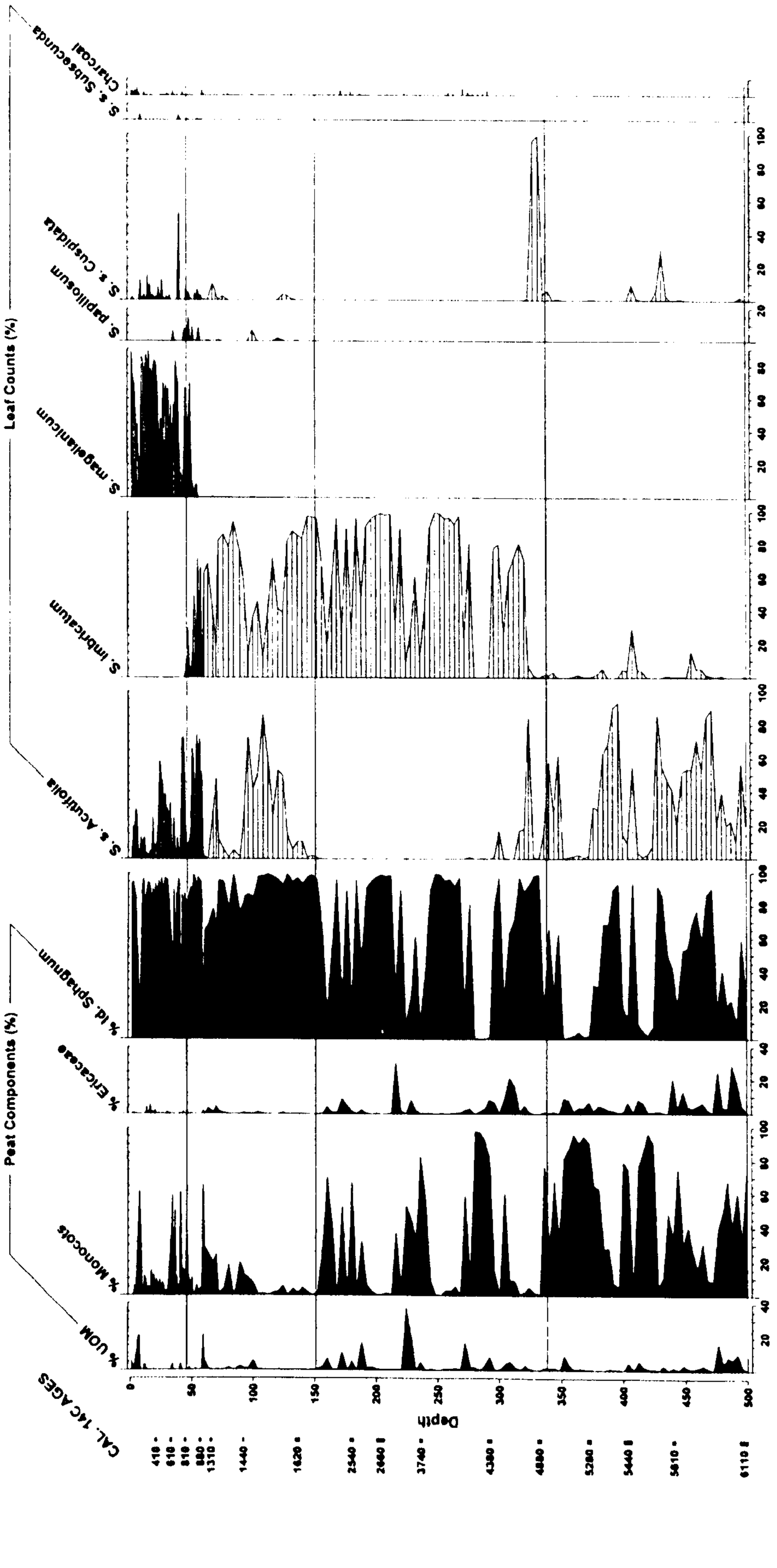

Figure 2.3. Macrofossil data of Bolton Fell Moss (Barber et al., 1994), showing the succession of plants with time influenced by wet/dry shifts on the bog. The peat components are derived from averaged quadrat counts under low power (*10) magnification, the leaf counts are a breakdown of per cent Identifiable *Sphagnum* and consists of proportions based on a random selections of leaves (>100 per sample interval) identified at high magnification (*400); UOM = unidentified organic matter.

A more recent study tested the replicability and variability of the macrofossil record within the bog (Barber et al., 1998). In this study several cores and monoliths were taken from Bolton Fell Moss and Walton Moss (discussion, see Section 2.3.2). The cores investigated by Barber were compared with the macrofossil profiles obtained from previous profiles. The investigation of a number of cores sampled along a transect indicated three stages in the development of the bog:

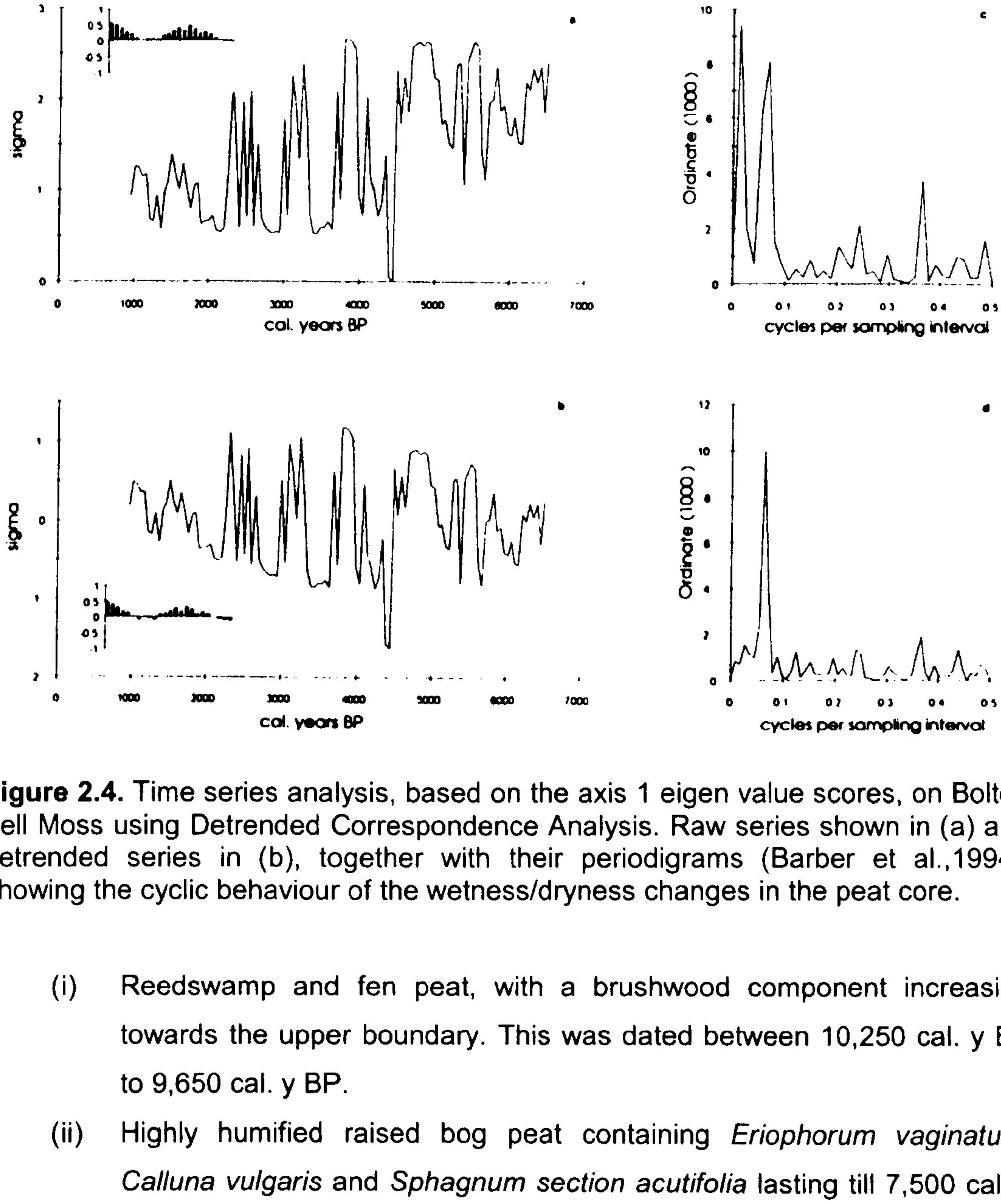

Figure 2.4. Time series analysis, based on the axis 1 eigen value scores, on Bolton Fell Moss using Detrended Correspondence Analysis. Raw series shown in (a) and detrended series in (b), together with their periodigrams (Barber et al.,1994), showing the cyclic behaviour of the wetness/dryness changes in the peat core.

(i) Reedswamp and fen peat, with a brushwood component increasing towards the upper boundary. This was dated between 10,250 cal. y BP to 9,650 cal. y BP.

(ii) Highly humified raised bog peat containing *Eriophorum vaginatum*, *Calluna vulgaris* and *Sphagnum section acutifolia* lasting till 7,500 cal. y BP.

(iii) Fresh *Sphagnum* peat. This was found in all cores and often with remarkable purity (up to 90% remains of *Sphagna*) and displays a horizontally layered stratigraphy visible for hundreds of metres.

Comparison of different cores revealed a similar pattern in the succession of different species of *Sphagnum*. The decline and extinction of the dominant Holocene taxa (*S. imbricatum*) was dated around 1300 to 1800 AD over the bog, possibly corresponding to the advent of the Little Ice Age, a wetter period starting around 1300-1400 AD. The observed shifts were explained as a climatically forced response due to changing hydrological conditions within the bog. All profiles displayed wetter plant assemblages at about 1300-1400 AD, during the 1600s and between 1750 and 1800, times characterised by wet summers with low temperatures (Lamb, 1977). The main problem in replicate analyses was obtaining accurate chronologies for the different cores.

Nott and Avsejs obtained molecular and stable isotopic stratigraphies from Bolton Fell Moss (Nott, 2000; Nott et al., 2000; Xie et al., 2000; Avsejs, 2001; Avsejs et al., 2002; Xie et al., in press). These authors studied one 40-cm monolith and a core of 250 to 500 cm depth (this section was also investigated in this thesis for its compound-specific δD record). In the first part of their study, they investigated the lipid composition of peat in a 40-cm monolith, which was ^{210}Pb dated and shown to range from 1770 to present (Nott et al., 2000; Xie et al., 2000; Xie et al. in press). This study yielded the following major conclusions:

(i) The abundance of the almost exclusively *Sphagnum* derived *n*-tricosane (C_{23} straight chain alkane), expressed as a ratio of *n*-C_{23} against *n*-C_{31} reflected changes in the plant community (Nott et al., 2000; Xie et al., in press), which correlated with recorded cooler growing season temperatures.

(ii) A suite of biomarkers for sedge plants, 5-*n*-alkyl resorcinols, showed an inverse correlation with climate (Avsejs et al., 2002).

(iii) Compound-specific δ^{13}C and δD isotope ratios reflected changes in climate and vegetation types (Xie et al., in press).

Figure 2.5 shows the abundances and δD values of the *n*-tricosane compared with temperature and rainfall. This study served as pilot study for this thesis and showed for the first time a correlation between δD values and *n*-C_{23}/*n*-C_{31} abundances and temperature and rainfall (Xie et al., 2000).

A down-core study between 250 and 500 cm was also performed, with the above conclusions being largely sustained, although several noticeable differences with the macrofossil record were found. The conclusions from this second study were:

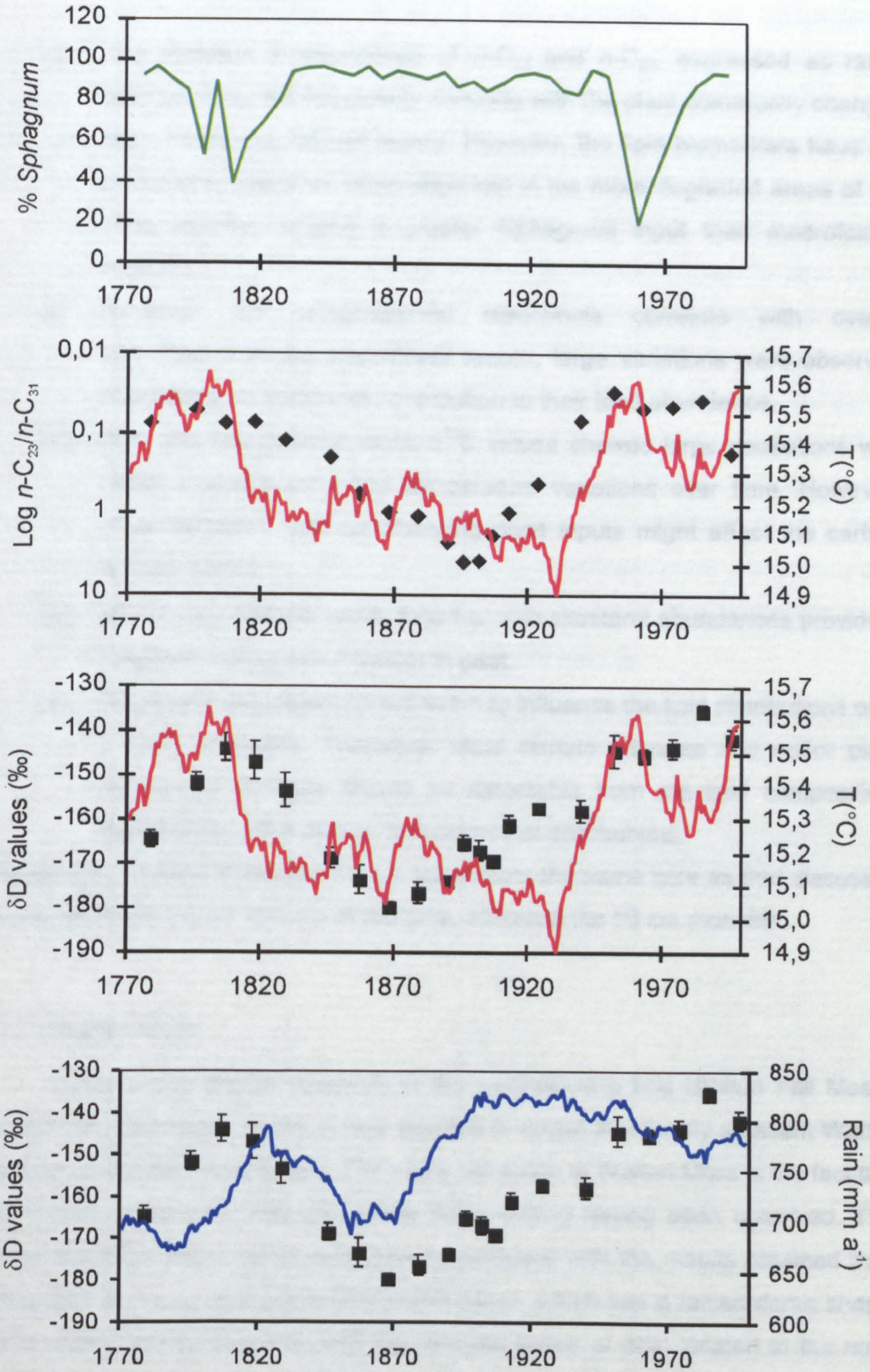

Figure 2.5. Profile showing the temporal variations of the biomarker (*n*-tricosane) abundance (♦; expressed as log n-C_{23}/n-C_{31}) and compound-specific δD values (■) correlating with temperature (red), rainfall (blue) and the macrofossil record (green) (after Xie et al., 2000).

(i) The variation in abundance of *n*-C_{23} and *n*-C_{25}, expressed as ratios against *n*-C_{31}, did not closely correlate with the plant community changes seen in the macrofossil record. However, the lipid biomarkers have the potential to preserve information lost in the more degraded areas of the core, usually implying a greater *Sphagnum* input than macrofossils indicate.

(ii) Although the sedge-specific resorcinols correlate with overall abundances in the macrofossil record, large variations were observed suggesting an additional contribution to their total abundance.

(iii) Bulk and compound-specific $\delta^{13}C$ values showed large oscillations with depth, possibly indicating temperature variations over time. However, other variables such as changing plant inputs might affect the carbon isotope record.

(iv) $\beta\beta/(\alpha\beta+\beta\beta)$ hopane ratios, together with sitosterol abundances provide a long-term diagenetic indicator in peat.

(v) Diagenetic processes do not seem to influence the lipid distributions over a short timescale. Therefore, rapid climate changes and major plant community changes should be detectable from the lipid composition, especially in the *n*-alkane and resorcinol distributions.

The samples studied in this thesis, are taken from the same core as that discussed above, spanning the full 500 cm of the core, including the 50 cm monolith.

2.3.2 Walton Moss

Since the extensive research in the neighbouring bog (Bolton Fell Moss), yielded very promising results, it was decided to target the closely adjacent Walton Moss for additional investigation. The major attraction of Walton Moss is the fact that it is almost untouched, with only minor hand cutting having been observed. This makes the latter site a prime candidate to compare with the results obtained from Bolton Fell Moss. In contrast to Bolton Fell Moss, which has a raised dome shape, Walton Moss is asymmetrical, with the deepest layers of peat located to the north east of the present centre of the bog. The decline of *Sphagnum imbricatum*, the main Holocene species, was also dated at around 1300 AD, with surviving pocket habitats until 1800 AD. The major species currently present is also *Sphagnum magellanicum*.

The first study published on Walton Moss investigated the replicability of records between the Walton and Bolton Fell Moss sites (Barber et al., 1998). The macrofossil and pollen records from the two were in good agreement. The same three stages as for Bolton Fell Moss could be observed (reedswamp and fen peat, highly humified peat and fresh *Sphagnum* peat; Section 2.3.1).

This study demonstrates the almost universal shifts noticeable in the cores. Even if not all transitions occur at the same time, a carefully chosen location of the cores could provide a representative profile, valid for the entire bog. In a second study (Hughes et al., 2000), a full 10-m core of Walton Moss was analysed. The macrofossil record for this core is shown in Figure 2.6. The age-depth model for this core provided an accumulation rate of 10.3 y cm^{-1}, which agrees well with the previously observed accumulation rates of Bolton Fell Moss. The study also demonstrated that wet shifts occur in both bogs, as summarised in Table 2.1. Since the establishment of the *Sphagnum* phase around 7,800 BP, shifts are more or less simultaneously recorded in both bogs, with a 100 and 600 year periodicity in the climate reconstruction inferred from the macrofossil records.

Table 2.1. Comparison of known wet shifts in Bolton Fell Moss and Walton Moss, inferred by Detrended Correspondence Analysis of macrofossil data (dates are in years BP).

Bolton Fell Moss (BFM)			Walton Moss (WM)
Barber, 1981	Stoneman et al. (1993)	Barber et al., 1994	Hughes et al.(2000)
c. 200	c. 350		c. 100
c. 500			c. 300-350
c. 1000			
		c. 1300	c. 1450
			c. 1650-1750
	c. 2400	c. 1900-2200	c. 2100-2140/2320
	c. 3100	c. 2650-2900	c. 2600-2680/3170
	c. 3550	c. 3300-3600	c. 3500
		c. 4000-4350	c. 3800-3990/4410
			c. 4900-5300
			c. 6800-7800

The results of another recent study by Mauquoy and co-workers (2002a) compared Walton Moss to a bog in Denmark (Lille Vildmose). Both bogs are remarkably intact and posses abundant *S. magellanicum*. Short, 90-cm cores were studied from both bogs. The Walton Moss core was radiocarbon dated and wiggle matched to obtain a precise chronology, with the wet shifts (1215; 1464; 1601 AD) corresponding to the Wolf, Spörer and Maunder minima for solar activity, suggesting a possible link between the solar activity and climate signals in peat bogs.

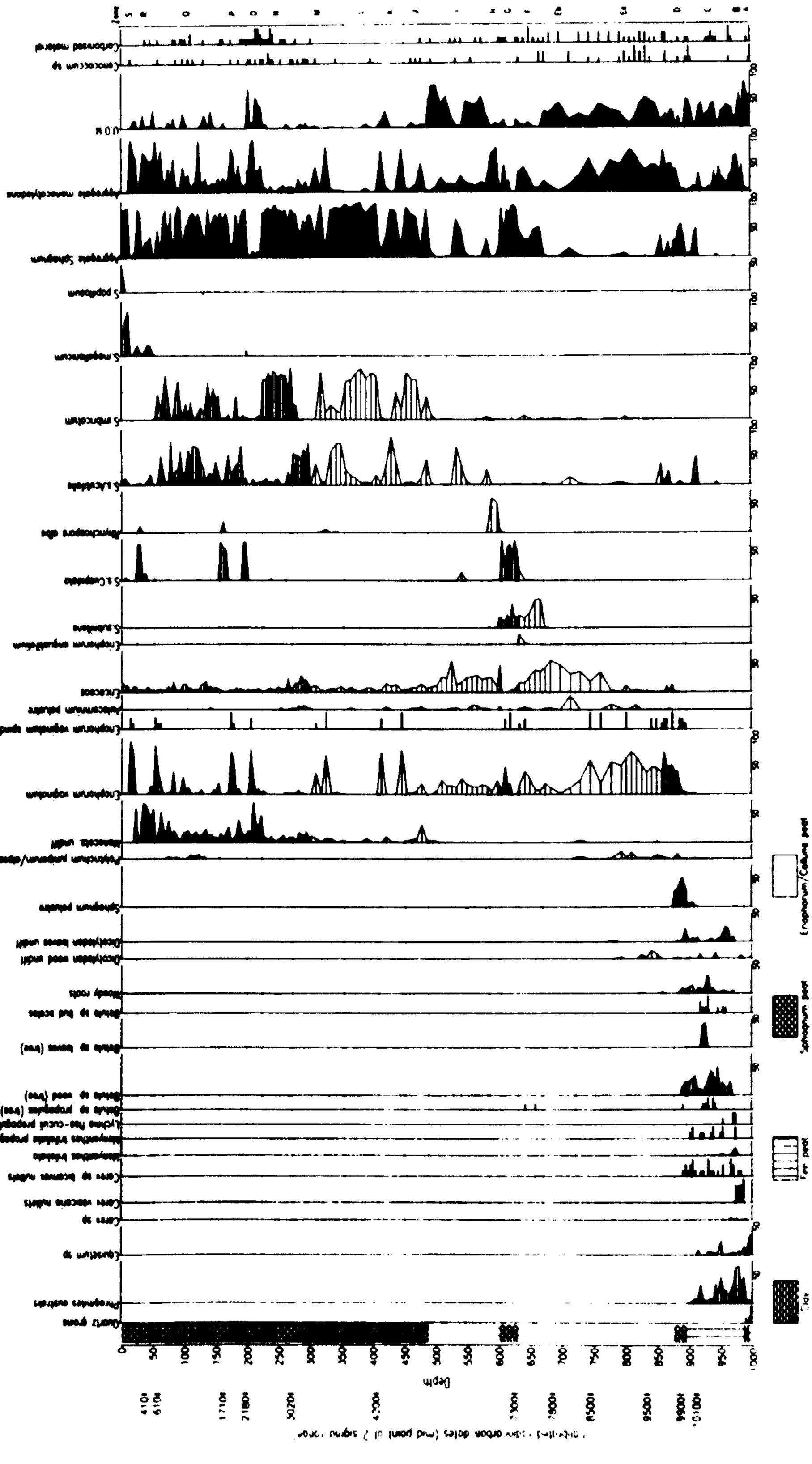
Depth
Figure 2.6. Macrofossil data from Walton Moss (Hughes et al., 2000).

The most recent of the studies published also used the above sites; however, three replicate cores of Walton Moss were used (Mauquoy et al., 2002b). Radiocarbon dates, macrofossil profiles and humification indices were all investigated. From pollen analysis a period of low agricultural activity from about 1000 to 1200 AD, corresponding to the Medieval warm period (low precipitation, dry bog surface) was noted. The wet shifts observed in this latest study confirmed previous findings.

2.4 Dating of cores

2.4.1 ^{210}Pb dating

2.4.1.1 Introduction

In order to allow down-core profiles of different cores to be compared with one another and with historical records, it is essential to date the cores. Historical records only span the last 200 years and as such an accurate dating method for the last 200 years has to be used. Due to the large errors involved in ^{14}C dating recent samples, a well-established alternative is ^{210}Pb dating. The ^{210}Pb is derived from the decay of ^{222}Rn following the decay of ^{226}Ra from ^{230}Th. Both ^{226}Ra and ^{222}Rn escape

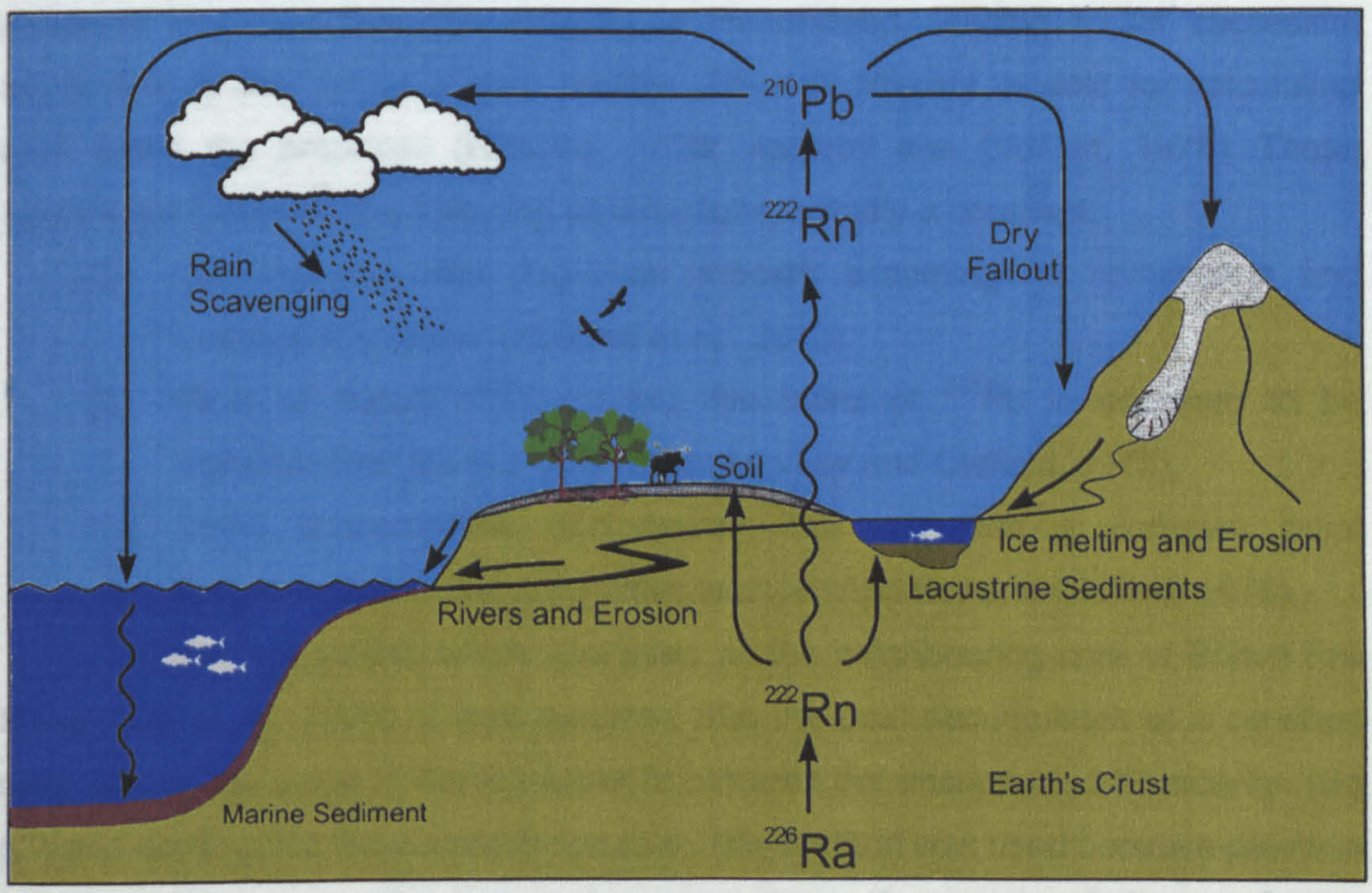

Figure 2.7. Schematic diagram of the ^{210}Pb global cycle (after Bradley, 1999).

from the Earth's surface and enter the atmosphere, where the ^{210}Pb is eventually produced. ^{210}Pb is then washed out of the atmosphere by precipitation or settles out as dry fall-out, where it accumulates in sedimentary deposits and decays (with a half-life of ca. 22 years) to stable ^{206}Pb. Assuming that the atmospheric flux of ^{210}Pb is constant, the decay rate of ^{210}Pb to ^{206}Pb with depth can be used to date sediment accumulation rates (Appleby and Oldfield, 1978; Figure 2.7). Due to its short half-life ^{210}Pb is only of value in dating sediments over the last 200 years; however, this is of particular value in isolating core-top floral and faunal elements for calibration with instrumental climatic data to derive accurate transfer functions for palaeoclimatic reconstructions. ^{210}Pb dating has been used to determine the accumulation rates of ombrotrophic peat (El-Daoushy et al., 1982; Mackenzie et al., 1998; Xie et al., 2000).

The total ^{210}Pb ($t_{1/2}$ = 22.26 years) is measured using its granddaughter ^{210}Po ($t_{1/2}$= 138 days). ^{210}Po is assumed to be in equilibrium with ^{210}Pb in all but the surface slice. It reaches equilibrium in about 2 years. The total ^{210}Pb of the samples comprises ^{210}Pb of atmospheric origin, the so-called unsupported ^{210}Pb and an additional in-situ component, which is produced from ^{226}Ra, the supported ^{210}Pb. The supported ^{210}Pb may not always be in equilibrium and a correction must be applied (El-Daoushy et al., 1982). Although questions relating to the mobility and retention of lead in peat samples have been posed (Urban et al., 1990), it is generally assumed that the majority is immobilised, leading to its successful application to the dating of peat profiles. Several different models for calculating peat dates are proposed (Robbins, 1978; Appleby and Oldfield, 1978). These models are based on the following assumptions, namely a constant:

(i) Accumulation rate (log-linear model); assuming no compaction and uniform deposition (Kotarba et al., 2002)

(ii) Rate of supply (CRS-model); the influx of ^{210}Pb is assumed to be constant over the last 200 years (Appleby and Oldfield, 1978).

(iii) Initial concentration (CIC-model); this assumes a constant initial concentration of the radioactive isotope (Appleby and Oldfield, 1978).

In the first model, which was used on the neighbouring core of Bolton Fell Moss, (Xie et al., 2000), it was assumed that the peat accumulates at a constant rate, so that the slope of the log-linear fit between the unsupported Pb activity (Bq g^{-1}) and depth gives the accumulation rate. This method was used because previous studies on the sample sites indicated a reasonably uniform accumulation rate for the bogs (Barber et al., 1994; Hughes et al., 2000).

The CRS-model is the most robust model (Appleby and Oldfield, 1978). It takes into account the different accumulation rates and the compaction of buried peat due to overburden. As such, this model will accurately reflect the post-deposition changes occurring in the bog and provide a true age estimate. The model has been successfully applied to dating peat samples (El-Daoushy et al., 1982; Appleby et al., 1997; Mackenzie et al., 1998) and is generally regarded as the best model. In this model dates are derived using the following formula:

$$t=(1/\lambda)*Ln(A_c(0)/A_c(X)).$$

With λ = 0.03114 (decay constant for ^{210}Pb)

$A_c(O)$ = cumulative specific activity (Bq cm^{-2})

$A_c(X)$ = cumulative activity below depth X (Bq cm^{-2})

Provided that a steady state exists between atmospheric supply and the radioactive decay, the influx of ^{210}Pb can be calculated using $^{210}Pb_{flux}= \lambda*A_c(O)$.

In the third model (Appleby and Oldfield, 1978), it is assumed that the initial concentration of ^{210}Pb in a sample has a constant initial concentration, despite the changes in accumulation rate and compactation that might occur. The age of a given sample is given by the formula:

$$t = (1/\lambda)*ln(C(O)/C(X))$$

With λ = 0.03114 (decay constant ^{210}Pb)

C(0) = initial concentration (Bq g^{-1})

C(X) = concentration on depth X (Bq g^{-1})

Since the initial concentration will increase with compaction, the deepest samples will be estimated to be younger then their real date. All three models will be evaluated and the most appropriate model used.

2.4.1.2 ^{210}Pb Dating of monolith samples

Lead dates were obtained from three different peat monoliths. These included one from Walton Moss (WM) and two from Bolton Fell Moss (BFM and BFX). One of the monoliths from Bolton Fell Moss (BFX; Xie et al., 2000; Nott, 2000; Nott et al., 2000; Xie et al., in press), previously dated using the constant accumulation model, has been reassessed to enable comparison between the previously published study and the results presented in this thesis. In all models the supported ^{210}Pb activity is estimated at 0.01 Bq g^{-1} and subtracted from the measured activity. No other previously published ^{210}Pb dated cores are known from these sample sites. In all three monoliths unsupported lead activities were very similar ranging between 60 and 100 Bq kg^{-1}, with unsupported levels reaching depths between 25 cm depth (BFX) to 39 cm depth (BFM). Logarithmic plots of the

^{210}Pb activity versus depth for all monoliths are presented in Figure 2.8. BFM and WM show similar behaviour characterised by a gradual decline in ^{210}Pb activity from 0 to 20-30 cm depth followed by a steepening of the curve, while BFX displays an irregular accumulation. Estimates of the ^{210}Pb activity of the top centimetre for the log-linear and CIC model were obtained using the intercept point of a log-linear trendline through the top 20 cm of each core, in order to obtain the initial concentration of ^{210}Pb.

Constant accumulation rate model (log-linear model)

Table 2.2 displays the age determinations for all three cores. The estimates are based on the slope of the natural logarithmic of the unsupported ^{210}Pb activity versus depth (Figure 2.8). This gave largely different values; core BFX and WM were of the same order, namely 4.9 and 4.6 y cm^{-1}, while core BFM gave a significantly lower rate (2.9 cm y^{-1}). These values appear to fit with the physical appearance of the monoliths, the latter appearing much better preserved than BFX and WM.

Constant initial concentration model (CIC)

The dates based on the CIC model are given in Table 2.3. As assumed, and noted by previous authors (Appleby and Oldfield, 1978; El-Daoushy et al., 1982; Mackenzie et al., 1998), this dating model tends to give rather erratic results; for example, the top 5 cm appears to be older than the next lower sample. It is also clear from their distribution that this model is fundamentally flawed, since it does not take into account the gradual compaction of the samples or differences in bulk density due to differences in plant input and, consequently, do not generate a constantly declining curve. Therefore, the model cannot be used for dating peat cores. These problems are illustrated in Figure 2.9, where all dating models are compared. The CIC model shows a non-uniform decline, inconsistent with the gradual degradation and compaction expected in decaying peat. Mass accumulation rates for the last 100 years are opposite to those obtained by the log-linear model, with all values falling in the same range, and no evidence of the doubling of the accumulation rate of BFM compared to BFX being revealed, hereby confirming that this model is unusable.

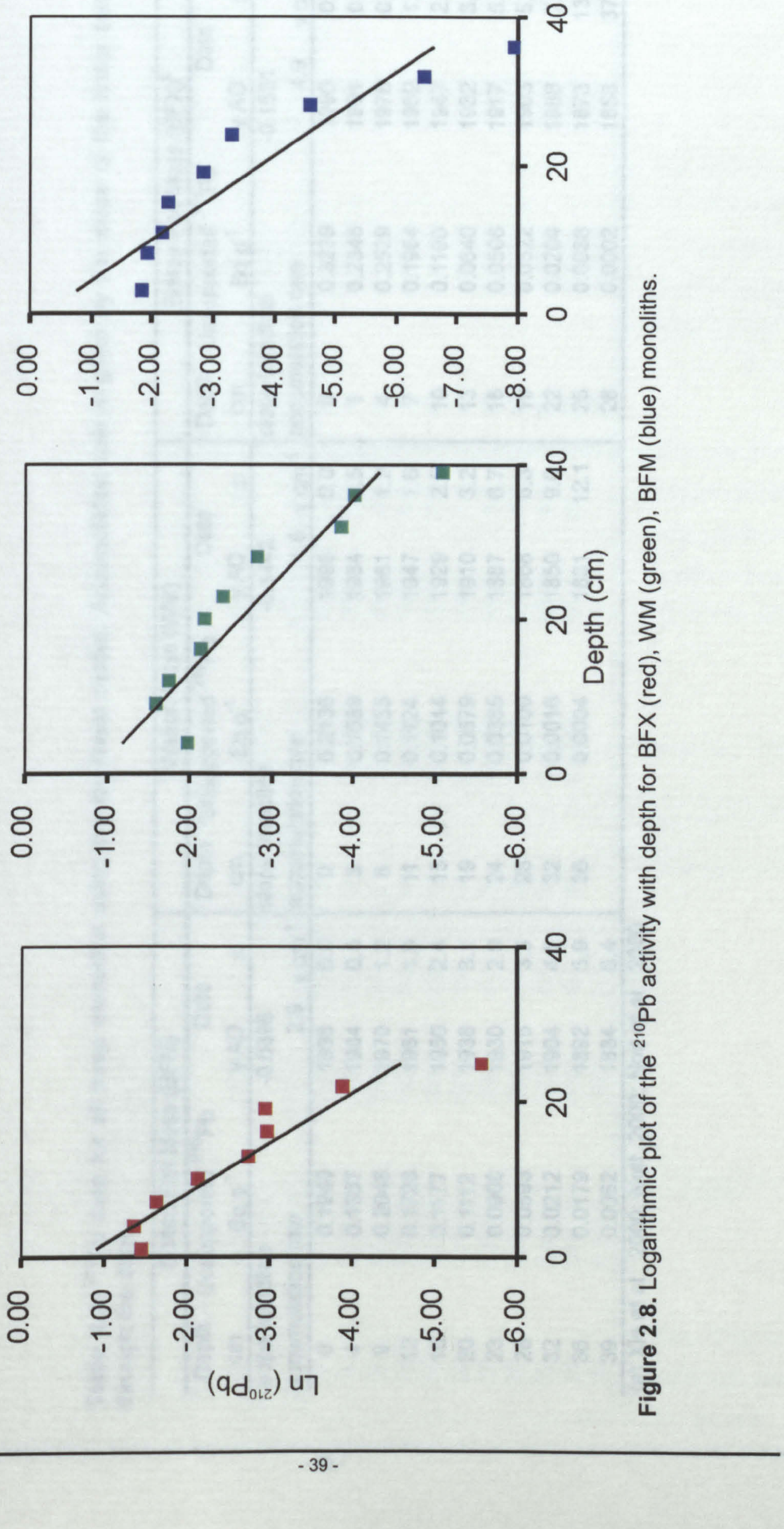

Figure 2.8. Logarithmic plot of the ^{210}Pb activity with depth for BFX (red), WM (green), BFM (blue) monoliths.

Table 2.2. ^{210}Pb data for all three monoliths using the log-linear model. Accumulation rate is given by the slope of the linear trendline through the data.

Bolton Fell Moss (BFM)				Walton Moss (WM)				Bolton Fell Moss (BFX)[a]			
Depth cm	Unsupported ^{210}Pb Bq g^{-1}	Date y AD	±	Depth cm	Unsupported ^{210}Pb Bq g^{-1}	Date y AD	±	Depth cm	Unsupported ^{210}Pb Bq g^{-1}	Date y AD	±
slope trendline		-0.0896		slope trendline		-0.1442		slope trendline		-0.1531	
accumulation rate		2.9	y cm^{-1}	accumulation rate		4.6	y cm^{-1}	accumulation rate		4.9	y cm^{-1}
0	0.1940	1996	0.0	0	0.2136	1998	0.0	0	0.3239	1996	0.0
4	0.1387	1984	0.5	3	0.1589	1984	0.5	1	0.2348	1991	0.2
9	0.2048	1970	1.2	8	0.1455	1961	1.2	4	0.2529	1976	0.8
12	0.1728	1961	1.9	11	0.1124	1947	1.6	7	0.1964	1962	1.5
16	0.1177	1950	2.4	15	0.1044	1929	2.5	10	0.1190	1947	2.1
20	0.1112	1938	3.1	19	0.0579	1910	3.2	13	0.0640	1932	3.4
23	0.0900	1930	2.9	24	0.0365	1887	6.7	16	0.0508	1917	5.4
28	0.0593	1915	3.3	28	0.0100	1868	6.3	19	0.0522	1903	5.6
32	0.0212	1904	4.5	32	0.0016	1850	9.0	22	0.0204	1888	7.1
36	0.0179	1892	5.9	36	0.0004	1831	12.1	25	0.0038	1873	13.2
39	0.0062	1884	6.4					28	0.0002	1858	37.3

(a) Xie et al., 2000; Nott, 2000; Nott et al., 2000

Table 2.3. ^{210}Pb data for all three monoliths calculated using the constant initial concentration model (CIC). Accumulation rates quoted are calculated over the last 100 years.

Bolton Fell Moss (BFM)				Walton Moss (WM)				Bolton Fell Moss (BFX)[a]			
Depth cm	Unsupported ^{210}Pb Bq g^{-1}	Date y AD	±	Depth cm	Unsupported ^{210}Pb Bq g^{-1}	Date y AD	±	Depth cm	Unsupported ^{210}Pb Bq g^{-1}	Date y AD	±
Average accumulation rate over last 100 years		0.0109	g cm^{-2}y^{-1}	Average accumulation rate over last 100 years		0.0136	g cm^{-2}y^{-1}	Average accumulation rate over last 100 years		0.0115	g cm^{-2}y^{-1}
0	0.1940	1996	0.0	0	0.2136	1998	0.0	0	0.3239	1996	0.0
4	0.1387	1985	0.5	3	0.1589	1987	0.4	1	0.2348	1986	0.4
9	0.2048	1998	0.1	8	0.1455	1984	0.4	4	0.2529	1988	0.3
12	0.1728	1992	0.2	11	0.1124	1975	0.7	7	0.1964	1980	0.7
16	0.1177	1980	0.8	15	0.1044	1973	0.8	10	0.1190	1964	1.4
20	0.1112	1978	1.0	19	0.0579	1954	1.6	13	0.0640	1944	2.8
23	0.0900	1971	1.1	24	0.0365	1939	3.5	16	0.0508	1937	4.1
28	0.0593	1958	1.6	28	0.0100	1898	4.8	19	0.0522	1937	3.5
32	0.0212	1925	3.4	32	0.0016	1838	9.7	22	0.0204	1907	5.8
36	0.0179	1920	4.3	36	0.0004	1791	15.1	25	0.0038	1853	15.4
39	0.0062	1885	6.3					28	0.0002	1751	66.4

(a) Xie et al., 2000; Nott, 2000; Nott et al., 2000

Constant rate of supply model (CRS)

This model should account for the various stages of the peat accumulation. The data given in Table 2.5 shows a gradual increase in compaction (more years per centimetre) with depth. It is also clear that this model gives the most accurate estimates of the sample age despite the larger standard errors. In this model, the accumulation rate for monolith BFM is twice that of BFX, correlating with the noticeable absence of advanced decay in the BFM monolith. The influx of ^{210}Pb into the bogs (67 and 71 Bq cm^{-2} y^{-1} per liter of rainfall), assuming an average yearly rainfall of 791 mm per year (Jones, 1983; Tabony, 1980, year books Meteorological library, Bracknel, UK) is within the limits of the UK average of 77 ± 14 Bq cm^{-2} y^{-1} (Table 2.4).

In the top 20 to 30 cm only a very gradual increase in age is observed, after which a pronounced steepening of the curve is apparent (Figure 2.9). This corresponds to the acrotelm/catotelm boundary in peat deposits. From previous studies (Okland and Ohlson, 1998) this boundary usually exists between 20 and 40 cm depth, and is in BFM and WM dated at around 100-150 years before present. Also of note are the larger errors inherent in the method.

Table 2.4. Yearly flux of ^{210}Pb calculated over the last 150 years compared with previously determined Cumbria and UK averages.

	Inventory of ^{210}Pb Bq cm^{-1}	^{210}Pb Flux Bq cm^{-2} y^{-1}	^{210}Pb flux per liter rainfall[a] Bq cm^{-2} y^{-1}
Bolton Fell Moss			
BFM	2032	63	80
BFX[b]	1362	42	54
Average	1697	52.5	67
Walton Moss			
WM	1801	56	71
Cumbria[c]			73
UK[c]			77

(a) yearly rainfall in Carlisle (average last 150 years): 791 mm y^{-1} (Jones, 1983)
(b) Xie et al., 2000; Nott, 2000; Nott et al., 2000
(c) Smith et al., 1997

Comparison of all dating models in Figure 2.9 leads to the conclusion that for the dating of peat monoliths only the constant rate of supply model fulfills all the criteria outlined in the above section. A gradual increase of age with depth, as well

Table 2.5. ^{210}Pb data for all three monoliths calculated using the constant rate of supply model (CRS). Accumulation rates calculated over the last 100 years.

Bolton Fell Moss (BFM)				Walton Moss (WM)				Bolton Fell Moss (BFX)[a]			
Depth cm	Mass accumulation rate g cm^{-2} y^{-1}	Date y AD	±	Depth cm	Mass accumulation rate g cm^{-2} y^{-1}	Date y AD	±	Depth cm	Mass accumulation rate g cm^{-2} y^{-1}	Date y AD	±
Average accumulation rate over last 100 years		0.0281	g cm^{-2} y^{-1}	Average accumulation rate over last 100 years		0.0229	g cm^{-2} y^{-1}	Average accumulation rate over last 100 years		0.0148	g cm^{-2} y^{-1}
0		1996	0.0	0		1998	0.0	0		1996	0.0
4	0.0147	1990	0.4	3	0.0113	1989	0.4	1	0.0058	1992	0.4
9	0.0099	1983	0.9	8	0.0124	1977	1.2	4	0.0054	1982	1.6
12	0.0118	1977	1.3	11	0.0160	1967	1.9	7	0.0069	1968	3.1
16	0.0173	1966	2.0	15	0.0172	1952	3.1	10	0.0114	1952	4.8
20	0.0183	1954	3.0	19	0.0311	1931	4.9	13	0.0213	1937	6.6
23	0.0226	1942	4.0	24	0.0493	1898	9.0	16	0.0268	1924	8.8
28	0.0343	1916	6.6	28	0.1808	1851	14.4	19	0.0261	1904	12.8
32	0.0958	1888	9.6	32	1.1478	1790	22.1	22	0.0666	1867	19.6
36	0.1135	1858	16.4	36	5.0188	1707	63.3	25	0.3600	1801	41.0
39	0.3289	1814	29.9					28	7.7492	1675	156.6

(a) Xie et al., 2000; Nott, 2000; Nott et al., 2000

as a difference in accumulation rate between the catotelm and acrotelm sections of the peat bog is accounted for. The upper 20-30 cm could be dated with the log-linear model, but extrapolation below the acrotelm leads to large errors in the dating and invalidates any comparison with historical records.

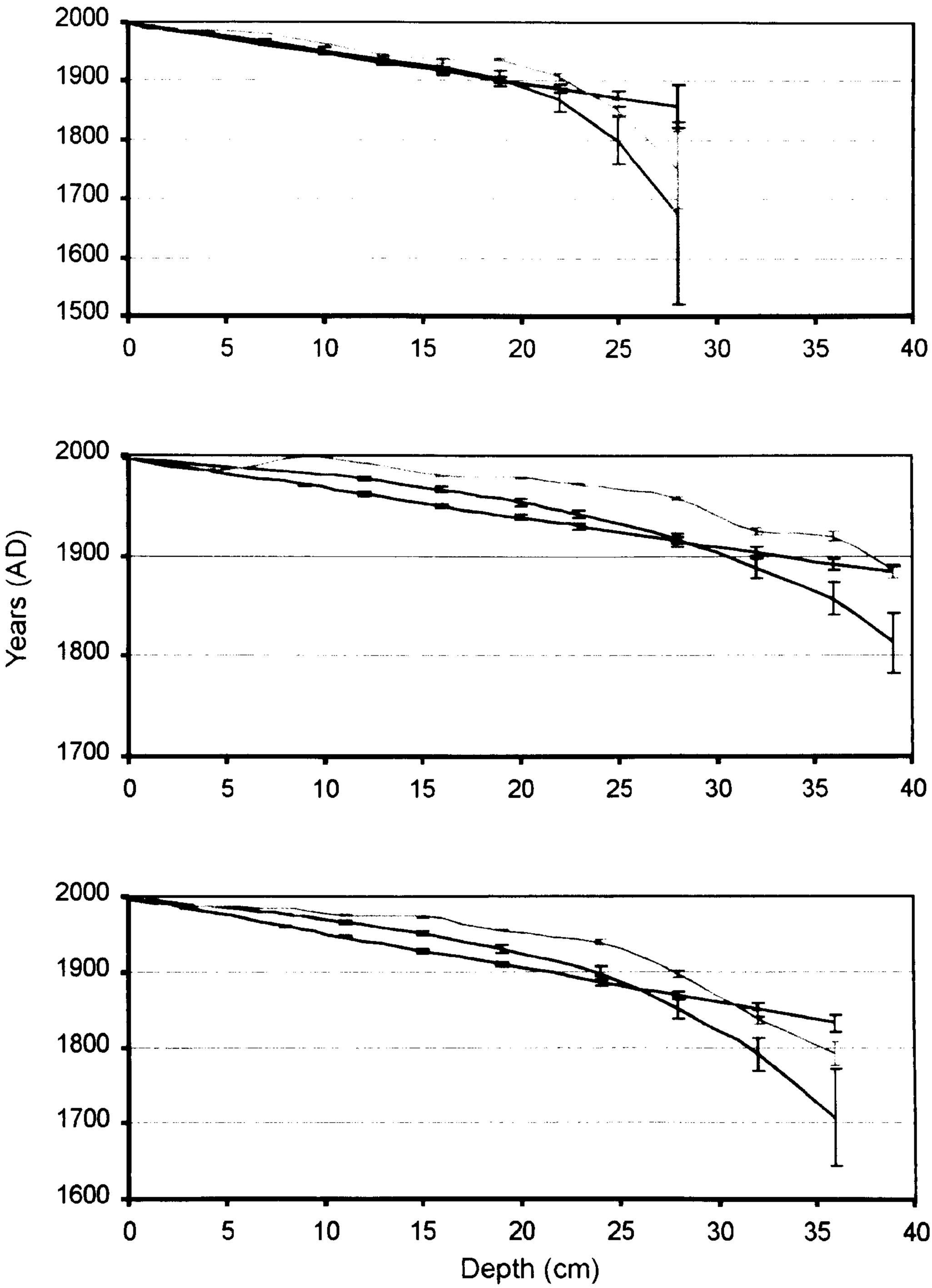

Figure 2.9. Comparison of all three dating models for each monolith. (a) BFX; (b) BFM, and (c) WM and within each graph: log-linear- (blue line), CIC- (green line), and CRS-dating model (red line).

2.4.2 Radiocarbon dating

2.4.2.1 Introduction

This is one of the earliest dating methods developed and is the most widely used dating method for Holocene samples. Radiocarbon is produced in the upper atmosphere by neutron bombardment of atmospheric nitrogen atoms. The carbon atoms are rapidly oxidized to CO_2, becoming mixed throughout the atmosphere and absorbed into the biosphere. In other words, ^{14}C, which is continually being produced in the upper atmosphere, becomes stored in various global reservoirs. Plants and animals assimilate a certain amount of ^{14}C in their tissues through photosynthesis and respiration. The ^{14}C content of these tissues is in equilibrium with that of the atmosphere because there is a constant exchange of new ^{14}C as old cells die and are replaced. However, as soon as an organism dies this exchange and replacement of ^{14}C ceases. Subsequently the ^{14}C content of the organism declines as the carbon decays to nitrogen, and the ^{14}C content is henceforth purely a function of time.

In order to detect ^{14}C activity in organic materials, extremely sensitive instrumentation is required. Two approaches are used to measure the residual ^{14}C activity in a sample: (i) conventional radiocarbon dating, which involves the detection and counting of β emissions from ^{14}C atoms over a period of time in order to determine the rate of emissions and hence the activity of the sample, and (ii) accelerator mass spectrometry, which uses particle accelerators as mass spectrometers to count the actual number of ^{14}C atoms in a sample of material (Aitkin, 1990; Fowler et al., 1986). The second approach was used to date the samples in this study.

It is necessary to consider the errors involved in dating samples using the radiocarbon method. Due to the nature of radiocarbon dating dates established are not absolute values, but are instead expressed as probabilities. Different errors have to be taken into account in doing so:

(i) Temporal variations in radiocarbon production.

Originally it was assumed that radiocarbon production was relatively constant. However, discrepancies were discovered between radiocarbon dates and the calendar age of recent wood samples (de Vries, 1958). Due to this discrepancy it is necessary to make a clear distinction between radiocarbon dates and calendar years. Attempts have been made to reconcile both timescales by comparing radiocarbon dates with those obtained from tree rings (Stuiver et al., 1998). In this way it is possible to calibrate the radiocarbon timescale. The causes of atmospheric

variations in radiocarbon production are factors influencing the cosmic ray flux. These include variations in the geomagnetic field of the earth and the sun, variations in solar activity, variations in the climate system and the distribution of the radiocarbon in the different reservoirs (especially the storage in oceans). Evidence for the solar forcing of our climate has been found in comparing $\delta^{14}C$ values of *Sphagnum* remains in peat with ^{14}C records (Speranza et al., 2002). Lately also the fossil fuel effect and the fall out of nuclear weapons testing have contributed to a changing concentration of radiocarbon.

(ii) Isotopic fractionation.

Although carbon isotopes are chemically indistinguishable, a tendency to take up the lighter isotope does exist in biochemical pathways. A correction for this effect is then also necessary, and is done by normalising radiocarbon activity against the mean $\delta^{13}C$ value of wood (-25‰).

(iii) Contamination problems.

Contamination by older or younger carbon can occur. A typical example is the intrusion of rootlets in older peat layers (Shore et al., 1995). Another source of such errors is the so-called hard water effect. This is a result of infinite age carbon dilution, which can result in living organisms taking up carbon with depleted ^{14}C content, and causes a sample to appear older than expected.

(iv) The biogeochemistry of the dated material.

It has been reported that different fractions of organic matter can give different ages (Shore et al., 1995; Avsejs, 2001) due to the different carbon sources used in the biogeochemical pathways e.g. uptake of CO_2 directly from the atmosphere or dissolved in bog water, which possibly contains older ^{14}C.

Notwithstanding the various problems, radiocarbon dating is widely applied in peat core research. In this thesis ^{14}C-dates will provide an independent control and further estimate of the accumulation rate of peat. Several studies (Kilian et al., 2000; Speranza et al., 2000) have demonstrated that ^{14}C AMS wiggle matching gives good results in dating peat. When dating materials that are deposited annually it is sometimes possible to use the wiggles that occur on the ^{14}C calibration curve to achieve a more accurate date. Taking a series of samples within a known interval and radiocarbon dating them does this. Once this is done it is possible to match the small wiggles that occur through the data set with those observed on the calibration curve. However, due to the nature of the procedure, the available resources (time and money) need to be very large. Therefore, it was concluded that such an

Table 2.6. Published radiocarbon dates on Walton Moss and Bolton Fell Moss.

Bolton Fell Moss					
Depth cm	Lab number	Mid-depth cm	Cal. Range (2σ) y BP		y AD/BC
Core J [a,f]					
20-22	SSR-4556	21	509	307	1540
26-28	SSR-4557	27	542	480	1440
32-34	SSR-4558	33	671	545	1340
38-40	SSR-4559	39	731	666	1250
44-46	SSR-4560	45	916	691	1150
50-52.5	SSR-4561	51.25	918	692	1150
56-58	SSR-4562	57	967	795	1070
63-65	SSR-4805	64	1347	1267	640
91-93	SSR-4806	92	1540	1344	510
100-108	SSR-4627	104	1284	1097	760
134-138	SSR-4807	136	1716	1521	330
3178-182	SSR-4808	180	2729	2349	-590
200-207	SSR-4628	203.5	2761	2558	-710
235-238	SSR-4809	236.5	3848	3629	-1790
260-268	SSR-4810	264	3697	3487	-1640
290-294	SSR-4629	292	4521	4229	-2430
330-334	SSR-4811	332	5031	4734	-2930
370-374	SSR-4630	372	5444	5116	-3330
400-407	SSR-4813	403.5	5563	5306	-3490
439-442	SSR-4813	440.5	5729	5493	-3660
485-489	SSR-4631	487	6279	5949	-4160
493-500	SSR-4815	496.5	6263	5955	-4160
Core L [f]					
400-408	SSR-4936	404	4237	3937	-2140
500-508	SSR-4937	504	5445	5053	-3300
Monolith BFX [c]					
39-40	OxA-9123	39.5	430	150	1660
Core BFM [c]					
420-421	OxA-9110	420.5	5030	4850	-2990
423-424	OxA-9177	423.5	4520	4410	-2515
426-427	OxA-9178	426.5	4520	4300	-2460
429-430	OxA-9111	429.5	5030	4860	-2995
432-433	OxA-9112	432.5	4830	4580	-2755
435-436	OxA-9179	435.5	4820	4550	-2735
438-439	OxA-9113	438.5	4790	4440	-2665
441-442	OxA-9114	441.5	5210	4870	-3090
444-445	OxA-9115	444.5	4830	4620	-2775
447-448	OxA-9180	447.5	4790	4420	-2655

Walton Moss					
Depth cm	Lab number	Mid-depth cm	Cal. Range (2σ) y BP		y AD/BC
Core 11 [b]					
32-40	SSR-5867	36	610	510	1390
52-60	SSR-5868	56	670	550	1340
156-164	SSR-5869	160	1840	1580	240
		Mid-depth cm	Wigglematched Date y AD		
			Core 19 [d,e]	Core 20 [d,e]	Core 21 [d,e]
	GrA-16651	28.5		1833	
	GrA-16689	31.5			1813
	GrA-16690	33.5			1800
	GrA-16654	34.5		1799	
	GrA-16692	35.5	1815		1788
	GrA-16660	37.5	1776	1771	1652
	GrA-16661	38.5		1762	
	GrA-12788	39.5	1737	1753	1583
	GrA-16693	40.5			1549
	GrA-16665	41.5	1699	1735	1515
	GrA-16666	42.5		1726	1481
	GrA-16667	43.5	1660	1717	1447
	GrA-16696	44.5	1640		1412
	GrA-16669	45.5	1621	1645	1378
	GrA-12853	46.5	1601		1344
	GrA-16700	47.5	1582		1265
	GrA-12861	48.5	1563		1255
	GrA-12862	49.5	1543		1246
	GrA-12863	50.5			1237
		52.5	1485		
	GrA-17518	54.5		1509	
		55.5	1464		
		57.5	1446		
	GrA-17457	59.5	1428		1156
		60.5	1419		
		61.5	1410		
	GrA-16663	62.5		1391	
		63.5	1392		
	GrA-12783	64.5		1351	
	GrA-16670	65.6	1374	1346	
	GrA-16671	67.5		1316	
	GrA-16673	68.5		1302	
	GrA-16674	69.5	1338	1287	1066
	GrA-16677	70.5		1197	
	GrA-16676	71.5	1247	1189	
	GrA-16679	72.5		1181	
	GrA-16680	73.5	1231	1173	
	GrA-12785	75.5	1215	1157	
	GrA-12786	76.5	1207	1149	
		77.5	1199		
		78.5	1191		
		84.5	1144		
		89.5	1104		
	GrA-17485	90.5			877
		94.5	1065		
	GrA-16681	99.5	1025	967	795

(a) Barber et al. (1994) (b) Hughes et al. (2000) (c) Avsejs (2001) (d) Mauqouy et al. (2002a) (e) Mauqouy et al. (2002b)
(f) Barber et al. (2003)

intensive study could not be undertaken and deemed unnecessary given the fact that the sample sites have been widely researched. Only the major excursions were dated (rangefinder dates) in order to establish if ^{210}Pb determined accumulation rate could be extrapolated further down-core or if corrections were necessary.

2.4.2.2 ^{14}C Dating of core samples

Previous studies (Section 2.3) all include radiocarbon dates from Bolton Fell Moss and Walton Moss. Table 2.6 gives an overview of the dates obtained in these studies (only dates obtained on depths used in this study are given in the table (Walton Moss, 100 cm; Bolton Fell Moss, 500 cm)). They comprise dates obtained using conventional radiocarbon dating and accelerator mass spectrometry. The results show that most cores accumulated in an almost linear mode below 50 cm depth.

For this thesis, bulk peat samples (20 mg) from Bolton Fell Moss and Walton Moss were submitted for pre-treatment and radiocarbon dating at the Oxford Radiocarbon Accelerator Unit (results in Table 2.7). The Bolton Fell Moss core used in this study has been previously dated between 420-448 cm depth (Avsejs, 2001) and the Bolton Fell Moss monolith (Xie et al., 2000) has been dated at 39-40 cm depth (Avsejs, 2001), shown in Table 2.6. Calibration of the radiocarbon determinations was achieved using the Oxcal v3.5 program (Bronk Ramsey, 1995, 2001), which uses the calibration record from Stuiver and co-workers (1998). The obtained age ranges are shown in Figure 2.10 and Table 2.7. For the age-depth model of the cores below 50 cm, the data ranges at 95.4% probability will be used.

Table 2.7. AMS radiocarbon dating of Walton Moss and Bolton Fell moss.

	Bolton Fell Moss		Walton Moss
	BFM-C2-94/95	BFM-C2-186/187	WM-C1-88/89
Lab number	OxA-11985	OxA-11986	OxA-11987
Depth (cm)	94.5	186.5	88.5
δ^{13}C value (‰)	-24.9	-26.5	-26.0
Radiocarbon date (y BP)	1033 ± 25	1740 ± 23	967 ± 25
Calibrated age range (y AD)			
68.2% probability	994 - 1020	245 - 265	1020 - 1050
		270 - 310	1090 - 1120
		315 - 345	1140 - 1160
95.4% probability	900 - 920	240 - 390	1000 - 1160
	960- 1040		

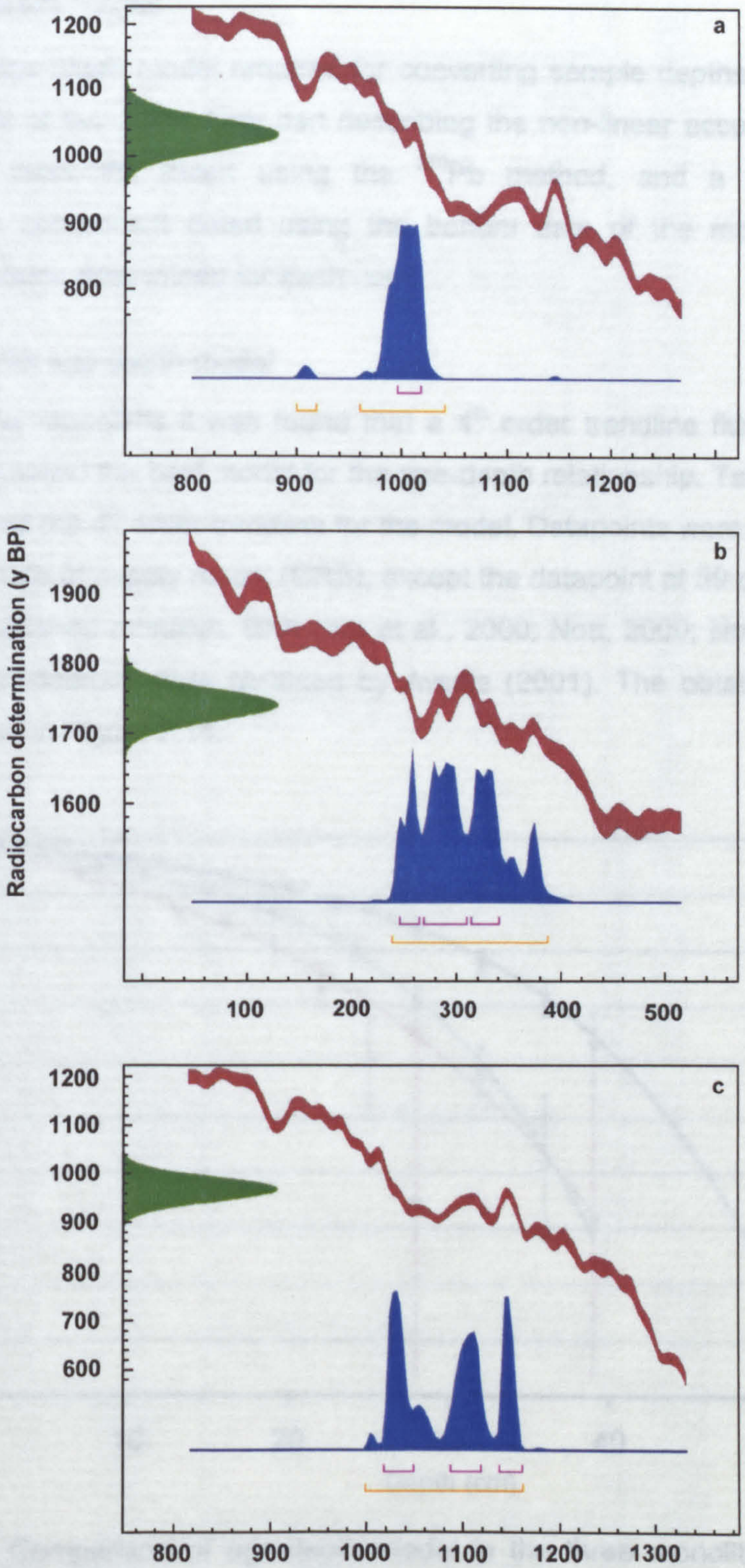

Figure 2.10. Calibration of radiocarbon determination for (a) BFM-C2-94/95; (b) BFM-C2-186/187, and (c) WM-C1-88/89. Calibrated age ranges indicated by (⌊⌋) at 68.2% and (⌊⌋) at 95.4% probability.

2.4.3 Age-depth model

The age-depth model required for converting sample depths into calibrated ages consists of two parts. One part describing the non-linear accumulation in the top 50 cm monoliths dated using the ^{210}Pb method, and a second, linear accumulation component dated using the bottom date of the monolith and the radiocarbon dates determined for each core.

2.4.3.1 Monolith age-depth model

For the monoliths it was found that a 4th order trendline fitted through the datapoints provided the best model for the age-depth relationship. Table 2.8 lists the dates used and the 4th order trendline for the model. Datapoints were obtained using the constant rate of supply model (CRS), except the datapoint at 39 cm depth of the previously published monolith, BFX (Xie et al., 2000; Nott, 2000; Nott et al., 2000), which is a radiocarbon date obtained by Avsejs (2001). The obtained calibration curve is shown in Figure 2.11.

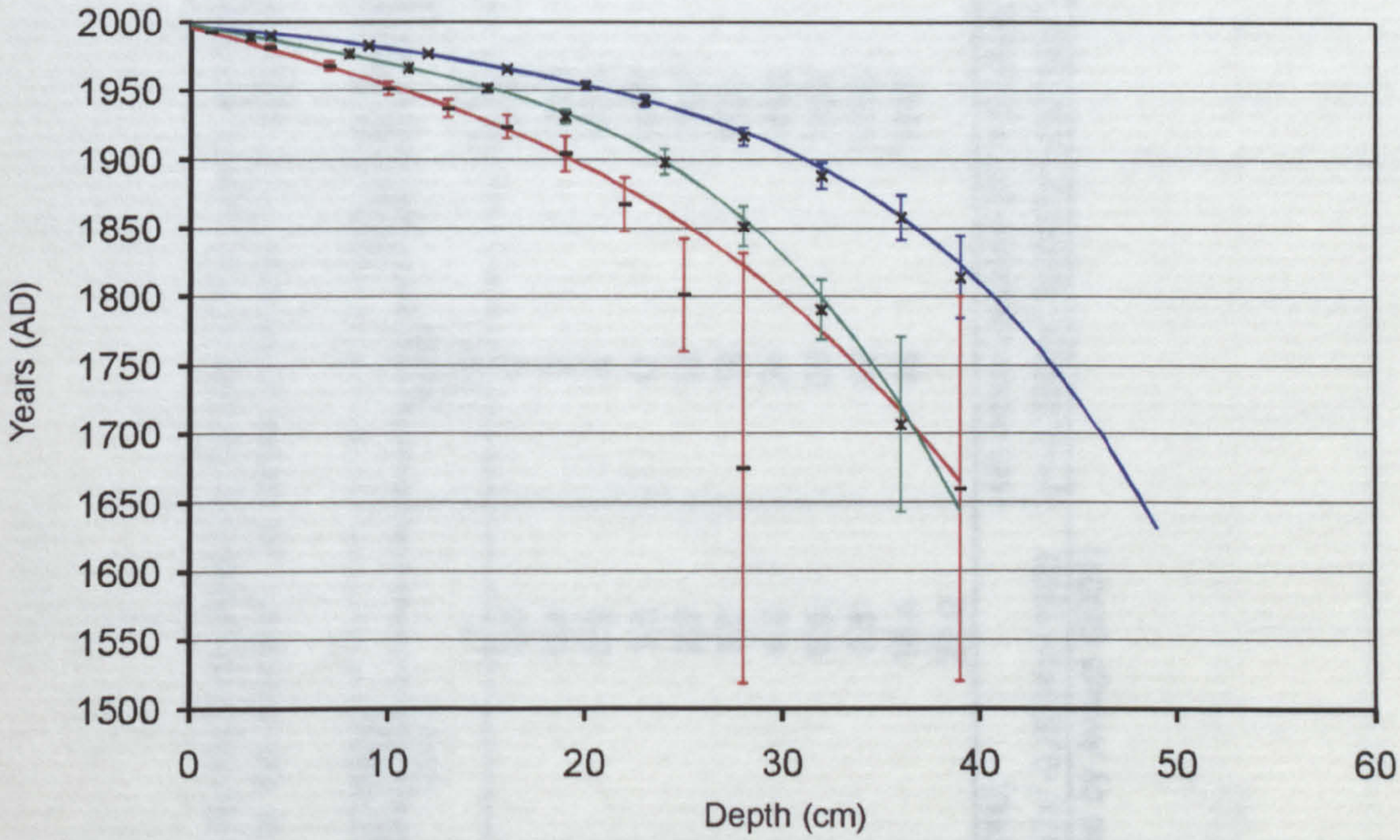

Figure 2.11. Comparison of age-depth model in the three monoliths: Bolton Fell Moss monoliths (BFM, blue line; BFX, red line) and Walton Moss (green line) monolith. Trendline uses formula given in Table 2.8, for which dates are provided by the CRS-model.

Table 2.8. Age-depth model for the monoliths (top 50 cm) of the cores investigated in this thesis. A 4th order trendline gives best fit and can be extrapolated to the bottom of the monolith. All dates used are ^{210}Pb dates (CRS-model), except for BFX date at 39 cm depth, which is a calibrated ^{14}C date.

Bolton Fell Moss (BFM)			Walton Moss (WM)			Bolton Fell Moss (BFX)		
Depth	Date		Depth	Date		Depth	Date	
cm	y AD	±	cm	y AD	±	cm	y AD	±
0	1996	0.0	0	1998	0.0	0	1996	0.0
4	1990	0.4	3	1989	0.4	1	1992	0.4
9	1983	0.9	8	1977	1.2	4	1982	1.6
12	1977	1.3	11	1967	1.9	7	1968	3.1
16	1966	2.0	15	1952	3.1	10	1952	4.8
20	1954	3.0	19	1931	4.9	13	1937	6.6
23	1942	4.0	24	1898	9.0	16	1924	8.8
28	1916	6.6	28	1851	14.4	19	1904	12.8
32	1888	9.6	32	1790	22.1	22	1867	19.6
36	1858	16.4	36	1707	63.3	25	1801	41.0
39	1814	29.9				39[(a)]	1660	140.0
4th order trendline (R^2 = 0,9990)			4th order trendline (R^2 = 0,9999)			4th order trendline (R^2 = 0,9991)		
$y=-0,0001x^4+0,0046x^3-0,1237x^2-0,6694x+1996$			$y=-0,0001x^4-0,0007x^3+0,0188x^2-2,8252x+1998$			$y=-0,00001x^4-0,0026x^3+0,0004x^2-3,9475x+1996$		

(a) Radiocarbon date reported by Avsejs (2001)

Table 2.8. Age-depth model for the monoliths (top 50 cm) of the cores investigated in this thesis. A 4th order trendline gives best fit and can be extrapolated to the bottom of the monolith. All dates used are ^{210}Pb dates (CRS-model), except for BFX date at 39 cm depth, which is a calibrated ^{14}C date.

Bolton Fell Moss (BFM)			Walton Moss (WM)			Bolton Fell Moss (BFX)		
Depth	Date		Depth	Date		Depth	Date	
cm	y AD	±	cm	y AD	±	cm	y AD	±
0	1996	0.0	0	1998	0.0	0	1996	0.0
4	1990	0.4	3	1989	0.4	1	1992	0.4
9	1983	0.9	8	1977	1.2	4	1982	1.6
12	1977	1.3	11	1967	1.9	7	1968	3.1
16	1966	2.0	15	1952	3.1	10	1952	4.8
20	1954	3.0	19	1931	4.9	13	1937	6.6
23	1942	4.0	24	1898	9.0	16	1924	8.8
28	1916	6.6	28	1851	14.4	19	1904	12.8
32	1888	9.6	32	1790	22.1	22	1867	19.6
36	1858	16.4	36	1707	63.3	25	1801	41.0
39	1814	29.9				39[(a)]	1660	140.0
4th order trendline (R^2 = 0,9990)			4th order trendline (R^2 = 0,9999)			4th order trendline (R^2 = 0,9991)		
$y=-0,0001x^4+0,0046x^3-0,1237x^2-0,6694x+1996$			$y=-0,0001x^4-0,0007x^3+0,0188x^2-2,8252x+1998$			$y=-0,00001x^4-0,0026x^3+0,0004x^2-3,9475x+1996$		

(a) Radiocarbon date reported by Avsejs (2001)

2.4.3.2 Core age-depth model

Previous authors (Barber et al., 1994; Avsejs, 2001) have reported that peat accumulation rates are fairly uniform in ombrotrophic mires below 50 cm depth. The age-depth model is then also provided by the linear trendline through the radiocarbon dates and the bottom calibrated date of the monolith-dating model. The author of this thesis is aware that the limited number of radiocarbon dates recorded cannot accurately describe all the variations possible in the peat accumulation process. However, it was deemed that for this study no further dates were necessary, since no wiggle-matching of the core was going to be performed. As such the linear accumulation model was deemed sufficient for the purposes of this study.

For the calibration of the profiles, the mid-point of the 95.4% or 68.2% probability ranges were used. The cores were assumed to be linear between the different radiocarbon determinations, and a piece wise linear trend established (Figure 2.12). Table 2.9 shows the trendlines used to calibrate sample depths with their respective ages. Overall accumulation rates of 11.5 cm y^{-1} (BFM) and 13.8 cm y^{-1} (WM) are in agreement with previous published results showing both bogs to have accumulation rates between 10 and 16 cm y^{-1} (Barber et al., 1994, 2002; Hughes et al., 2000; Avsejs, 2001), even if accumulation rates between separate radiocarbon dates varied between 7.5 and 14.1 cm.y^{-1}.

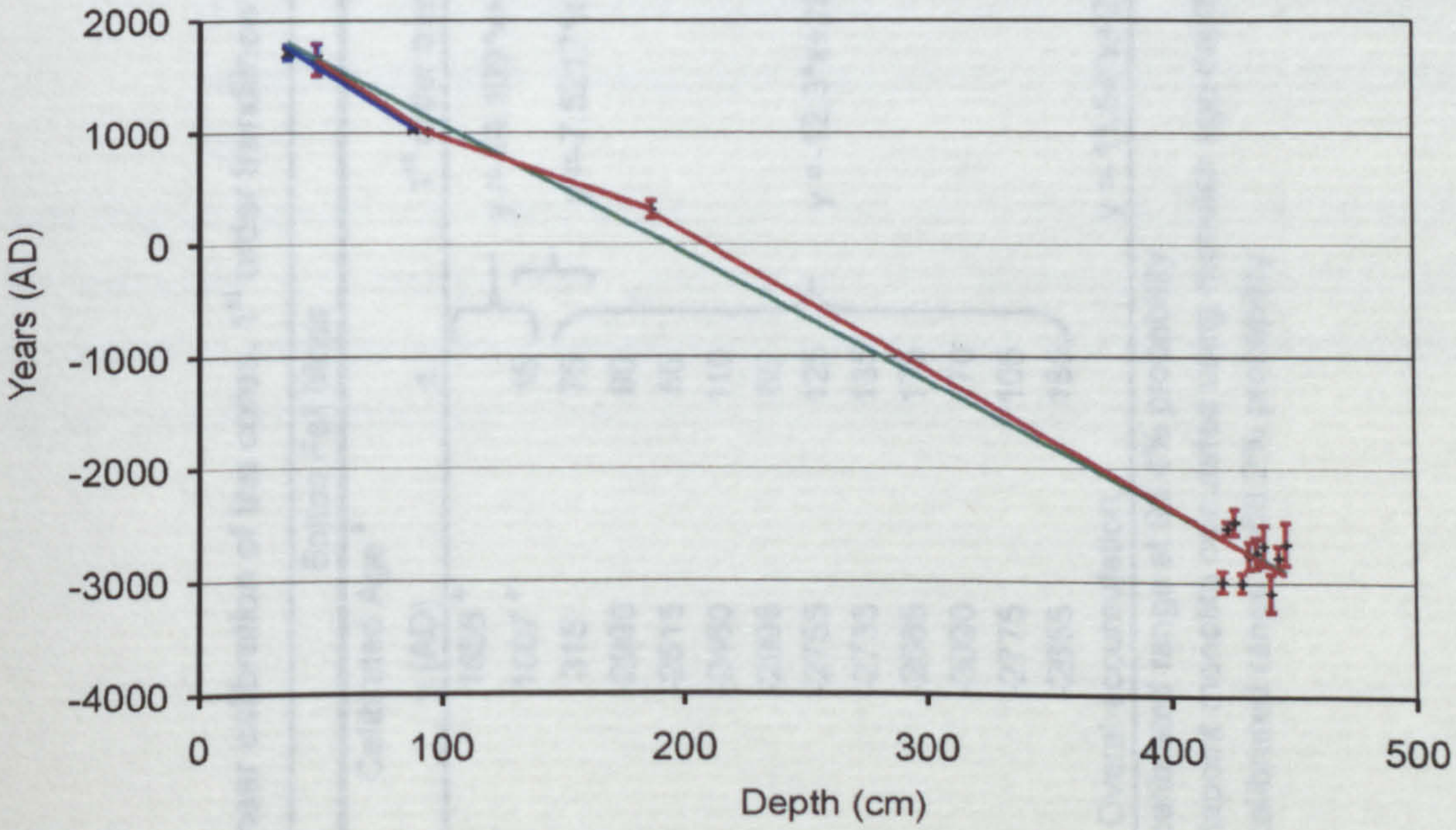

Figure 2.12. Linear calibration of sample depth into calibrated calendar years; Walton Moss (blue line), Bolton Fell Moss (brown line), green line gives overall accumulation rate in BFM profile. Top point provided by monolith age-depth model.

Table 2.9. Linear calibration of the cores. 1st order trendlines shown in Figure 2.12.

Bolton Fell Moss				Walton Moss			
Depth cm	Calibrated Age [a] y (AD)	±	1st order trendline	Depth cm	Calibrated Age [a] y (AD)	±	1st order trendline
48	1656 [b]		y =-14.109*x+2333.2	36	1720 [b]		y =-13.765*x+2259.5
94	1007 [c]	15		88	1035 [c]	15	
186	315	75	y =-7.5217*x+1714				
421	-2990	90					
423	-2515	55					
426	-2460	110					
429	-2995	85					
432	-2755	125	y =-12.3*x+2574.71				
435	-2735	135					
438	-2665	175					
441	-3090	170					
444	-2775	105					
447	-2655	185					
Overal accumulation:			y =-11.54*x+2249.00				

(a) Mid-point calibrated range at 95.4% probability
(b) Bottom datapoint monolith calculated using monolith age-depth model
(c) Mid-point calibrated range at 68.2% probability

2.5 Conclusions

The overview of previous studies on both sample sites showed that previously studied profiles do reflect past climatic changes and that the sample sites are suitable for the study of past climate undertaken in this thesis. In order to relate the results of this thesis to previously published studies, dating of the cores was necessary. Dating of the cores was achieved using a two-way strategy:

(i) The top part of the profile (the monolith, top 50 cm) was dated using ^{210}Pb dating technique. A comparison of the different dating models available (constant accumulation rate, constant initial concentration and constant rate of supply) yielded a dating model (constant rate of supply model), which described all the properties ascribed to decaying peat matter; gradual compaction and thus increase in accumulation rate with depth. All three monoliths used in this thesis gave an upper age range of about 200 to 350 years, consistent with previously published dating of peat monoliths. A fourth-order age-depth model was found to best describe the peat accumulation.

(ii) Rest of the profile dated using ^{14}C dating technique and described using a piece-wise linear model. The radiocarbon determinations were in-line with previous dating of cores from Bolton Fell Moss and Walton Moss. Overall accumulation rates were 11.5 cm y^{-1} (Bolton Fell Moss) and 13.8 cm y^{-1} (Walton Moss) and correspond to previously published results, indicating that peat accumulation rates are fairly uniform throughout the bog.

This chapter showed that dating of the peat cores could be achieved and as such the molecular and isotope data presented in the following chapters can be expressed in calendar years enabling inter-core comparison and providing a basis for comparison with historical records and other palaeoclimate records.

3 Biomarker Hydrocarbon Records in Two Neighbouring Ombrotrophic Peat Bogs

3.1 Introduction

There are relatively few applications of modern organic geochemical techniques to palaeoenvironment and palaeoclimate reconstructions based on peat deposits (Boon et al., 1986; Farrimond and Flanagan, 1995; Ficken et al., 1998; Kuder and Kruge, 1998). This is perhaps surprising considering: (i) the organic-rich nature of these facies; (ii) the high frequency of occurrence of peat deposits over the Northern Hemisphere; and (iii) that peat deposits provide reasonably continuous records spanning the last several thousand years and posses a diversity of potentially informative features that have made them a focus of interest in palaeoclimate and palaeoenvironmental research. Recently, a number of authors have begun to investigate the use of lipid biomarkers as proxies for past changes in bog vegetation (Farrimond and Flanagan, 1995; Ficken et al., 1998; Nott et al., 2000; Xie et al., 2000; Pancost et al., 2002; Avsejs et al., 2001).

The hydrology of ombrotrophic mires is governed by precipitation and evaporation (Barber, 1993). Moreover, sediment accumulation rates in mires are high, allowing the development of high-resolution climatic records with plant macrofossils reflecting the abundances of climatically sensitive bog vegetation and, hence, such records can be used to infer past hydrological changes (Barber et al., 2003 and references therein). However, macrofossil analyses are restricted to deposits and time intervals in which they are sufficiently well preserved, and this has prompted the development of supplemental proxies for vegetation change in highly humified peats. Several studies (Farrimond and Flanagan, 1995; Ficken et al., 1998; Nott et al., 2000; Pancost et al., 2002; Avsejs et al., 2001; Xie et al., in press) have attempted to use lipid biomarkers as molecular fingerprints to reconstruct changing plant inputs through a peat profile, and to use the changes in the biomarker stratigraphy as a basis for deriving new palaeoclimatic information. The overall aim of this chapter of the thesis will be to further develop such proxies as an independent tool to assess vegetation changes during bog development and relate these changes to bog wetness. The two neighbouring bogs were selected in order to provide replicate cores and test the hypothesis that synchronous biomarker records could be obtained from bogs of comparable type within a geographically restricted

area. Previous work had shown that these two bogs exhibited synchronicity in their macrofossil records to a depth of 1 m (Barber et al., 1998).

3.2 Lipids in peat and peat forming plants

3.2.1 Lipids in peat

Investigations of lipids of ombrotrophic mires include that of lipid sub-fractions of *Sphagnum* and *Carex* peats displaying various degrees of humification (Lehtonen and Ketola, 1990). They identified long-chain acyclic methyl ketones, which may derive from peat-forming mosses and sedges or via bacterial oxidation of *n*-alkanes and/or β-oxidation and decarboxylation of *n*-fatty acids. In a further study (Lehtonen and Ketola, 1993) the diagenetic changes to peat lipids in 4 different peat types, *Sphagnum*, *Carex*, *Bryales* and *Carex/Bryales* was explored; hydrocarbon, ketone, alcohol, sterol and acidic fractions were investigated. Although no specific humification effects were found in the *n*-alkanol distributions of *Sphagnum* and *Bryales* peats, the sterol fraction consisted of 4 major components i.e. β-sitosterol, stigmasterol, campesterol and stigmastanol, together with lower abundances of stanols that were most likely to be products of microbial reduction of the corresponding sterols. The acidic lipid fraction comprised *n*-alkanoic acids and ω-hydroxy acids, with the longer chain homologues ($>C_{22}$) of the former increasing in abundance with increased humification. In common with the *n*-alkanoic acids the longer-chain hydroxy acids ($>C_{22}$) increased in relative abundance with increased humification. Overall, the peat lipid components were attributed to moss and higher plant sources with changes in alkyl lipid distributions becoming more exaggerated with increased humification and interpreted as a microbial diagenetic effect.

Studies of lipids from peat deposits other than raised bogs have included the comparison of peats from tropical, subtropical, temperate and cool temperate climates (Dehmer, 1995). Dehmer (1995) suggested that the odd numbered *n*-alkanes (C_{25}, C_{27} and C_{29}) derived from higher plant waxes and those with chain lengths less than C_{23} may be due to bacterial activity. Hopanoids (17β,21β(H)-22*R*-homohopane), first observed by Maxwell and co-workers (Quirk et al., 1984) together with the C_{31} αβ hopane in temperate peats, were the main components in tropical peats and were assigned a microbial origin. Several non-hopanoid aromatic triterpenoids were identified in peats from subtropical regions, including 1,2,9- and 2,2,9-trimethyl-1,2,3,4-tetrahydropicene, the formation of which was attributed to bacterially mediated aromatisation of α- and β-amyrin. In his investigation of sub-recent peat horizons of Bolton Fell Moss, Nott (2000) observed the presence of

relatively high abundances of the C_{31}-homohopanes, taraxer-14-ene and taraxast-20-ene, while olean-12-ene and urs-12-ene were present in lower abundances. These compounds most likely derive from precursor triterpenols such as taraxerol, α- and β-amyrin (Nott, 2000; Pancost et al., 2002).

3.2.2 Lipids in peat forming plants

An important consideration in using the lipid compositions of peat for palaeoclimate reconstruction is the lipid composition of the peat-forming plants. The most extensively investigated class of lipids in peats are the hydrocarbons. The hydrocarbon fraction of peat-forming plants consists almost exclusively of straight-chain alkanes, which comprise part of their epicuticular waxes. The first description of the *n*-alkane distributions in *Sphagnum* plants was by Sever et al. (1972), who reported the *n*-alkane distribution of *S. affine* to be dominated by the C_{31} homologue. Marseli et al. (1972) analysed *S. teres* revealing *n*-alkanes ranging from C_{24} to C_{33} with the C_{31} homologue again dominant. In a study by Corrigan (1973) the major *n*-alkane reported in four other species of *Sphagna* was C_{23} or C_{25}. In all the investigated samples a clear odd-over-even-carbon number predominance was observed, typical of that generally found in higher plants. In a further investigation, Corrigan et al. (1976) reported considerable variation in the dominant *n*-alkane in a further six *Sphagna* species. Karunen and co-workers investigated the lipid composition of fresh and decaying *S. fuscum* (Karunen et al., 1979; Karunen and Salin, 1980; Karunen and Ekman, 1981), observing *n*-alkanes ranging from C_{21} to C_{33} with a strong odd-over-even predominance with a maximum at C_{23}/C_{25}.

A further series of studies into the lipid composition of other peat-forming plants appeared in the 1980s. Salasoo (1981) studied several *Ericaceae* species and found that the *n*-alkanes range from C_{25} to C_{33}, with a distinct odd-over-even predominance and a maximum at either C_{31} or C_{33}. In 1986, Salasoo reported the *n*-alkane composition of several heath plants from Alaska, demonstrating similar distributions to those reported in his 1981 study. Several other papers by the same author reported *n*-alkane compositions consistent with earlier reports (Salasoo, 1987a, 1987b, 1988, 1989).

Renewed interest in this area prompted several new studies of the *n*-alkane lipid distributions of peat-forming plants (Ficken et al., 1998; Nott, 2000; Nott et al., 2000; Baas et al., 2000; Pancost et al., 2002). The results of these latter studies of a total 36 peat-forming species are summarised in Table 3.1. Again a very distinct

Table 3.1. *n*-Alkane distributions expressed as percent composition of the sum of the odd carbon number *n*-alkanes for 36 peat-forming plants.

	% of total odd Alkanes							distribution mode[f]
	n-C_{21}	*n*-C_{23}	*n*-C_{25}	*n*-C_{27}	*n*-C_{29}	*n*-C_{31}	*n*-C_{33}	
Bog Moss								
Sphagnum magellanicum[c,d]	7.4	14.2	32.0	5.9	10.3	21.3	8.9	BI
Sphagnum palustre[c,d]	9.1	33.1	25.0	9.8	9.3	11.9	1.9	BI
Sphagnum papillosum[c,d]	11.0	37.3	22.1	4.7	4.9	16.5	3.5	BI
Sphagnum imbricatum[d,e]	26.6	42.4	21.2	4.2	2.1	3.5	0.0	UNI
Sphagnum compactum[d]	6.4	17.3	31.8	5.2	8.7	30.6	0.0	BI
Sphagnum fimbriatum[d]	4.1	18.2	37.6	21.2	7.6	11.2	0.0	BI
Sphagnum rubellum[d,e]	10.0	16.7	19.8	4.9	12.2	25.5	10.8	BI
Sphagnum fuscum[b]	8.6	21.5	41.0	15.7	4.7	7.5	1.1	UNI
Sphagnum capillifolium[b,c]	8.5	15.3	17.8	7.1	12.1	29.3	9.9	BI
Sphagnum molle[d]	11.4	17.8	30.1	6.4	10.2	24.2	0.0	BI
Sphagnum tenellum[d]	10.0	40.7	18.0	5.3	10.0	16.0	0.0	BI
Sphagnum cuspidatum[c,d,e]	11.0	45.2	10.3	3.5	6.5	18.7	4.7	BI
Sphagnum pulchrum[d]	13.5	36.9	19.8	8.1	9.0	12.6	0.0	BI
Sphagnum recurvum[c,d]	19.4	31.4	14.4	8.3	11.3	12.0	3.2	BI
Sphagnum sub-nitens[c]	3.2	5.4	4.4	4.8	9.5	39.6	33.1	UNI
Aulacomnium palustre[c]	0.8	0.9	5.1	38.6	9.8	29.7	15.1	BI
Hypnum cupressiforme[c]	1.2	4.4	9.6	19.1	31.5	25.4	8.8	UNI
Polytrichum sp.[c]	0.3	0.8	2.7	12.7	29.4	33.5	20.5	UNI
Huperzia selago[b]	0.0	3.0	6.1	27.3	31.8	24.2	7.6	UNI
Racomitrium lanuginosum[b]	1.1	1.1	2.3	6.8	28.4	46.6	13.6	UNI
Sedge								
Carex bigelowii[b]	4.9	7.3	4.9	39.0	17.1	20.7	6.1	BI
Eriophorum vaginatum[c]	0.5	1.2	1.8	3.4	15.4	56.3	21.5	UNI
Eriophorum angustifolium[c]	0.5	1.2	1.8	3.3	15.4	56.4	21.5	UNI
Trichophorum cespitosum[c]	0.1	0.3	0.7	2.0	11.5	59.3	26.1	UNI
Rhynchospora alba[c]	2.4	2.4	3.3	4.0	29.7	46.9	11.4	UNI
Ericaceae								
Calluna vulgaris[a,c,e]	1.4	1.2	2.4	4.4	8.6	36.2	45.8	UNI
Erica tetralix[c,e]	2.2	4.6	4.5	4.0	12.5	55.3	16.9	UNI
Empetrum nigrum[b,c]	0.0	0.0	0.1	3.1	29.4	49.9	17.4	UNI
Vaccinium oxycoccus[c]	0.3	0.7	1.1	13.9	53.7	28.2	2.1	UNI
Vaccinium vitis-idaea[b]	1.1	2.3	9.1	19.3	45.5	19.3	3.4	UNI
Andromeda polifolia[c]	0.1	0.6	3.3	6.6	40.3	46.7	2.5	UNI
Lichen								
Cetraria islandica[b]	1.2	1.2	3.5	11.6	29.1	43.0	10.5	UNI
Sphaerophorus globosus[b]	1.2	1.2	2.4	6.0	19.3	54.2	15.7	UNI
Cladonia sp.[c]	1.0	1.6	3.3	8.1	20.9	48.4	16.6	UNI
Cladonia uncialis[b]	1.2	1.2	2.3	7.0	22.1	51.2	15.1	UNI
Cladonia arbuscula[b]	1.1	1.1	2.2	6.7	26.7	51.1	11.1	UNI

(a) Huang et al. (1997) (b) Ficken et al. (1998) (c) Nott et al. (2000) (d) Baas et al. (2000)
(e) Pancost et al. (2002) (f) BI = Bimodal; UNI = Unimodal distribution

pattern of odd-over-even carbon number alkanes has been observed, as well as differences in the dominating *n*-alkane between *Sphagnum* species and other taxa. Except for three *Sphagna* species, which show hentriacontane (*n*-C_{31}) as the major *n*-alkane, all *Sphagna* have either C_{23} or C_{25} as dominant homologue. Another difference between *Sphagna* and other peat forming vegetation is the commonly seen bimodal distribution, while higher plants display unimodal distributions maximising at C_{29} or C_{31}. The occurrence of the shorter chain length *n*-alkanes has been proposed as a proxy for tracking vegetation changes (Nott 2000; Nott et al., 2000; Pancost et al., 2002). While these latter studies showed promising qualitative agreement between lipid distributions and the macrofossil records, the overall conclusion is that these *n*-alkanes records cannot be used to quantitatively asses plant inputs into the peat profile (Nott et al., 2000; Avsejs, 2001; Pancost et al., 2002).

3.3 Plant tissue and diagenetic effects on lipid distributions

The high quality of preservation of lipids in peat is primarily attributed to the slow rate of biodegradation in the anoxic, water-saturated environment (Clymo, 1983). Oxygen abruptly disappears at the groundwater/air boundary, as diffusion is unable to compensate for the rapid respiration of degrading organisms. The deeper, permanently saturated layers of peat (below the minimum height of groundwater level) are dominated by fermentative/methanogenic bacteria. In the top-most layer, oxygen is freely available and the most active organisms are fungi. Changes in the level of the water table result in the introduction or suppression of aerobic activity in a given interval of peat. Identification of a cumulative effect of exposure to aerobic processes on the chemistry of plant lipids has been proposed as a basis for the reconstruction of past peat surface wetness (Kuder and Kruge, 1998).

Two further factors controlling the lipid distribution of peat deposits are the selective preservation of specific plant tissues and the initial compositional differences within those tissues (Pancost et al., 2002). This latter study showed that (Table 3.2) the lipid distribution in two *Ericaceae* species (*Calluna vulgaris* and *Erica tetralix*) exhibited intra-specific differences in their *n*-alkane concentrations and to a lesser extent their distribution between different plant tissues. Such differences are is not a problem in major peat-forming plants, such as *Sphagna*, which do not posses such a range of tissues.

A study by Karunen and co-workers into the changes in the lipid concentration in relation to the age of the plant (Karunen, 1979; Karunen and Salin, 1980; Karunen and Ekman, 1981) revealed that the lipid concentration in the

Table 3.2. *n*-Alkane concentrations and distributions in different tissues of *Ericaceae* species (Pancost et al., 2002).

	Amount of odd alkanes (µg g^{-1} dry peat)						
	n-C_{21}	*n*-C_{23}	*n*-C_{25}	*n*-C_{27}	*n*-C_{29}	*n*-C_{31}	*n*-C_{33}
Erica tetralix (fine roots)	0	4	4	2	12	89	95
Erica tetralix (coarse roots)	5	6	5	4	14	52	0
Erica tetralix (stems)	1	3	3	2	6	18	0
Calluna vulgaris (leaves)	0	0	0	26	50	270	1043
Calluna vulgaris (roots)	1	1	1	1	2	17	8
Calluna vulgaris (stems + leaves)	21	13	16	28	160	700	3500
Sphagna[a]	17	39	31	9	14	30	10

(a) average of all known *Sphagna* species (shown in Table 3.1)

youngest shoots of *Sphagnum* species was 40-60% higher than the older parts. Six to Ten centimetres below the bog's surface only minor changes in composition were observed, with the *n*-alkane distribution showing a shift towards longer-chain homologues at the expense of shorter-chain components, although the *n*-C_{25} homologue continued to dominate in plant remains from all peat horizons. A loss of the straight chain hydrocarbons in older shoots was suggested to be the first sign of microbial attack before any morphological changes could be detected.

Lehtonen and Ketola (1993) studied the effect of humification on the lipid distributions of different peats (*Sphagnum*, *Carex*, *Bryales* and *Carex-Bryales* peat). Under the oxygen-poor or anaerobic conditions prevalent in peat bogs the lipids are subjected primarily to microbial changes, corroborating the findings by Karunen and co-workers, i.e. the carbon preference index of the *n*-alkanes shifted slightly towards longer-chain homologues with increasing burial depth.

Lethonen also studied the lipid content of bog water (Lethonen et al., 1991). The latter study showed a contribution of 15.7% *n*-alkanes to the dissolved organic matter (DOM) in the bog water, and the total lipids in the DOM were found to be only 2% of the water extractable lipids of peat. But this was almost insignificant compared with concentration of the solvent extractable lipids (2.35 mg g^{-1} vs. 98.8 mg g^{-1}; Avsejs, 2001), thereby confirming that hydrocarbons will not be transported to any significant extent through dissolution in bog water from their site of production/deposition.

Huang et al. (1997) in which degraded plant remains from a 23-year field decomposition of *Calluna vulgaris* were investigated. The decay of *n*-alkanes showed a first order exponential decrease in concentration with time. Effects on their distribution were very minor with no clear trends being established. In summary, while changes do occur in the concentrations of *n*-alkanes during the decay of peat-

forming plants, the overall distributions appear to be robust and hold promise for use in reconstructing vegetation changes during bog development.

3.4 Aims of this chapter

Based on the above review of the lipid composition of peat, the hydrocarbon components appear to hold considerable promise as climate proxies. Hence, this Chapter focuses specifically on the hydrocarbon fraction of the lipid components of peat due to: (i) the relatively high stability of the hydrocarbons to diagenesis; (ii) the presence of hydrocarbon components characteristic of key organisms involved in bog development; (iii) the relative ease of obtaining pure hydrocarbon fractions from complex lipid extracts (see Chapter 7), and (iv) the relative ease of determining compound-specific δD values of hydrocarbons compared to other functionalised lipids (relevant to the results presented later in Chapter 5).

The organic geochemical investigation presented in this Chapter will aim to achieve the following:

(i) Build on the work of Nott (Nott, 2000; Nott et al., 2000) and Avsejs (2001), on Bolton Fell Moss by extending the investigations to an adjacent bog, i.e. Walton Moss.

(ii) Comparison of two 1000 y peat profiles thereby providing a means of establishing whether or not synchronicity of climatic response of different peat bogs is manifested in their hydrocarbon distributions.

(iii) Extend investigations of the relationships between known climate phenomena and anomalies in the hydrocarbon distributions to a 5500 y ombrotrophic peat profile from Bolton Fell Moss.

(iv) Provide baseline information, i.e. distributions and concentrations, on hydrocarbon composition vital for subsequent compound-specific δD analysis.

3.5 Results and Discussion

3.5.1 Hydrocarbon composition of peat

Only lipid components detectable throughout the entire core were identified, because only these components would have the capacity to provide contiguous down-core molecular stratigraphic records for comparison with known past climate events. The lipids contained in the hydrocarbon fraction of ombrotrophic peat bogs fall into two classes: straight-chain alkanes and cyclic hydrocarbons with terpene and hopane structures and these are considered in turn in the following sections.

3.5.1.1 Straight-chain alkanes in peat

A typical gas chromatogram of the hydrocarbon fraction of both Bolton Fell Moss (BFM) and Walton Moss (WM) peat is shown in Figure 3.1. The *n*-alkanes are abundant components in all horizons in both bogs occurring as homologous series with a distinct odd-over-even carbon number preference, consistent with a higher plant origin. While the *n*-alkanes ranging between *n*-C_{19} and *n*-C_{33} are higher plant derived, the lower homologues (*n*-C_{14} to *n*-C_{19}) most likely derive from micro-organisms (Albro, 1976). However, they do not constitute a major part of the hydrocarbon fraction <1%. The *n*-alkanes from *n*-C_{19} to *n*-C_{29} are all accompanied by the analogous mono-unsaturated straight chain alkenes ($C_{19:1}$-$C_{29:1}$). These have been reported previously in oligotrophic (Dehmer, 1995) and in ombrotrophic peat bogs (Nott et al., 2000), a microalgal or cyanobacterial source being proposed by Dehmer (1995). No odd-over-even preference or even-over-odd preference was seen for these latter components.

The overall trends in the mean *n*-alkane compositions of the cores from both bogs were comparable with respect to both their concentrations (Figure 3.2) and carbon number distributions (Figure 3.3), the latter being characterized by a bimodal distribution, reflecting the different *n*-alkane distributions of the parent peat-forming plants. At this point it needs pointing out that intercomparisons of these distributions, as with the profiles discussed later in this Chapter, is somewhat hampered by the lack of macrofossil records. Comparison of these new results with those of a previous study of Bolton Fell Moss (Nott, 2000; Nott et al., 2000; Xie et al., in press; subsequently referred to as BFX monolith) reveals some marked differences in *n*-alkane composition. For instance, the BFX monolith was characterized by a remarkably high percentage (up to 55%) of *n*-tricosane. Although this compound was the most abundant shorter-chain alkane in the new cores, it was never as abundant (%) in BFM and WM, as in BFX. Interestingly, the mean concentration of *n*-C_{23} was found to be similar (18-22 μg g^{-1} dry peat) in both cores and comparable to BFX. Another difference is the greater abundance of the *n*-C_{25} and *n*-C_{27} homologues in the new cores compared to the BFX monolith where they were barely detectable. Generally, the most abundant compounds were the longer chain homologues, *n*-C_{31} and *n*-C_{33}. The observation that peat profiles are generally dominated by the higher molecular-weight homologues is in agreement with previous authors observations (Ficken et al., 1998; Pancost et al., 2002) that although the cores are dominated by *Sphagnum* taxa, this generally is not readily reflected in the *n*-alkane distribution. The observation by Pancost et al. (2002) that epicuticular wax *n*-alkanes are 10 to 30 fold more abundant in *Ericaceae* than in

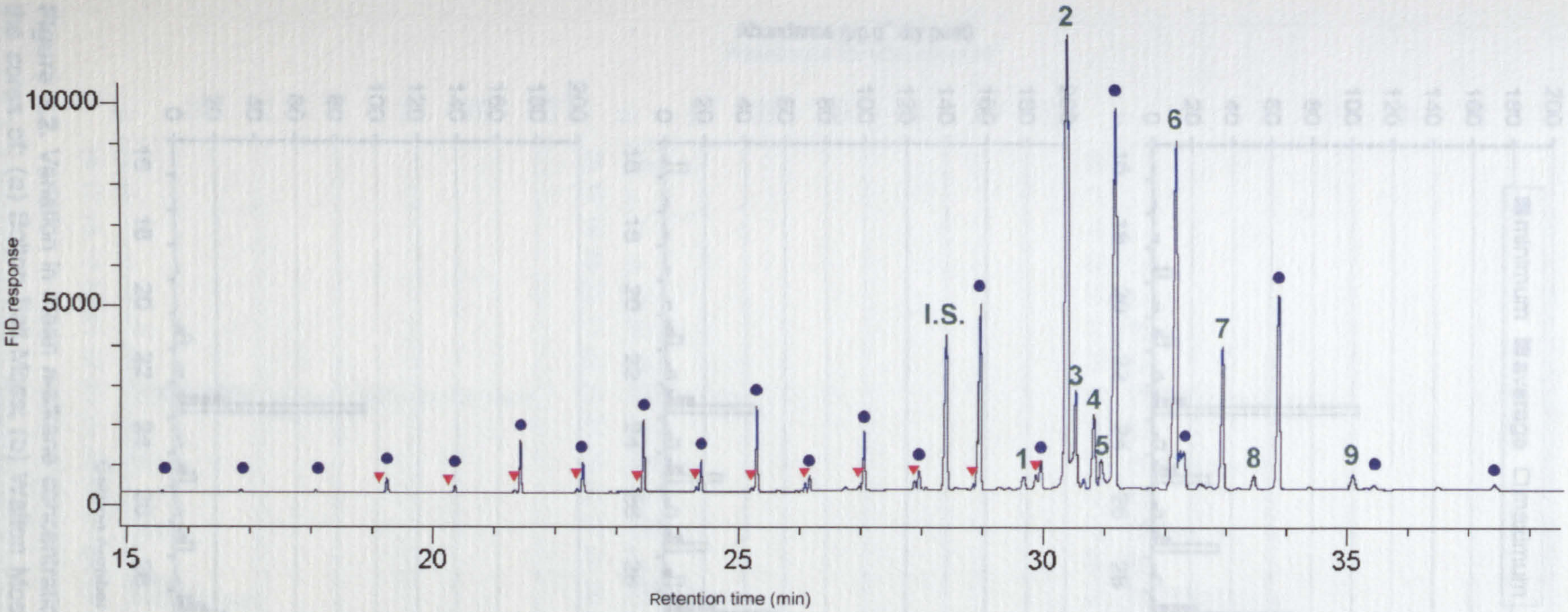

Figure 3.1. Typical partial gas chromatogram of the hydrocarbon fraction of a peat extract (Walton Moss, 78-79 cm depth).

- ● *n*-Alkanes ranging from *n*-C_{16} to *n*-C_{35}
- ▼ Alkenes ranging from $C_{19:1}$ to $C_{29:1}$
- I.S. Internal quantification standard (5-α-Cholestane)
- 1 17β(H)-Trisnorhopane
- 2 Taraxer-14-ene
- 3 Olean-12-ene
- 4 Unidentified triterpenoid
- 5 Urs-12-ene
- 6 Taraxast-20-ene
- 7 17α(H),21β(H)-Homohopane
- 8 Diploptene
- 9 17β(H),21β(H)-Homohopane

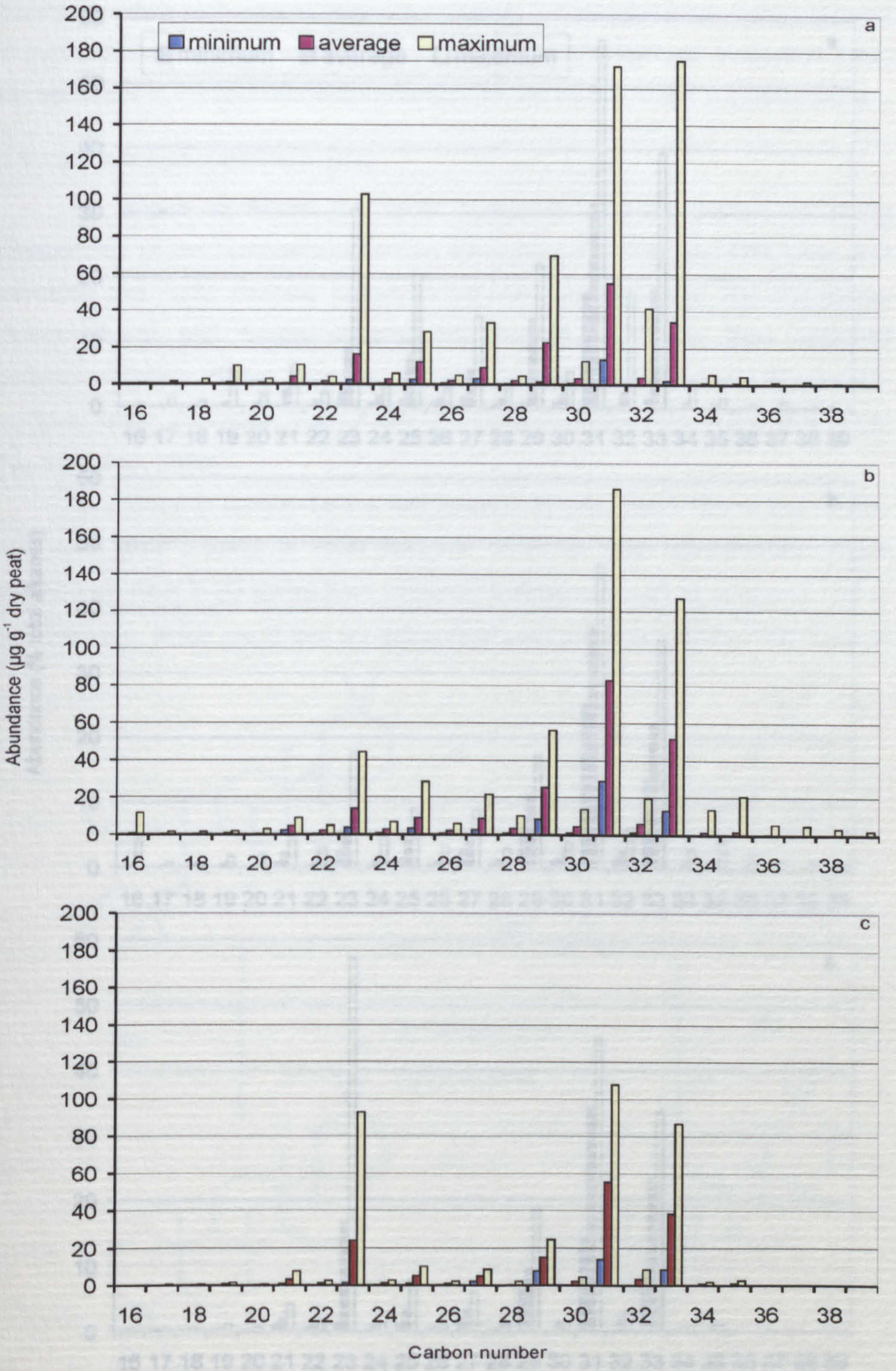

Figure 3.2. Variation in mean *n*-alkane concentrations (µg g^{-1} dry peat) throughout the cores of: (a) Bolton Fell Moss; (b) Walton Moss, and (c) previously published Bolton Fell Moss monolith (Nott, 2000; Nott et al., 2000; Xie et al., in press).

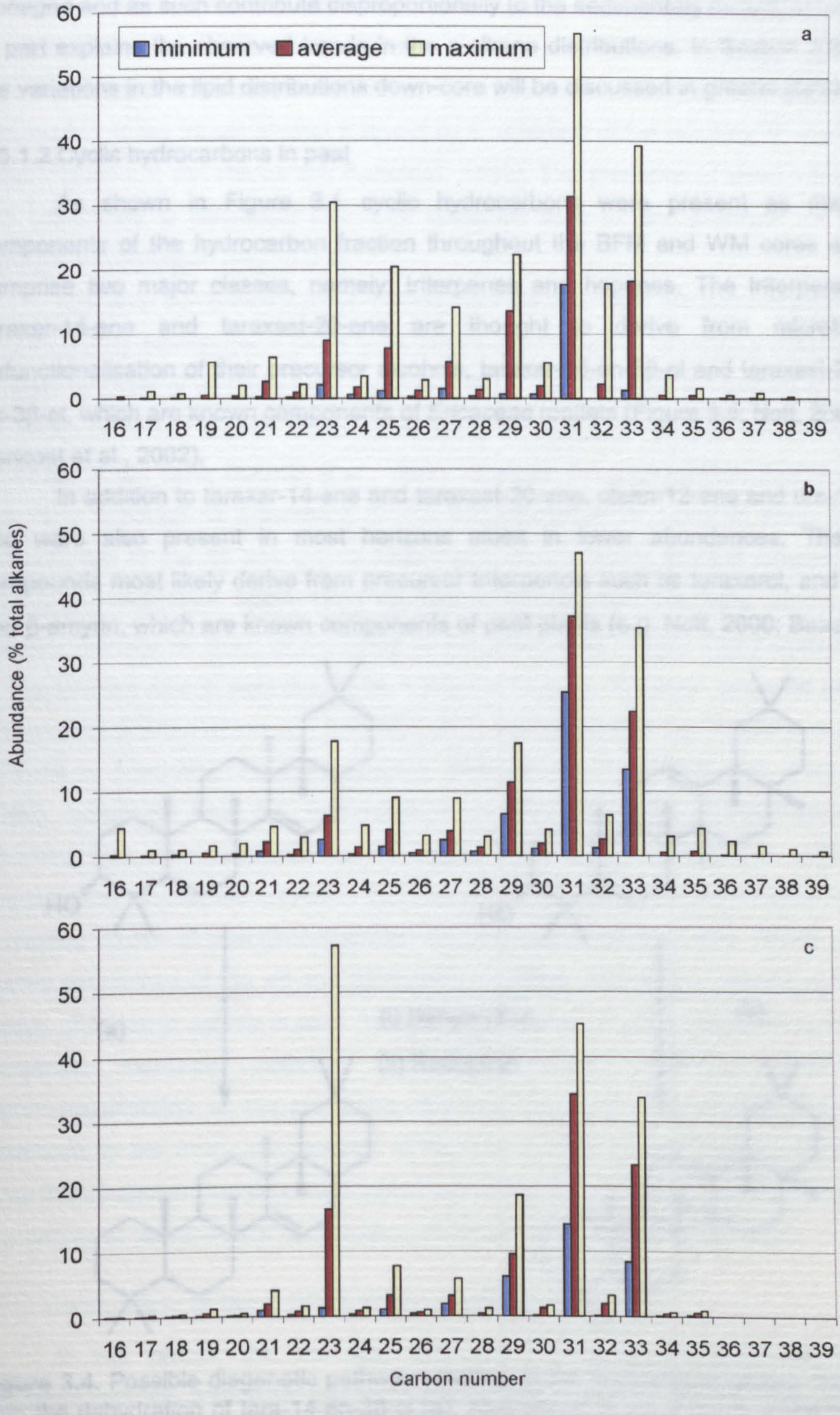

Figure 3.3. Variations in mean *n*-alkane abundances (% of total *n*-alkanes) through the cores of: (a) Bolton Fell Moss; (b) Walton Moss, and (c) previously published Bolton Fell Moss monolith (Nott, 2000; Nott et al., 2000; Xie et al., in press).

Sphagna and as such contribute disproportionally to the sedimentary record, at least in part explains the observed trends in the *n*-alkane distributions. In Section 3.5.2, the variations in the lipid distributions down-core will be discussed in greater detail.

3.5.1.2 Cyclic hydrocarbons in peat

As shown in Figure 3.1 cyclic hydrocarbons were present as major components of the hydrocarbon fraction throughout the BFM and WM cores and comprise two major classes, namely: triterpenes and hopanes. The triterpenes, taraxer-14-ene and taraxast-20-ene are thought to derive from microbial defunctionalisation of their precursor alcohols, taraxer-14-en-3β-ol and taraxast-20-en-3β-ol, which are known components of *Ericaceae* rootlets (Figure 3.4; Nott, 2000; Pancost et al., 2002).

In addition to taraxar-14-ene and taraxast-20-ene, olean-12-ene and urs-12-ene were also present in most horizons albeit in lower abundances. These compounds most likely derive from precursor triterpenols such as taraxerol, and α- and β-amyrin, which are known components of peat plants (e.g. Nott, 2000; Baas et

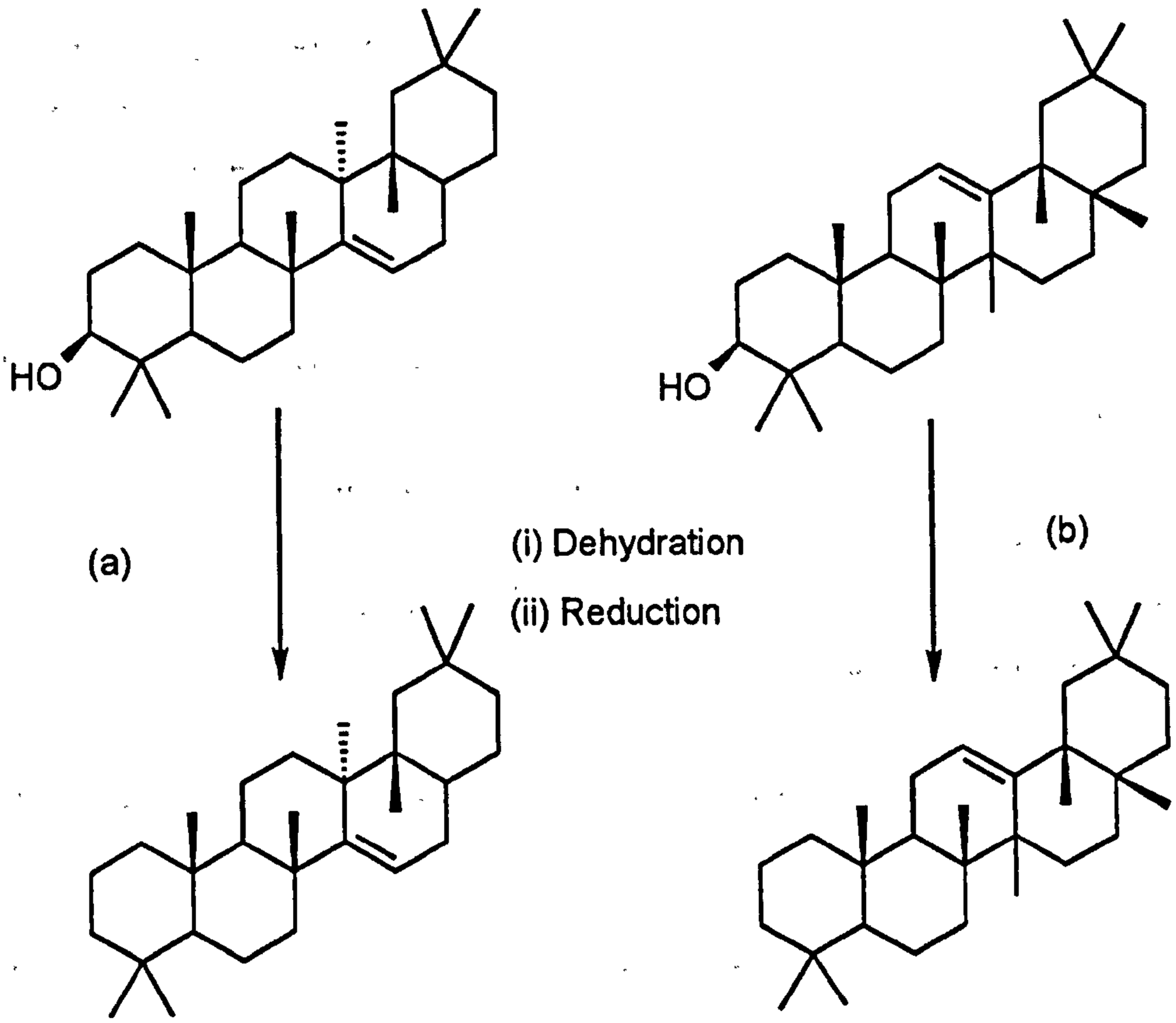

Figure 3.4. Possible diagenetic pathway resulting in the formation of taraxer-14-ene from the dehydration of tara-14-en-3β-ol (a). Also shown is the same reaction for β-amyrin, giving olean-12-ene (b) as end product.

al., 2000). Pancost et al. (2002) reasoned that since neither taraxer-14-ene and taraxast-20-ene were detectable in modern plants, a mechanism for their formation from their likely precursors, taraxast-20-en-3β-ol and taraxer-14-en-3β-ol, involved a dehydration of the parent alcohol followed by a reduction of the resulting Δ^2 double bond (Figure 3.4; ten Haven and Rullkötter, 1988). The presence of olean-12-ene and urs-12-ene is consistent with their formation from α- and β-amyrin via an analogous mechanism (Figure 3.4).

The other components present throughout the core were two homo-hopanes: 17α(H),21β(H)–homohopane and 17β(H),21β(H)–homohopane, previously observed in peats by Quirk et al. (1984) and Dehmer (1995). The presence of hopanes of the ββ series is almost always regarded as being indicative of bacterial populations (Ourisson et al., 1979; Rohmer et al., 1980). However, the origin of the αβ series is less clear although its occurrence is well documented in all types of peat. The isomerisation of the ββ into the αβ homologue occurs during thermal maturation (Peters and Moldowan, 1993). Thus, the ββ/(αβ+ββ) ratio has been long used as a maturity indicator for crude oil (reviewed by Farrimond et al., 1998). The occurrence of this epimerisation in peat cannot be a thermal process. However, since the peat environment is often of low pH, Dehmer (1995) suggested that this maybe a factor involved in promoting the epimerisation. Alternatively, Reis-Kautt and Albrecht (1989) suggested that the epimerisation process might be microbiologically mediated. The latter suggestion would explain the findings of Quirk et al. (1984), who observed an increasing relative abundance of 17α(H),21β(H)–homohopane with increasing degree of peat decomposition and is thus a function of time. Hence, the relative abundance of the αβ and ββ-hopane could be used as an indicator of the degree of bacterial activity in peat. Their overall pathway was suggested to involve microbially mediated oxidative and decarboxylation reactions involving bacteriohopanetetrol as the precursor, with acid catalysed epimerisation at C-17 influenced by the acidic environment of the bog. In Bolton Fell Moss and Walton Moss the αβ epimer was present in higher abundances than the ββ epimer, which is in accordance with previous observations (Dehmer, 1995; Quirk et al., 1984).

3.5.2 Comparison of two 1,000 y hydrocarbon records

In this section the two new hydrocarbon records are discussed and compared with the analogous record previously developed for the 40 cm monolith from Bolton Fell Moss (Nott, 2000; Nott et al., 2000; Xie et al., in press).

3.5.2.1 *n*-Alkanes

Figure 3.5 shows the variations in the abundances in the major *n*-alkanes in the Bolton Fell Moss and Walton Moss peat cores spanning the last 1,000 years. The plots are presented as variations in a specific *n*-alkane as a percentage of total *n*-alkane abundances, in order to compare the distribution changes down the core and exclude differences in absolute concentrations; in general variations in the abundances of individual *n*-alkanes show little co-variation with one another. This is not unexpected since plant inputs (the main source of the hydrocarbons) have been shown, from earlier macrofossil analyses of other cores, to vary between the cores, and as discussed above a small increase in the growth of *Ericaceae* can cause a substantial increase in total *n*-alkane input due to the higher *n*-alkane content of *Ericaceae* species compared with *Sphagnum* species (Table 3.2).

Within each core the variations in abundance of individual *n*-alkanes show similarities among *n*-C_{21}, *n*-C_{23}, *n*-C_{25} and, to a lesser degree, *n*-C_{27}. In contrast, the longer-chain length alkanes (*n*-C_{29}, *n*-C_{31} and *n*-C_{33}) do not correlate with one another with depth. Such differences in the patterns of variations between the short- and long-chain *n*-alkanes are to be expected since the shorter-chain alkanes (*n*-C_{21}, *n*-C_{23}, *n*-C_{25}) almost exclusively derive from *Sphagnum*, while the longer-chain alkanes are contributed by a variety of different plant species. The largest variations within the down core records are seen in the shorter-chain-length alkanes, especially with the respect to the high abundance of *n*-tricosane (*n*-C_{23}) in the BFX core (Nott, 2000; Nott et al., 2000), which has previously been linked with climate and vegetation changes recorded in the peat profile. The *n*-alkane down-core profiles derived for the new cores (BFM, WM) examined in this thesis do not show such large variations in *n*-tricosane component over the past thousand years.

A comparison of all three cores does not reveal obvious similarities between their respective *n*-alkane down-core profiles when expressed as percent relative abundances. Correspondingly, Average Chain Length and Carbon Preference Index do not show co-varying trends for the three cores (Figure 3.7).

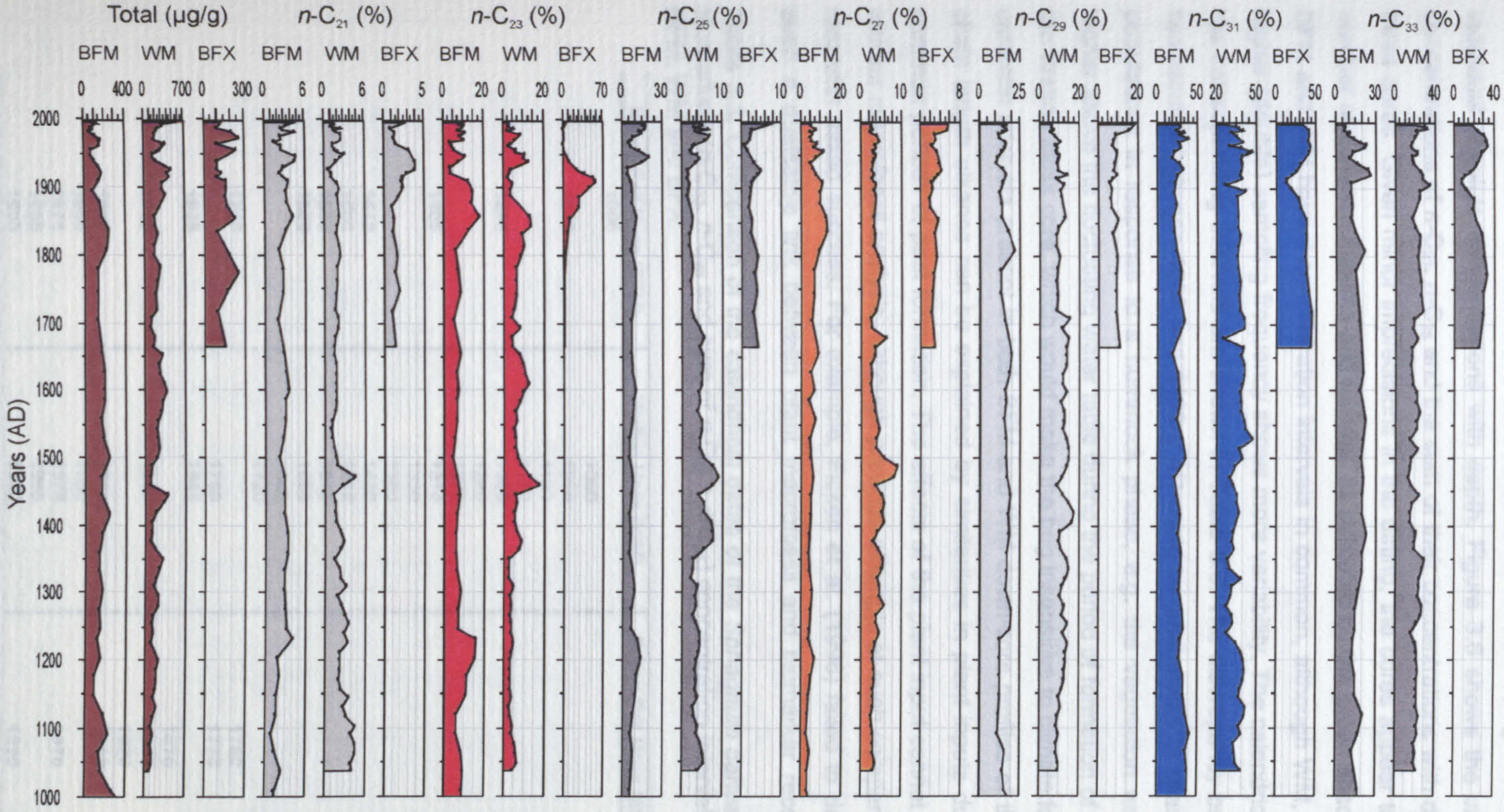

Figure 3.5. Down-core variations in *n*-alkane abundances presented as percent of total *n*-alkanes abundances against the calendrical age model developed in Chapter 2 for Bolton Fell Moss (BFM) and Walton Moss (WM), compared with the results of the previous study by Nott (BFX, Nott, 2000; Nott et al., 2000; Xie et al., in press).

The shorter-chain length alkanes do show co-varying trends in their individual absolute concentrations with depth. Figure 3.6 shows the variations in concentrations of *n*-C_{23}, *n*-C_{25} and the sum of their concentrations with depth for all three cores. Given minor imprecisions in the dating, the cores appear to display a number of common maxima and minima, as indicated by the green shaded blocks. BFM and WM have 9 concentration intervals in common, although WM, due to the higher (double) sampling frequency shows more variability. The calendrical dates of the corresponding intervals are shown in Table 3.3. The discrepancy between the two records between 1050 and 1190 y AD could be attributable to changing plant populations in response to a hummock phase, e.g. the vegetation was growing higher above the fluctuating water table during the period of formation of this part of the Walton Moss core, which would make the bog insensitive to climate forcing. The common intervals present in both BFM and WM down-core profiles of the shorter-chain length alkanes can be explained by similarities in plant inputs during those common periods of peat formation. The effects of the plant input cannot be verified without macrofossil analysis, although previous attempts at such comparisons have met with mixed success. For example, Ficken et al. (1998) failed to demonstrate even a qualitative link between plant macrofossil and biomarker records, while

Table 3.3. Comparison of the calendrical dates of the *Sphagnum* derived *n*-alkane biomarkers (*n*-C_{23}, *n*-C_{25} and sum of *n*-C_{23} + *n*-C_{25}) concentration intervals for cores BFM, WM and BFX.

Bolton Fell Moss (BFM)	Walton Moss (WM)	Bolton Fell Moss (BFX)[a]
1000		
	1050	
1090	1090	
	1130	
	1170	
1205	1200	
	1240	
	1275	
1305	1310	
	1330	
	1360	
1410	1430	
1500	1515	
1600	1610	
1650	1650	
	1680	
	1720	
1740		1750
	1780	1775
1835	1845	
		1870
1905	1905	1905
		1920
1940	1940	1940
1960	1960	
1971	1975	1970
1985	1985	
1990	1990	1990

(a) Nott, 2000; Nott et al., 2000

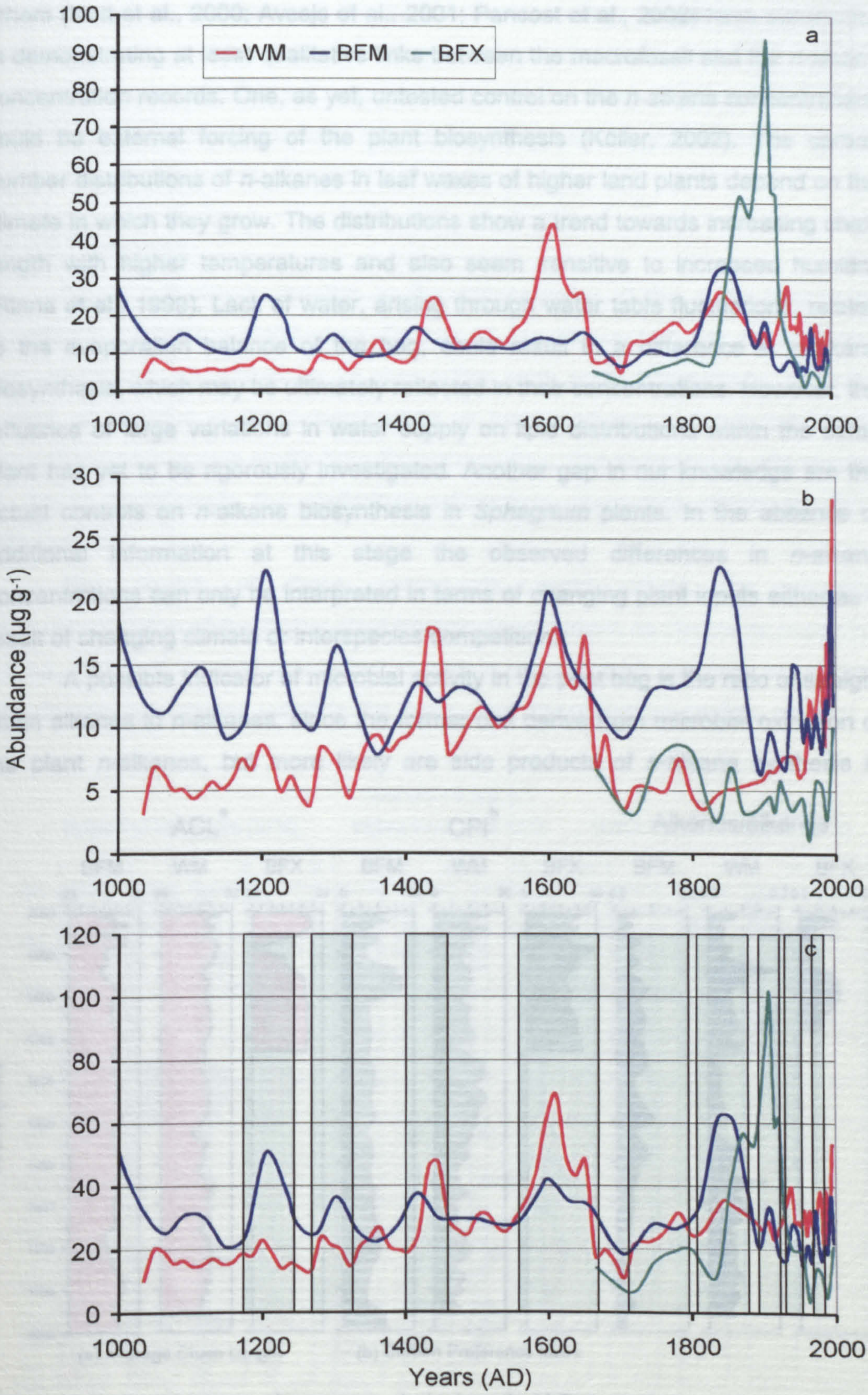

Figure 3.6. Variation of concentrations of (a) *n*-C_{23}; (b) *n*-C_{25}, and (c) sum *n*-C_{23} + *n*-C_{25}, of for BFM, WM and BFX. Green boxes highlight time intervals showing co-varying trends in *n*-alkanes concentration.

others (Nott et al., 2000; Avsejs et al., 2001; Pancost et al., 2002) have succeeded in demonstrating at least qualitative links between the macrofossil and the *n*-alkane concentration records. One, as yet, untested control on the *n*-alkane concentrations could be external forcing of the plant biosynthesis (Köller, 2002). The carbon number distributions of *n*-alkanes in leaf waxes of higher land plants depend on the climate in which they grow. The distributions show a trend towards increasing chain length with higher temperatures and also seem sensitive to increased humidity (Rinna et al., 1999). Lack of water, arising through water table fluctuations, related to the evaporation balance of the bog, could result in a difference in *n*-alkane biosynthesis, which may be ultimately reflected in their concentrations. However, the influence of large variations in water supply on lipid distributions within the same plant has yet to be rigorously investigated. Another gap in our knowledge are the actual controls on *n*-alkane biosynthesis in *Sphagnum* plants. In the absence of additional information at this stage the observed differences in *n*-alkane concentrations can only be interpreted in terms of changing plant inputs either as a result of changing climate or interspecies competition.

A possible indicator of microbial activity in the peat bog is the ratio of straight chain alkenes to *n*-alkanes, since the former can derive from microbial oxidation of the plant *n*-alkanes, but more likely are side products of *n*-alkane synthesis in

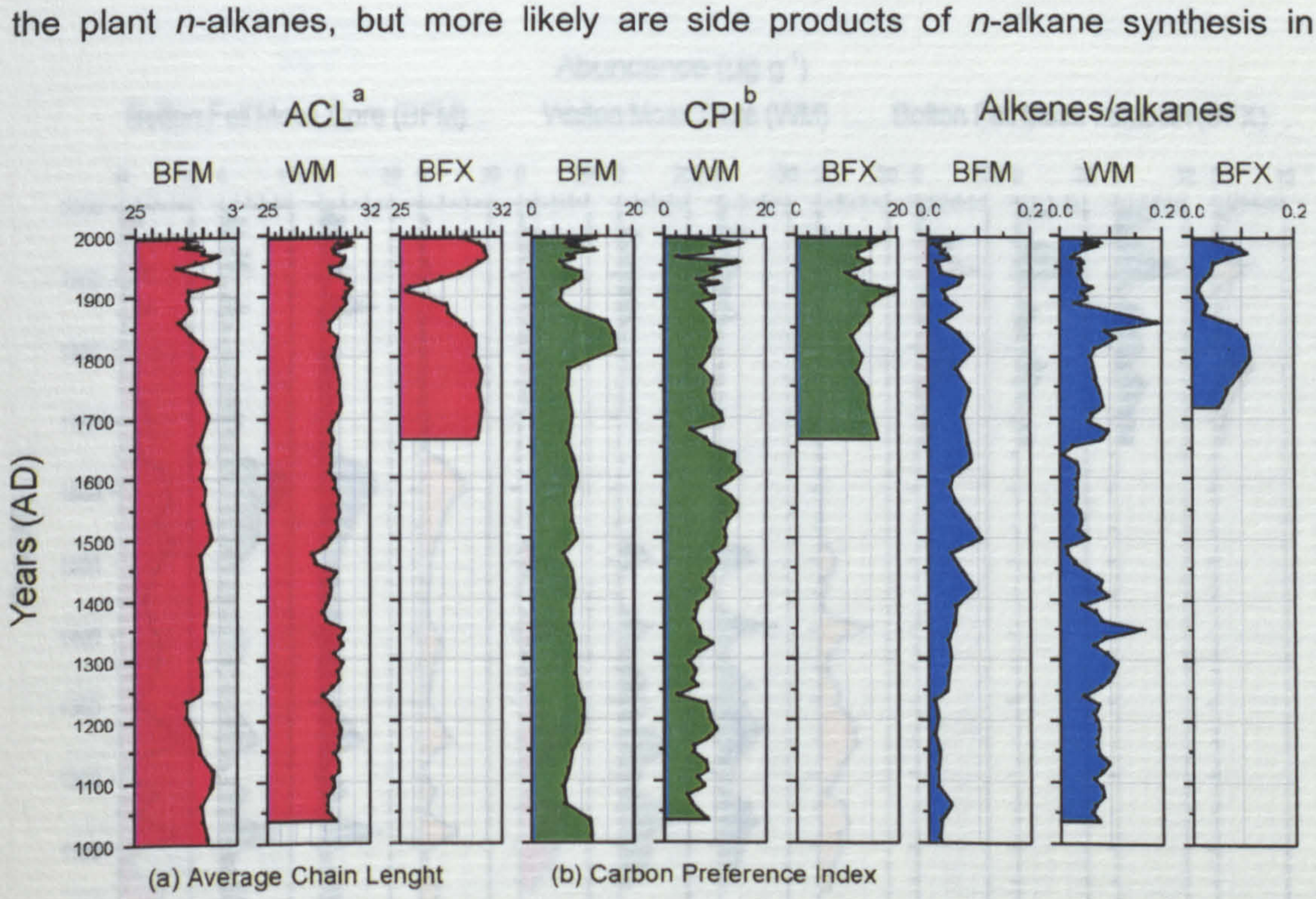

Figure 3.7. Comparison of average chain length (ACL), carbon preference index (CPI) and $C_{19:1}/C_{29:1}$-alkene/alkane ratio for Bolton Fell Moss (BFM; BFX, Nott, 2000) and Walton Moss (WM) plotted against the calendrical age model developed in Chapter 2.

organisms (plants and bacteria). Figure 3.7 shows no clear co-varying trend in the relative proportions of the alkenes/*n*-alkanes between the three cores. The lack of a coherent trend is perhaps not unexpected due to sampling uncertainties and the different local micro-environments needed for the growth of populations of specific groups of organisms.

3.5.2.2 Triterpenes

Figure 3.8 shows variation in the concentration of the major triterpenes identified in the BFM and WM cores. Taraxer-14-ene, taraxast-20-ene, olean-12-ene and urs-12-ene concentrations co-vary within each core. Interestingly, a similar pattern of variation in the concentrations of taraxer-14-ene and taraxast-20-ene were observed in a peat profile from Bargerveen Bog, The Netherlands, (Pancost et al., 2002). Significantly, few similarities exist among down-core profiles for BFM, WM and BFX.

The record of these compounds might reflect the microbial defunctionalisation of the higher plant triterpenol precursors as discussed in section 3.5.1.2. However, it might also reflect change in input through changing vegetation. The co-varying patterns noted in the down-core concentration profiles suggest a

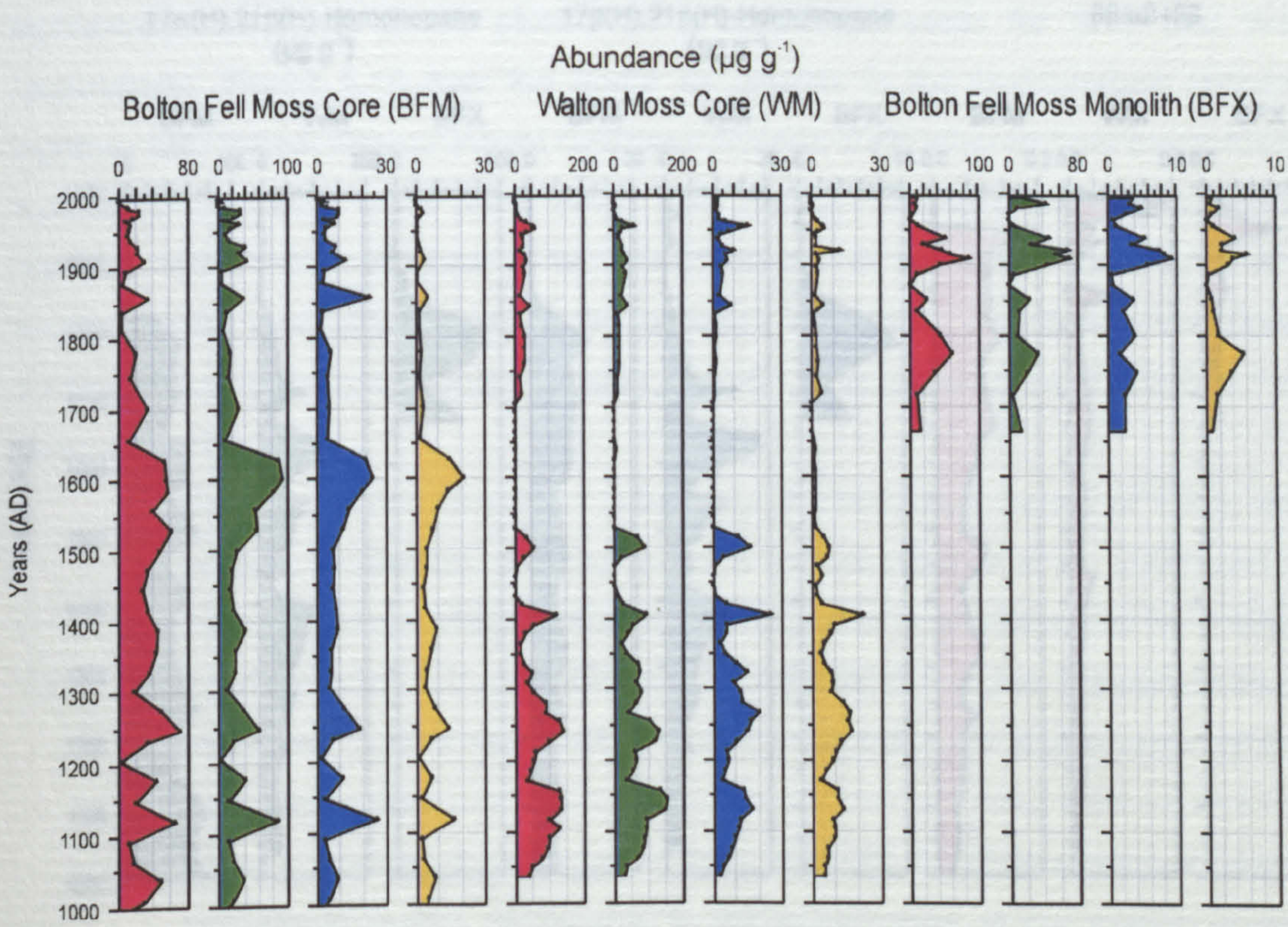

Figure 3.8. Down-core plots of the variations in concentrations (µg g^{-1}) of the major triterpenes: taraxer-14-ene (red), taraxast-20-ene (green), olean-12-ene (blue), and urs-12-ene (yellow) for the BFM, BFX and WM.

common source. Most likely this is the changing plant inputs (input of the precursor material).

3.5.2.3 Hopanes

Figure 3.9 shows the variations in the concentration of the αβ and ββ-homohopanes with depth in the BFM, WM and BFX cores. The abrupt increase in the concentration of both epimers at the depth at which the catotelm (anoxic zone) begins is striking, since these compounds are thought to drive primarily from aerobic bacteria (Ourisson et al., 1979; Rohmer et al., 1980). An explanation for their appearance is that they are diagenetic products, formed via microbial transformations of functionalised hopanoids, e.g. bacteriohopanetetrol, which occur widely in aerobes. As such they are indicative of microbial diagenesis. Within each core the αβ epimer is ca. 10 times more abundant than the ββ epimer. As discussed above for the triterpenes the similarities between the down-core concentration profiles of the different hopanes within the same core clearly suggests a common source of functionalised precursors, with the variations in concentration probably being controlled by variations in microbial populations (hopanoid producers) and/or in the degree of microbial activity (hopanoid degraders). Overall, there is no obvious

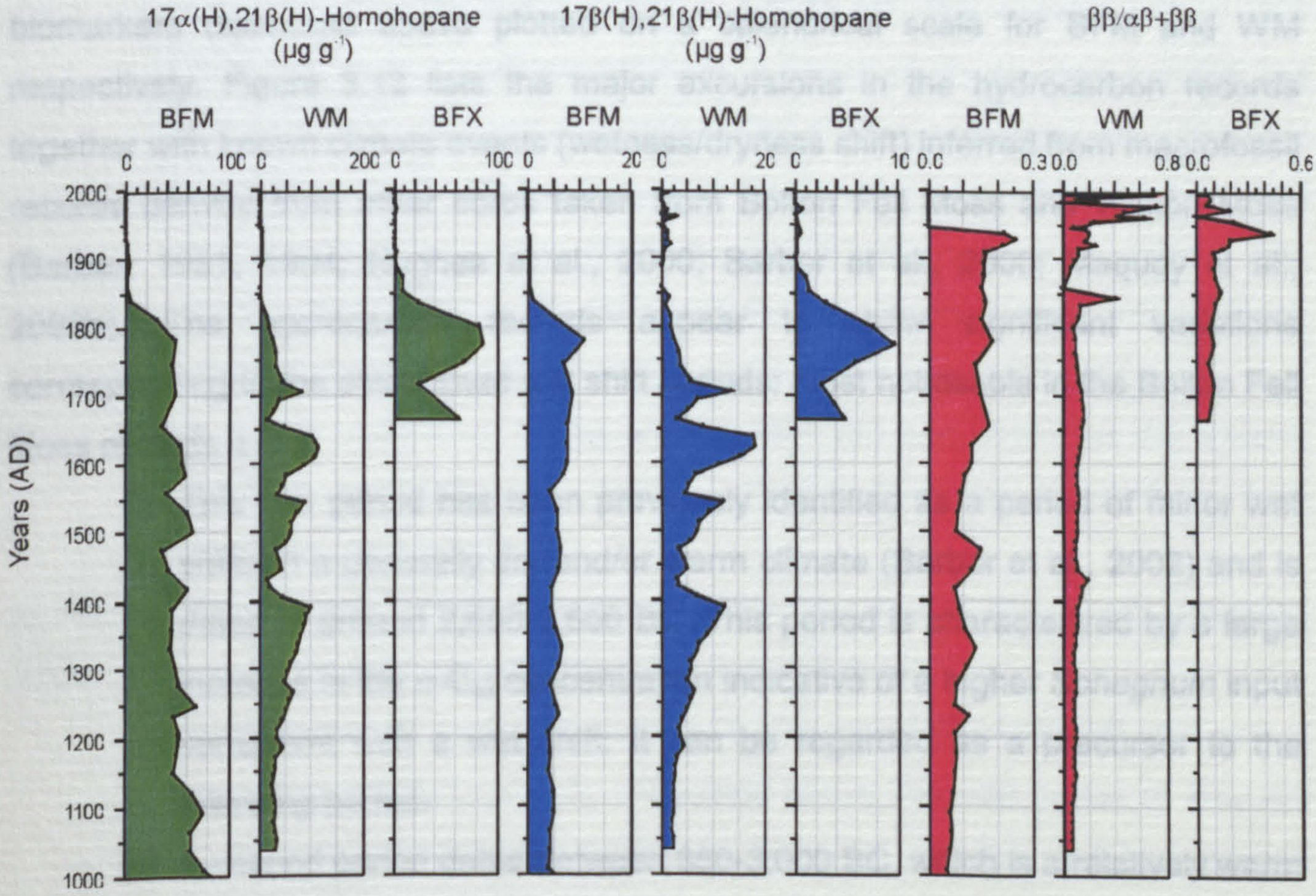

Figure 3.9. Down-core plots of the variations in the concentrations of 17α(H),21β(H)-homohopane and 17β(H),21β(H)–homohopane abundances, and the diagenetic ratio: ββ/(αβ+ββ), for BFM, WM and BFX.

trend in the concentrations of the hopanes that can be matched with other biomarker proxies or known climatic events.

The ββ/(αβ+ββ) ratio, which in crude oils is a known maturity indicator (Farrimond et al., 1998), describes the conversion of the ββ epimer into the αβ epimer. However, as discussed above, this epimerisation cannot be thermally driven in peat bogs as it is in oil source rocks. Several have made the link between the varying abundances of the two epimers and the acidic nature of peat bogs. Indeed, Pancost et al. (2003) proposed the ββ/(αβ+ββ) ratio as a possible indicator of pH of the bog, which is influenced by plant species and dilution factors due to water content. An increased abundance of the ββ-hopane relative to the αβ epimer may be the result of increased water content of the peat reducing the pH in the region of the catotelm. The ββ/αβ+ββ ratio is seen to decline gradually through the core, which is presumably indicative of progressive diagenetic alterations.

3.5.3 5,500 y hydrocarbon record from Bolton Fell Moss

Radiocarbon dating (Chapter 2) of a 500-cm core from Bolton Fell Moss indicated that the core spanned a period from the present back to 5,500 y BP. Figure 3.10 and Figure 3.11 shows the concentrations and ratios of the major biomarkers discussed above plotted on a calendrical scale for BFM and WM respectively. Figure 3.12 lists the major excursions in the hydrocarbon records together with known climate events (wetness/dryness shift) inferred from macrofossil records derived from other cores taken from Bolton Fell Moss and Walton Moss (Barber, 1981, 1994; Hughes et al., 2000; Barber et al., 2000; Maquoy et al., 2002b). The hydrocarbon records appear to show significant variations corresponding to the established wet shift periods; most noticeable in the Bolton Fell Moss records is:

(i) This first period has been previously identified as a period of minor wet shifts in a generally dry and/or warm climate (Barber et al., 2002) and is dated at around 2,600-3,600 BC. This period is characterized by a large increase in the *n*-C_{23} concentration indicative of a higher *Sphagnum* input consistent with a wet shift. It can be regarded as a precursor to the following period.

(ii) A second period dated between 850-3,000 BC, which is a relatively warm and stable period. Noticeable is the appearance of the homohopanes around 1700 BC, mainly due to the increased conversion of the ββ epimer into the αβ epimer (decrease in the ratio, which achieves its

highest ratio in this period). Also remarkable is the almost constant concentrations of most components and their respective ratios. Proof that the climate has stabilised over a long period of time. Nonetheless, macrofossil data have indicated a small number of minor wet shifts during this period (Figure 3.12).

(iii) A third period dated between 220-850 BC evident in the hopane concentration and *n*-alkane ACL records correspond to the Sub-boreal/Sub-atlantic transition (van Geel et al., 1996; Barber et al., 2002). The onset of this period is regarded as involving a shift towards wetter and/or cooler climate and this is reflected in the lower ACL values as a result of an increased relative abundance of the shorter chain *n*-alkanes derived from *Sphagmun spp*. The wet shift at this time is mirrored by the ca. 4-fold decrease in the concentration of the *n*-C_{31}, which is characteristic of higher plants, such as *Ericaceae*. The increase in the higher plant derived triterpenes from the mid-point to the end of this period is consistent with root penetration from the new growth of higher plants during the Roman period.

(iv) A period of high amplitude, frequent and rapid change occurs in all of the biomarker records between 500 and 1200 AD. This corresponds to what is known as the medieval optimum, a period of dry summer months, but relatively high annual precipitation. The $\delta^{18}O$ records from ice cores, tree rings and speleothems show that this period was followed by a trend towards climatic cooling (Roberts, 1998; McDermot et al., 2001). This latter period is not easily discerned from the biomarker records although all the records appear to become more stable after 1,200 AD.

(v) A period of cooling, dating around 1850 AD and known as the second part of the Little Ice Age is characterized by a relatively high concentration of *n*-C_{23}.

In Figure 3.11 the same overview is presented for the Walton Moss core, spanning 1000 y. The most distinct periods detectable in the core are:

(i) A third period of marked change is between 1100-1400 AD, the end of the Medieval Optimum. As discussed above this was period of frequent and rapid change due to the dry summer months and high annual precipitation. The period is characterised by a large increase in and fluctuations in triterpene concentrations, together with strong fluctuations in the *n*-alkane ACL and CPI; in contrast the concentration of the *n*-C_{23}

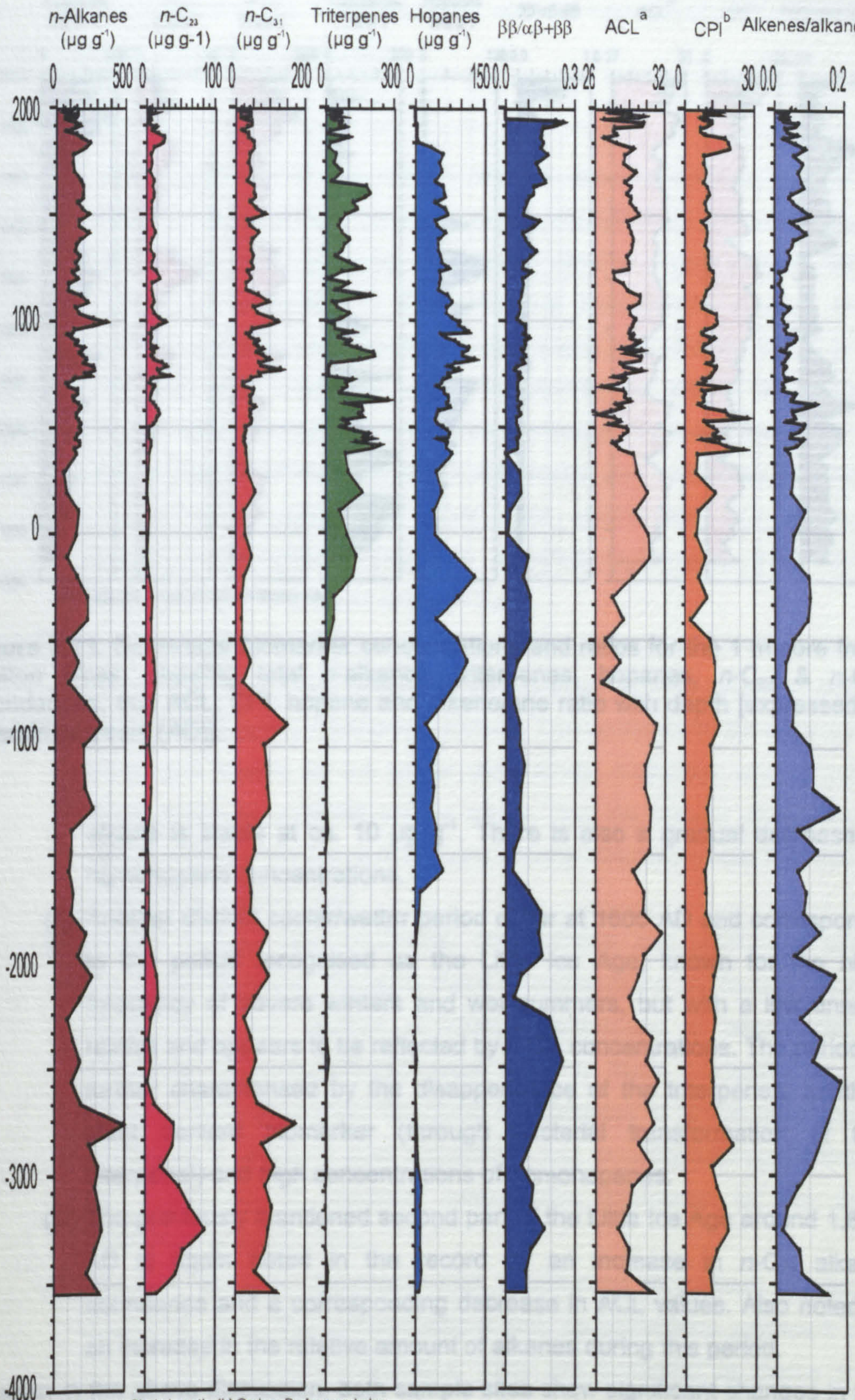

Figure 3.10. Down-core biomarker concentrations and ratios for the 5 m core from Bolton Fell Moss; showing total *n*-alkanes, triterpenes, hopanes, *n*-C_{23} & *n*-C_{31} abundances, and ACL, CPI, hopane and alkene/ane ratio with depth [expressed in calendrical years (AD)].

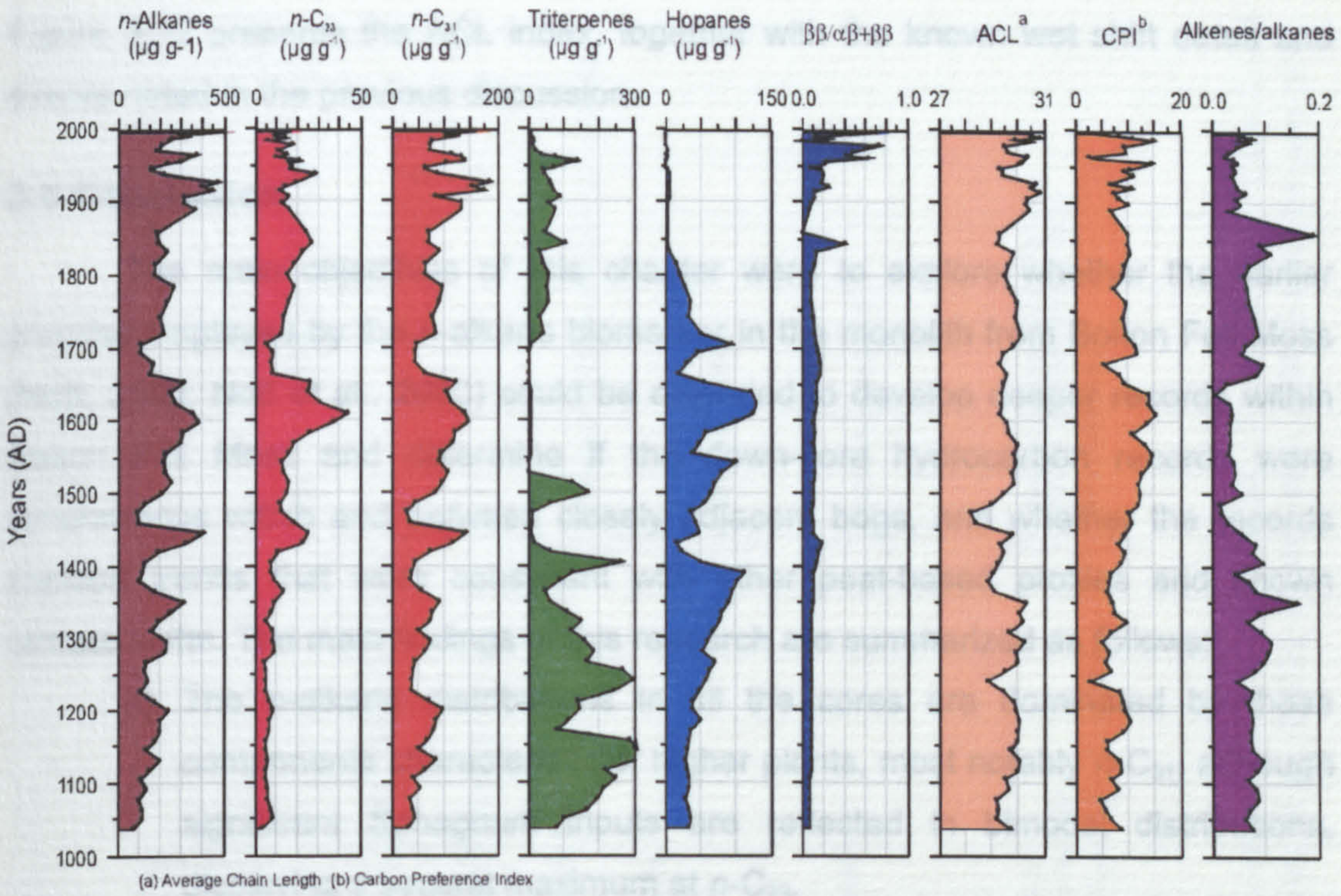

Figure 3.11. Down-core biomarker concentrations and ratios for the 1 m core from Walton Moss; showing total *n*-alkanes, triterpenes, hopanes, *n*-C_{23} & *n*-C_{31} abundances, and ACL, CPI, hopane and alkene/ane ratio with depth [expressed in calendrical years (AD)].

alkane is stable at ca. 10 µg g^{-1}. There is also a gradual decrease in homohopane concentrations.

(ii) Another distinct cooler/wetter period occur at 1600 AD and corresponds to the period recognised as the Little Ice Age, known for the high frequency of severe winters and wet summers, but with a low annual rainfall and appears to be reflected by *n*-C_{23} concentrations. The period is further characterised by the disappearance of the triterpenes, another plant derived biomarker (through bacterial transformation of the triterpenol) and high concentrations of homohopanes.

(iii) The previously mentioned second part of the Little Ice Age around 1,850 AD is again noted in the record by an increase in *n*-C_{23} alkane abundance and a corresponding decrease in ACL values. Also noted is an increase in the relative amount of alkenes during this period.

As seen in the above discussion, both sample sites show significant changes in the hydrocarbon abundances at times of changing climate. Although not conclusive by themselves, taken together they form a record of climatic change, either due to differences in input through changing plant species or due to direct climatic forcing.

Figure 3.12 presents the ACL index, together with the known wet shift dates and events noted in the previous discussion.

3.6 Conclusion

The main objectives of this chapter were to explore whether the earlier promise displayed by the *n*-alkane biomarker in the monolith from Bolton Fell Moss (Nott, 2000; Nott et al., 2000) could be extended to develop deeper records within Bolton Fell Moss and determine if the down-core hydrocarbon records were synchronous within and between closely adjacent bogs, and whether the records showed trends that were consistent with other peat-based proxies and known climate shifts. The main findings of this research are summarized as follows:

(i) The *n*-alkane distributions in all the cores are dominated by those components characteristic of higher plants, most notably *n*-C_{31}, although significant *Sphagnum* inputs are reflected in bimodal distributions, displaying a second maximum at *n*-C_{23}.

(ii) Synchronicity of the down-core concentration records of the shorter chain length alkanes (*n*-C_{21}, *n*-C_{23} and *n*-C_{25}) point to their common origin, namely being purely *Sphagnum* derived. This contrasts to the behavior of down-core records for the longer chain length *n*-alkanes, which have a wider range of potential source plants. But the shorter chain length alkane records are not synchronous among different cores, this due to differences in plant input.

(iii) Taraxer-14-ene, taraxast-20-ene, olean-12-ene and urs-12-ene occur throughout the cores. Because these compounds are not found in higher plants and have obvious structural relationships to triterpenols, a diagenetic precursor-product relationship is likely. Variations in the concentrations throughout the cores are assumed to reflect variations in inputs due to changing plant populations and, possibly heterogeneities in the distribution of microbial communities influenced by the local conditions within the mire.

(iv) Hopanes occur in reasonably high abundances throughout the cores especially within the catotelm where their concentrations approach that of the most abundant *n*-alkane. They are assumed to derive from diagenetic alterations of functionalised hopanoids biosynthesized by aerobic bacteria living in the acrotelm. The ββ/αβ+ββ hopane ratio decreased with depth, which was attributed to a microbially mediated epimerisation promoted by the elevated pH of the peat bog.

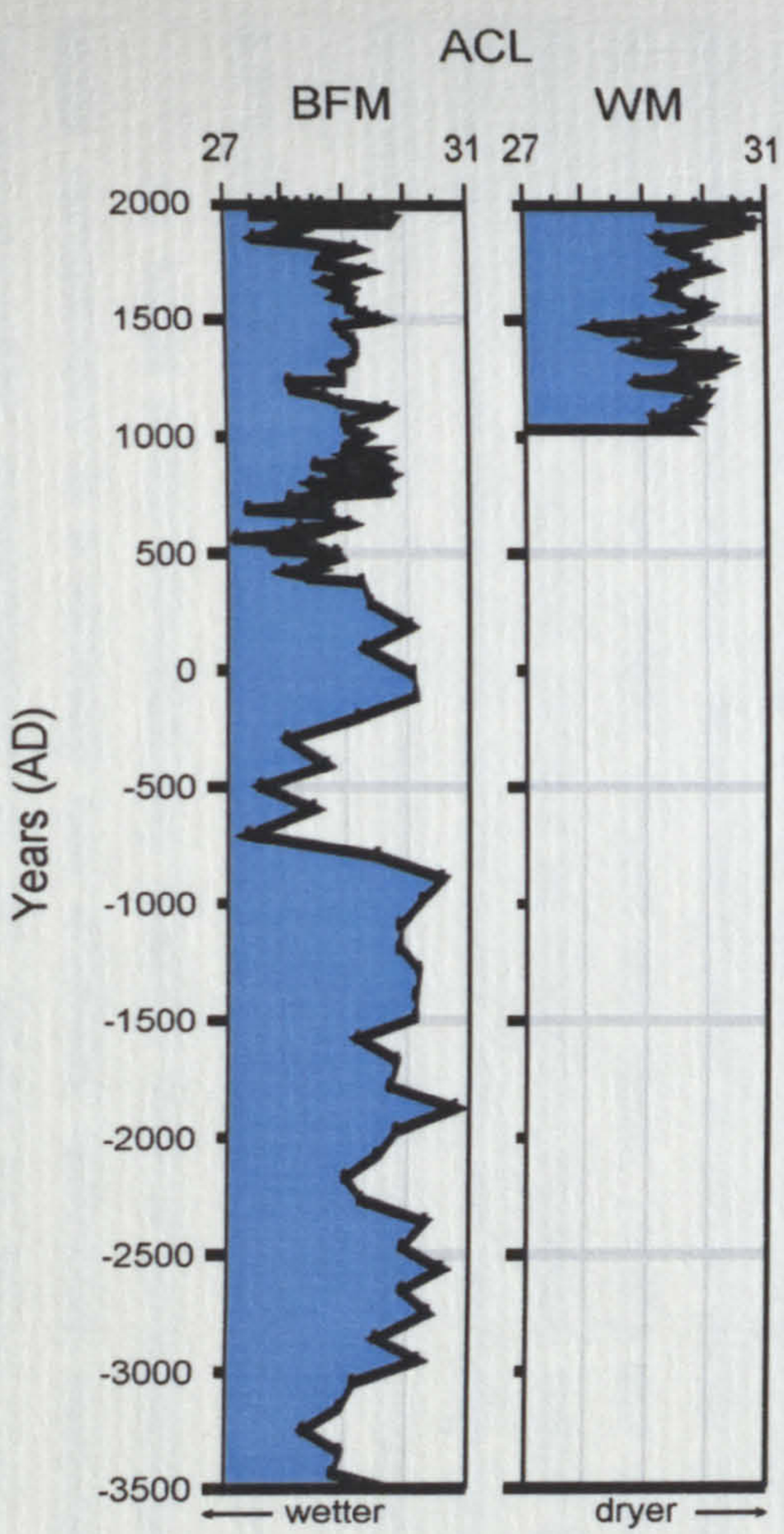

Wet shift dates WM	Wet shift dates BFM	Events in the hydrocarbon record	
1850		maxima in alkanes and CPI	
1770	1740		
1600		maxima n-C_{23}; no triterpenes	
1580			
1440	1450		
1380	1330		large fluctuations in all records
1230	1230		
1200			
	950	maxima alkanes, hopanes	
	780	maxima alkanes, hopanes; minima triterpenes	
	650		
	550		
500			
200		minima alkanes; maximum triterpenes	
-90		maxima triterpenes	
	-250		
-370		maximum n-C_{23} abundance and alkene/alkane	
	-400	minima in hopanes	minima in ACL, maximum in hopanes
	-490		
	-630		
-910	-950	triterpenes appear in record	
	-1070		
-1220	-1250		maxima alkanes
-1440			
-1550	-1650		
	-1800		
	-2070	start larger amounts of hopanes	maxima ββ/αβ+ββ
	-2330		
-2460	-2400	maxima ββ/αβ+ββ	
	-2670		
		maxima ββ/αβ+ββ	
		maxima alkene/alkane ratio	maxima alkane abundances
		maxima n-C_{31}; n-C_{23} abundance	minima alkene/alkane ratio
-3350	-3300	maxima n-C_{23} abundance and ββ/αβ+ββ ratio	some hopanes
	-3470		

Figure 3.12. Major excursions in the 5500 y hydrocarbon record from Bolton Fell Moss and Walton Moss (see also Figure 3.10 & Figure 3.11) compared with wet shift dates derived from BFM and WM [Barber, (1981, 1994), Hughes et al. (2000), Barber et al. (2000) and Maquoy et al. (2002b)]. Also shown is the ACL index showing all the major periods of fluctuation.

(v) Finally, a possible link between climate and hydrocarbon concentrations and abundance ratios is reflected in the matching of major excursions of the hydrocarbon profile with known climatic events, thereby confirming that meaningful links exist between climate, vegetation and biomarker hydrocarbon records. Especially noteworthy is the link between known climate periods and the fluctuations in the ACL index.

When studying the other fractions in the peat lipid extract, the results obtained will be comparable to the results given by the hydrocarbon fraction, since investigations of all the fractions suffer the same difficulties in interpreting their profiles. As seen by Avsejs and Nott (Nott, 2000, Nott et al. 2000, Avsejs, 2001, Avsejs et al., 2002) biomarkers have been identified in the other fractions, but yield the same information as the hydrocarbons studied in this thesis, or they are indicative of the other plants in the bog (e.g. 5-alkylresorcinols are sedge-specific biomarkers). The relative ease of analyses of the hydrocarbons make them ideal in providing basic climatic information, supplementing the data obtained by macrofossil analyses. In addition to providing biomarker proxy records in their own right the concentrations of hydrocarbons determined in this Chapter provide additional baseline information required for the compound-specific δD determinations reported in Chapter 5. However, before reporting these results the following Chapter discusses important aspects of instrument performance and calibration necessary to ensure reliable down-core δD records are obtained on which to base climate reconstructions.

4 Deuterium Isotope Ratio Mass Spectrometry: Practical Considerations during Data Acquisition

4.1 Introduction

The use of deuterium isotope ratios in palaeoclimate studies has a long history, with most work having been performed on stable isotope variations in ice cores (Jouzel et al., 1990). However, increasing attention is being placed on other natural isotope recorders, such as speleothems (Atkinson et al., 1986), tree rings (Yapp and Epstein, 1982) and peat (Xie et al., 2000). The determination of δD values in water of ice cores has been used to reconstruct long temperature records (>400 ky, Vostok record, Jouzel et al., 1990). Another major area where δD values are implemented is the study of climate reconstructions using tree rings. The major component being measured is 5α-cellulose; however, the method is problematic due to the isotopic fractionations occurring within the plants. Nevertheless, a number of studies have revealed strong correlations with temperature and humidity (Burk and Stuiver, 1981; Yapp and Epstein, 1982). The same technique has been applied to the study of peat cellulose, however, since peat is a complex mixture of decaying plant species, no clear signal could be obtained. The combined signal from the different species was found to complicate the generation of any coherent climate record (Brenninkmeijer et al., 1982; Dupont and Mook, 1987; van Geel and Middeldorp, 1988). With the discovery of species-specific biomarkers (Nott et al., 2000; Baas et al., 2000; Avsejs et al., 2002 and this thesis, Chapter 3) and the development of a new instrument for the determination of compound-specific δD values, the possibility was recognised of further developing δD records in peat for palaeoclimate reconstructions. Hence the promise shown by earlier studies of peat by Brenninkmeijer et al., (1982), Dupont and Mook, (1987) and van Geel and Middeldorp, (1988), can now perhaps be achieved. However, before δD records based on individual components can be constructed, the operating conditions and analytical performance of the new technique needed to be fully assessed.

4.1.1 Overview of the compound-specific δD technique

As noted in the introductionary chapter, thermal conversion isotope ratio mass spectrometry is a relatively new analytical technique, developed for the compound-specific measurements of δD values by Hayes and co-workers (Burgoyne and Hayes, 1998). The instrument used in this study is based on their

design. Its main characteristic is an open ceramic reactor tube, while other designs have been proposed and are in use, notably the filling of the reactor with a catalyst (Tobias et al., 1995; Tobias and Brenna, 1997).

A combined gas chromatograph isotope ratio mass spectrometer possesses the following essential characteristics:

(i) Components are separated by gas chromatography.

(ii) Components are converted post GC into a characteristic analyte.

(iii) Connection between GC/reactor and the mass spectrometer is made through an open split interface, with as much effluent passing in the source as possible (typically 0.4 ml He min^{-1}).

(iv) A dedicated high precision magnetic sector field instrument, records the analyte simultaneously in Faraday cups.

These characteristics are the same for all kinds of GC-IRMS instrumentation, whether they are designed for carbon, nitrogen or deuterium determinations. Two major hurdles exist in relation to the determination of compound-specific δD values (Hilkert et al., 1999):

(i) The isotopic analysis is carried out on hydrogen gas, meaning that all compounds have to be converted into this gas from their original structure and it is vital that this conversion is quantitative. Burgoyne and Hayes (1998) have shown that pyrolysis using temperatures above 1400°C converts all compounds quantitatively to hydrogen gas, thereby overcoming the problem.

(ii) The determination of relative abundances of *m/z* 2 and 3 in the presence of helium carrier gas. The main hurdle is the conversion in the ion source of helium into the $^4He^{+\cdot}$ ion, which interferes with the weak HD *m/z 3* ion. The instrument developers at Finnigan MAT have solved this problem using a precup electrostatic sector, also called a retardation lens, in front of the *m/z 3* Faraday cup. This is able to completely suppress the contribution of the $^4He^{+\cdot}$ ion to the *m/z 3* measurements.

With these developments, the major technical problems have been overcome such that accurate and precise measurement of compound-specific δD values can be achieved for nanogram quantities of various analytes delivered via a GC effluent stream. Although these developments have enabled the construction of a commercial system, the ThermoFinnigan MAT-DELTA^{PLUS}XL, the precise operating conditions required for developing long and coherent compound-specific δD records of the type demanded by this thesis needed to be evaluated. Such factors as linearity, accuracy and precision of repeated δD determinations made over a period of several years have to be assessed for the instrument used in this investigation.

The analytical precision and accuracy of the obtained values (expressed in ‰ against a V-SMOW-standard) are dependent on several factors:

(i) The determination of the H3-factor, which provides a correction for the production of H_3^+ in the ion source. H_3^+ and HD are not resolved by a typical isotope ratio mass spectrometer, and the H_3^+ contribution is dependant on the peak voltage of the analyte. As a consequence a correction factor has to be determined (Sessions et al., 2001a; Sessions et al., 2001b).

(ii) The way in which the δD values are calculated, either using an H_2-reference gas or a calibration using a suite of alkanes with known δD values or using co-injected standards with known δD values. Investigations of post-acquisition data treatments will determine which is the most effective means of standardisation.

(iii) The effect of the amount of analyte introduced in the system will be assessed. The δD values obtained can be affected (Ruff et al., 2000; Bilke and Mosandl, 2002) by sample size. Also differences between δD values determined by elemental analysis and compound-specific approaches have been observed (Hör et al., 2001; Bilke and Mosandl, 2002).

In the following section, a more detailed discussion of the above factors is presented.

The most important correction factor to be taken into account is the so-called H_3-factor. As stated before this is a correction for the production of a H_3^+ ion in the source, through the following reaction: $H_2^+ + H_2 \rightarrow H_3^+ + H^\cdot$. Unfortunately, this reaction occurs readily in the ion source. As a result a correction factor needs to be determined and applied to the acquired data. A very detailed study of H3-factors was undertaken by Hayes and co-workers (Sessions et al., 2001a; Sessions et al., 2001b). In these studies, several different approaches to H_3-factor determination were considered, among them the bellows-method or peak-wise correction, as used by the ThermoFinnigan DELTA^{PLUS}XL (for a description of this see Chapter 7). Their conclusion was that both methods are highly precise, but can introduce systematic errors when applied to the acquired data that cannot be assessed in this study (different software and inlets not available for the instrument used herein); the source of these errors were unknown. Peak-wise corrections, based on peak height only can be very accurate, but only to the extent that peak shapes and background are constant, which rarely occurs during data acquisition. The peak-based methods are less precise, but give consistently more accurate δD values. The uncertainty

associated with measuring the H3-factor can limit the analytical precision unless sample and standard peaks are carefully matched in both size and δD value. The H_3^+ production in the ion source is also dependent on the pressure of helium. If the variations in pressure are relatively small the H3-factor is not significantly affected. Other factors such as the presence of CH_4 or H_2O, possible contaminants or non-ideal operation of the reactor, or the presence of column bleed do not affect the H_3-factor.

A consequence of the findings of Hayes and co-workers (Sessions et al., 2001a; Sessions et al., 2001b) relates to the second operational parameter; the data evaluation. Isotope ratios are always calculated against a reference standard of known isotopic composition. Two ways of standardising a sample run exist: (i) either using pulses of hydrogen gas at the beginning and the end of the run, or (ii) using co-injected standards. Both should theoretically yield the same δD value.

The last characteristic is the influence of the amount of effluent introduced into the IRMS and the conditioning necessary for the reactor to function optimally. Previous publications have already noted the problems involved in comparing δD values obtained from analytes by elemental analysis (EA) and gas chromatography (GC). Bilke and Mosandl (2002) noticed that linearity between the two values is only obtained at peak heights >3 volt, and pyrolysis is only complete at low carrier gas flow rates. The dependency on signal height was also observed by Ruff et al. (2000), noting that the δD-values changed until reaching a plateau starting at a certain sample size (>0.6 µg of benzaldehyde). An offset up to 20-40‰ between EA and on-line analysis was also noted by Hör et al. (2001). In the operating manual and the original study of the instrument (Hilkert et al., 1999) no conditioning of the reactor was recommended, although the original reactor design involved a graphite deposit (Burgoyne and Hayes, 1998). Several studies since have noted that conditioning the reactor to provide a carbon deposit improves the accuracy of the δD values obtained (Ruff et al., 2000; Bilke and Mosandl, 2002).

4.1.2 Aims

Although several studies (Sessions et al., 2001a; Sessions et al., 2001b; Hilkert et al., 1999; Bilke and Mosandl, 2002) have documented the conditions necessary to obtain deuterium isotope ratios, no detailed study of the acquisition and treatment of data for the development of down-core profiles exist. The necessary conditions for data acquisition and treatment have to be known in order to eliminate any influence of instrument performance on the actual trends noted in the δD values obtained. This chapter aims to specify and explain the procedures used in

this thesis, keeping in mind that our main goal was to obtain reliable δD values, required for the development of climate records based on lipid biomarker proxies preserved in peat bogs. As such, the aims of this chapter can be summarised as:

(i) A set of standard *n*-alkanes will be analysed using both bulk (elemental analysis (EA)) and compound-specific (gas chromatographic (GC)) methods to determine the effect on their δD values with signal magnitude.

(ii) The linearity, precision and accuracy of the δD determinations will be assessed. For this purpose a series of standards, both official international reference materials, as well as cross-referenced standards will be evaluated.

(iii) Two different approaches to raw data treatment in compound-specific analysis will be examined in order to obtain the most accurate and precise compound-specific δD records possible.

(iv) A standard protocol will then be proposed in order to provide the most reliable δD values. Only factors that normal users can influence will be addressed, so no rewriting of software or technical adaptations will be necessary for the developed procedure.

4.2 Results and Discussion

4.2.1 Bulk standard measurements (TC/EA-IRMS)

4.2.1.1 Normal operational procedure

The operational procedure described is a combination of the instructions by the manufacturer and our own observations, obtained during the course of our research. Several important factors have to be considered before the instrument could be used for TC/EA-IRMS determinations.

The first factor to be considered is the tuning of the instrument with regard to the sensitivity and the H3-factor. In contrast to the tuning of a carbon isotope ratio monitoring IRMS, the HD measurements not only require tuning to obtain high sensitivity but also low H3-factors have to be taken into account. The instrument is operated with a background signal on *m/z* 2 of lower than 200 mV, while tuning the highest voltage on the *m/z* 3 cup. When these parameters have been optimised, an H3-factor measurement is made. For this 5 pulses of reference gas were introduced with the amount of each manually adjusted to give a different peak voltage. When the value obtained is below 10 ppm nA^{-1}, the measurement is repeated until an

average σ = 0.1 is achieved on three consecutive measurements, otherwise the tuning was repeated. During tuning the reactor was slowly brought to the operational temperature of 1450°C, ensuring that no cracking of the reactor tube occurred through thermal stress. During the whole procedure a He flow was maintained through the system.

Before measuring of the samples could take place, the reference gas is calibrated against an internationally recognized standard material (PEF1). Hereafter an H3-factor is determined every day to within the allowed deviation; otherwise the operation of the IRMS has to be reassessed. The sample measurements were obtained using two reference H_2 pulses before and two after the sample peak and these were then used to calculate the δD value of the sample.

All samples are introduced into the reactor using silver capsules (3 to 6 mm diameter). The capsules are folded in such a way that no air is enclosed with the sample hereby ensuring no influence from humidity and contaminants.

4.2.1.2 Standards

Standards used to assess the performance of the instrument were *n*-alkanes. Since they do not posses exchangeable hydrogen atoms their δD values will not be altered by any process other then an incomplete combustion or post-combustion fractionations. This property makes them ideal for monitoring the performance of the instrument. Moreover, they are analogues to the major compound class that is the focus of this thesis. Test standards (*n*-alkanes) were obtained from Sigma Aldrich: *n*-pentadecane (*n*-C_{15} alkane), *n*-eicosane (*n*-C_{20} alkane), *n*-tetracosane (*n*-C_{24} alkane,) *n*-octacosane (*n*-C_{28} alkane), *n*-dotriacontane (*n*-C_{32} alkane), *n*-hexatriacontane (*n*-C_{36} alkane) and *n*-octatriacontane (n-C_{38} alkane). These compounds cover the entire molecular weight range of hydrocarbons to be measured from the peat hydrocarbon fraction. Independent δD values for these test standards were obtained by triplicate off-line measurements at the application laboratory of Finnigan MAT (Bremen, Germany), and calibrated against Vienna Standard Mean Ocean Water (V-SMOW, O‰). In addition to these *n*-alkanes, PEF1 (polyethylene foil, its δD value determined relative to V-SMOW (Vienna Standard Mean Ocean Water, reference material 8535)) was obtained from the National Institute of Standards and Technology for the calibration of the reference gas. The independent δD values of these test compounds are given in Table 4.1.

Table 4.1. Bulk δD values of reference materials.

Reference standard	δD values (‰)	Standard Deviation (‰)
n-C_{15} alkane	-171.1 ‰	0.9 ‰
n-C_{16} alkane	-64.2 ‰	5,0 ‰
n-C_{20} alkane	-83.7 ‰	1.0 ‰
n-C_{24} alkane	-40.0 ‰	1.0 ‰
n-C_{28} alkane	-45.7 ‰	1.0 ‰
n-C_{32} alkane	-234.2 ‰	1.7 ‰
n-C_{36} alkane	-241.2 ‰	1.4 ‰
n-C_{38} alkane	-107.3 ‰	1.2 ‰
PEF1 (polyethylene film)	-100.3 ‰	2.0 ‰

4.2.1.3 Relationship between signal size and δD value

According to Hilkert et al. (1999) no relationship exists between the amount of sample introduced and its measured δD value. Bilke and Mosandl (2002) observed that linearity between the two δD values is only obtained at signal sizes greater than 3 V. This dependency on signal amplitude was also noted by Ruff et al. (2000). Before the determinations of the test standards at a range of concentrations, the reference gas value was obtained using repeated measurements of the NIST PEF1 standard. Each time the reactor was changed or the graphite crucible replaced, the reference gas was recalibrated using the NIST standard. This resulted in different δD values (ranging from –200‰ to -165‰) of the reference gas. A possible explanation for this phenomenon is that the silver capsules used for introducing the samples gradually poison the reactor, especially the first reactor. Experience showed that not more then 450 consecutive analyses could be performed using the same reactor, without the graphite crucible being changed. Hence, a regime was implemented whereby the crucible was changed every 150-200 runs in order to prevent the deteriorations observed. The δD value of the NIST standard is plotted in Figure 4.1 and shows no dependency on signal size.

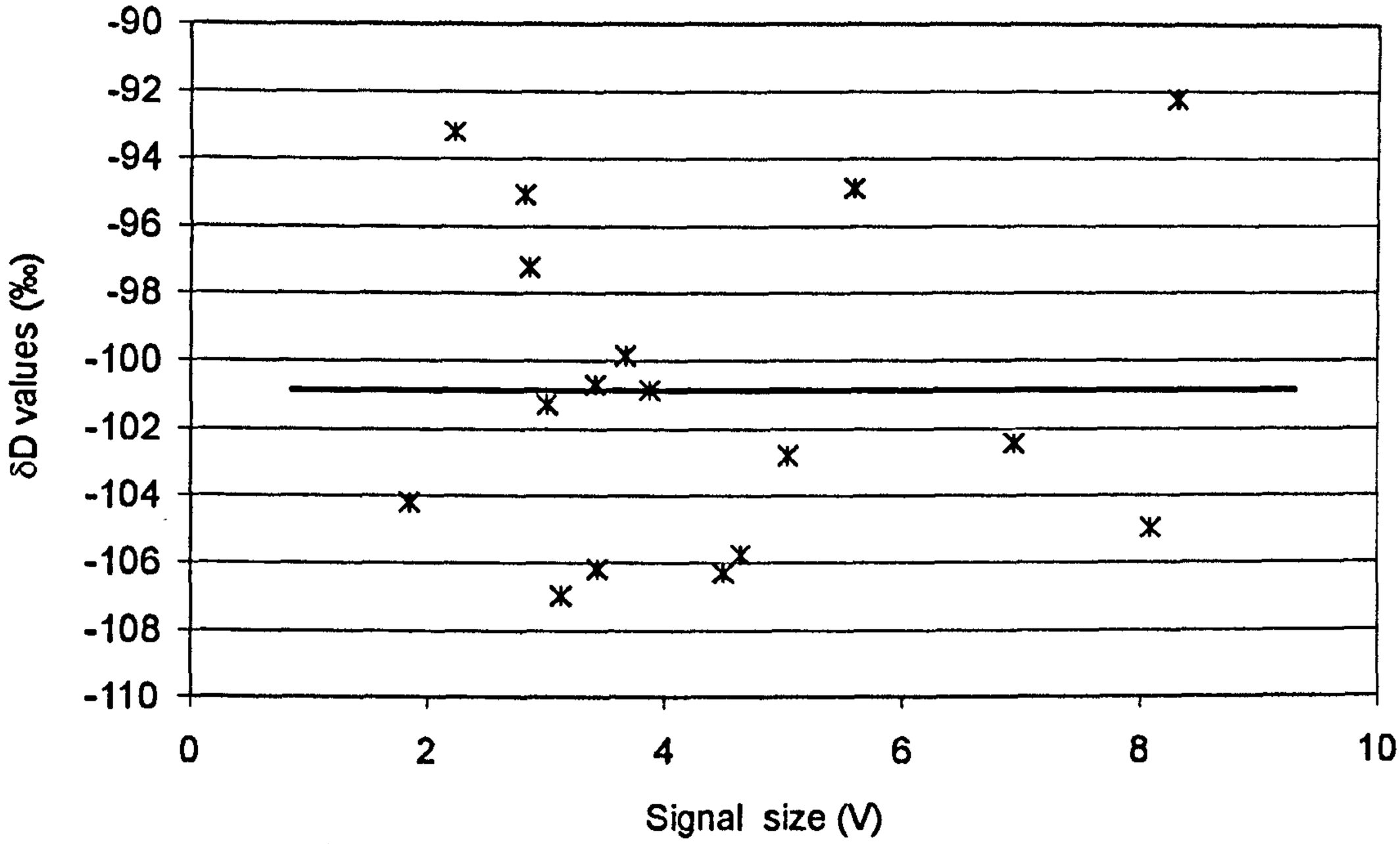

Figure 4.1. Plot of δD values of PEF1 NIST standard in relation to signal amplitude. Trendline shows no effect of sample size.

However, a dependency between the signal amplitude of the peak and the δD value is observed below 3 volts and can be best described by a logarithmic trendline. These results are summarised in Figure 4.2. When a large enough signal size range is used, a small dependency above 2.5 V is observed, however, this falls within the standard deviation range of the method. Lower then 2.5 V, there is a large bias in the data. This means that samples have to be run at voltages >2.5 V. All data show a trend towards more positive δD values at lower signal sizes. Another noticeable effect is the data scatter, with larger scatter occurring at lower voltages, probably due to incorrect H_3-factor correction, since this is determined using peak heights between 1.5 and 5 V. These data indicate that peak heights should be ideally between 2.5V to 5V to ensure full linearity between peak amplitude and δD values obtained. Another phenomenon is the larger bias on the more depleted standards. No obvious explanation can be given for this.

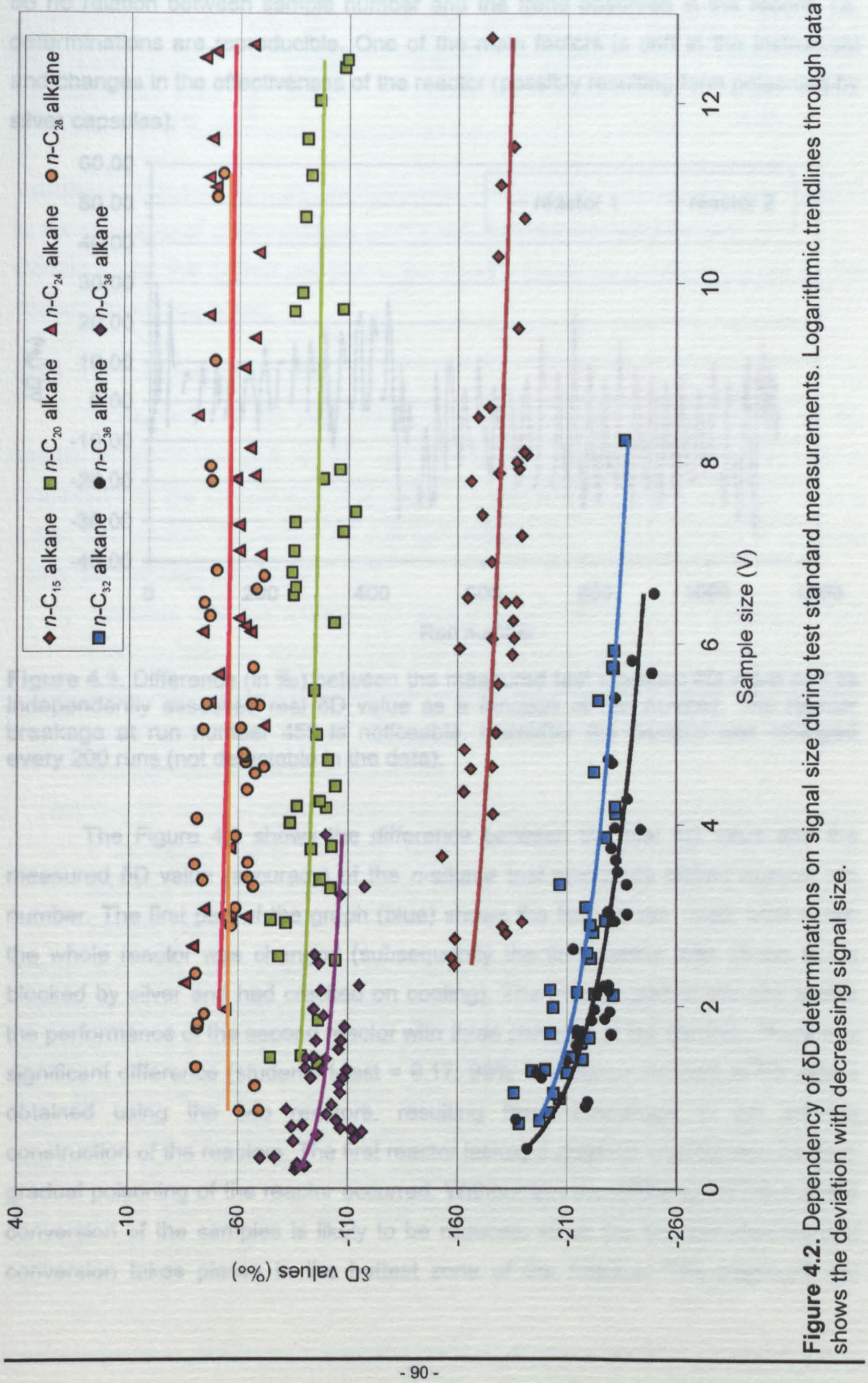

Figure 4.2. Dependency of δD determinations on signal size during test standard measurements. Logarithmic trendlines through data shows the deviation with decreasing signal size.

4.2.1.4 Linearity over time (reproducibility)

It will be important when trying to establish a climate record that there should be no relation between sample number and the trend observed in the record, i.e. determinations are reproducible. One of the main factors is drift in the instrument and changes in the effectiveness of the reactor (possibly resulting form poisoning by silver capsules).

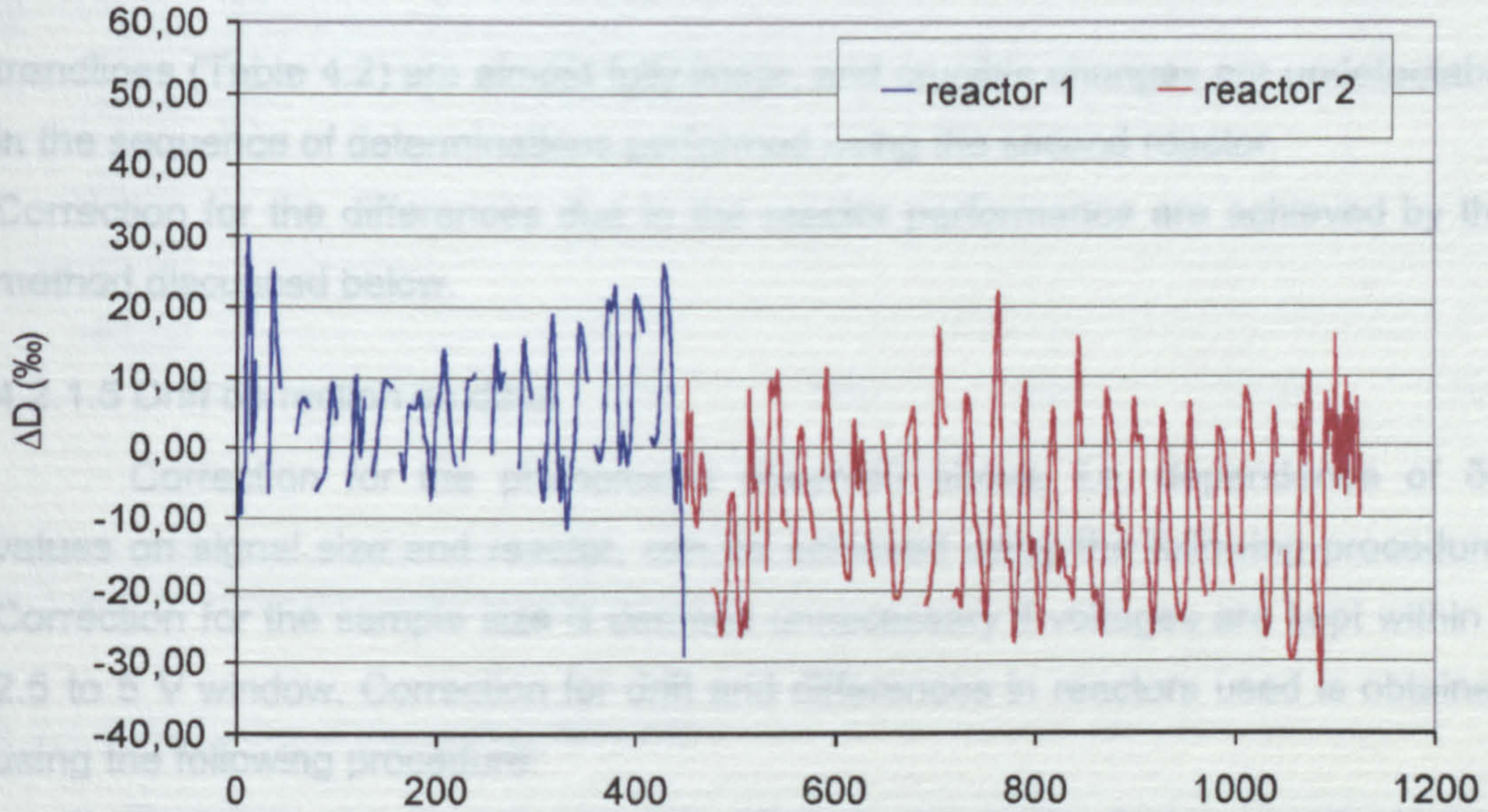

Figure 4.3. Difference (in ‰) between the measured test standard δD value and its independently assessed real δD value as a function of run number. The reactor breakage at run number 450 is noticeable. Hereafter the crucible was changed every 200 runs (not detectable in the data).

The Figure 4.3 shows the difference between the real δD value and the measured δD value (accuracy) of the *n*-alkane test standards plotted against run number. The first part of the graph (blue) shows the first reactor used, after which the whole reactor was changed (subsequently the first reactor was shown to be blocked by silver and had cracked on cooling). The second part of the plot shows the performance of the second reactor with three changes of the crucible. There is a significant difference (students t-test = 9.17; 99% confidence interval) in δD values obtained using the two reactors, resulting from differences in the internal construction of the reactors. The first reactor lacked a graphite crucible, and as such gradual poisoning of the reactor occurred. Without this the efficiency of the thermal conversion of the samples is likely to be reduced, since the crucible ensures that conversion takes places in the hottest zone of the furnace. The slopes of the

Table 4.2. Linearity of the δD values >1100 determinations of all test standards over time plotted in Figure 4.3, showing the values of the trendline between run number and the deviation between real and measured δD values (ΔD).

	R^2	Slope	Intercept	Mean diff (‰)
First reactor (blue)	0.0006	0.0018	4.3157	4.68
Second reactor (red)	0.0107	0.0054	-11.655	-7.33
total (two reactors)				-3.46

trendlines (Table 4.2) are almost fully linear, and crucible changes are undetectable in the sequence of determinations performed using the second reactor. Correction for the differences due to the reactor performance are achieved by the method discussed below.

4.2.1.5 Drift correction on data.

Correction for the phenomena observed above, i.e. dependence of δD values on signal size and reactor, can be achieved using the following procedure. Correction for the sample size is deemed unnecessary if voltages are kept within a 2.5 to 5 V window. Correction for drift and differences in reactors used is obtained using the following procedure:

(i) Samples are run interspaced with test standards: first a standard, then triplicate sample, then a further standard, and so on.

(ii) Each test standard provides a measure of the deviation of the recorded δD value from the standards' real δD value, and allows the effectiveness of the thermal conversion to be assessed.

(iii) The δD value of each sample (run triplicate) can then be corrected using the 3 standards run in triplicate before and after the sample. This gives an average deviation over 21 data points, which is then used to correct the sample value.

Figure 4.4 plots ΔD values for the test standards obtained after applying this correction method. Comparison with Figure 4.3 shows that no significant difference is detected in the ΔD values derived from the two reactors (student T-test = 0.16, 99% significance level). Thus, data from the two reactors can be meaningfully compared. Also noticeable is an improvement in the spread of the values observed (differences between maximum and minimum values: 64.8‰ against 48.6‰ before and after). All data (precision and accuracy) measurements will be compared before and after drift correction.

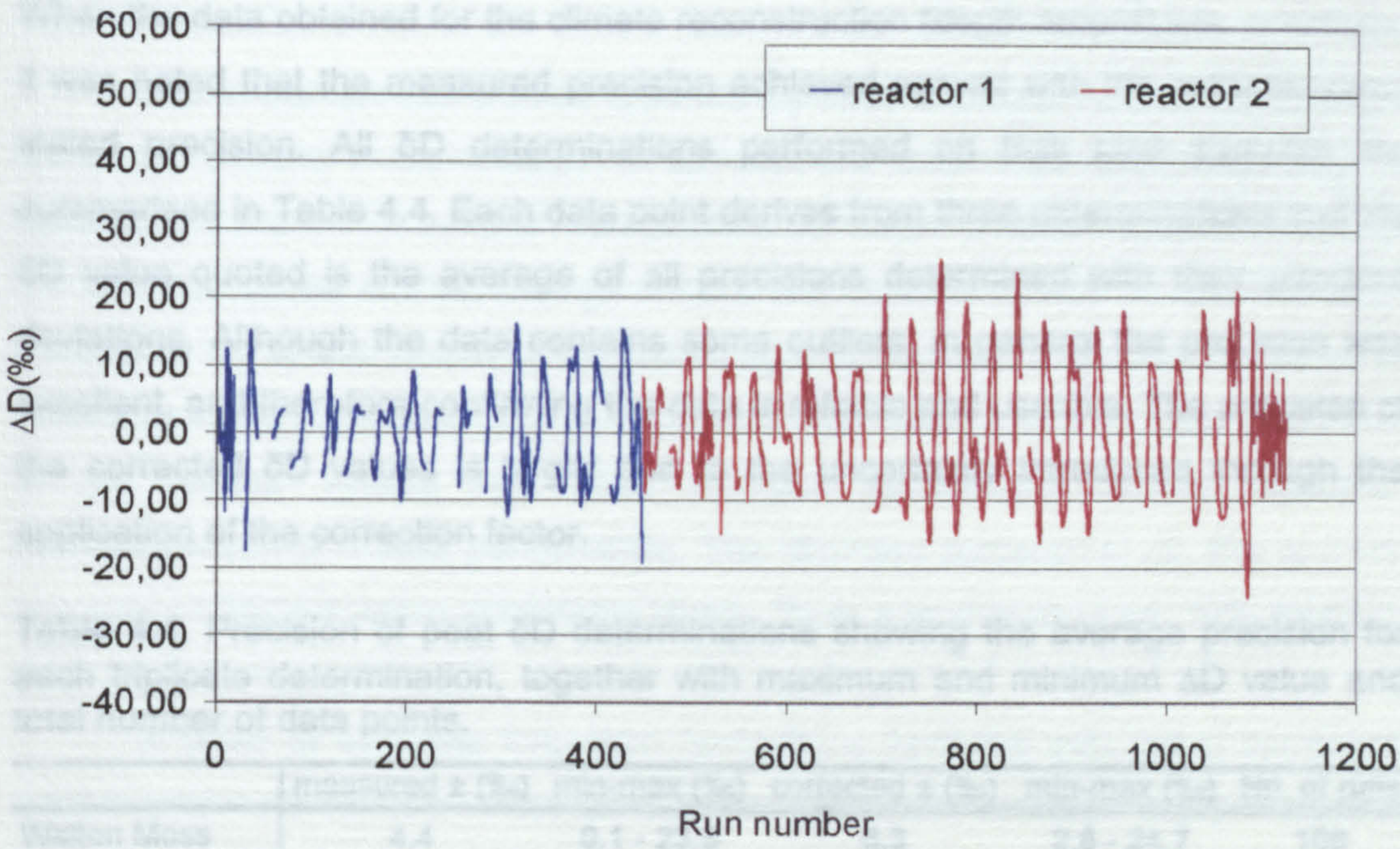

Figure 4.4. Plot of ΔD values (‰) as a function of run number after correction for drift due to changing reactor performance.

4.2.1.6 Precision of the measurements

Precision is defined as the degree to which several consecutive measurements give the same δD value. Here the precision is represented by the standard deviation of the measured δD values. The precision of the instrument of 10 consecutive measurements is defined by the manufacturer as 4‰. In Table 4.3 the precision of the alkane δD determinations is shown. The measured δD values yield a precision more then twice that stated by the manufacturer. This due to the differences in performance shown above for the two reactors (Section 4.3.3.3). After correcting for reactor drift, the precision is only influenced by small fluctuations in the instrument operating parameters.

Table 4.3. Precision of measured values for test standards for X consecutive runs.

Reference standard	δD measured (‰)	± (‰)	δD drift corrected (‰)	± (‰)	No. of runs
n-C_{15} alkane	-176.8	9.6	-172.1	5.2	39
n-C_{20} alkane	-94.5	9.9	-88.7	5.2	45
n-C_{24} alkane	-54.2	10.7	-48.7	5.3	35
n-C_{28} alkane	-54.8	11.5	-51.5	5.9	46
n-C_{32} alkane	-224.1	8.7	-223.3	5.1	40
n-C_{36} alkane	-234.1	8.2	-233.6	5.4	40
n-C_{38} alkane	-105.9	9.2	-105.3	6.1	45
PEF1	-100.9	4.8	-100.9	6.7	17
Total all standards		*9.1 ± 2.0*		5.6 ± 0.6	307

When the data obtained for the climate reconstruction (depth record) was assessed, it was noted that the measured precision achieved agreed with the manufacturers stated precision. All δD determinations performed on bulk peat samples are summarised in Table 4.4. Each data point derives from three determinations and the δD value quoted is the average of all precisions determined with their standard deviations. Although the data contains some outliers, in general the precision was excellent, and therefore confirming the data is reliable and useable. The precision of the corrected δD values is larger due to the uncertainty introduced through the application of the correction factor.

Table 4.4. Precision of peat δD determinations showing the average precision for each triplicate determination, together with maximum and minimum ΔD value and total number of data points.

	measured ± (‰)	min-max (‰)	corrected ± (‰)	min-max (‰)	No. of runs
Walton Moss	4.4	0.1 - 23.5	6.3	2.6 - 24.7	108
Bolton Fell Moss	4.8	0.23 - 17.7	8.1	3.12 - 18.4	154

4.2.1.7 Accuracy of the measurements

The accuracy is the degree to which the measured δD value agrees with the real sample δD value. In this case the deviation between the independently measured off-line δD value and the δD value recorded herein. The accuracy for each compound is then given by the average off all deviations for that compound and are summarised in Table 4.5. The accuracy for the various standards ranges from 1.4‰ for the *n*-C_{38} alkane to 14.2‰ for the *n*-C_{24} alkane. The average deviation is 3.1 ‰ over all standards. Correcting for drift obviously improves the accuracy of the measurement (2.2‰ vs. 3.1‰), but with an operating precision of 6-10‰ this improvement is relatively insignificant.

Table 4.5. Accuracy of δD determination of test standards given as difference between measured δD value and real δD value. Both real time measured δD values and drift corrected δD values are shown.

Reference standard	δD real (‰)	δD meas. (‰)	diff (‰)	δD corr. (‰)	diff (‰)	No. of runs
n-C_{15} alkane	-171.1	-176.8	-5.7	-172.1	-1.0	39
n-C_{20} alkane	-83.73	-94.5	-10.8	-88.7	-5.0	45
n-C_{24} alkane	-40.03	-54.2	-14.2	-48.7	-8.6	35
n-C_{28} alkane	-45.67	-54.8	-9.1	-51.5	-5.8	46
n-C_{32} alkane	-234.22	-224.1	10.1	-223.3	10.9	40
n-C_{36} alkane	-241.23	-234.1	7.2	-233.6	7.6	40
n-C_{38} alkane	-107.31	-105.9	1.4	-105.3	2.0	45
PEF1	-100.3	-100.9	-0.6	-100.9	-0.6	17
Total all standards			3.1 ± 0.5		2.2 ± 0.6	307

4.2.2 Discussion

Due to the fact that a small dependency exists between the sample size and δD value, resulting in non-linearity, all samples are determined using peak heights between 2.5 and 5 V. A trend to more positive δD values is observed between 0 and 2.5 V, which agrees with the findings of Bilke and Mosandl (2002). To ensure overall linearity all δD values should be measured against secondary isotope standards, to ensure accurate monitoring of system performance. Each time a physical parameter of the reactor system has been changed recalibration allows numerical intercomparison of reactor performance. The recorded precision of ca. 6‰ and the accuracy of 3‰ are within acceptable levels. Thus, a total error of ca. 10‰ exists in each triplicate measurement.

In order to eliminate long-term fluctuations from the data set a correction system was devised. The mean sample δD value was corrected using the mean deviation between real and measured standard δD value of the three standards before and after the sample. By using this procedure an average standard error for each data point of 6‰ was obtained, which, after taking the 3‰ accuracy into account, gives a total error of 9‰. A spread of 50-60‰ in values was obtained on peat samples, which is considerably larger than the uncertainty in the individual determinations. No obvious correlation exists between the correction and the corrected values (R^2 of 0.001). All bulk data presented in this thesis have been corrected using this procedure.

4.2.3 Compound-specific determinations using GC-TC-IRMS

4.2.3.1 Normal operational procedure

The operational procedure described here is based on the operating instructions provided by the manufacturer and observations made during the course of this study.

The first factor to be considered is the tuning of the instrument with regard to the sensitivity and the H_3-factor. In contrast to the tuning of a carbon isotope ratio monitoring IRMS, the HD measurements not only require tuning to obtain high sensitivity, but also low H_3-factors. The machine is operated with a background signal on *m/z* 2 of < 200 mV, while tuning the highest voltage on the *m/z* 3 cup. When these parameters have been optimised an H_3-factor measurement is made. For this, 5 pulses of reference gas are measured, each manually adjusted to a different peak voltage. When the signal obtained is below 10 ppm nA^{-1}, the

measurement is repeated until an average $\sigma = 0.1$ is achieved for three consecutive measurements, otherwise the tuning is repeated.

Simultaneously the reactor can be slowly brought up to the operational temperature of 1450°C, obviously ensuring that no cracking of the reactor tube occurs, due to thermal stress. During the whole procedure a He flow is maintained through the system. Before any measuring of samples can take place, the reference gas is calibrated against an internationally recognized standard material (V-SMOW). Hereafter, an H_3-factor is determined every day within the allowed deviation and if necessary the deviation is corrected by retuning.

The size of all injections made in splittless mode was 2 µl. The samples were dissolved in iso-octane (25 µl). This high boiling solvent was used to prevent concentration of the samples in the vials due to evaporation during autoruns. All sample vials contained co-injected alkane standards (*n*-pentadecane and *n*-octatriacontane) for post-acquisition data calculations. These internal standards were used to monitor the performance of the instrument during acquisition. The GC program employed is the same as that used for quantitative analysis of the hydrocarbon fraction (1 min @ 50°C, 50-200°C @ 10° min^{-1}, 200-300°C @ 4° min^{-1}, @ 300°C for 20 min). The column used was a 50 m CPSil-5CB (0.32 mm i.d., 0.12 µm film thickness). To prevent the solvent peak from being transferred into the reactor, the eluent was vented outside the furnace for 5 min at the start of each analysis using a backflush valve. Each sample peak δD value within each run was calculated using four reference gas pulses before and after the sample peaks (two with backflush on, two with backflush off). A typical standard run is shown in Figure 4.5.

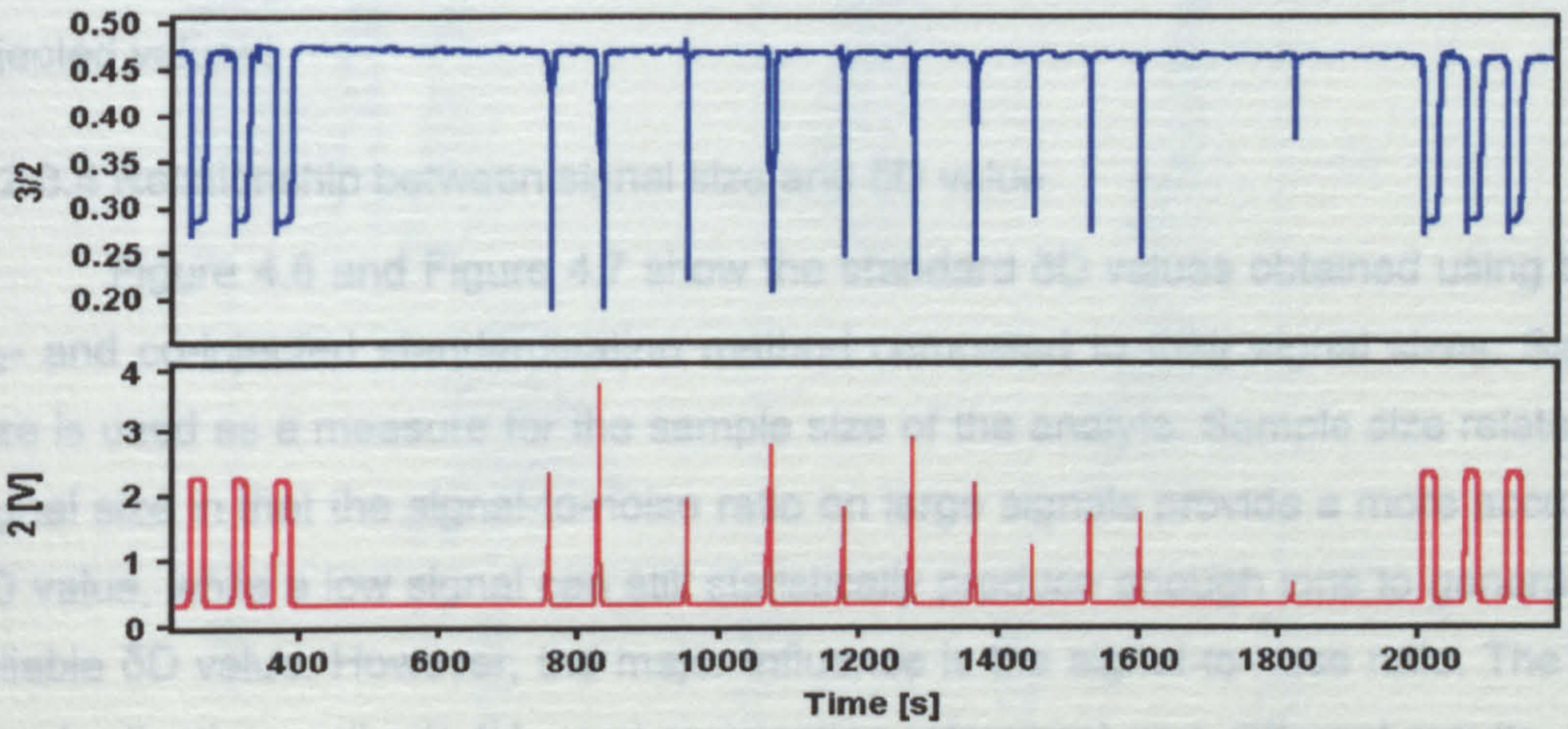

Figure 4.5. Typical GC-TC-IRMS output showing in blue the DH vs. H_2 signal, and in red the voltage of total signal.

4.2.3.2 Standards

The same suite of *n*-alkanes used for the bulk analyses was used in the compound-specific study. Several test standard solutions containing different concentrations of test standards were prepared for evaluation purposes. The δD values for the standards were measured off-line (Table 4.1). The reference gas was calibrated against a set of *n*-alkanes (so called Indiana-standards, obtained from Dr A. Schimmelmann, Indiana University). This standard comprises a homologous series of *n*-alkanes containing 16 to 32 carbon atoms, and was calibrated against V-SMOW, using a dual-inlet IRMS. Ten measurements were made presetting the δD value of the standards, thereby obtaining a δD value for the reference gas. Before an accurate determination of the reference gas could be made the reactor was conditioned by running standard samples (consisting of the test standards) until the δD values reached a plateau.

4.2.3.3 Data acquisition and treatment

The results presented here are drawn from 110 sample runs, collected using the reference gas to calculate the individual δD values for the various *n*-alkanes. After each analysis all the individual δD values for each test component were recalculated using the *n*-C_{15} alkane and *n*-C_{38} alkane reference δD values. These two test *n*-alkanes were co-injected with every sample to monitor instrument performance during acquisition. This produced an additional 786 standard δD values, as well as an added reference, since all samples contained an internal quantification standard (5α-cholestane, unknown off-line δD value). For subsequent discussions, δD values obtained using reference gas pulses are called H_2-values, reference values obtained using the co-injected alkane standards are called co-injected values.

4.2.3.4 Relationship between signal size and δD value

Figure 4.6 and Figure 4.7 show the standard δD values obtained using both H_2- and co-injected standardisation method compared to their signal sizes. Signal size is used as a measure for the sample size of the analyte. Sample size relates to signal size in that the signal-to-noise ratio on large signals provide a more accurate δD value, while a low signal can still statistically produce enough ions to generate a reliable δD value. However, the major influence is the signal-to-nose ratio. The two standardisation methods (H_2- and co-injection reference) give different results. The explanation lies in the difference in peak shapes used to calculate δD values. The

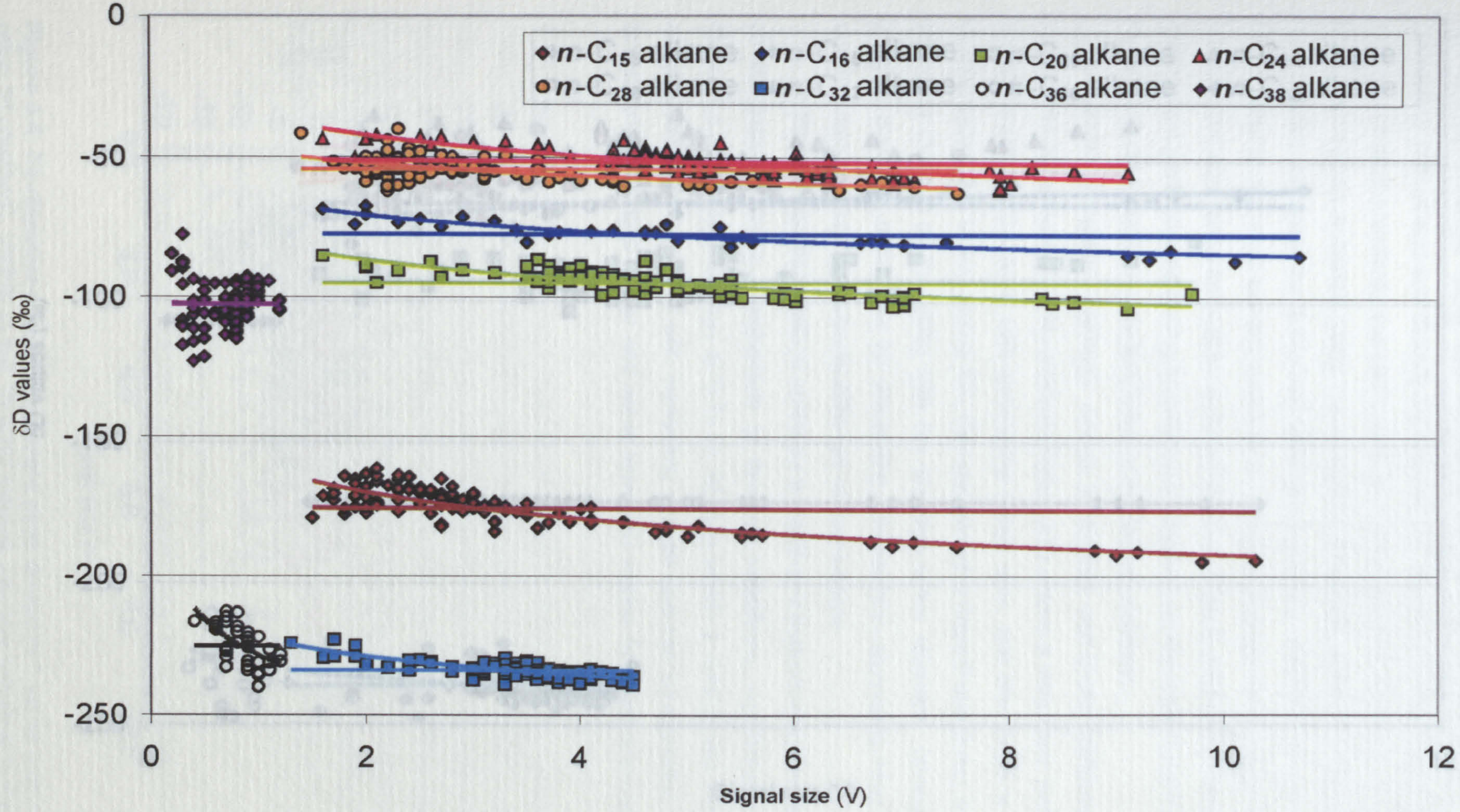

Figure 4.6. Plot of variations in δD values of *n*-alkane standards with signal size, calculated using the H_2-method. Logarithmic trendlines shows deviations from the horizontal line around the measured mean δD value.

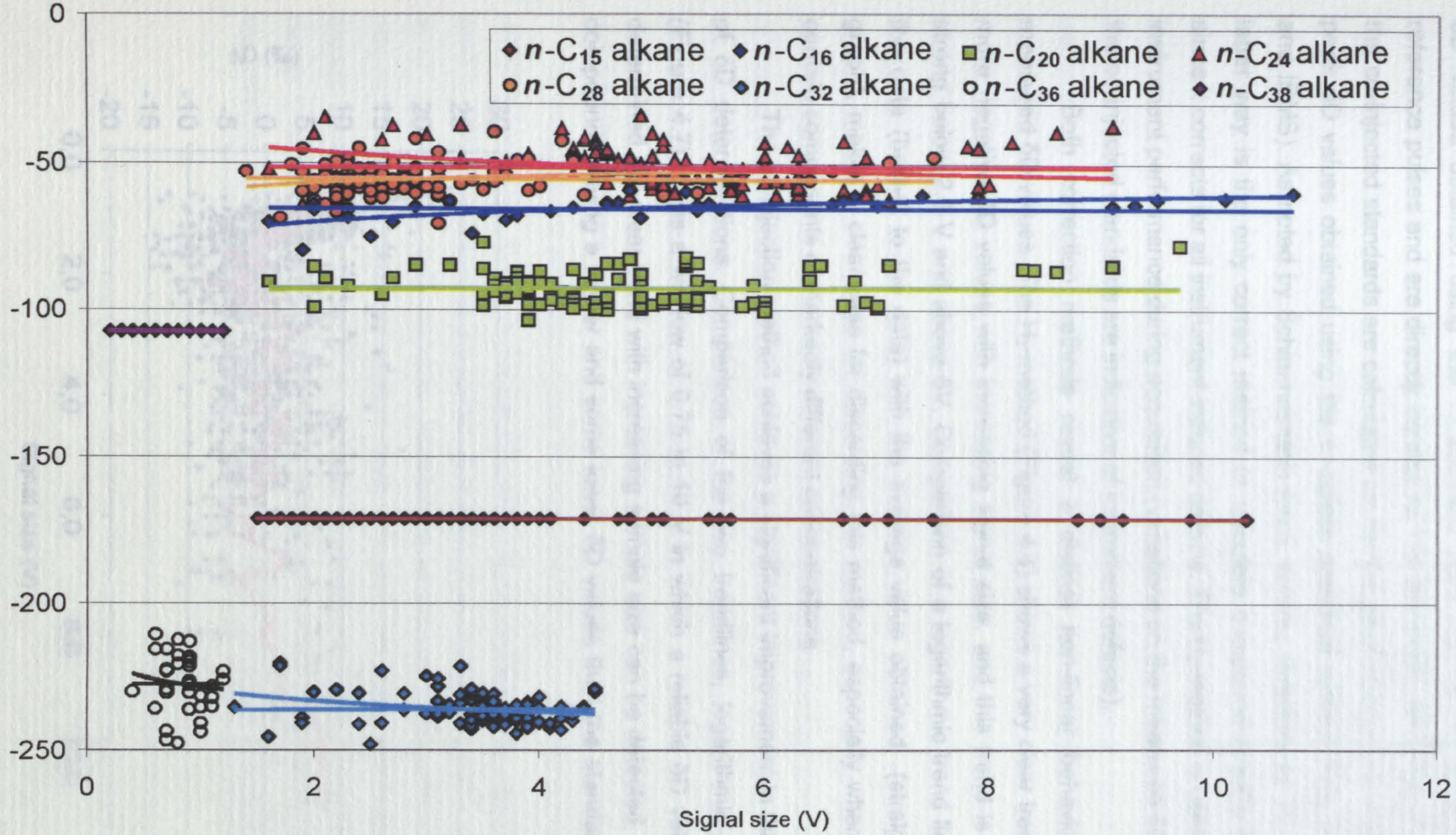

Figure 4.7. Plot of variations in δD values of *n*-alkane standards with signal size, calculated using the co-injection method, using *n*-C_{15}; *n*-C_{38} alkane as co-inject standards. Logarithmic trendlines show deviations from the horizontal line around the measured mean δD value.

δD values obtained using the H_2-standardisation are calculated using square reference pulses and are directly introduced into the IRMS, while the δD values of the co-injected standards are calculated on normal peak shapes with the reference peak δD values obtained using the complete analytical system (GC, plus reactor and IRMS). As noted by Schimmelmann (pers. comm.; Sessions et al., 1999), the latter way is the only correct method to calculate compound-specific δD values, since it corrects for all instrument-induced defects. The H_2-method is used to assess instrument performance during acquisition (variations on the measured δD values of the co-injected standards are indicative of instrument defects).

Both correction methods reveal a distinct non-linear behaviour of the measured δD values. The H_2-method (Figure 4.6) shows a very clear trend towards more negative δD values with increasing signal size, and this trend is especially strong below 2.5 V and above 5V. Comparison of a logarithmic trend line through the data (best-fit to the data) with the average value obtained (straight line on graph), makes a clear case for discarding this method, especially where mixtures contain components of markedly different concentrations

The co-injection method achieves a significant improvement in the accuracy of δD determinations. Comparison of the two trendlines, logarithmic and linear (Figure 4.7), gives a window of 0.75 to 10 V in which a reliable δD value can be determined. No clear trend with increasing sample size can be detected, with some compounds having a higher and some lower δD values than the standards off-line

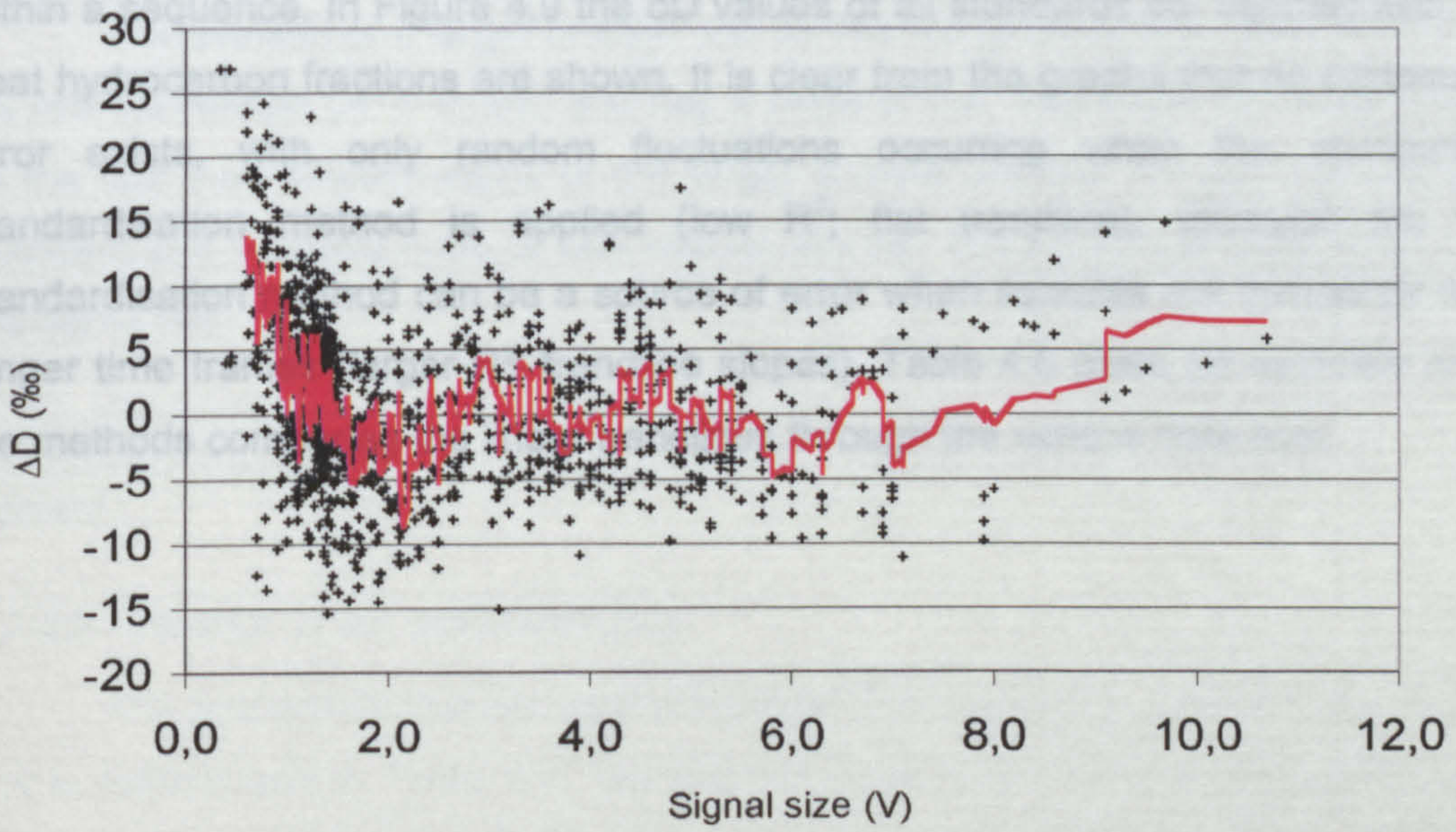

Figure 4.8. 5α-cholestane internal standard peak deviation from its mean 2-12V δD value (H_2-method). Visible in the 15 point moving average trendline is the deviation below the 1V sample size (larger then 5V accuracy).

δD value. Below 1.5 V it is difficult to make an accurate determination of the signal size effect. The δD values determined above 1,5 V produce no clear evidence for a large effect with decreasing signal size. Although below 1.5 V the *n*-C_{36} alkane is offset from its real value, no large trend in the measured δD values can be observed. Also noticeable is that no correlation exists between elution order and δD values. The co-injection method must be used to determine δD values and enables the comparison of δD values of a series of compounds in a sequence of samples. A good measure of the signal height effect is obtained through the monitoring of the internal quantification standard, 5α-cholestane, in each peat sample run. A dependency on signal amplitude after recalculating the δD values using the co-injection standardisation method still is still observed (Figure 4.8). The skew towards more positive δD values is in the order of 20‰ per V, below 1 V signal height. As noted from Figure 4.7 the different compounds show different directions for the skew of the δD values below 1.5 V, hence, no correction is possible. However, the δD values obtained on 5α-cholestane do allow a signal window to be defined within which reliable δD values can be determined. Assuming an average error of 10‰ any δD value determined at a signal intensity between 0.75 and 9 V can be deemed to be accurate and uninfluenced by the signal height effect; this assuming a maximum deviation of 5‰ due to the signal amplitude effect

4.2.3.5 Linearity over time

No apparent correlation exists between the δD value and the sample position within a sequence. In Figure 4.9 the δD values of all standards co- injected with the peat hydrocarbon fractions are shown. It is clear from the graphs that no systematic error exists, with only random fluctuations occurring when the co-injection standardisation method is applied (low R^2; flat trendline), although the H_2-standardisation method can be a source of error when samples are compared over longer time frames (larger R^2; trendline slopes). Table 4.6 gives an overview of all the methods comparing the linear trendlines through the various data sets.

Table 4.6. Linearity of co-injected standards (*n*-C_{15}; *n*-C_{38} alkane, internal quantification standard (5α-cholestane) and a target analyte (*n*-C_{23} alkane)), showing correlation (R^2), slope and intercept of the linear trendline through the data points with run number, and between internal standard and sample with run number.

	R^2	Slope	Intercept	Mean value (‰)
H_2-method				
5α-cholestane	0.222	-0.019	-253.1	-260.3
n-C_{15} alkane	0.084	-0.010	-167.9	-172.0
n-C_{38} alkane	0.202	-0.020	-94.1	-101.9
n-C_{23} alkane	0.166	-0.030	-160.1	-172.0
co-injection method				
5α-cholestane	0.078	-0.008	-260.7	-263.8
n-C_{15} alkane	0.000	0.000	-171.1	-171.1
n-C_{38} alkane	0.000	0.000	-107.3	-107.3
n-C_{23} alkane	0.087	-0.020	-166.4	-174.3
5α-cholestane vs. *n*-C_{23} alkane				
H_2-method	0.211	0.867	54.5	
co-injection method	0.069	0.612	-12.2	

Comparison of a target analyte with its internal quantification standard shows no real correlation (R^2 = 0.069) and has a slope of 0.6. The slope can be attributed to the fact that concentrations of the target analyte and the internal quantification standard can fluctuate more or less simultaneously, since they are both drawn from the same vial.

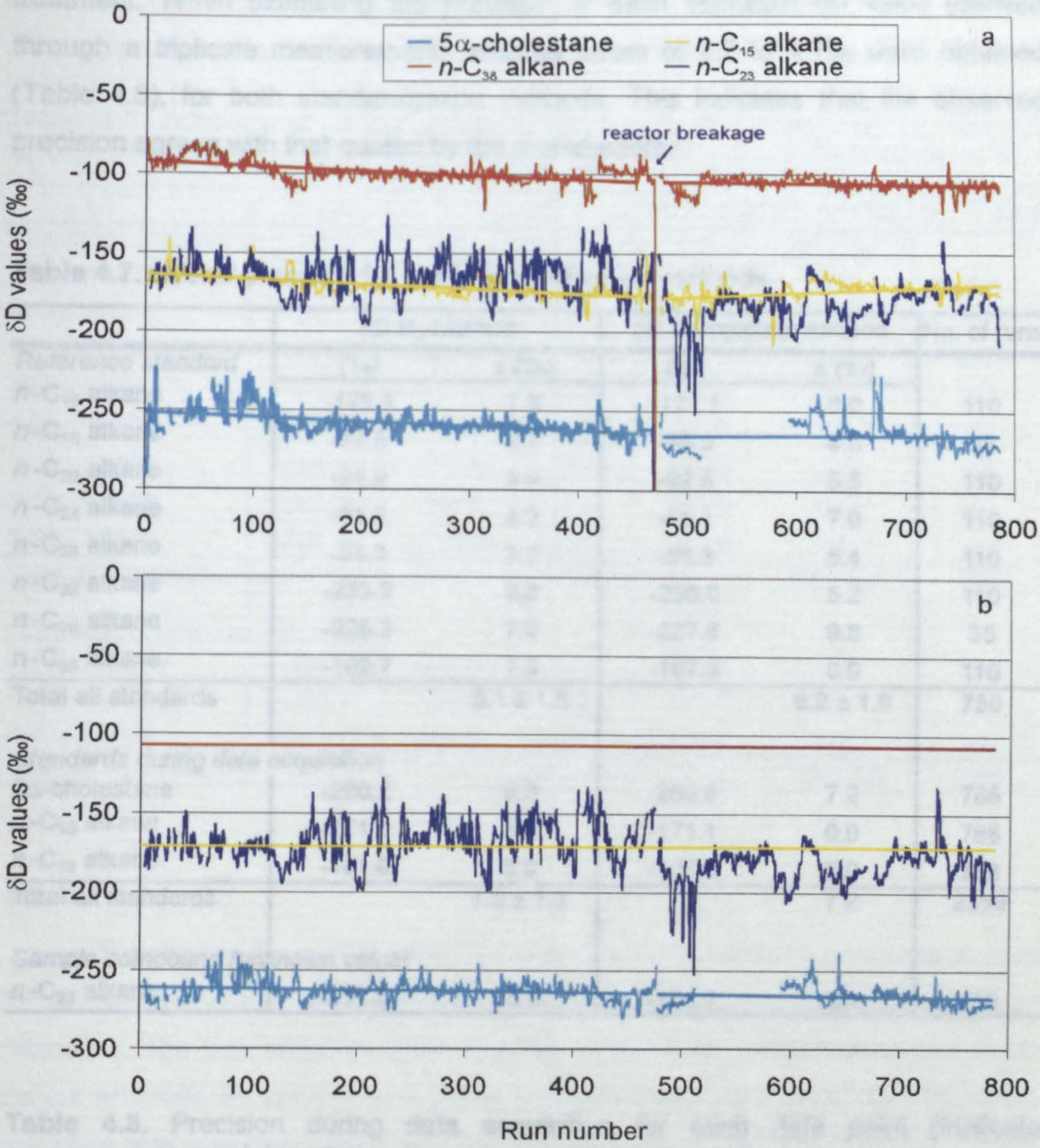

Figure 4.9 Variation in the δD values of *n*-alkane standards over time in compound-specific analyses. The figure shows δD values for all standards (co-injection and internal quantification) plus a target analyte with unknown value for (a) H_2-standardisation method and (b) co-injection standardisation method. Clearly visible is the improvement of the linearity in the co-injection standardisation method (as shown for 5α-cholestane) and the reactor breakage in the H_2-standardisation method.

4.2.3.6 Precision of the measurements

The precision is defined as the repeatability of a measurement in the system and is summarized in Table 4.7. The manufacturer quotes the instrument precision as 4‰. The precision obtained for each individual compound was higher than quoted (7.5 - 8‰). No difference existed between the methods of standardisation employed, confirming that precision is not influenced by the post acquisition data

treatment. When examining the precision of each individual δD value (derived through a triplicate measurement) average errors of 2.2 to 4.7‰ were obtained (Table 4.8), for both standardisation methods. This indicates that the observed precision agrees with that quoted by the manufacturer.

Table 4.7. Overall precision for both standardisation methods.

	δD H_2-method		δD co-injection method		No. of runs
Reference standard	(‰)	± (‰)	(‰)	± (‰)	
n-C_{15} alkane	-175.9	7.3	-171.1	0.0	110
n-C_{16} alkane	-77.5	4.7	-65.3	4.5	35
n-C_{20} alkane	-94.9	3.9	-92.5	5.5	110
n-C_{24} alkane	-51.7	4.2	-51.1	7.0	110
n-C_{28} alkane	-54.3	3.9	-55.3	5.4	110
n-C_{32} alkane	-233.9	2.8	-236.0	5.2	110
n-C_{36} alkane	-225.3	7.0	-227.6	9.8	35
n-C_{38} alkane	-102.7	7.3	-107.3	0.0	110
Total all standards		5.1 ± 1.8		6.2 ± 1.9	730
Standards during data acquisition					
5α-cholestane	-260.2	9.0	-263.8	7.2	786
n-C_{15} alkane	-171.8	6.6	-171.1	0.0	786
n-C_{38} alkane	-101.6	6.9	-107.3	0.0	786
Total all standards		7.5 ± 1.3		7.2	2358
Sample compound (unknown value)					
n-C_{23} alkane	-171.8	15.8	-174.1	15.0	786

Table 4.8. Precision during data acquisition for each data point (triplicate measurement per data point).

Standards	H_2 ± (‰)	min-max (‰)	co-inject ± (‰)	min-max (‰)	No. of runs
5α-cholestane	3.2 ± 3.5	0.1 - 32.2	3.3 ± 2.3	0.2 - 18.6	786
n-C_{15} alkane	2.2 ± 2.0	0.1 - 14.9	0.0 ± 0.0	0.0 - 0.0	786
n-C_{38} alkane	2.7 ± 1.7	0.2 - 13.3	0.0 ± 0.0	0.0 - 0.0	786
n-C_{23} alkane	4.4 ± 4.2	0.0 - 30.3	4.7 ± 4.2	0.1 - 29.0	786

4.2.3.7 Accuracy of the measurements

The accuracy, the degree of deviation from the real value is given in Table 4.9. The accuracy is of the same order as that achieved for TC/EA determinations. A mean accuracy of 3.6‰ was obtained for all the reference standards. Although a trend towards more positive δD values with elution order can be seen in the H_2-

standardisation method, no such trend was observed with the co-injection method. This is possibly linked to the signal size effect noted previously in Section 4.2.3.4.

Table 4.9. Accuracy of on-line measurements. Accuracy measured vs. real δD values (off-line determined at ThermoFinnigan Gmbh (Table4.1). Differences in ‰.

	δD real	δD H_2-method		δD co-injection method		No. of runs
Reference standard	(‰)	(‰)	diff. (‰)	(‰)	diff. (‰)	
n-C_{15} alkane	-171.1	-175.9	-4.8	-171.1	0.0	110
n-C_{16} alkane	-64.2	-77.5	-13.3	-65.3	-1.1	35
n-C_{20} alkane	-83.73	-94.9	-11.2	-92.5	-8.8	110
n-C_{24} alkane	-40.03	-51.7	-11.6	-51.1	-11.0	110
n-C_{28} alkane	-45.67	-54.3	-8.6	-55.3	-9.6	110
n-C_{32} alkane	-234.22	-233.9	0.3	-236.0	-1.8	110
n-C_{36} alkane	-241.23	-225.3	15.9	-227.6	13.7	35
n-C_{38} alkane	-107.31	-102.7	4.6	-107.3	0.0	110
Total all standards			3.6 ± 2.0		3.7 ± 2.8	730
Standards during data acquisition						
5α-cholestane	-261.5	-260.2	1.3	-263.8	-2.3	786
n-C_{15} alkane	-171.1	-171.8	-0.7	-171.1	0.0	786
n-C_{38} alkane	-107.31	-101.6	5.7	-107.3	0.0	786
Total all standards			2.0 ± 4.7		2.3 ± 3.0	2358

4.2.3.8 Discussion

The dependency of δD values on signal size when the reference gas is used to calculate δD values, is partially eliminated by using the co-injected standards for reference. The only influence peak size has is the larger amount of scatter in δD values recorded for components giving voltages lower then 1.5 V. The observed precision and accuracy are within the specifications of the manufacturer. Three consecutive measurements gave precisions of 2-4‰ that agrees with the manufacturers specifications (4‰). An accuracy of 4‰ is within the expected δD value; the observed δD values reveal no systematic errors.

4.3 Comparison and conclusions

4.3.1 Comparison of elemental analysis and compound-specific δD values

Previous studies have noted large differences between δD values determined via elemental analysis and compound-specific approaches. Up to 20% deviations were reported (Hör et al., 2001; Bilke and Mosandl, 2002). No such deviations were observed in this study. Large differences were observed between the δD values used as real values (determined by Finnigan MAT) and our own measurements. If this is a result of the two different instruments, or not, we can only speculate. No real difference was observed between the elemental analyser and compound-specific measurement; they yielded statistically identical δD values as summarised in Table 4.10.

Table 4.10. Comparison of all δD values of all standards determined by elemental analysis and compound-specific approaches and using the different standardisation methods.

	δD bulk			δD compound-specific					
				δD H_2-method			δD co-injection method		
	(‰)	diff (‰)	± (‰)	(‰)	diff (‰)	± (‰)	(‰)	diff (‰)	± (‰)
n-C_{15} alkane	-172.1	-1.0	5.2	-175.9	-4.8	7.3	-171.1	0.0	0.0
n-C_{20} alkane	-88.7	-5.0	5.2	-94.9	-11.2	3.9	-92.5	-8.8	5.5
n-C_{24} alkane	-48.7	-8.6	5.3	-51.7	-11.6	4.2	-51.1	-11.0	7.0
n-C_{28} alkane	-51.5	-5.8	5.9	-54.3	-8.6	3.9	-55.3	-9.6	5.4
n-C_{32} alkane	-223.3	10.9	5.1	-233.9	0.3	2.8	-236.0	-1.8	5.2
n-C_{36} alkane	-233.6	7.6	5.4	-225.3	15.9	7.0	-227.6	13.7	9.8
n-C_{38} alkane	-105.3	2.0	6.1	-102.7	4.6	7.3	-107.3	0.0	0.0
total		2.2	5.6		3.6	5.4		3.7	6.2

4.3.2 Conclusions

The results presented in this chapter have shown that by using an appropriate standardized procedure δD values can be obtained with accuracies and precisions suitable for establishing reliable down-core δD profiles.

The following criteria for operating the IRMS must be met for such determinations:

(i) The reactor must be slowly brought to its operating temperature (1450°C; in a stepwise fashion, with sufficient (1-2 hours) time allowed between the different ramps for equilibration).

(ii) The IRMS should be tuned using the procedure described in the manufacturers instructions until three consecutive H_3-factor determinations are within 0.1 ppm nA^{-1} of each other. H_3-factors should

be determined with the open split set in the open position (hereby delivering background from the entire system).

(iii) The water background signal should be checked using the universal triple collector.

(iv) Tuning should be checked again and H_3-factor determined.

(v) A series of bulk samples of known δD values should be determined until the reactor is conditioned.

(vi) A suitable set of reference materials should be run to check accuracy and precision.

(vii) During the sequence of runs the tuning of the instrument can shift; if this occurs the instrument should be retuned using the above procedure.

The following additional criteria must be met when making bulk δD determinations:

(i) Reference standards (with known δD values) should be run before attempting to run unknown samples in order to evaluate the accuracy and precision of the IRMS. Changes in reactor configuration (e.g. after crucible change) can lead to changes in δD value of reference gas.

(ii) Samples should be run in triplicate and interspaced with reference materials for monitoring of the IRMS.

(iii) After 150-200 runs, the crucible should be changed to prevent poisoning of the thermal conversion reactor; after the change the tuning procedure must be repeated.

(iv) Sample sizes providing signal sizes between 2.5 and 5 V should be used to avoid the signal size effect (skew on the δD values in lower signal range).

(v) The obtained δD value (mean of triplicate measurement) should then be corrected for instrument drift using the deviation on the reference δD value of the interspersed standards.

For compound-specific δD determinations the following additional criteria must be fulfilled:

(i) On start-up of the IRMS a series of standards should be run to condition a new reactor (until the δD values stabilise).

(ii) Suitable co-injection standards should be added to all samples to enable recalculation using the co-injection standards. It is advisable to add two co-injection standards at front of the sample peaks and two at the back, to ensure that a control on the recalculation exists.

(iii) The data should be acquired using the H_2-standardisation method, to enable monitoring of the IRMS through the co-injected reference standards δD values.

(iv) Signal sizes should be between 0.75 and 10 V to ensure no signal height effect exists.

(v) After data acquisition the δD values should be recalculated using the co-injected reference peak δD values.

5 Compound-Specific δD Values of Lipid Biomarkers

5.1 Introduction

The relationship between hydrogen isotope ratios and climate is well established (Dansgaard, 1964). The basic source for deuterium in the organic material of an autotrophic plant is the water on which it is growing. Schiegl (1972) was the first to observe that the hydrogen isotope ratio of plant matter is therefore, also related to climate. Schiegl analysed various peat samples for hydrogen isotope ratios and found a correlation between δD values and temperature. As such, peat is one of the earliest established settings for the study of climate using hydrogen isotope ratios. Subsequently, several authors have tried to improve on the latter correlation (Brenninkmeijer et al., 1982; Dupont and Mook, 1987; van Geel and Middeldorp, 1988) by using α-cellulose instead of bulk peat. A link between the isotopic composition of cellulose from tree rings and climate was established by Epstein and co-workers (Epstein et al., 1976; Epstein et al., 1977). Two principal errors associated with the measuring of hydrogen isotope ratios in bulk plant matter were identified. The first error was associated with the measurement of total plant biomass. Epstein reasoned that different fractions of plant matter, i.e. lignins, lipids and resins, have different isotope ratios, such that differences in two unpurified (bulk) samples may merely reflect differences in the relative proportion of different plant biochemical components rather than true isotopic effects. The second error associated with measurement of isotope ratios in plant biomass was the measurement of exchangeable hydrogens. Plant organic matter including cellulose contains a high proportion of hydroxyl hydrogens that are readily exchangeable with water. Thus, a measurement of hydrogen isotope ratio of all hydrogens may not reflect the true hydrogen isotope ratio of hydrogens incorporated into cellulose at the time of its formation, but rather it may reflect the hydrogen isotope ratio of the water to which the components were most recently exposed. By selecting a single compound (α-cellulose) and using suitable derivatisation methods, analysis of plant material for their hydrogen isotope ratios became possible. Cellulose was established as a compound for hydrogen isotope ratio determinations for tree rings, and is also found in peat deposits.

Peat deposits occur over a wide geographical area and are frequently found to span the period of the last 10,000 years. A major advantage of peat for palaeoclimate reconstruction is that pollen and macrofossil analysis of a peat core

can provide palaeoclimatological information paralleling the isotopic records, thereby allowing direct comparison of the two records. However, unlike tree rings some complications have to be resolved. For example, peat is a mixture of partially decayed plants of different species, which may posses different isotopic compositions resulting from differing isotopic fractionations during biosynthesis. This has been confirmed by the observation that freshly collected *Sphagnum* mosses and vascular plants exhibit consistent differences in isotopic composition (Brenninkmeijer et al., 1982). Thus, the variations in δD values in down-core profiles could be due to variations in species composition rather than being driven by a climate variable. However, it is known that the fluctuations in the δD values without physically separating plant macrofossils are influenced by temperature. There is also an indirect effect of temperature; during relatively warm periods plants favouring relatively dry conditions often dominate the vegetation on raised bogs and those species exhibit relatively high δD values. During periods when the climate is wetter, plant species with lower δD values thrive (Dupont and Mook, 1987). A direct comparison between a peat core from Carbury bog (Ireland) and Lamb's climate indices (van Geel and Middeldorp, 1988) also revealed a species effect on the profile and concluded that physical separation of the plant taxa might be necessary in order for isotopic records in peat to be a useful tool in palaeoclimate research. With the advent of compound-specific hydrogen isotope ratio mass spectrometry (see Chapter 4) and the selection of species-specific biomarkers, the latter goal might be achievable. A pilot study, on which the work discussed in this thesis is based, demonstrated a strong correlation between climate (temperature) and compound-specific δD values of *n*-alkanes (Xie et al., 2000). In this chapter the factors influencing compound-specific δD values are discussed. New results are then presented from two cores taken from two neighbouring bogs.

5.2 Factors influencing the δD values of individual lipids

The δD values of peat lipids from raised bogs mainly depend on three factors:

(i) The δD value of precipitation, since this is the only source of water for the growing vegetation.

(ii) The isotopic fractionation occurring during evapotranspiration from the plants leaves.

(iii) The isotopic fractionations occurring during photosynthesis and the biochemical reaction involved in the formation of the individual lipid classes.

In this section a discussion of all the above factors will be presented, with the aim of providing a basis for subsequent discussions of compound-specific δD down-core profiles. Figure 5.1 shows a schematic representation of all the fractionation effects involved in the uptake of hydrogen atoms in plants.

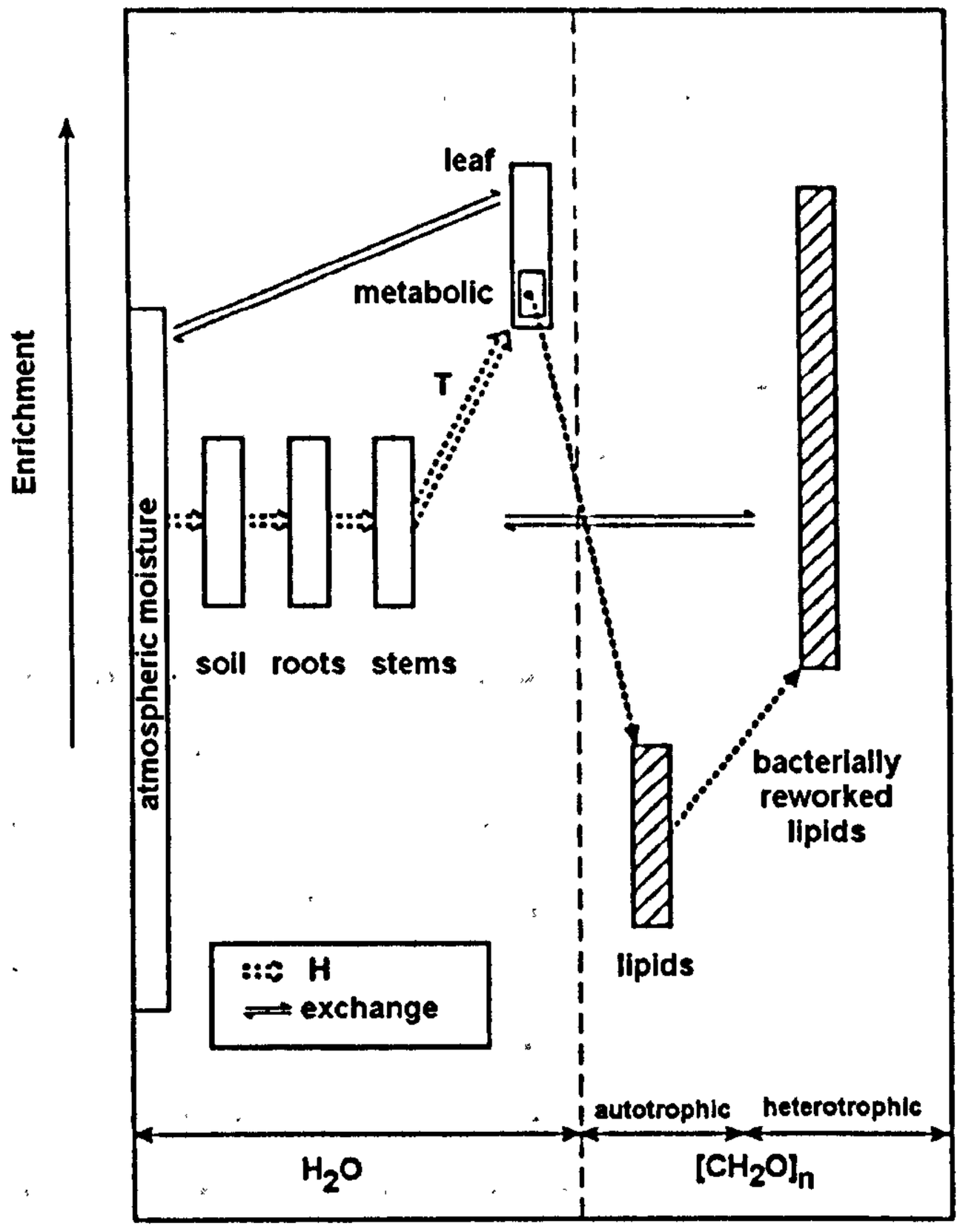

Figure 5.1. Schematic representation of the major steps in the development of the isotope ratios of hydrogen in plant lipids (after Yakir, 1992).

5.2.1 Isotopic composition of precipitation.

A detailed discussion of the various factors controlling the hydrogen isotope ratios of water was given in Section 1.4.2. Among the important considerations are:

(i) Condensate from water vapour is enriched in deuterium relative to the vapour with the result that the remaining vapour is depleted.

(ii) The water vapour content of the atmosphere is temperature dependant (Ziegler, 1988). The deuterium content of the water vapour is also temperature dependant, with decreasing temperature resulting in

increasing depletion of the water vapour and enriched precipitation (Dansgaard, 1964).

(iii) A dependency on the amount of rain is noticed (Dansgaard, 1964), with intense rain events being isotopically depleted relative to then light rain events.

In addition to precipitation, many areas of the world have fog, a source of water for plants. Fog is depleted in the heavier isotopes relative to the source water from which it was formed. While it has been argued that fog precipitation can comprise a third or more of annual precipitation in certain coastal areas, its importance as a water source for plants remains unquantified (Ehleringer and Dawson, 1992).

5.2.2 Evaporative factors influencing leaf and bog water.

After deposition of the precipitation on the bogs surface, isotopic fractionation due to evaporation can occur before the water is taken up by the plants. Evaporation can occur either directly from the bog water or from the leaves through evapotranspiration. Evaporation from raised bogs is considerably higher than from the same area of open water (Nichols and Brown, 1980). At all temperatures the rate of evaporation is about twice that of water, due to the larger surface area (water wicked up by the *Sphagnum* mosses) available for evaporation. However, since the bog surface is highly permeable, infiltration proceeds rapidly with the result that the isotopic composition of the peat pore water is very close to that of the local precipitation. However, local differences in the isotopic composition of bog water have been seen with water in hollows being more depleted in deuterium compared to water in hummocks (± 8-15‰, with hummocks having a δD value around -35‰ and hollows around –47‰; Ménot-Combes et al., 2002). The observed difference between hummocks and hollows is the result from the increased evaporation above *Sphagnum* covered hummocks over the water covered hollows. Seasonal changes in the bogs water as well as a gradual depletion in deuterium is observed down to a depth of 50 cm, i.e. well below the living plant matter. At this point a fairly uniform mixing of the bog water (through lateral flow in the acrotelm) results in a uniform isotopic composition of pore water (around -70‰; Ménot-Combes et al., 2002).

Raised bogs usually have a mix of vascular plants and non-vascular (i.e. *Sphagnum* species) plants. These two groups have developed distinctly different systems for transporting water to the photosynthetic cells. Vascular plants transport water through stems (xylem water) and no enrichment is noted during uptake of

water in the root system of vascular plants, since the influx of water into plants is governed by viscous rather than molecular flow (Ziegler, 1988). Isotopic enrichment of xylem water can happen due to the slow mixing of the water present in the roots, xylem and leaf compared to the velocity of the upward flow of water (White et al., 1985). This process does not play a role in the isotopic fractionation for vascular plants on peat bogs, because they are sampling fairly uniform source water compared to plants growing on soil that can sample isotopically different source waters, depending on their root system (Ehleringer and Dawson, 1992). During water transport no change in isotopic composition is expected in vascular bog plants until the water reaches tissues undergoing water loss, i.e. leaves or non-suberized stems, where evaporative enrichment in the heavier isotope takes place. Leaves are the primary site of evaporative enrichment and the magnitude of this enrichment is a function of temperature and relative humidity (Aravena and Warner, 1992). A change from high to low relative humidity will produce enrichment in the deuterium in the residual water in the leaves, due to the slower rate of diffusion of HDO into undersaturated air (White, 1988). The enriched isotope signal is then transmitted to the plant lipids during photosynthesis.

In contrast, the *Sphagnum* mosses grow nearly submerged and the water transport to the growth-tops is effected by capillary action through the voids between the stems and leaves (see Chapter 1). Because of the shorter pathway and the larger cross-section of the vertical water column, vertical mixing of water is larger than for vascular plants. Consequently, the isotopic enrichment of the water adhering to the growth tops of *Sphagnum* plants and of the water stored in their hyaline cells is less pronounced than in vascular plants. Since *Sphagnum* plants lack stomata and therefore the ability to control their rate of water loss, enrichment of the available source water happens exclusively through evaporation.

5.2.3 Isotopic fractionation during biosynthesis

The biggest differences in the isotopic composition of individual compound classes are due to isotopic discrimination during biosynthesis. While all the isotopic alterations mentioned in the previous sections tended to enrich, biosynthesis tends to discriminate against the heavier isotope. Different plants have different biosynthetic pathways. Three different carbon assimilation pathways operate in higher plants: C_3, C_4 and CAM plants (Ehleringer and Cerling, 2001). Differences in carbon isotope ratios ($\delta^{13}C$ values) are related to their photosynthetic pathway (Raven, 1992; Proctor et al., 1992). All the available data indicate that *Sphagnum* and other peat-forming mosses are C_3 photosynthesising plants (Proctor et al.,

1992). However, among monocot species (such as sedges and grasses) C_4 photosynthesis is very common (Ehleringer and Cerling, 2001). Differences in δD values of bulk biomass and cellulose from plants with different biosynthetic pathways have been noted (Sternberg, 1988), but these differences are inconclusive for determining the photosynthetic pathways. Plants of the C_4 photosynthesis type show highly variable D/H ratios (bulk and α-cellulose) that are in some cases, higher than those found in C_3 plants but are in other cases indistinguishable (Yakir, 1992). However, δD values of the saponifiable lipid fraction are not substantially different between C_3 and C_4 plants (Sternberg, 1988). The major difference between the two photosynthetic pathways is shown in Figure 5.2. Photosynthesis is a multistep process in which carbon is fixed into stable organic products. In the C_3 pathway, RuBP carboxylase-oxygenase (Rubisco) combines RuBP with CO_2 and H_2O to form two molecules of phosphoglycerate (PGA). The Calvin cycle and subsequent biochemical pathways then convert PGA into substrates for subsequent reactions. However, Rubisco is also capable of catalysing another reaction with O_2 as substrate, called photorespiration. It oxygenates PGA while consuming ATP and releases fixed CO_2. C_4 Photosynthesis represents a biochemical and morphological modification of C_3 photosynthesis to reduce Rubisco oxygenase activity and thereby increase the photosynthetic rate. In C_4 plants, the C_3 cycle of photosynthetic pathway is restricted to interior cells within the leaves and provides a concentrating mechanism for CO_2 delivery to the Rubisco incorporation mechanism. Since both mechanisms use leaf water, fractionations, only small differences would be

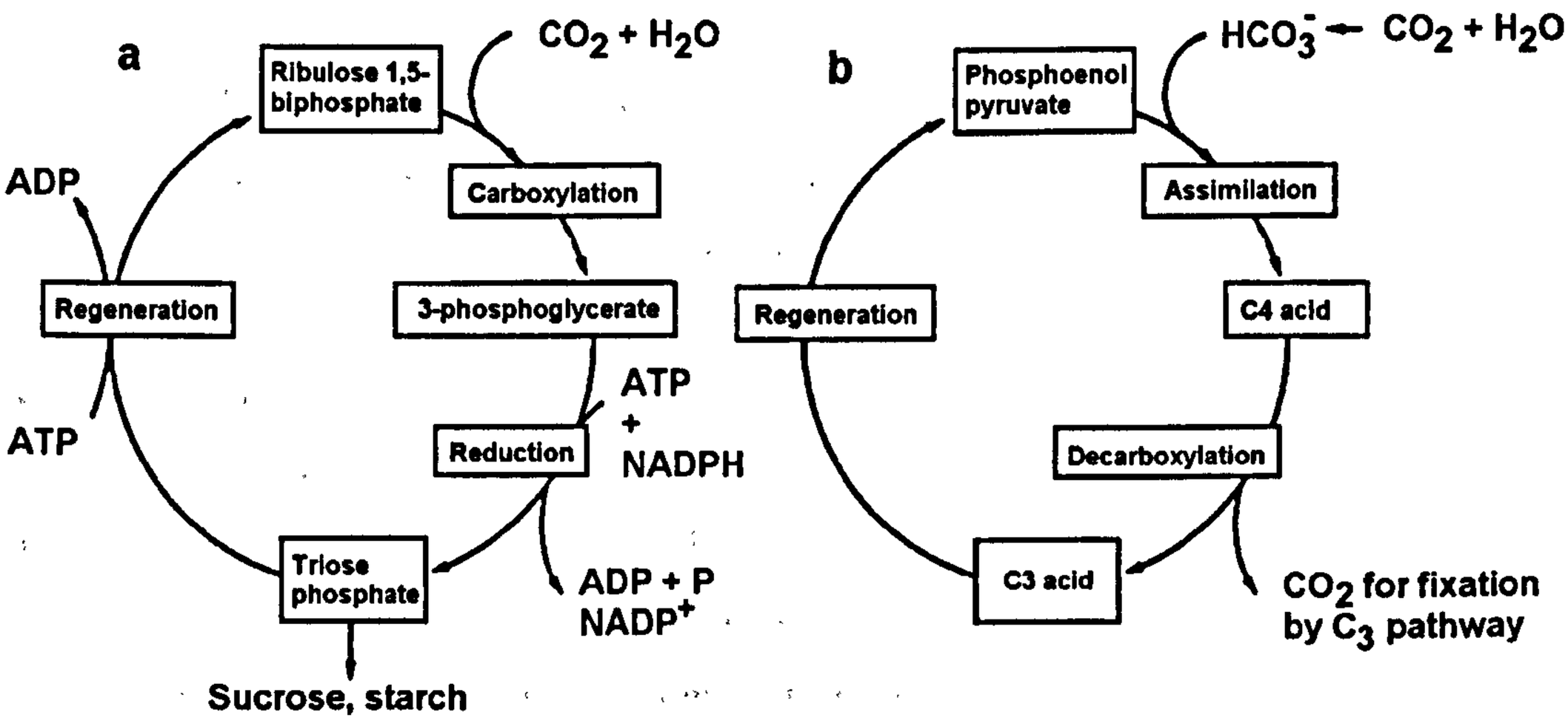

Figure 5.2. The difference between C_3 (a) and C_4 (b) biosynthetic pathways. C_4 pathway introduces extra steps to the C_3 pathway and as such creates extra isotopic fractionations.

expected between δD values obtained from plants through the two photosynthetic systems. Chikaraishi and Naraoka (2003) found on average a difference of 15‰ between *n*-alkane δD values obtained from C_3 and C_4 plants, with C_4 plants being more depleted in deuterium.

Different compound classes in a single organism exhibit different δD values (Estep and Hoering, 1980). Such differences can be explained by the different hydrogen pools used for biosynthesis of the different compound classes and the different biosynthetic pathways employed. During lipid biosynthesis there are three immediate sources for organic hydrogen:

(i) The biosynthetic precursor (dependant on source water).

(ii) Water which can exchange with other organic H atoms.

(iii) The hydrogen added from NADPH, during biosynthesis (Sessions et al., 1999).

The third source of hydrogen is an extra factor controlling the isotopic composition of lipids compared to the factors governing the assembly of the carbon skeleton, and provides extra information on biosynthetic mechanism.

Lipids are divided into two major classes: acetogenic lipids (including *n*-alkanes, *n*-alkanols and *n*-fatty acids) and isoprenoid lipids (triterpenes, hopanes, steroids). All acetogenic lipids in plants are formed via the fatty acid biosynthetic pathway, while isoprenoidal lipids are formed by two distinct biosynthetic pathways: (i) mevalonic acid pathway, and (ii) non-mevalonic acid pathway (1-deoxy-D-xylose-5-phosphate pathway, MEP) (Figure 5.1; Sessions et al., 1999). Hence, it is expected that acetogenic lipids could have different δD values than isoprenoid lipids. Indeed, isoprenoid lipids were found to be depleted relative to acetogenic lipids (Estep and Hoering, 1980; Sessions et al., 1999).

In Figure 5.3 the sources of the isotopic differences in the biosynthesis of lipids is shown. Fatty acid synthesis proceeds with the head-to-tail linkage of acetate molecules in a chain that grows by 2-carbon increments. After addition of acetate, the carboxyl of the previous acetate is reduced by addition of H^+ from NADPH. Dehydration removes the resulting hydroxyl group and one hydrogen from the adjacent methylene group. Addition of a second H^- from NADPH, and H^+ from water, hydrogenates the double bond. The net result of this process is that roughly 25% of lipid hydrogen is derived from the methyl group of acetate, 25% directly from water, and 50% is supplied by NADPH. Given the fact that all acetogenic lipids are produced from the fatty acid biosynthetic pathway (Kolattukudy, 1976), similar δD values can be expected. However, hydrocarbons have distinctly different values compared with fatty acids and *n*-alcohols, whose δD values are similar.

Hydrocarbons have been found to be enriched (Sessions et al., 1999) or depleted (Estep and Hoering, 1980) relative to the other acetogenic lipids, possibly due to the influence of source materials (organic substrates and NADPH).

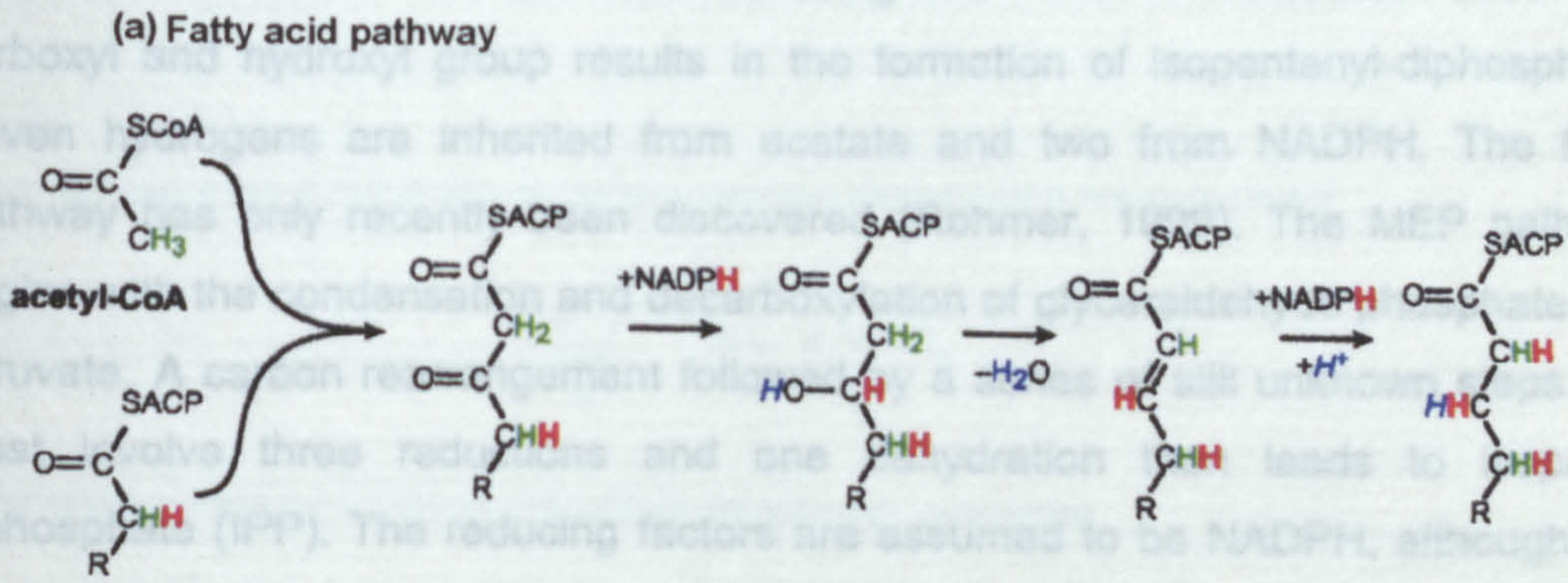

Figure 5.3. Sources of hydrogen during (a) fatty acid synthesis (b) mevalonic acid (MVA) isoprenoid synthesis and (c) methylerythitol phosphate (MEP) isoprenoid synthesis (after Sessions, 2002). Hydrogen shown in red is supplied by NADPH, in blue is obtained from water and green is inherited from organic substrates. Two arrows indicate multiple steps.

In isoprenoid lipids the amount of hydrogen derived from NADPH is less (22% for MVA pathway and 33% for MEP pathway) than for the acetogenic lipids. Figure 5.3b and c shows the major sources of hydrogen for both pathways used in isoprenoid synthesis. In the MVA pathway three acetyl coenzyme A (CoA) molecules condense and are reduced using two NADPH molecules. Loss of a carboxyl and hydroxyl group results in the formation of isopentenyl-diphosphate. Seven hydrogens are inherited from acetate and two from NADPH. The MEP pathway has only recently been discovered (Rohmer, 1999). The MEP pathway begins with the condensation and decarboxylation of glyceraldehyde phosphate and pyruvate. A carbon rearrangement followed by a series of still unknown steps that must involve three reductions and one dehydration then leads to isopentyl diphosphate (IPP). The reducing factors are assumed to be NADPH, although this has still to be demonstrated. Three of nine hydrogens in IPP are inherited from the methyl group of pyruvate and two or four are supplied by glyceraldehyde phosphate; the remainder are then either supplied by NADPH (or another reductant) or by water. Differences between the two pathways, with phytol (MEP) being consistently depleted relative to sterols and triterpenoids (MVA) have been observed (Sessions et al., 1999; Sessions et al., 2002). At present it is assumed that steroids and triterpenes in plant systems are derived using the MVA pathway, while the MEP pathway is used for hopanoid biosynthesis in bacteria (Rohmer, 1999).

To make a connection between the isotopic composition of lipids and the isotopic composition of source water (the ultimate source of hydrogen and deuterium), it is necessary to trace the exact source of hydrogen on NADPH and in the organic substrates for each biosynthetic pathway. A mechanism for the depletion of lipids versus source water is found in the use of NADPH as reductor in many biosynthetic pathways. The source of hydrogen in NADPH is not very well understood. A major source is the oxidation by Rubisco in the photorespiration in organisms. The H^+ at the oxidized position is quantitatively transferred to $NADP^+$. In addition it is assumed that protons are in equilibrium with water and are available for reduction of $NADP^+$ (Yakir, 1992). So several sources of hydrogen precursor molecules are possible, which can lead to the observed depletion of lipids versus source water.

Post-synthetic alterations can influence the final isotopic composition of the lipids, and such heterotrophic processing leads to deuterium enrichment. Post-synthetic metabolism can enrich the lipids through hydrogen exchange. Although carbon bound hydrogen is considered to be non-exchangeable, there are numerous opportunities for its exchange during metabolism and isomerisations via complex

enzyme-catalyzed reactions (Yakir, 1992). Most of these reactions involve enol intermediates, and as such a possible kinetic isotope effect through the abstraction of a proton (for binding to the enzyme) and the breaking of a C-H bond. An overview of all the possible reactions influencing the hydrogen isotopic composition of lipids is given in Figure 5.4 (Schimmelmann et al., 1999).

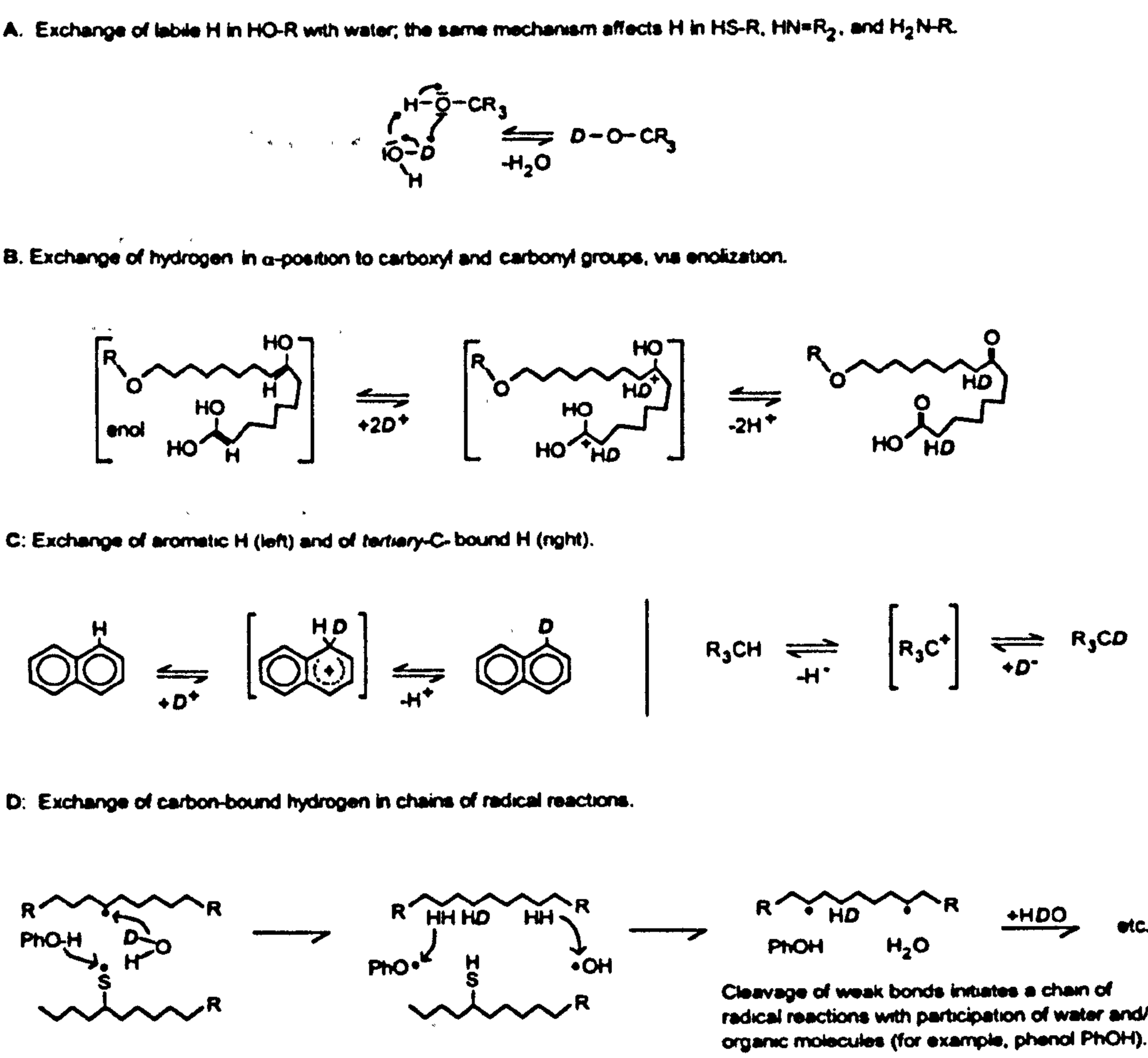

Figure 5.4. Different exchange mechanisms for isotopic alterations to synthesised biomolecules (taken from Schimmelmann et al., 1999).

5.2.4 Aims of the chapter

The investigation of compound-specific δD values in two ombrotrophic peat cores will aim to:

(i) Using compound-specific δD values of peat-forming plants previously obtained in this laboratory by Xie et al. (in press), an assessment of the water usage of the different peat forming plants will be undertaken and

δD values of lipid biomarkers in peat can then be compared with the presumed δD of the source water.

(ii) Comparison of a 1000-year record from two neighbouring bogs will provide a means of investigating synchronous profiles.

(iii) Comparison of the δD profiles for selected compounds with documentary climate records.

(iv) Application of the relationship between climate and δD values of individual lipid biomarkers.

5.3 Results and discussion

5.3.1 δD values of individual peat lipids

5.3.1.1 δD values of *n*-alkanes in peat forming plants

In previous work performed in this laboratory (Xie et al., in press) six *Sphagnum* and three sedge species were evaluated for the δD values of their straight chain hydrocarbons (summarized in Table 5.1). Mean total *n*-alkane δD values agree with a later study that reported plant *n*-alkane δD values ranging between –115 and –210‰ (Chikaraishi and Naraoka, 2003). Using the average fractionation factor determined for C_3 photosynthesising plants (-116‰ ± 15; Chikaraishi and Naraoka, 2003), which is lower than the estimate by Sessions et al. (1999) of –160‰, but falls within the fractionation range (-80 to -167‰) reported by Sauer et al. (2001), the δD value of the plant source water (bog water) was determined and estimated to be ca. –45‰. However, large differences exist between the different plants. Differences between sedge species and *Sphagnum* would be expected, because biochemical fractionation could be species specific. *Sphagnum* species are enriched in deurerium relative to sedge plants by about 20‰ (Table 5.1). However, there is evidence to suggest that biochemical fractionation is

Table 5.1. δD values of *n*-alkanes (‰) in three sedge and six *Sphagnum* species (Xie et al., in press). δD of source water determined using –116‰ fractionation factor for C_3 plants (Chikaraishi and Naraoka, 2003).

	n-C_{23}	*n*-C_{25}	*n*-C_{27}	*n*-C_{29}	*n*-C_{31}	*n*-C_{33}	average	δD water
Trichophorum cespitosum	-130 ± 7	-148 ± 5	-195 ± 7	-231 ± 4	-231 ± 0	-222 ± 1	-193 ± 44	-77 ± 23
Eriophorum angustifolium	-144 ± 5	-127 ± 4	-154 ± 2	-194 ± 2	-210 ± 1	-199 ± 1	-171 ± 34	-54 ± 19
Eriophorum vaginatum	-140 ± 4	-155 ± 11	-178 ± 6	-180 ± 3	-176 ± 1	-195 ± 5	-171 ± 20	-54 ± 12
Sphagnum capillifolium	-147 ± 1	-155 ± 3	-128 ± 5	-143 ± 3	-149 ± 1	-139 ± 8	-143 ± 9	-26 ± 9
Sphagnum palustre	-161 ± 1	-162 ± 1	-147 ± 7	-154 ± 6	-163 ± 2	-148 ± 6	-156 ± 7	-39 ± 8
Sphagnum magellanicum	-160 ± 6	-168 ± 4	-141 ± 11	-140 ± 1	-159 ± 3	-161 ± 6	-155 ± 12	-38 ± 9
Sphagnum papillosum	-157 ± 4	-148 ± 6		-143 ± 0	-169 ± 3	-157 ± 1	-155 ± 10	-38 ± 9
Sphagnum recurvum	-167 ± 5	-147 ± 6	-147 ± 13	-172 ± 2	-141 ± 5	-142 ± 0	-153 ± 13	-36 ± 10
Sphagnum cuspidatum	-171 ± 2	-156 ± 3	-145 ± 3	-161 ± 5	-192 ± 4	-193 ± 7	-170 ± 19	-53 ± 12

not only species-specific, but also similar within the same genus (Aravena and Warner, 1992). Hence, the differences in hydrocarbon δD values cannot be attributed to differences in plant biosynthesis, but to differences in source water. The study by Ménot-Combes et al. (2002) supports this suggestion. These authors determined the δD values of water in hummocks and hollows of ombrotrophic peat bogs and observed a mean depletion of between 8-15‰ for hollows compared to hummocks. Surprisingly, the measured and estimated δD values of source water in hummocks (-30 to -45‰) and hollows (-40 to -70‰) are nearly identical for the two different sites (oceanic climate, UK, this study and Mountain climate, Switzerland, Ménot-Combes et al., 2002). The difference in bog water is reflected in the different *Sphagna* taxa, which all inhabit different microenvironments (hummocks/hollows or lawns) and as such will take up isotopically different water. The differences between sedge species, and their relative depletion compared to most *Sphagnum* plants can thus also be explained by source water. The roots of sedges penetrate deeper into the bog, where the source water is relatively depleted in deuterium compared with the surface bog water (Ménot-combes et al., 2002). Since the δD values of sedge plants are depleted relative to *Sphagnum*, a contribution to the enrichment process by evapotranspiration expected in the leaf water can be ruled out.

When comparing individual *n*-alkane δD values between the two classes of peat forming vegetation (Figure 5.5), it is obvious that a gradual depletion in deuterium occurs with increasing longer-chain length homologues in sedges. This is contrary to what has been observed before in fatty acids (Sessions et al., 1999), where enrichment in δD was seen. No such trend was observed for *Sphagnum* species. *n*-Alkanes in *Sphagnum* display similar δD values for all homologues, although minor enrichment is evident for the *n*-C_{27} homologue. This pattern of depletion in *Sphagnum* versus the depletion in sedges reflects those seen in the relative abundance distributions for *n*-alkanes (see Chapter 3). As such it can be assumed that biosynthetic differences lie at the basis of these isotopic variations. However, since so little is known about the hydrogen incorporation into the different plant species it is impossible to make any firmer statement concerning the precise source of variation.

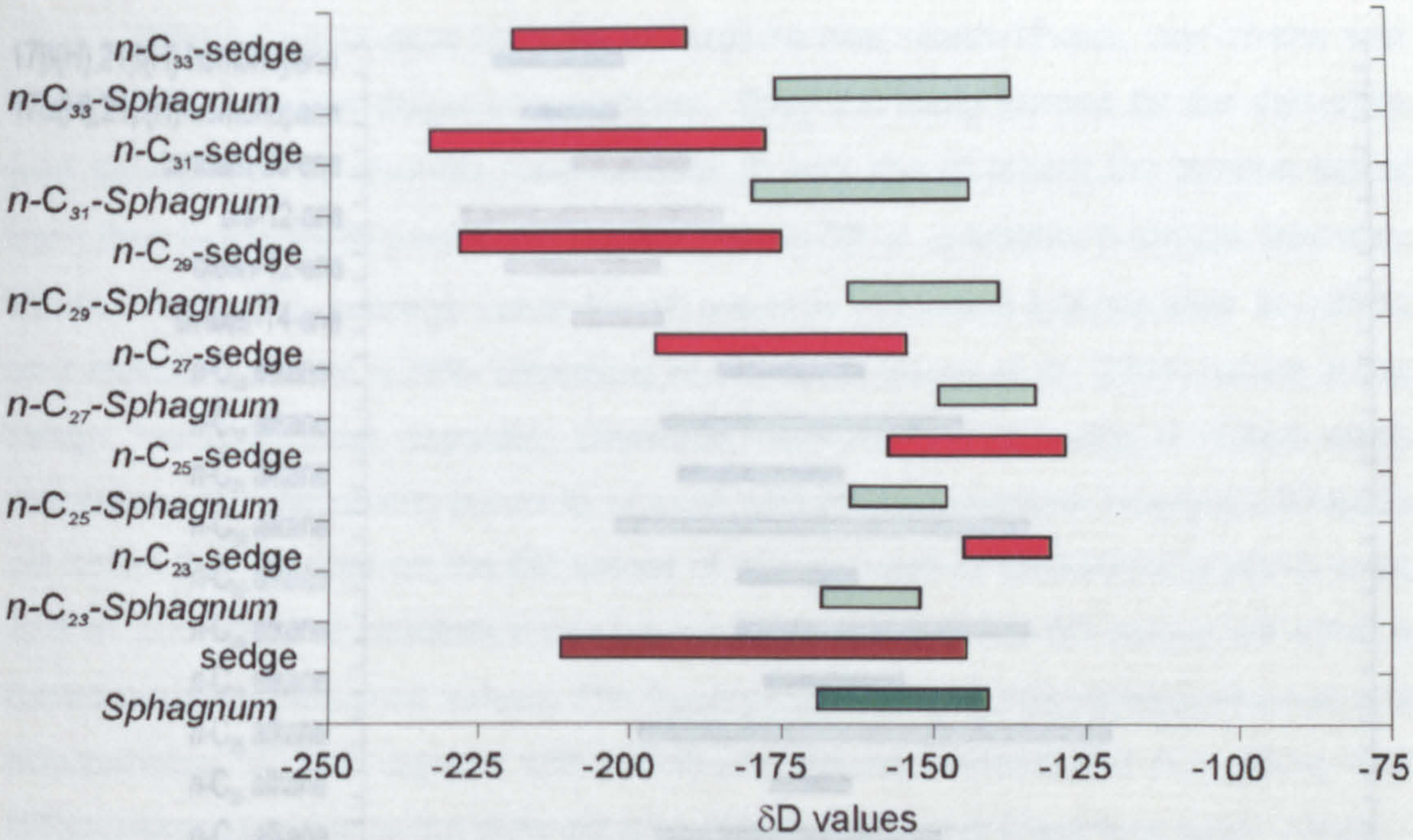

Figure 5.5. Range of δD values for individual *n*-alkanes in *Sphagnum* (green) and sedges (red), showing distinctly different δD value ranges. Average range for all *n*-alkanes for *Sphagnum* (dark green) and sedges (dark red).

5.3.1.2 δD values of hydrocarbons in peat

Since the major hydrocarbons in peat are derived from peat forming plants (Chapter 3) a correlation between their δD values (see Section 5.3.1.1) and the δD values of peat is expected. Figure 5.6 shows the average δD values of peat hydrocarbons, together with bulk peat δD values. Bulk δD values (on average –86‰ ± 10‰ for all samples of both cores), obtained using the procedure described in section 4.3, are similar to those reported by Schiegl (1972; -77‰ ± 20‰). Bulk values are always more enriched in deuterium than individual lipids, since their value is determined by the δD values of all the plant components, i.e. not only lipids but also carbohydrates, amino acids, tannins, lignin, and represent a large proportion of exchangeable hydrogens. Since lipids are only a minor part of the total plant components, their relatively large depletion will not be reflected in the bulk δD values. Bulk δD values reported in this thesis are similar to those obtained from α-cellulose (Dupont and Mook, 1987; van Geel and Middeldorp, 1988).

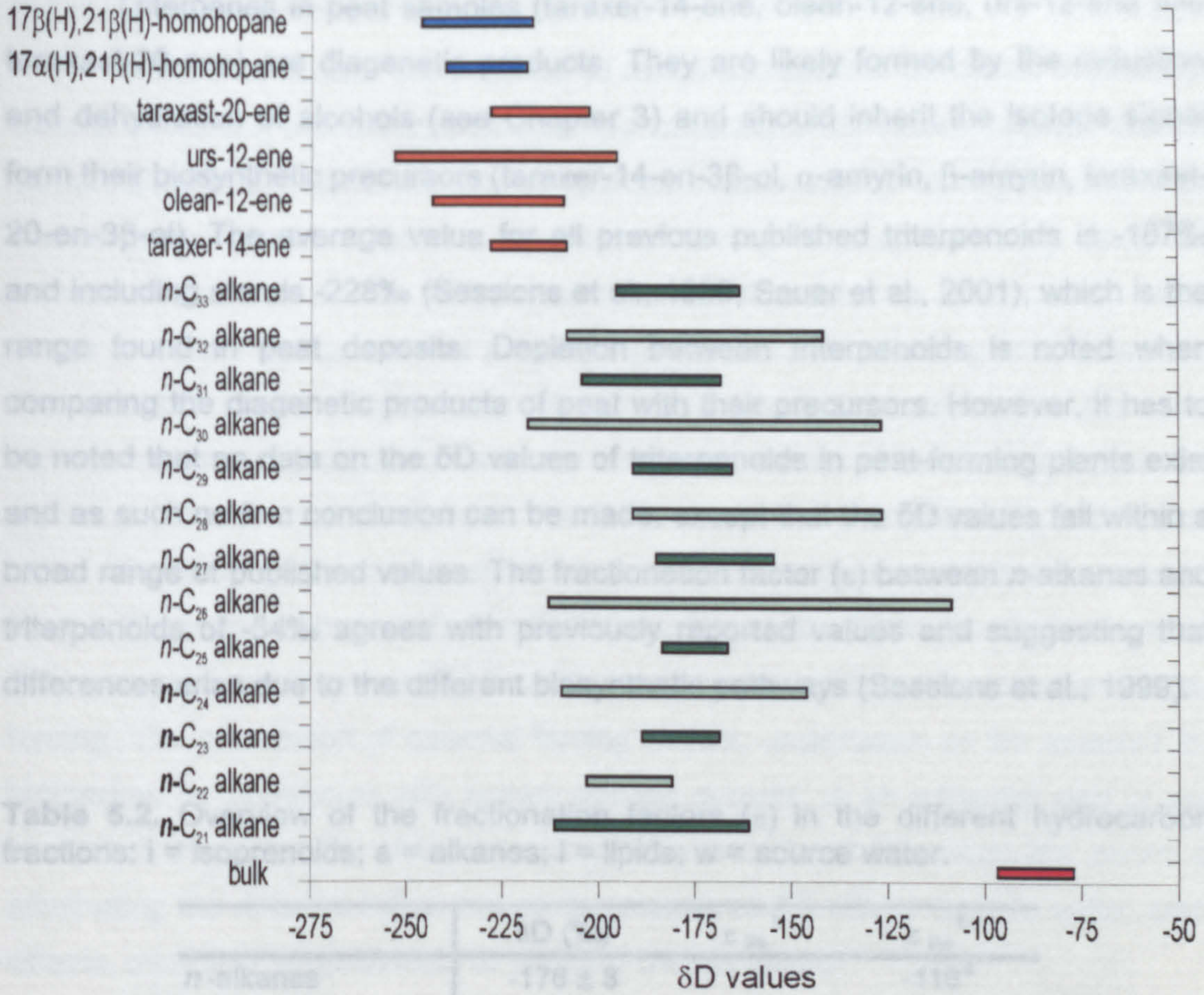

Figure 5.6. Range of hydrocarbon δD values in two peat cores (Bolton Fell Moss and Walton Moss). Range exists of average value over the two cores plus standard deviation on the measurements (± 750 data points per compound).

Comparing the δD values of *n*-alkanes (Figure 5.5 and Figure 5.6) from peat with the δD values of *n*-alkanes from peat forming plants, the distribution of individual *n*-alkanes δD values in peat is comparable with the distribution of the δD values of individual *n*-alkanes obtained from *Sphagnum* and not with the δD distribution from sedges. A similar mean δD value for all of the *n*-alkanes is noted, with a minor enrichment for the *n*-C_{27} homologue. However, the freshly collected peat-forming plants are less depleted in deuterium than the actual peat lipids. No obvious explanation exists for this observation since alkanes are considered to be relatively isotopically stable (lack of exchangeable hydrogens). A possible reason is the time of collection of the fresh *Sphagnum* plants. The freshly collected plants will exhibit the isotope signal from the most recent precipitation events, while the peat samples will represent a mean δD value of the source water over a longer period of time (years). The larger variation of the even-numbered-alkanes is due to lower abundances, which induce larger errors in the measurements (see Chapter 4).

Triterpenes in peat samples (taraxer-14-ene, olean-12-ene, urs-12-ene and taraxast-20-ene) are diagenetic products. They are likely formed by the reduction and dehydration of alcohols (see Chapter 3) and should inherit the isotope signal form their biosynthetic precursors (taraxer-14-en-3β-ol, α-amyrin, β-amyrin, taraxast-20-en-3β-ol). The average value for all previous published triterpenoids is -187‰ and including sterols -228‰ (Sessions et al., 1999; Sauer et al., 2001), which is the range found in peat deposits. Depletion between triterpenoids is noted when comparing the diagenetic products of peat with their precursors. However, it has to be noted that no data on the δD values of triterpenoids in peat-forming plants exist and as such no firm conclusion can be made, except that the δD values fall within a broad range of published values. The fractionation factor (ε) between *n*-alkanes and triterpenoids of -54‰ agrees with previously reported values and suggesting that differences arise due to the different biosynthetic pathways (Sessions et al., 1999).

Table 5.2. Overview of the fractionation factors (ε) in the different hydrocarbon fractions: i = isoprenoids; a = alkanes; l = lipids; w = source water.

	δD (‰)	$\varepsilon_{l/a}$ [b]	$\varepsilon_{l/w}$ [b]
n-alkanes	-176 ± 8		-116[a]
triterpenes	-221 ± 9	-54	-164
homohopanes	-231 ± 9	-66	-174
water [a]	-68 ± 9		

(a) determined using -116‰ (Chikaraishi, 2003)
(b) $\varepsilon_{a/b} = 1000[(\delta_a+1000)/(\delta_b+1000)-1]$

The bacterial derived homohopanes are supposed to be biosynthesised via a different pathway to the triterpenoids (see Section 5.2.3). The mean δD values of the hopanes present in peat samples are enriched compared with published δD value for phytol, which reportedly uses the same photosynthetic pathway), namely -229 and -231‰ in peat vs. -330‰ (Sessions et al., 1999).

Using the isotopic fractionation factor for *n*-alkanes in C_3 synthesising plants (Chikaraishi and Naraoka, 2003) an average source water value can be derived. The derived source water δD value of -68‰ (see Table 5.2) is slightly more depleted than that expected from the peat forming plants (-46‰). However, both values fall within δD values measured for precipitation in the UK (-40‰ for the summer and -70‰ for the winter; Heathcote and Lloyd, 1986).

5.3.2 Down-core study of δD values of lipid biomarkers

In order to assess the potential of compound-specific δD values in peats as climate indicators, a down-core study of the variability of δD values between the two sample sites was undertaken. The comparison of two records of neighbouring bogs should reveal similar responses to external forcing. The synchronicity study will provide information on the differences between the cores in local source water usage and plant inputs, but also provide a sound basis for selecting δD biomarkers. The selection of two neighbouring sample sites, which are subjected to the same climatic variations, provides a basis for further discussion of similar patterns in the δD values of individual biomarkers. The Bolton Fell Moss site (5500 yrs) and Walton Moss site (1000 yrs) were examined and compared with data obtained previously from a 300 yr monolith from Bolton Fell Moss (Xie et al., 2000; Xie et al., in press). This comparison will reveal which similarities can be attributed to external climatic forcing. The elucidation of external forcing factors, undertaken on the selected δD biomarker, by correlation with known climatic records, is an essential part of any study into the variability of the record. All the aspects of this study are aimed at eliminating the different influences on the measured δD values (source water, plant effects, analytical uncertainties) to obtain a climate record.

5.3.2.1 Down-core synchronicity of δD *n*-alkane values

Comparison of the δD values for all homologues provides the opportunity to gradually eliminate all the influences on the δD record not related to climate. Figure 5.7 and Figure 5.8 show δD profiles for bulk δD values and all *n*-alkane homologues for all three peat cores. This section discusses the selection of the profiles for climate analysis taking account of analytical and biological factors.

5.3.2.1.1. Instrument effects on low concentration down-core profiles

As discussed in Chapter 4 instrument parameters affect the measured δD values generated. The most pronounced effect on the accurate determination of δD values is the signal size effect. The linearity of the instrument with regard to the signal size can only be guaranteed above 0.75 V. Signal sizes below 0.75 V systematically enrich the determined δD values and show large scatter on repeat determinations. The shorter-chain alkanes suffer from this effect (low overall concentrations), because they do not occur in sufficient concentrations to determine their δD values correctly within mixtures containing higher concentrations of the higher carbon number *n*-alkanes. The substantial offset between the shorter-chain even-numbered

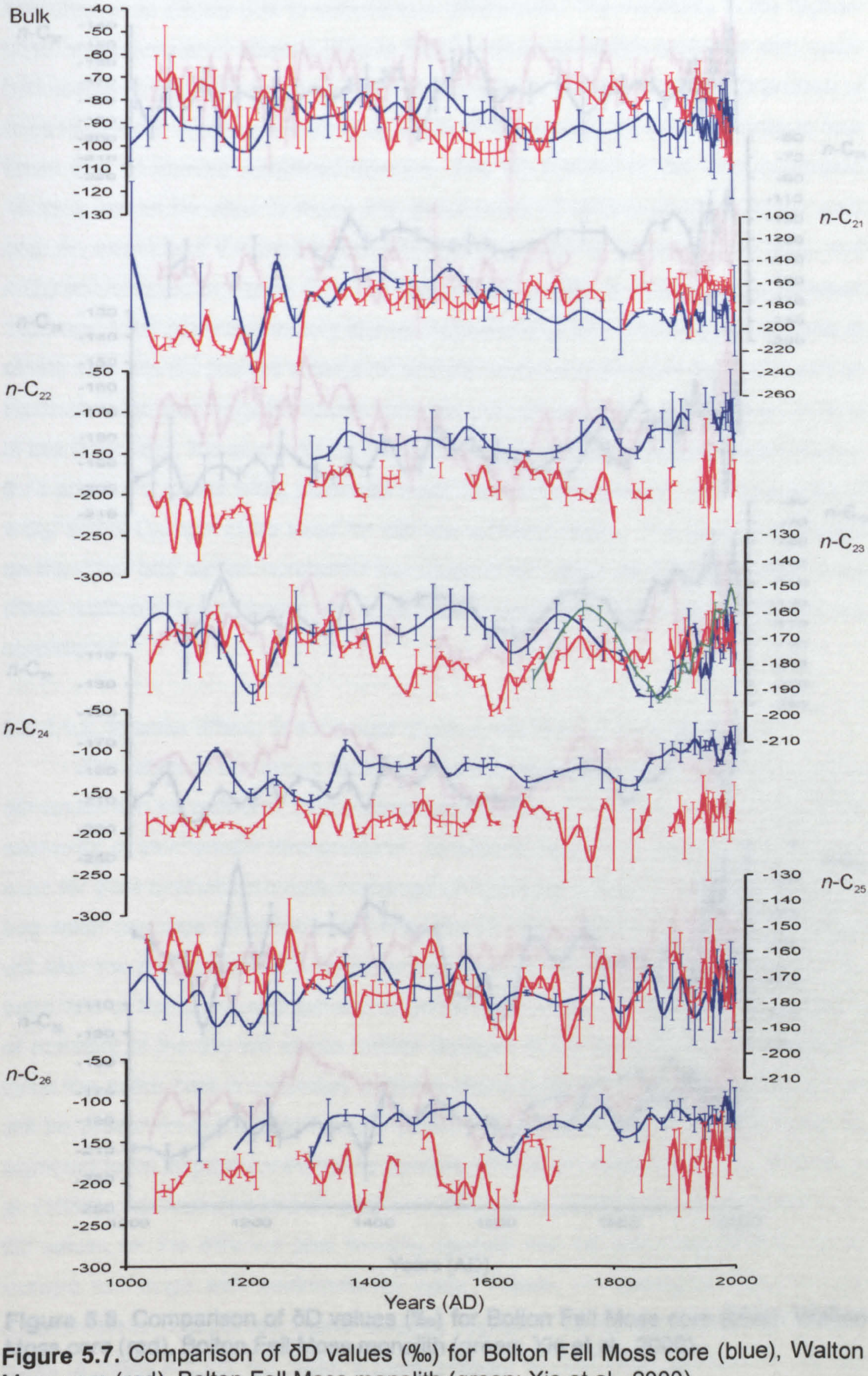

Figure 5.7. Comparison of δD values (‰) for Bolton Fell Moss core (blue), Walton Moss core (red), Bolton Fell Moss monolith (green; Xie et al., 2000).

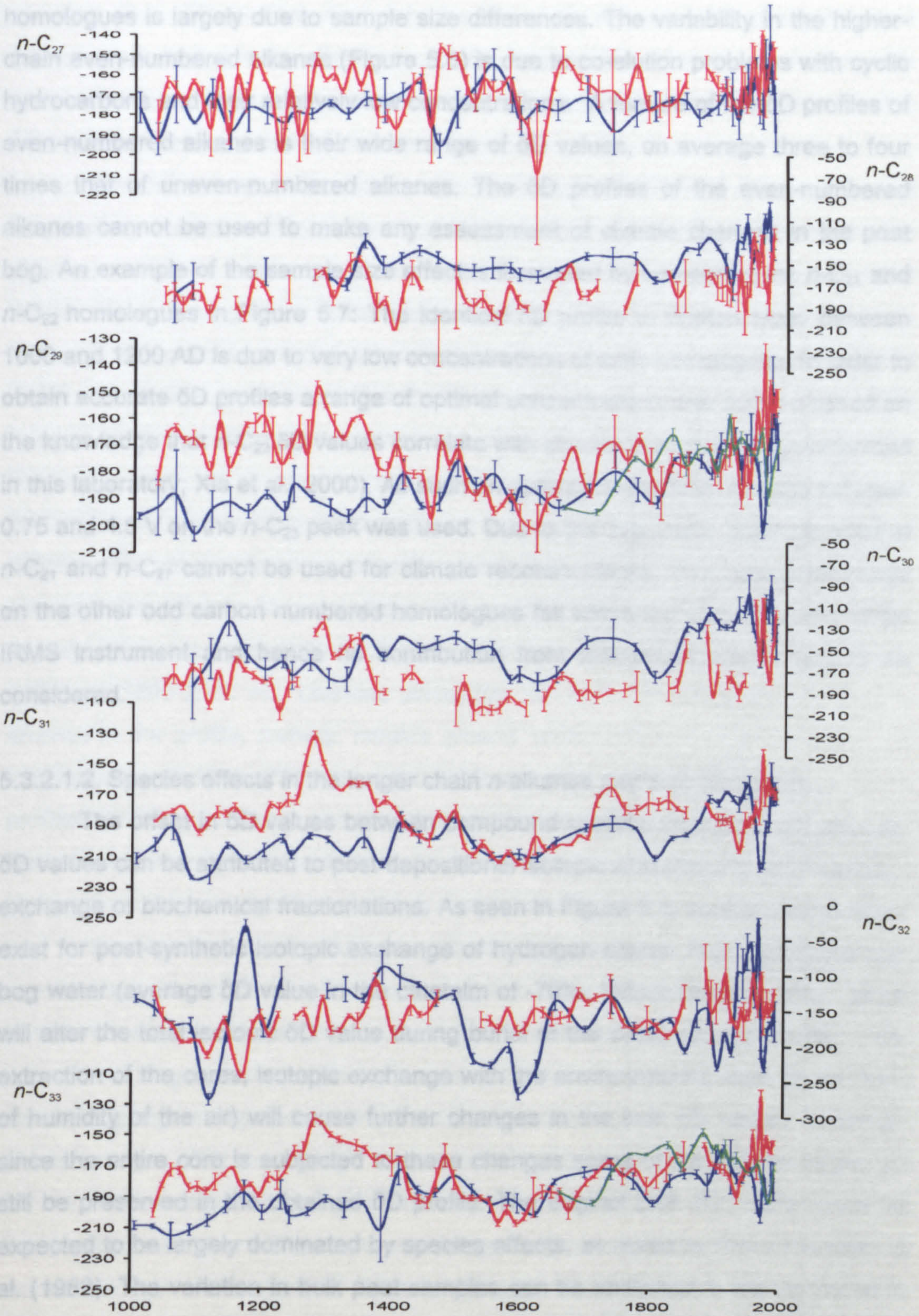

Figure 5.8. Comparison of δD values (‰) for Bolton Fell Moss core (blue), Walton Moss core (red), Bolton Fell Moss monolith (green; Xie et al., 2000).

homologues is largely due to sample size differences. The variability in the higher-chain even-numbered alkanes (Figure 5.8) is due to co-elution problems with cyclic hydrocarbons and their relatively low concentrations. A feature of the δD profiles of even-numbered alkanes is their wide range of δD values, on average three to four times that of uneven-numbered alkanes. The δD profiles of the even-numbered alkanes cannot be used to make any assessment of climate changes in the peat bog. An example of the sample size effect is illustrated by comparing the *n*-C_{21} and *n*-C_{22} homologues in Figure 5.7: The identical δD profile in Walton Moss between 1000 and 1200 AD is due to very low concentrations of both homologues. In order to obtain accurate δD profiles a range of optimal concentrations was defined based on the knowledge that *n*-C_{23} δD values correlate with climate (see pilot study performed in this laboratory; Xie et al., 2000). As such an optimal concentration range between 0.75 and 4.5 V on the *n*-C_{23} peak was used. Due to this approach, the δD profiles of *n*-C_{21} and *n*-C_{27} cannot be used for climate reconstructions. The peak sizes range on the other odd carbon numbered homologues fell within the linearity range of the IRMS instrument and hence no contribution from instrument effects had to be considered.

5.3.2.1.2. Species effects in the longer chain *n*-alkanes and bulk δD values

The offset in δD values between compound-specific measurement and bulk δD values can be attributed to post-depositional isotopic alterations due to hydrogen exchange or biochemical fractionations. As seen in Figure 5.4, several mechanisms exist for post-synthetic isotopic exchange of hydrogen atoms. First, exchange with bog water (average δD value in the catotelm of -70‰; Ménot-Combes et al., 2002) will alter the total isotopic δD value during burial of the decaying peat matter. After extraction of the cores, isotopic exchange with the environmental water (in the form of humidity of the air) will cause further changes in the bulk δD values. However, since the entire core is subjected to these changes some of the original signal will still be preserved in the obtained δD profile. The original bulk δD profile would be expected to be largely dominated by species effects, as noted by Brenninkmeijer et al. (1982). The variation in bulk peat samples can be attributed to the variations in δD values for the different peat forming species and the smoothing effect due to isotopic exchange with environmental water. Hence, no correlation between the different cores is expected. Some features appear to be common between the two cores: a valley around AD 1200, a peak/ plateau around 1400 and then a gradual lowering of the curve towards 1700. The similarity in overall trend probably reflects similar changes in plant communities due to changes in external forcing (dry/wet

climate). Bulk δD profiles can only be seen as indicative of changing plant communities and due to alterations to it's original δD value by exchange with environmental water/humidity, no real value can be attached to the changes in the δD profiles reflecting actual climate events.

The differences in the down-core stratigraphic profiles of the shorter- and longer-chain *n*-alkanes δD values are striking. Differences in δD profiles among the different *n*-alkanes within the same core (blue = Bolton Fell Moss Core; red = Walton Moss Core; green = Bolton Fell Moss Monolith) are expected and observed. Although all *n*-alkanes are derived from the same biosynthetic pathway, differences in δD of individual lipids occur due to differences in water uptake in different peat forming plants, i.e. difference between the shorter (*n*-C_{23} and *n*-C_{25}) and longer (*n*-C_{29}, *n*-C_{31} and *n*-C_{33}) alkanes is expected as the shorter chain alkanes are predominantly derived from *Sphagnum* and the longer chain alkanes exhibit a mixed species δD value. However, overall certain similarities can be observed. For example, the Walton Moss *n*-alkane δD profiles exhibit similar overall patterns, namely: minima around 1000-1200 and 1400-1600 AD, and maxima around 1200-1400 and 1800-2000 AD. Likewise similarities are seen for all Bolton Fell Moss *n*-alkanes in the profile, namely: minima around 1000-1300 and 1800-1850 AD and maxima around 1300-1700 and 1900-2000 AD (see Figure 5.10b). Although the profiles for the individual *n*-alkanes show deviations from each other, which cannot really be explained since the individual lipids should all be derived through the same biochemical pathway, the overall trends can be seen in all records.

The differences in individual *n*-alkanes δD profiles between the two cores can be explained by invoking the following two factors: differences in lipid source (different taxa) and different source water (hummock vs. hollow).

The longer-chain length *n*-alkanes, *n*-C_{29} to *n*-C_{33}, derive from two sources namely: *Sphagnum* species (low concentrations with high plant inputs) and higher plants (sedges, *Ericaceae*, high concentrations with low plant inputs). In section 5.3.1.2 a discussion of the disparity between the peat lipids and their plant species composition was given. This discussion is again relevant in the discussion of the δD values of longer chain alkanes. Within each core, the *n*-alkane profiles show nearly identical patterns for the higher chain lengths (*n*-C_{29}, *n*-C_{31} and *n*-C_{33}), which could be expected looking at the provenance of these lipids. Between the two cores similarities exist during the Little Ice Age (±1400-1700 AD), possibly due to a climate forcing. The differences between the two cores can be attributed to differences in plant inputs. This corresponds to the findings of previous authors (Brenninkmeijer et

al., 1982; Dupont and Mook, 1987; van Geel and Middeldorp, 1988) whom observed the same species influence on δD values of peat α-cellulose.

Both bulk and compound-specific δD stratigraphic profiles are influenced by species variations, so much so that the profiles obtained from bulk peat and the higher homologues can be almost exclusively assigned to the changes in plant composition. Hence, the δD profiles reflect changing plant communities.

5.3.2.2 Shorter-chain *n*-alkane δD values: species and source-water effects

As mentioned several times before in this thesis, the shorter-chain *n*-alkanes (*n*-C_{23} and *n*-C_{25}) are highly specific biomarkers for the *Sphagnum* inputs into peat. From the study of δD values of *Sphagnum* lipids, it was concluded that little variation exists between the different *Sphagnum* species and most of this variation could be attribuated to differences in δD values of the source water. Hence, the δD profiles obtained from these shorter-chain *n*-alkanes should reflect climate, (through the relationship of their δD values to that of their source water).

Within the shorter-chain-length alkanes the difference in the down-core δD stratigraphic profiles is striking. *n*-C_{25} shows considerable variation in its down-core δD profile. Very few similarities exist with the *n*-C_{23} down-core δD profile. The possibility of species effects also dominating *n*-C_{25} has to be considered. The study of the *n*-alkane distributions in peat-forming plants revealed a minor input of shorter-chain alkanes from sedge species, proportionally larger for *n*-C_{25} than for *n*-C_{23}. Thus, the differences in the *n*-C_{25} δD profiles could be partially attributed to the small differences in plant inputs combined with variations in δD source water for the different species (hummock/hollow). A possible alternative explanation is differences in biosynthesis in periods of climatic stress on the hydrocarbon abundances and isotopic values affecting individual lipids. However, insufficient information is currently available on the biosynthetic pathways and the effect of climatic forcing to make a firm independent statement concerning its possible effects. The different effects make it impossible to filter the interfering species signal from the climate signal.

The n-C_{23} δD profile is shown in Figure 5.9. The succession of depletion and enrichment in δD values is surprisingly similar in both peat bogs. This leads to the conclusion that besides minor plant input effects also an external forcing factor (climate) controls *n*-C_{23} δD values. The largest difference between the two cores is situated between 1400-1700 AD and around 1850 AD. This can be explained by differences in source water coming from hummock/hollow differences, with hollows being depleted vs. hummocks.

In Table 5.3 the different deviations from the long-term trend in δD values is compared to the abundance data (discussion see Chapter 3) and wet-shift data. From this table it is obvious that several data are recurring in all three data sets. As such it can be concluded that indeed climate in general or at least one of its variables lies at the basis of the observed shifts.

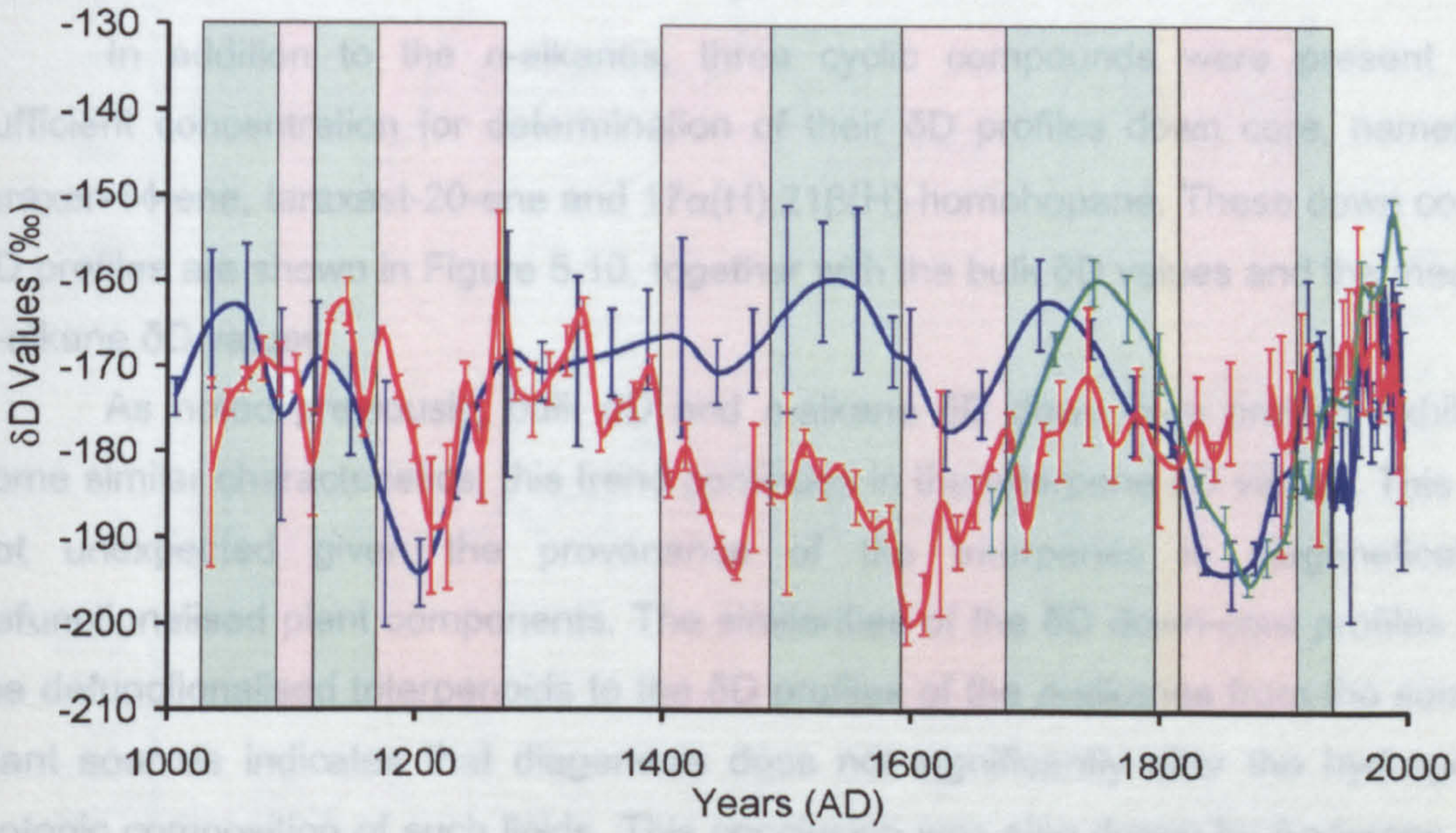

Figure 5.9. Comparison of the *n*-C_{23} alkane profile in all three cores: red = Walton Moss; blue = Bolton Fell Moss Core; green = Bolton Fell Moss Monolith (Xie et al., 2000). Similarities are marked with coloured bands: valleys (red) and peaks (green).

Table 5.3. Comparison of the episodes noted in the δD values (depletion from mean values) and abundance data (higher abundance than mean value) of *n*-C_{23} and known wet-shift (years AD, see Table 3.5) episodes occuring during the last millennium.

abundance	δD values	wet-shifts
1990	1990	
1970	1970	
1940	1935	
1905		
1840	1840	1850
1780		1770
1750		1740
1650		
1610	1610	1600
		1580
1510		
1430	1460	1440
1310		1330
1200	1210	1200
1090	1100	

In order to determine which variables of the climate system cause the shifts in the records, a comparison of the δD values with known climatic parameters will be undertaken (Section 5.3.3).

5.3.2.3 Down-core δD values of the non-cyclic hydrocarbons

In addition to the *n*-alkanes, three cyclic compounds were present in sufficient concentration for determination of their δD profiles down core, namely: taraxer-14-ene, taraxast-20-ene and 17α(H),21β(H)-homohopane. These down core δD profiles are shown in Figure 5.10, together with the bulk δD values and the mean *n*-alkane δD values.

As noted previously, bulk δD and *n*-alkane δD down core profiles exhibit some similar characteristics; this trend continues in the triterpene δD values. This is not unexpected given the provenance of the triterpenes is diagenetically defunctionalised plant components. The similarities of the δD down-core profiles of the defunctionalised triterpenoids to the δD profiles of the *n*-alkanes from the same plant sources indicates that diagenesis does not significantly alter the hydrogen isotopic composition of such lipids. This conclusion was also drawn by Andersen et al. (2001) during their studies of the δD values of *n*-C_{22} alkane and 5α-cholestane in a Messinian sediment core. The major difference between the down core profiles of the *n*-alkane components and the diagenetically altered components occurs in the uppermost part of the cores (1950 to present), where instead of enrichment, a depletion of δD values is noted. This, however, is much more likely since the influence of increasing temperature should, in theory, give rise to a depletion of deuterium in the source-waters. Comparison of the two cores (BFM and WM) does not yield any useful information, since δD values are not determined (low signal strength) on a large section of the Walton Moss core. Within each core the δD profiles of all components are very similar and this can be, (see Section 3.4.1.2) attributed to a similar diagenetic pathway for their formation, probably mediated by the same microbial population.

The αβ-homohopane component, a bacterial derived compound, does not show the same general trends as the plant derived triterpenes. This is not unexpected since the hydrogen isotopic fractionations in micro-organisms can deviate substantially from those in plants (Sessions et al., 2002). The patterns of variation between the two cores shows some similarities, but overall little variation is observed, except again at the top part of the core where the hopanes start to

appear. Both cores show rather different profiles, presumably due to the microenvironments responsible for the development of the microbial communities.

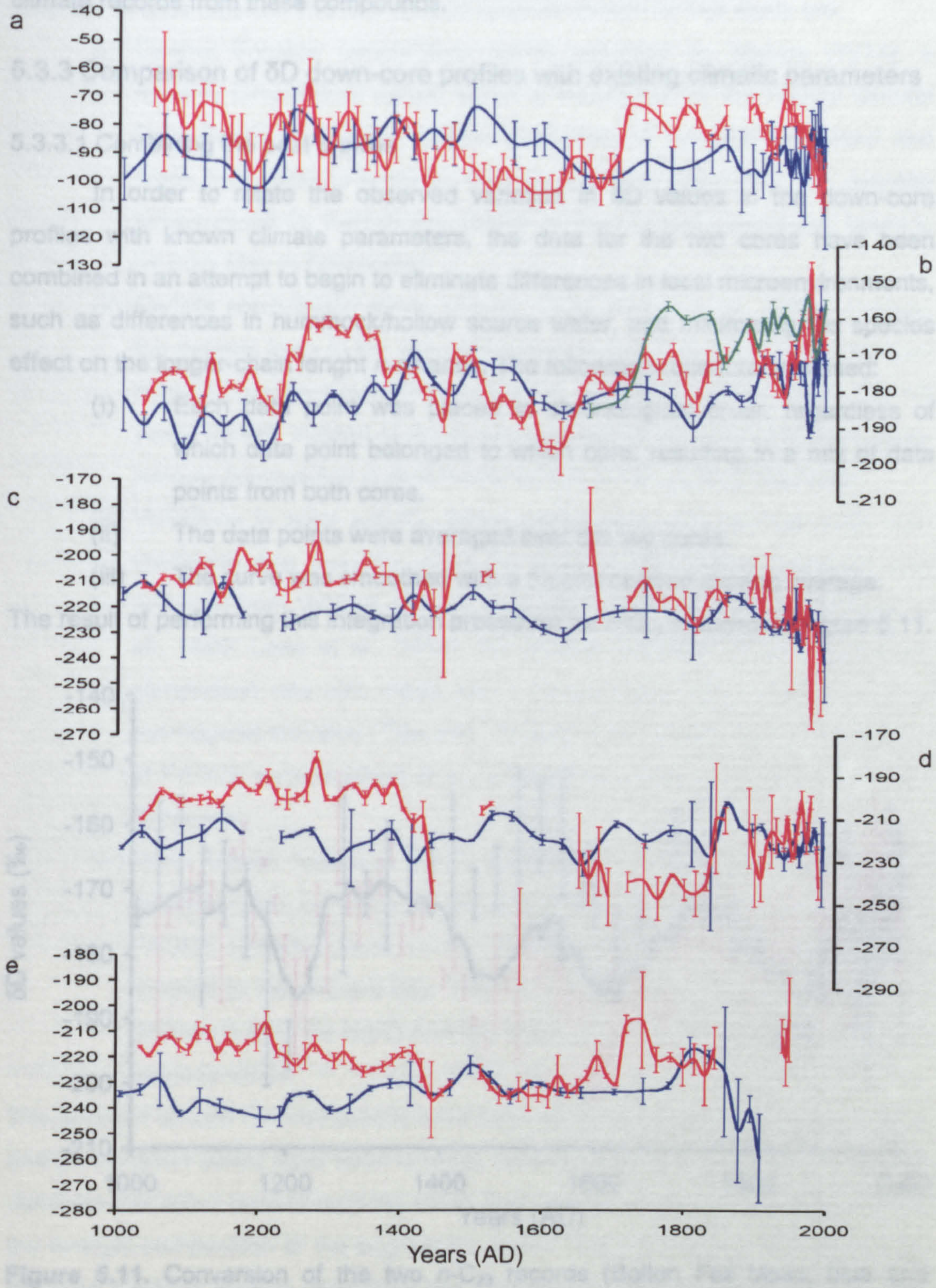

Figure 5.10. Comparison of δD values from (a) bulk, (b) average of all odd-carbon numbered *n*-alkanes, (c) taraxer-14-ene, (d) taraxast-20-ene and 17α(H),21β(H)-homohopane for Bolton Fell Moss Core (blue), Walton Moss Core (red) and Bolton Fell Moss Monolith (green).

The links between climate and these microbially derived components is currently rather unclear. As such it is deemed impossible at present to derive useful climate records from these compounds.

5.3.3 Comparison of δD down-core profiles with existing climatic parameters

5.3.3.1 Combining the peat profiles

In order to relate the observed variation in δD values in the down-core profiles with known climate parameters, the data for the two cores have been combined in an attempt to begin to eliminate differences in local microenvironments, such as differences in hummock/hollow source water, and minimising the species effect on the longer-chain lenght *n*-alkanes. The following procedure was used:

(i) Each data point was placed in chronological order, regardless of which data point belonged to which core, resulting in a mix of data points from both cores.

(ii) The data points were averaged over the two cores.

(iii) The curve was smoothed with a 5-point centred moving average.

The result of performing this integration procedure for *n*-C_{23} is shown in Figure 5.11.

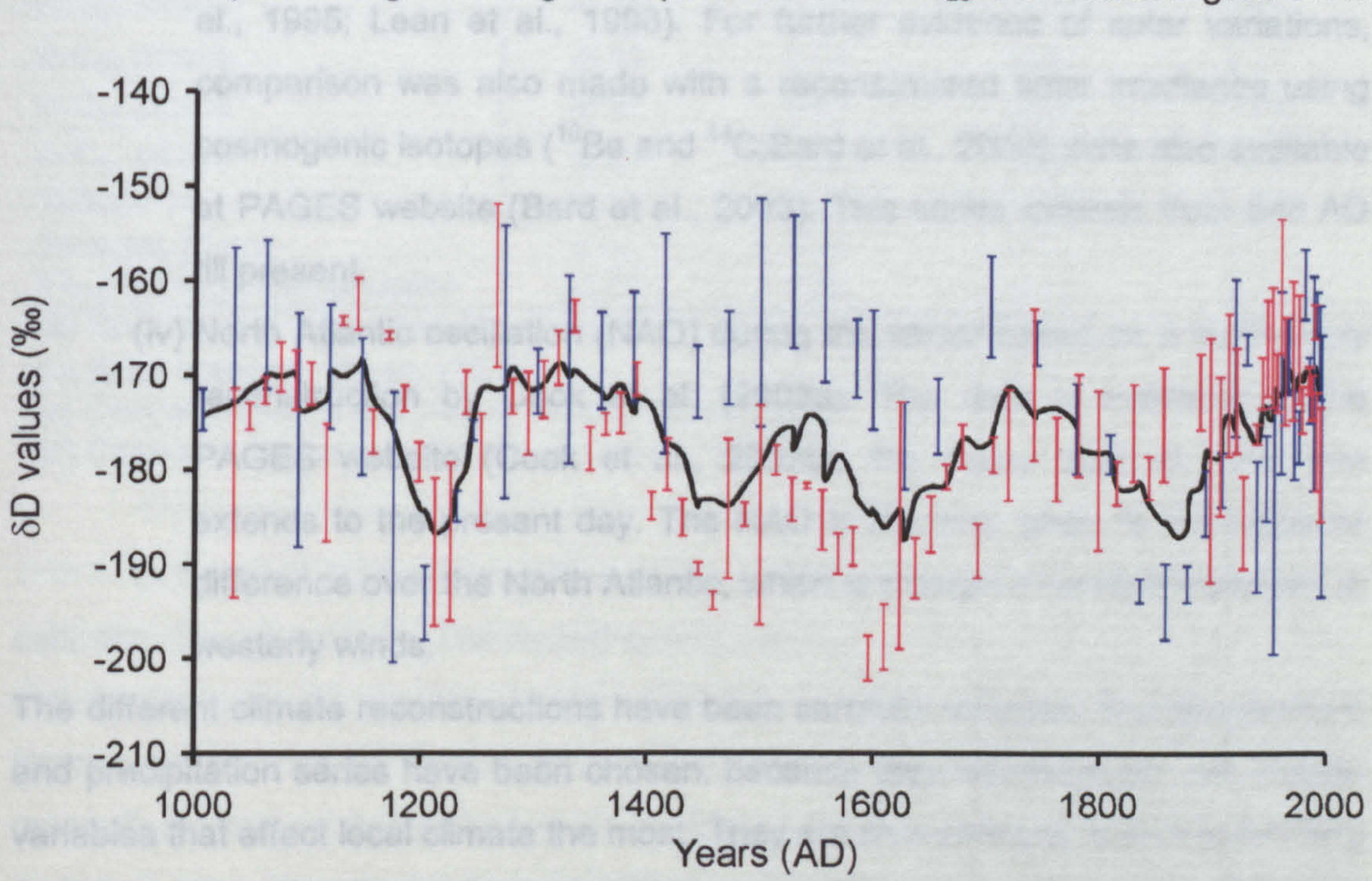

Figure 5.11. Conversion of the two *n*-C_{23} records (Bolton Fell Moss, blue and Walton Moss, red) into one single record (black line) using a five-point moving average smoothing of the data.

5.3.3.2 Possible links with known climate parameters

To investigate possible existence of climate signals in the composite deuterium record (see section 5.3.3.1), the δD profiles will be compared with different climate records. The four climate records chosen for this study are:

(i) Central England temperature series compiled by Manley (1974), a monthly temperature series, which is maintained by the Hadley Climate Data Centre and is the longest observational temperature record and dates from 1659 to present. The temperatures taken here are average temperatures for the growing season of peat forming vegetation, taken to be from May to September.

(ii) Carlisle precipitation series (Jones, 1983; Parker et al., 1992). Carlisle, the nearest town to the two peat bog deposits (Figure 2.1), has the third longest homogeneous rainfall series in the UK, Tabony (1980). The full yearly rainfall, instead of the growing season is used, since the bog water isotopic composition is determined by the entire years precipitation.

(iii) Variations in solar activity. Direct comparison with reconstructed solar irradiance was possible using the reconstructed solar irradiance data recorded from 1610 till present, available at the PAGES website (Lean et al., 1995; Lean et al., 1998). For further evidence of solar variations, comparison was also made with a reconstructed solar irradiance using cosmogenic isotopes (^{10}Be and ^{14}C;Bard et al., 2000); data also available at PAGES website (Bard et al., 2003). This series extends from 843 AD till present.

(iv) North Atlantic oscillation (NAO) during the winter based on a multi-proxy reconstruction by Cook et al. (2002a). The data is available at the PAGES website (Cook et al., 2002b); the series start at 1400 and extends to the present day. The NAO is the term given to the pressure difference over the North Atlantic, which is thought to govern variations in westerly winds.

The different climate reconstructions have been carefully selected. The temperature and precipitation series have been chosen, because they represent the two climate variables that affect local climate the most. They are also principal factors controlling the isotopic composition of the bog source water. The solar data has been chosen because previous studies (Blackford and Chambers, 1995; Speranza et al., 2002) have found evidence for solar forcing of the climate by linking peat bog properties (humification data and ^{14}C content) to solar activity. The link between solar activity and climate has been widely established (Bradley, 1999) and as such deserves

attention. The fourth data series, the reconstructed NAO index is a measure for the pressure difference over both ends (Iceland and the Azores) of the North Atlantic along the same longitude and is thought to influence the variation in westerly winds above the Atlantic (can be compared to the El-Ninõ phenomena).

Table 5.4 gives the correlation coefficients between the 5-point composite δD records of the different components and a 30-year moving average for the climate data. Noticeable, is the moderate correlation with the solar activity record. The correlation coefficients for the composite *n*-C_{23} record is lower than was expected through a visual comparison of the profiles. This is probably due to the scatter in the records and the fact that the δD down core records are unevenly spaced data, while the historical records are evenly spaced.

Table 5.4. Correlation coefficient (r) between the 5-point moving average δD values for each compound with a thirty-year moving average climate component.

	NAO[a]	Solar[b]	Temperature[c]	Rainfall[d]
Bulk	-0.13	-0.06	0.05	0.02
Average all alkanes	-0.41	0.76	0.31	0.29
n-C_{21} alkane	-0.23	0.23	0.25	0.14
n-C_{23} alkane	-0.35	0.58	0.44	0.42
n-C_{25} alkane	-0.34	0.51	0.16	0.21
n-C_{27} alkane	-0.45	0.52	0.16	0.07
n-C_{29} alkane	-0.33	0.74	0.25	0.15
n-C_{31} alkane	-0.27	0.61	0.25	0.28
n-C_{33} alkane	-0.33	0.65	0.16	0.16
Taraxer-14-ene	0.25	-0.80	-0.43	-0.43
Taraxast-20-ene	0.04	0.54	0.01	0.05
17α(H),21β(H)-homohopane	-0.07	0.05	0.36	-0.04

(a) North Atlantic oscillation (Cook, 2000b)
(b) Solar irradiance (Lean, 1998)
(c) Central England temperature series (Manley, 1972)
(d) Carlisle composite rainfall record (Jones, 1983)

In Figure 5.12 the δD profiles of the composite record is compared to the 4 selected climate records. The record spans a period of climatic shifts (noticeable in the climate data). As discussed before (Section 3.5.3) the last thousand years of the Earth's climate can be divided into several climatic episodes. Around 1,400 AD is the end of what is generally known as the medieval optimum, a relatively warm period of dry summers and high precipitation. This is followed between 1,450-1,700 AD by a general cooling and is known as the Little Ice Age, a period of severe winters and wet summers. Then a gradual improvement of the climate is observed, with a second climatic cooling around 1,850 AD, known as the second part of the Little Ice Age, and then the present warming of the climate system.

In the period studied here, the bulk isotope values do not show a correlation with the observed climatic parameters. This was not unexpected, since species effects are thought to dominate the δD signal (Brenninkmeijer et al., 1982). It has been demonstrated that bulk δD values are affected by atmospheric moisture during storage by exchange with environmental moisture (Sessions et al., in press) and differences in δD values are most likely due to differences in storage time and humidity on the days the samples were prepared.

When considering the higher correlation coefficient between the δD profiles of the *n*-alkanes and the solar activity, it has to be noted that the correlation is mainly due to the trend of increasing solar activity since 1,600, together with a gradual enrichment of δD values. A precise matching of the wiggles in both curves is not observed (see also Figure 5.13), although several minima and maxima do coincide in both curves, noticeably between 1,400-1,600 AD and around 1,800 AD. This points towards a generally accepted influence of solar activity on the climate system. A possible link between the Little Ice Ages and the decreased solar activity has been observed before in peat humification data (Blackford and Chambers, 1995) and in climate reconstructions of peat plant inputs (Speranza et al., 2002).

A negative correlation between the variations in westerly winds over the North Atlantic (as measured by the NAO) and the δD profiles is observed. Much of the UK climate system is governed by westerly winds, and as such it is not surprising that a correlation should exist between a closely atmospherically coupled ecosystem and the variations in the dominant wind. However, no obvious reason for this negative correlation can be given, except that the atmospheric circulation patterns, of which the wind direction is a dominant parameter, determine the amount of precipitation through the control on which weather front (rain) reaches the sample site.

When considering the triterpenoid hydrocarbons, the bacterially derived homohopane is not strongly related to any climate parameter. The curve is not very indicative of any climate component, suggesting that the dominant control is the local microenvironment and the composition of the bacterial populations (which may or may not be dependant on climate). The triterpenes show opposite trends to each other in the composite record, solely due to one data point (around 1,640, see Figure 5.10c). The record, except for the depletion in the top of the record, follows the same general pattern as for the other compounds (Figure 5.12. The reversal of the correlation coefficient (negative instead of positive) for taraxer-14-ene, is due to the large depletion in the top of the record, instead of an enrichment; no obvious explanation can be given for this, except for the local microenvironment.

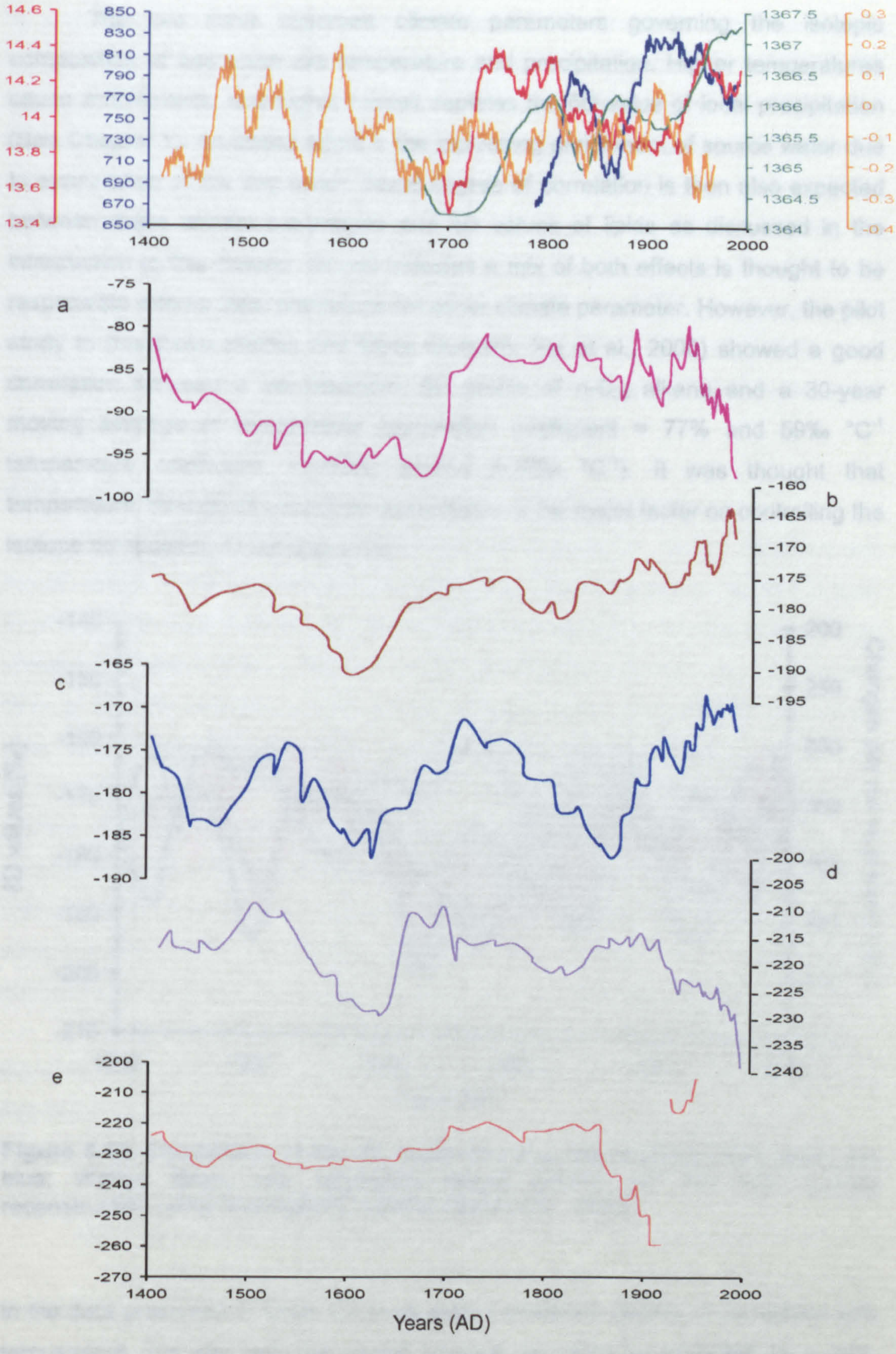

Figure 5.12. Comparison of documentary climate records (Temperature, red, °C and Rainfall, Blue, $mm.yr^{-1}$) and climate reconstructions (Solar irradiance, green, W/m^2 and NAO index, yellow) with δD profiles (in ‰) for (a) bulk, (b) average all *n*-alkanes, (c) *n*-C_{23}, (d) taraxer-14-ene and (e) 17α(H),21β(H)-homohopane during the last 600 years.

The two most important climate parameters governing the isotopic composition of bog water are temperature and precipitation. Higher temperatures cause enrichments, and higher rainfall depletes the δD value of local precipitation (See Chapter 1). An added effect is the increasing enrichment of source water due to evaporation of the bog water. Some degree of correlation is then also expected between these climate parameters and δD values of lipids as discussed in the introduction to this chapter. At mid latitudes a mix of both effects is thought to be responsible with no clear preference for either climate parameter. However, the pilot study to this thesis (Bolton Fell Moss Monolith; Xie et al., 2000) showed a good correlation between a low-resolution δD profile of *n*-C_{23} alkane and a 30-year moving average of temperature (correlation coefficient = 77% and 59‰ $°C^{-1}$ temperature coefficient, normally around 5-10‰ $°C^{-1}$). It was thought that temperature, through its control on evaporation, is the major factor on controlling the isotope composition of the bog water.

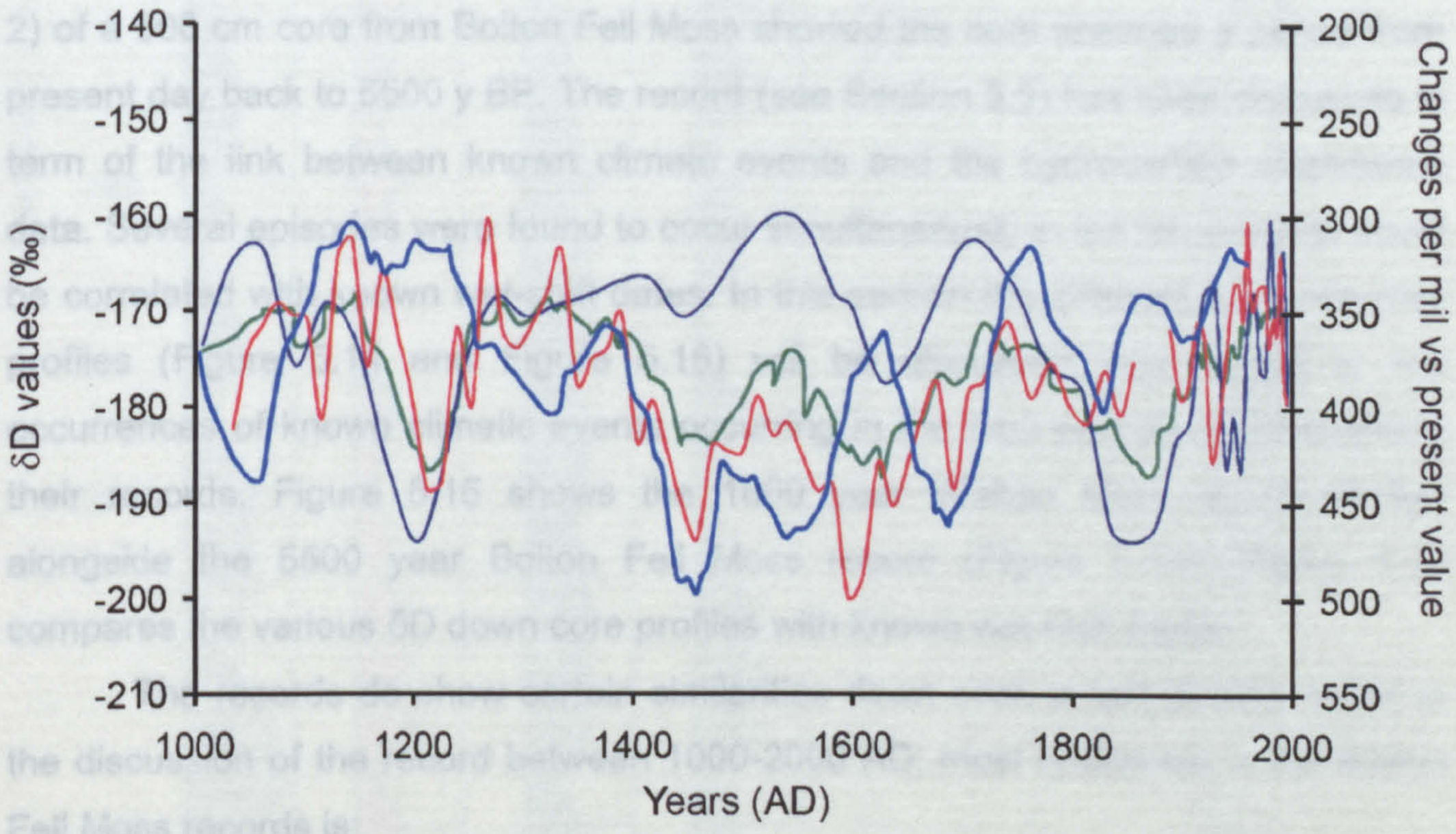

Figure 5.13. Comparison of the δD profile of *n*-C_{23} alkane (Bolton Fell Moss, thin blue; Walton Moss, red; composite record green) with the solar activity reconstruction using cosmogenic nuclides (Bard et al., 2003).

In the data presented in Table 5.4 there exist a moderate degree of correlation with temperature, but also with the rainfall amount, as might be expected for a mid-latitude site (Dansgaard, 1964). When considering the composite δD record of the *n*-C_{23} alkane the mixed control of both parameters seems to explain the variation in the δD record. The depletion in δD between 1870-2000 AD could have been caused

by a lowering of the temperature to 1910 combined with stable rainfall amounts, while before 1910 an increase in temperature is noticed, together with a decrease in rainfall, the overall effect of which could have been a lowering of the δD values. Before 1850 an increase in temperature and rainfall results in an enrichment in δD values. Overall, it is thought that temperature is the main factor in controlling the isotopic composition of the bog, but the influence of rainfall should not be underestimated. The temperature coefficient of the composite record is between 34 and 59‰ $°C^{-1}$, still remarkably high for any biomarker. At this moment no clear evidence exists that isotopic studies might help explain the wetter/cooler and drier/warmer episodes noted in macrofossil analysis, due to the inseparable signal they appear to record in the bog ecosystem.

5.3.4 5,500 year climate record

In the previous section correlations between certain climate variables and the δD values of lipid biomarkers have been observed. Radiocarbon dating (Chapter 2) of a 500 cm core from Bolton Fell Moss showed the core spanned a period from present day back to 5500 y BP. The record (see Section 3.5) has been discussed in term of the link between known climate events and the hydrocarbon abundance data. Several episodes were found to occur simultaneously in the records and could be correlated with known wet-shift dates. In this section the different δD down core profiles (Figure 5.14 and Figure 5.15) will be discussed with regard to the occurrences of known climatic events occurring in the time periods encompassing their records. Figure 5.15 shows the 1000 year Walton Moss record plotted alongside the 5500 year Bolton Fell Moss record (Figure 5.14). Figure 5.16 compares the various δD down core profiles with known wet shift dates.

The records do show certain similarities down core, a fact already noted in the discussion of the record between 1000-2000 AD; most noticeable in the Bolton Fell Moss records is:

(i) A period of depletion in the δD record around 1850 AD, known as the second part of the Little Ice Age (LIA).

(ii) A second period of depletion corresponding to the middle of the Little Ice Age (ca. 1600 AD); both minima are linked with the general cooler climate.

(iii) A third period is characterised by enrichment in deuterium between 1300 and 1500 AD, corresponds to the onset of the LIA. This contrasts with the expected depletion through the colder climate.

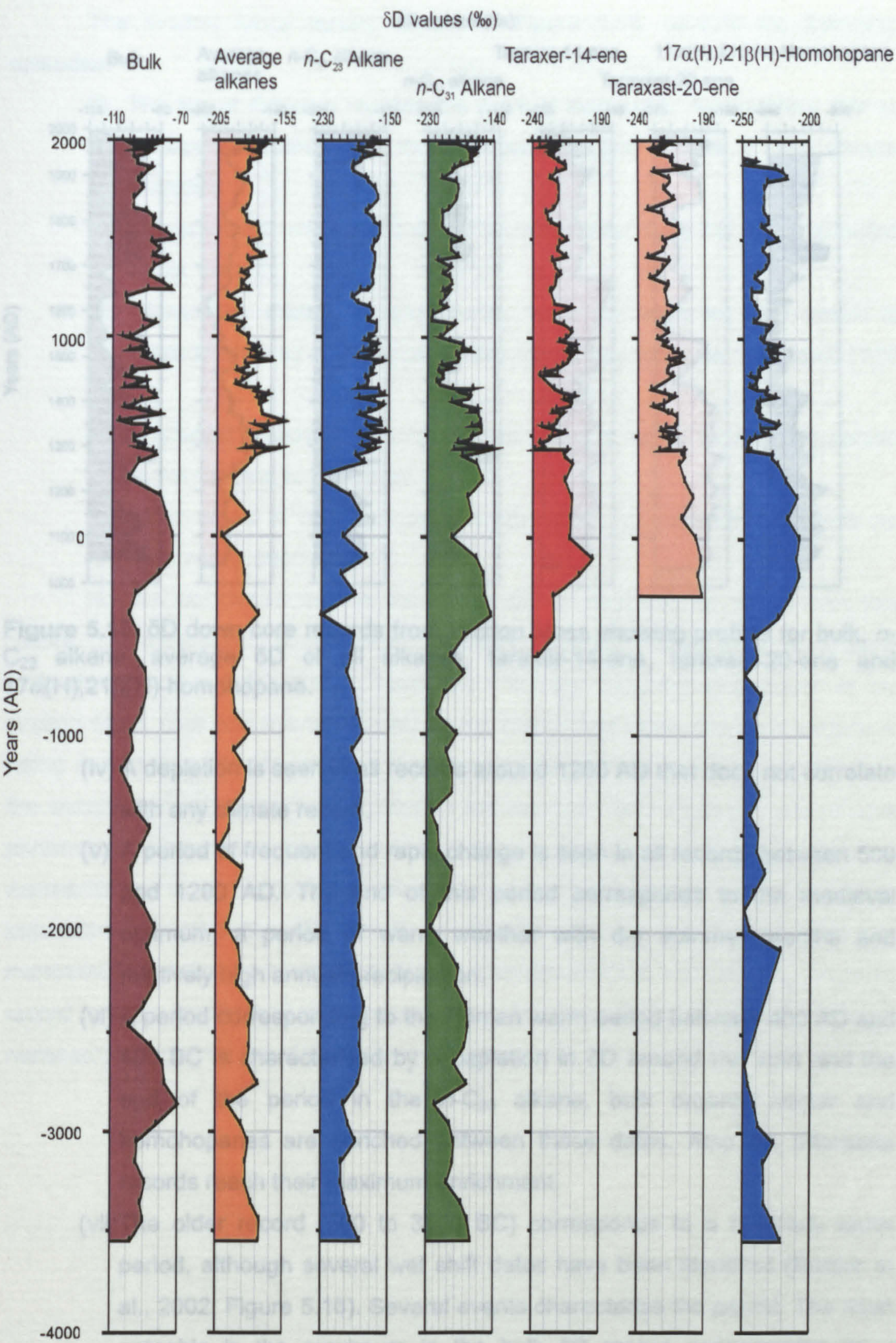

Figure 5.14. δD down core records from Bolton Fell Moss showing profiles for bulk, *n*-C_{23} alkane, average δD of all alkanes, taraxer-14-ene, taraxast-20-ene and 17α(H),21β(H)-homohopane.

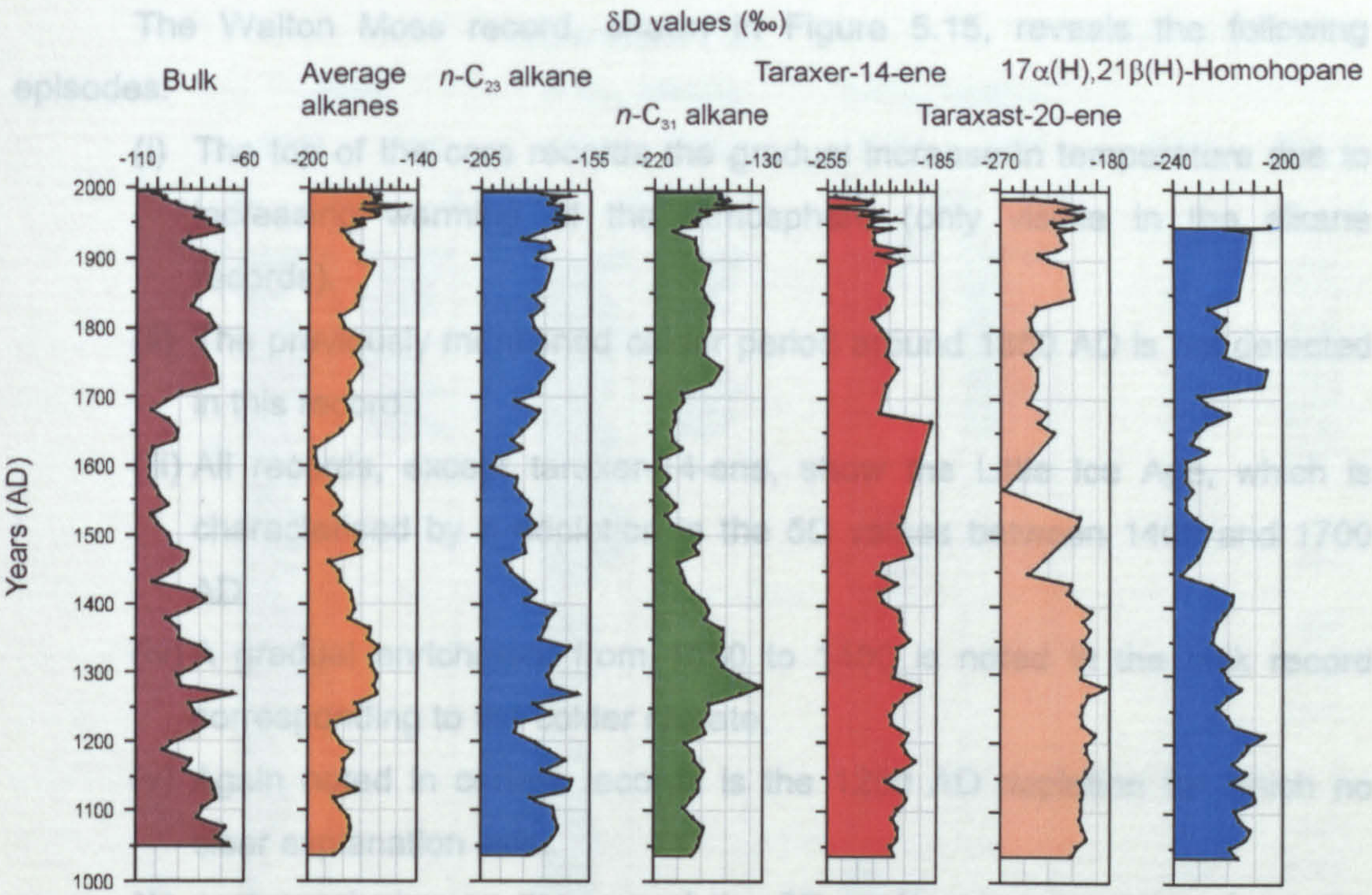

Figure 5.15. δD down core records from Walton Moss showing profiles for bulk, *n*-C_{23} alkane, average δD of all alkanes, taraxer-14-ene, taraxast-20-ene and 17α(H),21β(H)-homohopane.

(iv) A depletion is seen in all records around 1200 AD that does not correlate with any climate record.

(v) A period of frequent and rapid change is seen in all records between 500 and 1200 AD. The end of this period corresponds to the medieval optimum, a period of warm weather with dry summer months and relatively high annual precipitation.

(vi) A period corresponding to the Roman warm period between 400 AD and 400 BC is characterised by a depletion in δD around the start and the end of the period in the *n*-C_{23} alkane, bulk organic matter and homohopanes are enriched between these dates. Also the triterpene records reach their maximum enrichment.

(vii) The older record (500 to 3500 BC) corresponds to a relatively warm period, although several wet shift dates have been identified (Barber et al., 2002; Figure 5.16). Several events characterise the period. The most noteable is the maximum in the bulk δD record accompanied by a depletion in the other records, dated around 2800 BC. Also seen is a depletion in all δD records around 3300 BC, which coincides with the period of a known wet shift. Most of the fluctuations in this part of the record cannot be correlated with any known climate event.

The Walton Moss record, shown in Figure 5.15, reveals the following episodes:

(i) The top of the core records the gradual increase in temperature due to increasing warming of the atmosphere (only visible in the alkane records).

(ii) The previously mentioned colder period around 1850 AD is not detected in this record.

(iii) All records, except taraxer-14-ene, show the Little Ice Age, which is characterised by a depletion in the δD values between 1400 and 1700 AD.

(iv) A gradual enrichment from 1050 to 1400 is noted in the bulk record corresponding to the colder climate.

(v) Again noted in certain records is the 1250 AD depletion for which no clear explanation exist.

No real conclusion on the use of the δD profiles can be drawn from this record. The insensitivity of the record between –500 and –3500 BC was noted in both abundance and δD studies. However, it is clear from the comparison of the Walton Moss core and the upper part of the Bolton Fell Moss core that climate is being recorded in the δD profiles. The interpretation of the record is hampered by the complex climate relationship between the recorded δD values and the climate parameters. Enrichment and depletion in the record can be explained either by warmer/colder or by wetter/dryer climate, and the two signals cannot be readily separated by solely the δD record. Local differences make one or the other microenvironment more sensitive to climate change and if a full temperature/rainfall record is to be established then several cores from the same or adjacent sites are necessary to obtain a full climatically sensitive record.

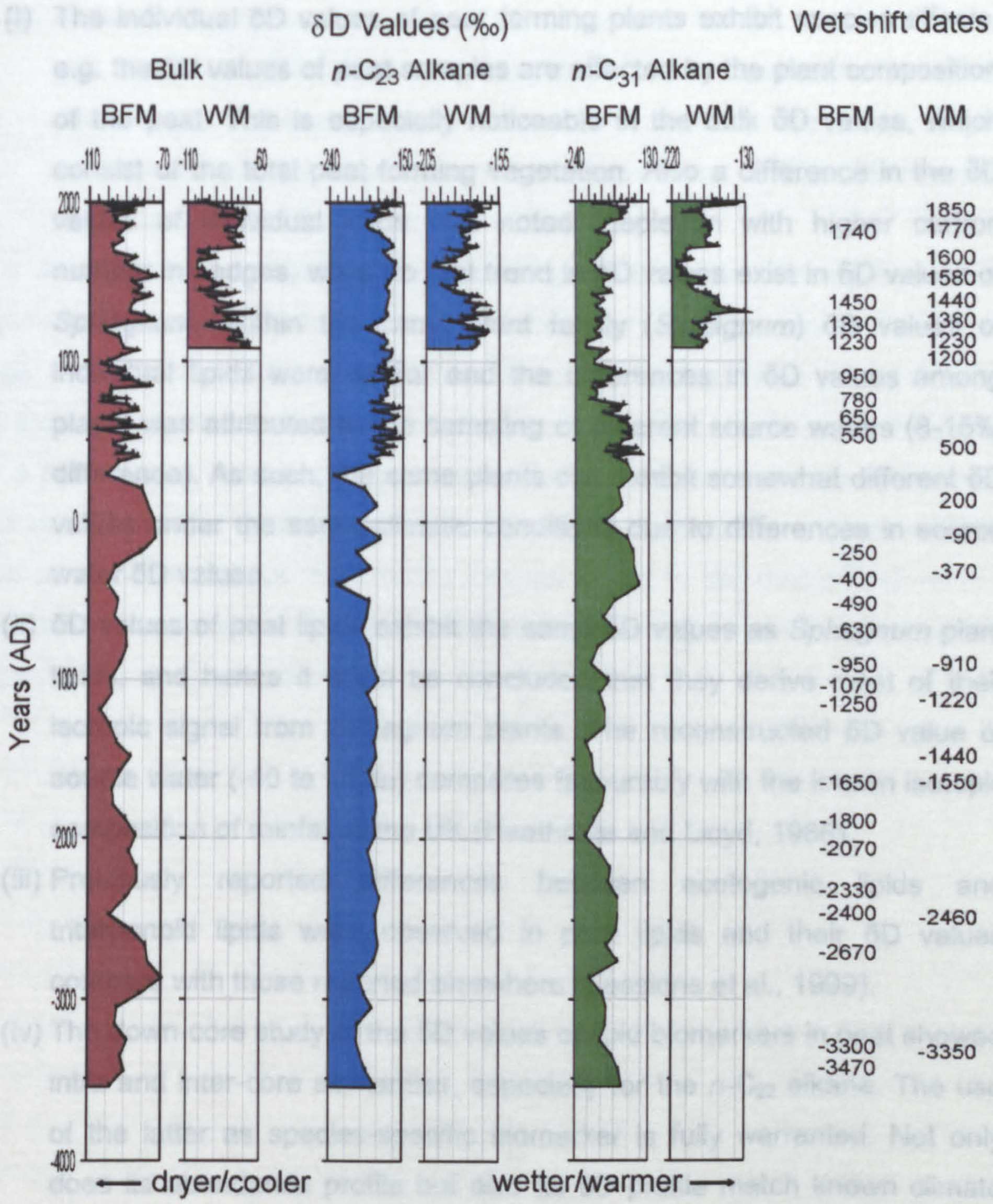

Figure 5.16. Comparison of known wet shift dates, identified using macrofossil analysis (Barber, 1981, 1994; Hughes et al., 2000; Barber et al., 2000; Maquoy et al., 2002b), and the BFM and WM δD profiles (bulk and *n*-C_{23} and *n*-C_{31} alkanes).

5.4 Conclusion

The establishment of compound-specific deuterium isotope ratio mass spectrometry as a tool in palaeoclimate analysis has been partially achieved. In this thesis several underlying assumptions concerning the factors influencing individual lipid δD values have been confirmed. The main findings of this research are summarized as follows:

(i) The individual δD values of peat forming plants exhibit species effects, e.g. the δD values of peat samples are affected by the plant composition of the peat. This is especially noticeable in the bulk δD values, which consist of the total peat forming vegetation. Also a difference in the δD values of individual lipids was noted (depletion with higher carbon number in sedges, while no real trend in δD values exist in δD values of *Sphagnum*. Within the same plant family (*Sphagnum*) δD values of individual lipids were similar and the differences in δD values among plants was attributed to the sampling of different source waters (8-15‰ difference). As such, the same plants can exhibit somewhat different δD values under the same climatic conditions due to differences in source water δD values.

(ii) δD values of peat lipids exhibit the same δD values as *Sphagnum* plant lipids, and hence it could be concluded that they derive most of their isotopic signal from *Sphagnum* plants. The reconstructed δD value of source water (-40 to -70‰) compares favourably with the known isotopic composition of rainfall in the UK (Heathcote and Lloyd, 1986).

(iii) Previously reported differences between acetogenic lipids and triterpenoid lipids were observed in peat lipids and their δD values compare with those reported elsewhere (Sessions et al., 1999).

(iv) The down-core study of the δD values of lipid biomarkers in peat showed intra and inter-core similarities, especially for the *n*-C_{23} alkane. The use of the latter as species-specific biomarker is fully warranted. Not only does its abundance profile but also its δD profile match known climate phenomena. Differences in the lipid δD values could be attributed to differences in source water, arising from hummock/hollow effects. As such it was deemed that a combination of both records (Walton Moss and Bolton Fell Moss) would partly eliminate the influence on source water differences.

(v) The correlation with climate did not reveal a single underlying mechanism for explaining the variations in the δD profiles. A mixture of wind (NAO), temperature and rainfall accounts for the variability in the record. The combined effect of these influences yields remarkably similar patterns in δD values between the different components. The major correlation was with the reconstructed solar activity, which is known to force climate and thus control the other climate parameters.

(vi) A partial correlation with known climate events for the past 5500 year was achieved. The δD record appeared rather insensitive to most climatic changes known in the older record, possibly due to the single record used. On this basis it is recommended that multiple δD records are integrated for climate reconstructions.

After the development of suitable derivatisation procedures, δD records based on other lipid fractions may help to provide further support to interpretations based on *n*-alkanes. Climate trends should be detectable in all fractions, since all are derived through similar biosynthetic pathways utilising similar source water. In the following chapter a combination of both methods (biomarker abundances and δD values) will be used to address the question of whether or not wetter/cooler or warmer/dryer episodes are responsible for the climatic change noted in the macrofossil record (wet shift dates are indicative of wetter/cooler or warmer/dryer episodes, but cannot distinguish between wetter and cooler events).

6 Overview and future work

6.1 Overview

The aim of this thesis was to investigate the potential of the biomarker hydrocarbons derived from the peat forming organisms (plants and micro-organisms) to provide high-resolution stratigraphic records that could be used in palaeoclimate reconstructions. The thesis presents stratigraphic records based on both changes in hydrocarbon distributions with time (depth) and their compound-specific δD values.

Chapters 3 and 5 demonstrate the climate sensitivity of the records obtained through a concerted response in the different components studied. In Chapter 3 the Average Chain Length, which is a measure of the different plant inputs into the peat bog, was identified as the most promising tool to record wetter and/or cooler versus dryer and/or warmer climate. The reason for this is the changing plant communities, which are highly dependent on the input of nutrients through precipitation, on the peat bog. In Chapter 5 the previous observation in this laboratory (Xie et al., 2000) of the δD profile of the *n*-C_{23} alkane as an indicator of the climatic conditions in which the *Sphagnum* moss grew is confirmed. However, while the previously published data set (in this thesis the monolith called BFX) showed a strong correlation with temperature only (cooler and warmer), the data presented in this thesis suggest a somewhat more complex picture. The δD signal is a function of both the growing season temperature and annual rainfall, as previously described by Dansgaard (1964) for a mid-latitude side. The correlation with the two most prominent climate parameters is a positive one, and depletion in δD values is then also caused by wetter and/or cooler climate, while enrichment is caused by warmer and/or dryer climate. As such both records (ACL and δD) can be used to reconstruct the climate in which the peat had accumulated.

In Figure 6.1 both records are shown plotted alongside one another, together with wet shift data derived from several peat bogs from Northern England and Scotland (Langdon, 2003), together with recognised climate periods in the time interval covered by the cores. The biomarker records shown are the composite record (see Chapter 5) for the last 1000 years, the older record is from the BFM core only. Both records have been smoothed using a three point moving average trendline. Theoretically both records represent the same climate intervals. However, the ACL index describes the changing plant composition due to changing

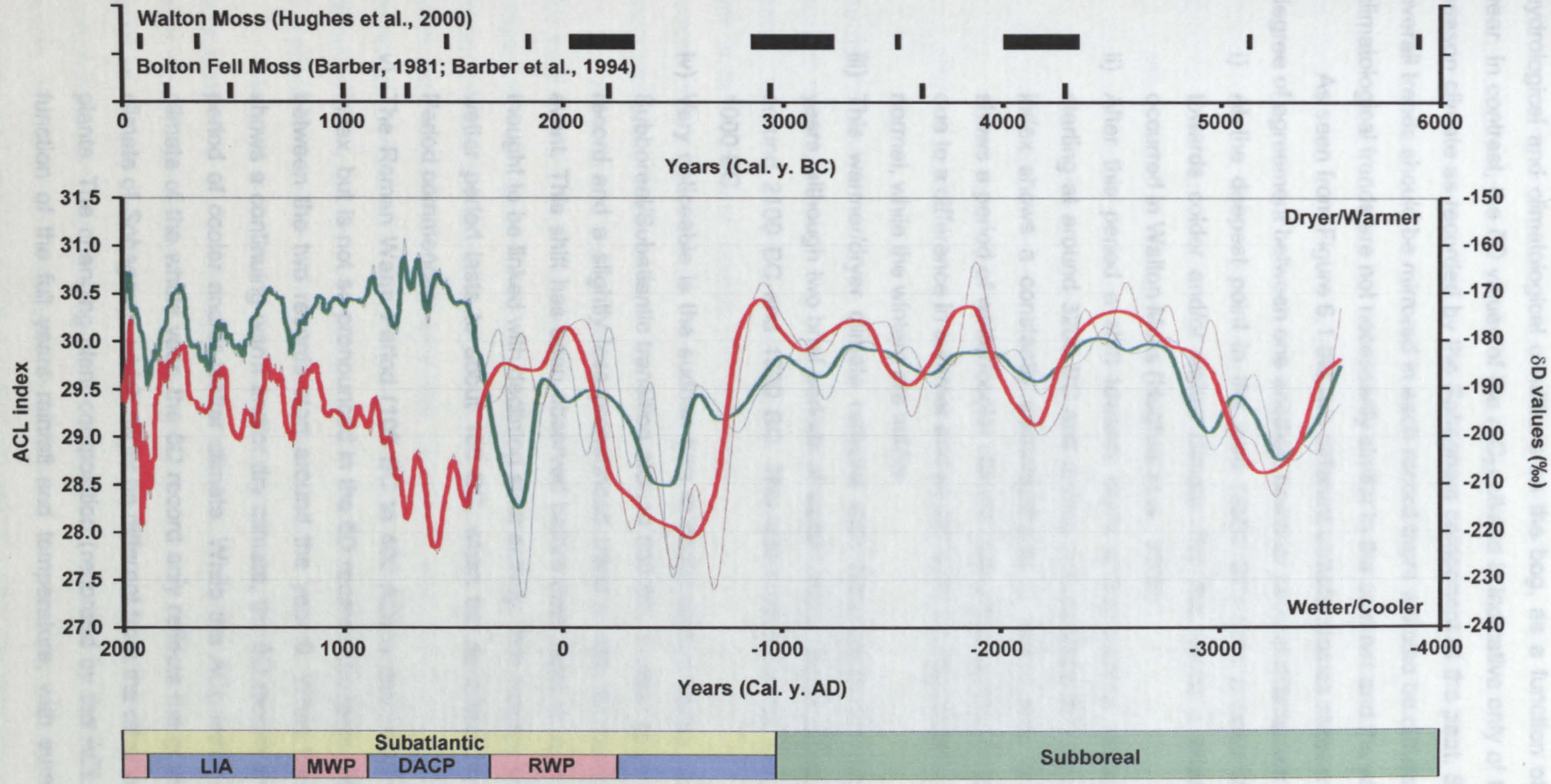

Figure 6.1. Comparison of two climate proxies revealed in this thesis: δD values (‰) of the *n*-tricosane biomarker (green) and the ACL index of the *n*-alkanes. Also shown are the known climate periods (lower box; LIA = Little Ice Age; MWP = Medieval Warm Period; DACP = Dark Ages Cold Period; RWP = Roman Warm Period) and wet-shift dates (upper graph).

hydrological and climatological conditions on the bog, as a function of the whole year. In contrast, the δD values of the *n*-C_{23} alkane is indicative only of the growing season climate as recorded by the *Sphagnum* component of the peat. So while the overall trends should be mirrored in each record there will also be differences, since climatological trends are not necessarily similar in the summer and the winter.

As seen from Figure 6.1 the two different climate proxies show a reasonable degree of agreement between one another, however several differences exist:

i) At the deepest point in the core (3500 BC) both proxies show a shift towards colder and/or wetter climate. For this period a known wet-shift occurred in Walton Moss (Hughes et al., 2000).

ii) After this period a shift towards dryer and/or warmer climate is noted starting at around 3200 BC and ending around 2800 BC. While the ACL index shows a constantly warming/drying of the climate the δD proxy shows a period of wetter/cooler climate during this period. This probably is due to a difference in summer and winter; summer being wetter/cooler then normal, while the winters are milder.

iii) This warmer/dryer climate remains then fairly stable for the next 1700 years, although two brief periods of wetter and/or cooler periods are noted around 2100 BC and 1500 BC. This warm period ends abruptly around 1000 BC.

iv) Very noticeable is the sudden turn to cooler and/or wetter climate at the Subboreal/Subatlantic transition around 850 BC. A clear switch in the ACL record and a slightly less pronounced trend in the δD record mark this event. This shift has been observed before (van Geel et al., 1996) and is thought to be linked with declining solar activity. The ensuing colder and/or wetter period lasts to about 100 BC, when the so-called Roman Warm Period commences.

v) The Roman Warm Period (100 BC to 400 AD) is detectable in the ACL index, but is not so pronounced in the δD record. The large discrepancies between the two records start around the year 0. While the ACL index shows a continuing warm and/or dry climate, the δD record shows a brief period of cooler and/or wetter climate. While the ACL index records the climate of the whole year, the δD record only reflects the growing season climate of *Sphagnum*, which might be different from the other peat forming plants. The changing plant composition (recorded by the ACL index) is a function of the full years rainfall and temperature, with summer losses

being replenished by winter precipitation. This difference in which component is recorded might explain the differences seen in the record.

vi) For the two following periods (medieval warm period and dark ages cold period) the two proxies are not synchronous. As explained before this is mainly due to the different time frames recorded by both proxies. This period is known to have had warm summers, but an overall high rainfall. As such the two records demonstrate this by deviating from each other. While overall plant species composition is in keeping with a wet surface, the deuterium record shows high summer warmth during the growing season.

vii) In the final climate episode of the record, the Little Ice Age, shows up remarkably well in both records, which behave synchronously. The LIA is characterised by a shift towards colder temperatures during the 15th and 17th century as well as a very considerable shift during the mid 1850's (so-called second part of the LIA).

viii) This is then followed by the warming of the climate towards the present day.

As demonstrated here both records together can help us to identify major climate periods recorded in peat bogs. Noteworthy, also is the fact that established wet-shift dates, do not necessarily coincide with the shifts noted in this record. The reason for this is that individual records (like the lower part of the BFM core) do not always record the same climate events due to insensitivities arising through bog topography, e.g. hummock periods.

As seen in Chapter 2 peat is mainly the remains of plants that once grew on the surface of the bog. The plant communities on the peat bog replace each other in response to changing climate. A consequence of these permanently changing plant communities is the changing bog topography. Although Bolton Fell Moss and Walton Moss have a subdued topography (see Chapter 2), their still remains the occasional hummock complex (the climate insensitive part). These hummocks can be readily identified on the surface of the bog, but the changing stratigraphy of the bog makes it impossible to predict their occurrence down-core.

As seen in Chapter 5 most of the variation down a profile is repeated in each core taken from the same bog or from neighbouring bogs. However it is also clear from the data presented in Figure 5.9 that not all the trends are replicated. This was deemed to be caused by insensitivities due to hummock periods in the peat accumulation. In order to be able to reconstruct a reliable down-core profile, which shows all the climate variations, multiple cores from the same locality have to be examined and combined into a composite record using the procedure outlined in

Section 5.3.3.1. The composite records, which can be obtained from multiple cores, will be able to show all the climate variations recorded in the bog.

In Figure 6.2 a theoretical peat bog is shown with several cores taken throughout the profile. Two cores are fully climate sensitive and four are only partially sensitive. Figure 6.2 shows a theoretical composite peat bog profile. As can be noted it combines all the individual records and shows all the variation down core. However, the composite record does not portray the full range of values, due to averaging. As such this approach can only be employed in a qualitative study and does not provide quantitative proxies.

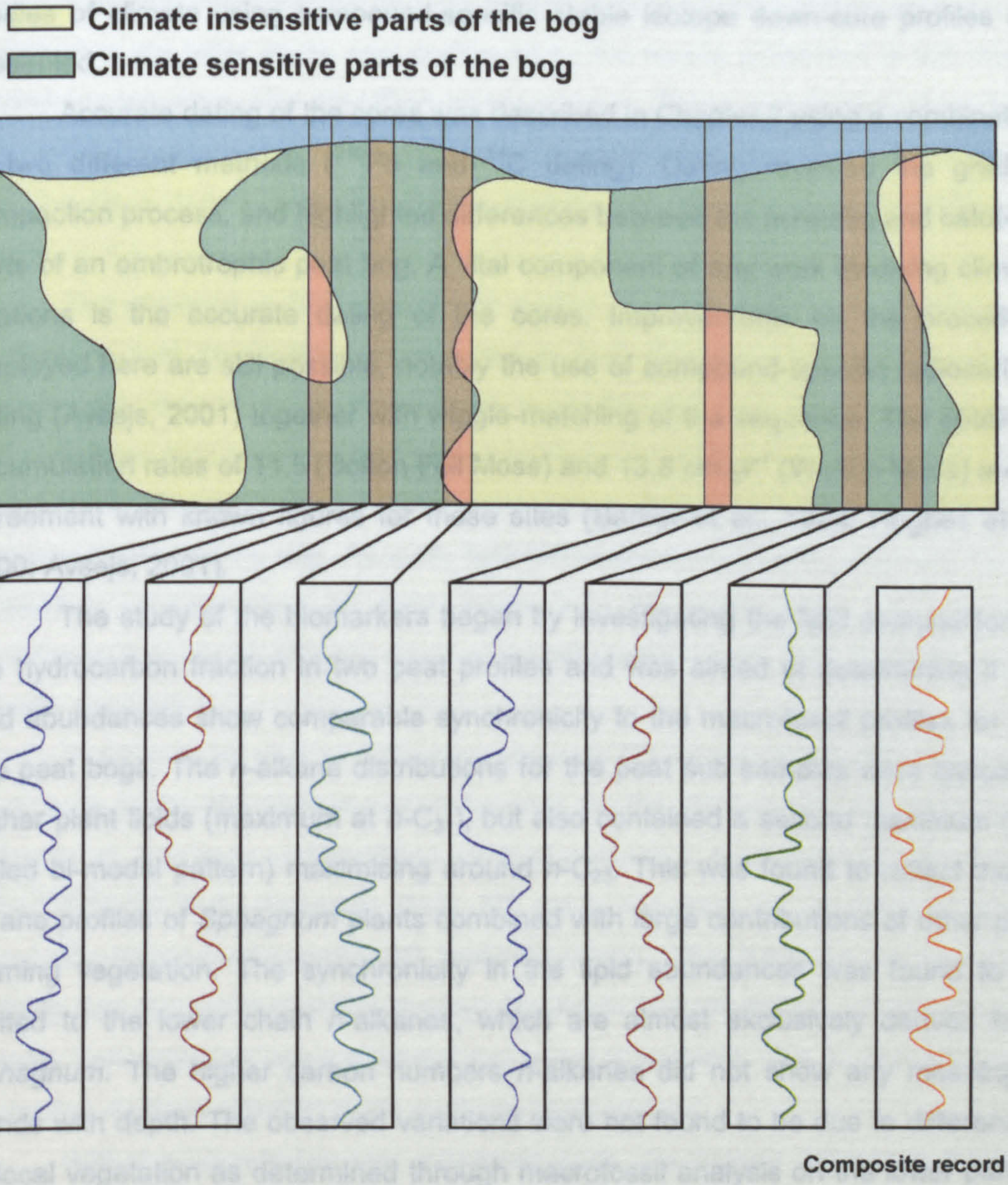

Figure 6.2. Theoretical peat bog showing profiles at different places in the bog. The composite record then averages all these out, showing the larger trends in the peat bog.

6.2 Conclusions

This thesis has been concerned with the biogeochemical and deuterium isotope study of individual lipid biomarker components of the hydrocarbon fraction in raised peat deposits. This involved the study of the hydrocarbon fraction using GC, GC/MS and GC-TC-IRMS in order to establishing down-core records and attempt to relate the observed variations in those records to climate and vegetation influences.

The hypothesis of this thesis is partly confirmed, namely the close link with climate does indeed make peat a valuable setting for deriving compound-specific δD records of past climate. In the following conclusions the general requirements for studies of climate using compound-specific stable isotope down-core profiles are presented.

Accurate dating of the cores was described in Chapter 2 using a combination of two different methods (^{210}Pb and ^{14}C dating). Dating revealed the gradual compaction process, and highlighted differences between the acrotelm and catotelm parts of an ombrotrophic peat bog. A vital component of any work involving climate relations is the accurate dating of the cores. Improvements on the procedure employed here are still possible, notably the use of compound-specific radiocarbon dating (Avsejs, 2001) together with wiggle-matching of the sequence. The obtained accumulation rates of 11.5 (Bolton Fell Moss) and 13.8 $cm.yr^{-1}$ (Walton Moss) are in agreement with known figures for these sites (Barber et al., 1994; Hughes et al, 2000; Avsejs, 2001).

The study of the biomarkers began by investigating the lipid composition of the hydrocarbon fraction in two peat profiles and was aimed at determining if the lipid abundances show comparable synchronicity to the macrofossil profiles for the two peat bogs. The *n*-alkane distributions for the peat sub samples were typical of higher plant lipids (maximum at n-C_{31}), but also contained a second maximum (so-called bi-modal pattern) maximising around n-C_{23}. This was found to reflect the *n*-alkane profiles of *Sphagnum* plants combined with large contributions of other peat forming vegetation. The synchronicity in the lipid abundances was found to be limited to the lower chain *n*-alkanes, which are almost exclusively derived from *Sphagnum*. The higher carbon numbers *n*-alkanes did not show any meaningful trends with depth. The observed variations were not found to be due to differences in local vegetation as determined through macrofossil analysis on the lower part of the BFM core (Nott, 2000). Thus no complete correlation with known climate events was achieved, although a qualitative reconstruction of climate was provided through the ACL index.

Two more classes of compounds were detected in appreciable abundances in the hydrocarbon fraction. Pentacyclic triterpenes most likely derive diagenetically from triterpenols, the latter being abundant in peat forming plants. A mechanism for their formation, proposed by Pancost et al. (2002), explains their appearance in the cores below the living surface layers. The mechanism, involving dehydration followed by a reduction of their precursors, was corroborated by the finding that all triterpenes show the same variations down the core. Also the triterpenes identified are products of the 4 major triterpenols known to comprise the lipids of peat forming plants. The prediction by Pancost et al. (2002) that besides taraxer-14-ene and taraxast-20-ene, olean-12-ene and urs-12-ene should be produced in peat, but not observed in the latter study, was confirmed by the results presented in this thesis. Homohopanes were also identified in abundance. These compounds have been reported before in peat deposits and are likely to be bacterially derived; in common with the plant derived triterpenes their abundances were found to increase with depth.

The study of a 5500 year peat profile revealed that large simultaneous changes in lipid distributions as reflected in their average chain lengths, carbon preference index and hopane ratios which correlated with climatic changes, given by wet shift dates obtained from macrofossil profiles obtained from adjacent cores. This points to the climatic forcing of plant communities, which is reflected in the changing lipid composition of the bog. As such, lipid biomarker distributions provide at least a qualitative representation of plant inputs into the peat profile and as such simultaneous study of different down-core lipid profiles might indeed identify major climatic changes.

In order to be able to determine accurate δD values of individual lipids in a down-core study, the instrumental influences on the δD values were determined (Chapter 4). Accuracy and precision were all deemed to be acceptable when using either external bulk standards (bulk δD measurements) or co-injected internal standards (compound-specific δD measurements). The influence of instrument stability over long analytical time frames, inevitable in such studies, or differences in sample concentration, were deemed not to be a problem, due to the necessary correction routines included in the methods implemented.

With the knowledge that individual lipids are indeed influenced by local climatic conditions (through changing plant species), attention turned to the isotopic composition of these lipids. The link between climatic parameters and isotopic composition is well established (Dansgaard, 1964). In Chapter 5 this linkage was explored through the compound-specific δD approach. It was found that δD values

of individual lipids are controlled by two main factors: source water and plant species (biochemical fractionation). Plant biomarkers displayed δD values dependent on plant family, i.e. sedges or *Sphagnum*. Variations within the same plant genus (*Sphagnum*) were attributed to differences in source water. Previous studies have shown that bog water exhibits different isotopic compositions depending on the local microenvironment, due to evaporative effects. Differences in the δD values of the two major lipid classes, i.e. acetogenic vs. triterpenoids, were confirmed, agreeing with the different biochemical pathways leading to their formation (Sessions et al., 1999). Overall, synchronous variations were observed between the individual biomarkers, especially the *Sphagnum* specific biomarker *n*-C_{23} alkane.

The variations in the δD profiles were found to correlate with climate parameters (temperature, rainfall and wind variations). In addition, a possible link with solar forcing of the climate system during the Little Ice Age was observed in the composite δD record. None of the variables was found to be dominant, but instead a mix of all the climate components was thought to be responsible for the δD values observed. As such, no clear correlation in the 5,500-year record could be established, but general trends were observed for species-specific biomarkers.

Overall it was concluded that highly species-specific biomarkers can be used for the development of δD down-core profiles and currently they offer a qualitative climate proxy. However, no single climate parameter specific to a single biomarker has been identified. It is therefore recommended that records from multiple cores should be integrated in order to reconstruct climate records, hereby minimising the impacts of climatically insensitive parts of a single core. The two most successful proxies (ACL index and δD profile of *n*-tricosane) developed during this research offer means of distinguishing between annual climate and growing season.

6.3 Future work

In order to build on the work of this thesis and to further validate some of the new findings, several new avenues of research are suggested:

(i) In order to deconvolute a climate component from lipid biomarkers, more detailed studies of the influences of climate parameters on the plant biosynthesis of these compounds is necessary. The influence of growth temperature on chain length and abundance of individual lipids is unknown and should be investigated.

(ii) In addition, the same study should try to elucidate the influence of species, within the same genus, on the δD values. The effects of

morphological differences between *Sphagnum* taxa and other vascular species on compound-specific δD values are unknown.

(iii) Furthermore, replicate longer, parallel cores from a single region should be collected and a multi-proxy approach (macrofossil, humification, biomarker abundances and isotope studies) should be undertaken in order to yield more information on the exact nature of the link between the δD values of individual lipid biomarkers and eliminate variability. This should be undertaken in combination with better dating methods (wiggle-matching of specific events) hereby leading to the better identification of periods of climatic change.

(iv) The compound-specific δD down-core profiles of other lipid fractions (alcohols, sterols, fatty acids), that are more abundant then the hydrocarbon fraction should, provide additional detailed information concerning the factors influencing the response of peat forming plants to climate change. This research can validate the findings of this study. However, the δD determination of functionalised compounds is more problematic then for *n*-alkanes due to the need for derivatisation prior to GC analysis. The exchangeable hydrogens on the functional groups need to be removed since they will not exhibit the isotopic ratio imprinted at the time of biosynthesis, but instead they will reflect the isotopic composition of the water, with which they have exchanged during sampling, transport, storage and/or chemical treatments (purification and derivatisation). This problem will be overcome by using appropriate derivatisation procedures, however care must be taken to prevent exchange of secondary hydrogens, thus the derivatisation procedures employed in carbon isotope ratio determinations cannot be used, namely: a trimethylsilylation using BSTFA, and methylation using BF_3-methanol (Meier-Augustein, 2002). Both procedures are used in carbon isotope analysis to enhance volatility and improve the separation of components. Although no isotope effects are known for carbons these derivatisation methods can not be used for compound-specific hydrogen determinations. For example, acid catalysed methylation reactions are prime candidates for secondary isotope effects, due to the nature of their formation (the attacking group of the derivatisation reagent displaces the leaving group of the protected compound). Base-catalysed reactions are much more preferable, since they should minimise the possibility of secondary isotope effects (still to be fully evaluated). Another

requirement is to minimise the number of new hydrogens introduced into the derivatised compound, for this reason a base catalysed methylation is preferable. A very suitable derivatisation procedure for fatty acids, and possibly for alcohols, uses an adaptation (Allen et al., 1984) of the method of Ciucanu and Kerek (1984), and involves the use of methyl iodide in N,N-Dimethylacetamide (DMA) with pyridine as base catalyst. The method has the advantage of requiring only low amounts of reagents and can be performed in one reaction vessel, limiting sample losses during repeated transfers. It should be possible to determine hydrogen, oxygen and carbon isotopes on the same derivatised compound. The method shows great promise, but will have to be assessed for kinetic isotope effects.

7 Experimental

7.1 General

7.1.1 Glassware

All Glassware was rigorously cleaned before use. The procedure involved sonication for 20 min (for each different solvent) of all the glassware using the following solvents: detergent (Micro™), tap water, de-ionised water, solvent mix of 1:1 dichloromethane and acetone. Afterwards the glassware was oven dried (90°C, overnight), and rinsed with an appropriate solvent before use.

7.1.2 Solvents

All solvents used were Rathburns® HPLC grade. Water was double distilled prior to use.

7.1.3 Storage

Peat samples were frozen at –20°C prior to analysis. Freeze-dried samples were kept in airtight containers and stored in a dark place prior to extraction. Lipid extracts were kept at 4°C in a refrigerator.

7.2 Peat coring

7.2.1 Bolton Fell Moss

A 5 m peat core was recovered from Bolton Fell Moss, Cumbria UK, national grid reference NY490690. Coring took place in September 1996. The core consisted off a 50 cm monolith (depth 0 till 50 cm), and a core taken with a 9 cm bore Russian corer (Barber, 1984), which covered 25 till 500 cm. Each sub-section of the core was taken with enough overlap to ensure a reliable record. The core was frozen at –20°C until sectioned.

7.2.2 Walton Moss

A 90 cm core was recovered from Walton Moss, Cumbria UK, national grid reference NY 504667. Coring took place in September 1996. The core consisted of a 50 cm monolith covering the first 50 cm and then a further core (depth 35 till 90

cm), taken with a 9 cm Russian corer (Barber, 1984). Each sub-section of the core was taken with enough overlap to ensure a reliable record. The core was frozen at –20°C until sectioned.

7.2.3 Plant samples

Peat plant samples were recovered from both Bolton Fell Moss and Walton Moss and immediately air-dried.

7.3 Lipid extraction and sample preparation

7.3.1 Sample preparation

The peat cores were sectioned in 1 cm sub-sections. The outer layers were discarded to eliminate contamination. Sub-samples (4 cm^3) were stored under distilled water for macrofossil analysis. The remaining peat sub-sections were then freeze-dried and crushed using pestle and mortar to pass through a 500 µm sieve, yielding between 0.3 and 7 g of material.

7.3.2 Internal Standards

A mixture of internal standards was prepared for the quantification of the components in each fraction. A solution in 100 ml of dichloromethane (more or less 200 ng/µl of standard) containing 5α-cholestane (hydrocarbon fraction, 210 µg), 2-hexadecanol (alcohols, 203 µg), 5β-pregnan-3-α-ol (sterols, 16 µg), 10-nonadecanone (alkenones, 206 µg), hexadecyl octadecanoate (esters, 204 µg) and heptadecanoic acid (acids, 211 µg) was prepared. Standard mixes were used at room temperature and well shaken beforehand. All flask were sealed with PTFE tape to ensure no evaporation occurred during storage.

7.3.3 Lipid extraction

From the obtained crushed and freeze-dried peat sample, between 0.25 and 0.5 g were taken, 50 µl (20 $\mu g.g^{-1}$ peat) of the standard mixture added and then solvent extracted. The extraction procedure involved sonication of the sample with ± 50 ml of 9:1 dichloromethane and acetone mixture and this in 7 cycles (1*10 ml and 6*6.5 ml of solvent mixture). The resulting supernatants were then decanted and blown to dryness under a gentle stream of nitrogen. This yielded the total lipid extract (TLE) for each sub-section.

A one-quarter aliquot of the TLE was then separated in its different compound classes, using a silica 'flash' column eluting with a series of solvents of increasing polarity. The TLE was separated using: 3.5 ml of hexane (hydrocarbon fraction), 1.5 ml of 9:1 hexane and dichloromethane (aromatic fraction), 5.5 ml dichloromethane (ketones and wax esters), 3 ml 1:1 dichloromethane and methanol (alcohol and sterol fraction), 2.5 ml methanol (polar fraction). The polar fraction remaining on the silica and was discarded. All fractions were blown to dryness under a nitrogen stream and stored in a refrigerator at 4°C. Figure 8.1 shows the complete extraction, separation and analysis scheme.

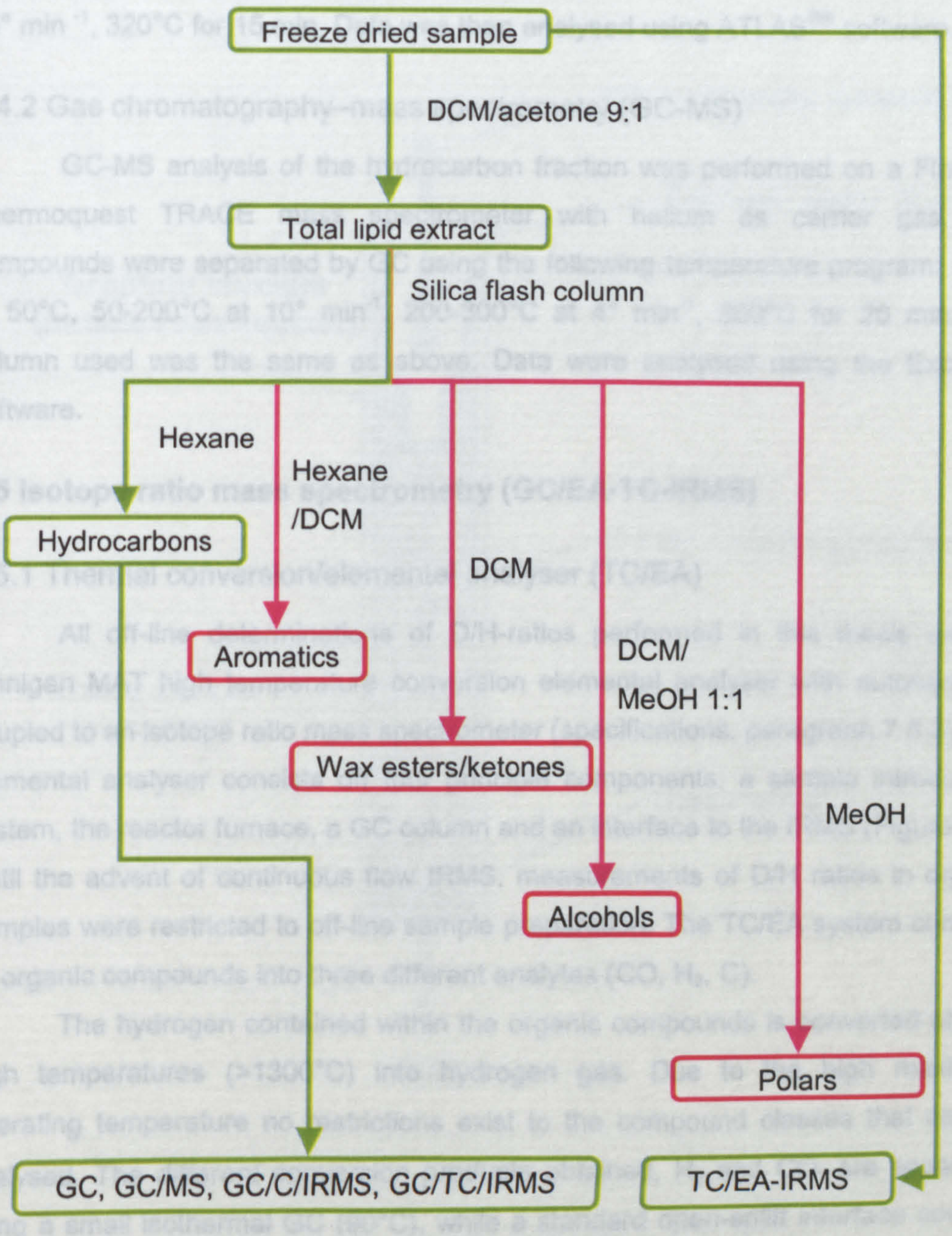

Figure 7.1. Schematic of the extraction, separation and analysis protocol.

7.4 Lipid analysis

7.4.1 Gas chromatography (GC)

In this thesis only the hydrocarbon fraction was investigated. The total fraction was dissolved in ca. 25 µl of hexane and then 1 or 2 µl (depending on concentration) of this analysed using a Carlo Erba 5300 Gas chromatograph, equipped with a flame ionisation detector (FID) and an on-column injector. Separation of the compounds was achieved using a 50 m CPSil-5CB capillary column (0.32 mm i.d., 0.12 µm film thickness, dimethyl polysilaxane equivalent) and helium as carrier gas. The temperature program used: 1 min at 40°C, 40 to 320°C at 10° min^{-1}, 320°C for 15 min. Data was then analysed using ATLAS©® software.

7.4.2 Gas chromatography–mass spectrometry (GC-MS)

GC-MS analysis of the hydrocarbon fraction was performed on a Finnigan Thermoquest TRACE mass spectrometer with helium as carrier gas. The compounds were separated by GC using the following temperature program: 1 min at 50°C, 50-200°C at 10° min^{-1}, 200-300°C at 4° min^{-1}, 300°C for 20 min. The column used was the same as above. Data were analysed using the Excalibur software.

7.5 Isotope ratio mass spectrometry (GC/EA-TC-IRMS)

7.5.1 Thermal conversion/elemental analyser (TC/EA)

All off-line determinations of D/H-ratios performed in this thesis used a Finnigan MAT high temperature conversion elemental analyser with autosampler, coupled to an isotope ratio mass spectrometer (specifications, paragraph 7.5.3). The elemental analyser consists off four principle components: a sample introduction system, the reactor furnace, a GC column and an interface to the IRMS (Figure 7.2). Until the advent of continuous flow IRMS, measurements of D/H ratios in organic samples were restricted to off-line sample preparation. The TC/EA system converts all organic compounds into three different analytes (CO, H_2, C).

The hydrogen contained within the organic compounds is converted at very high temperatures (>1300°C) into hydrogen gas. Due to the high maximum operating temperature no restrictions exist to the compound classes that can be analysed. The different conversion products obtained, H_2 and CO, are separated using a small isothermal GC (90°C), while a standard open-splitt interface couples the TC/EA with the IRMS, via a modified ConFlo-II (Finnigan MAT). The conversion

reaction takes place in the reactor, which consists of a ceramic tube (Al_2O_3) containing a graphite tube, which ensures that neither sample nor reaction gases can come into contact with oxygen containing compounds at high temperature. The reactor is further filled with glassy carbon beads, on to which a graphite crucible is placed, into which the sample (contained in a silver capsule) drops, and is flash incinerated. This crucible prevents the silver introduced to spread through the reactor and, hence, can be readily exchanged thereby preventing poisoning of the active reactor surface (Figure 7.2). The interface allows the automatic generation of reference gas pulses, enabling referencing of the sample gas peaks using high purity hydrogen.

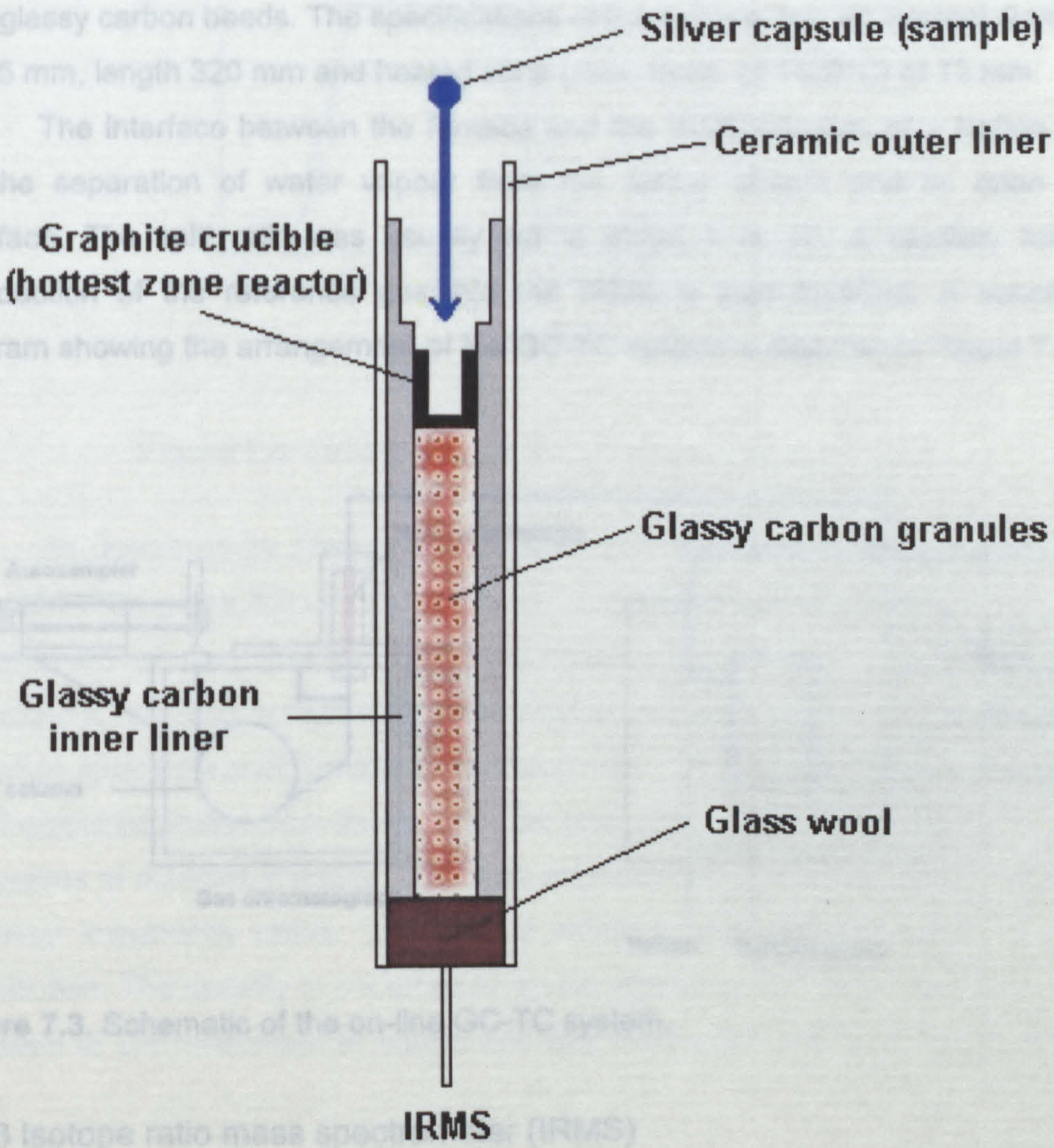

Figure 7.2. Schematic of the reactor design in a TC/EA instrument.

7.5.2 Gas chromatograph-thermal conversion-interface (GC-TC)

The on-line determination of D/H ratios was performed using a HP6890 gas chromatograph equipped with an autosampler coupled to a thermal conversion reactor, which itself was coupled using a GC/C interface to an IRMS. The interface and reactor are manufactured commercially by Finnigan MAT.

The mixtures of components were introduced into a HP6890 gas chromatograph via a splitt/splittless injector, operated in splittless mode. The reactor for the thermal conversion of the analytes replaces the normal GC FID detector. The reactor consisted of a heating element (temperature ±1400°C) into which a reactor tube was fitted. The reactor tube consists of an open ceramic tube (Al_2O_3), containing no packing, in contrast to the elemental analyser reactor, which is filled with glassy carbon beads. The specifications of the furnace are: an internal diameter of 0.5 mm, length 320 mm and heated zone (max. temp. of 1400°C) of 12 mm.

The interface between the furnace and the IRMS consists of a Nafion tube for the separation of water vapour from the carrier stream and an open split interface. The split ratio was usually set to about 1 to 10. A capillary for the introduction of the reference gas into the IRMS is also installed. A schematic diagram showing the arrangement of the GC-TC system is depicted in Figure 7.3.

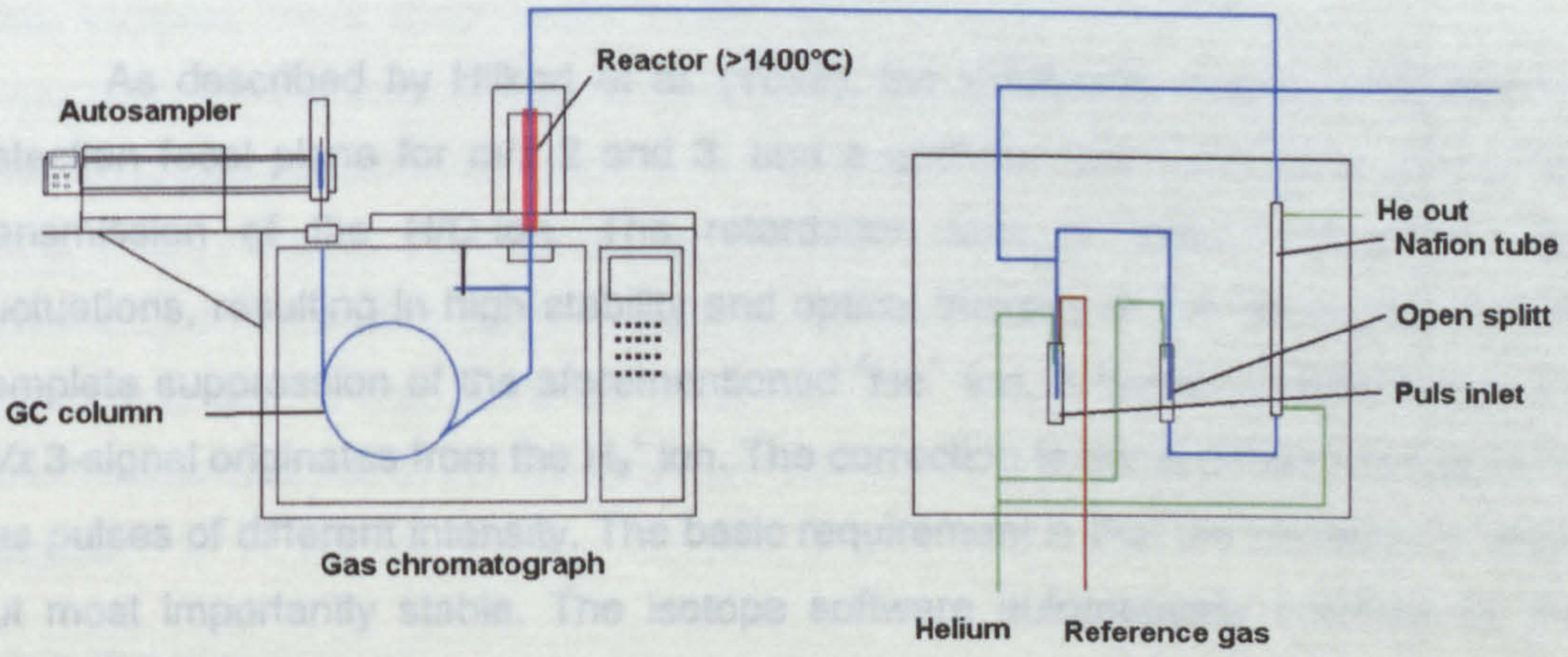

Figure 7.3. Schematic of the on-line GC-TC system.

7.5.3 Isotope ratio mass spectrometer (IRMS)

The isotope ratio mass spectrometer is used to determine ratios of H_2 (*m/z* 2) and HD (*m/z* 3). The instrument used for this research, Finnigan MAT DELTA^{PLUS}XL, is the first commercially available isotope ratio mass spectrometer that allows the simultaneous detection of *m/z* 2 and 3. The main problem with measuring D/H ratios

is the contribution from $^{4}He^{+\cdot}$ ion to the *m/z* 3 measurement (Figure 7.4). In the DELTA^{PLUS}XL the problem was solved by the manufacturers by introducing a small electrostatic sector before the Faraday cups. The $^{4}He^{+\cdot}$ ion energy does not allow it to pass through this electrostatic lens, such that only the desired HD-ions will reach the Faraday cup.

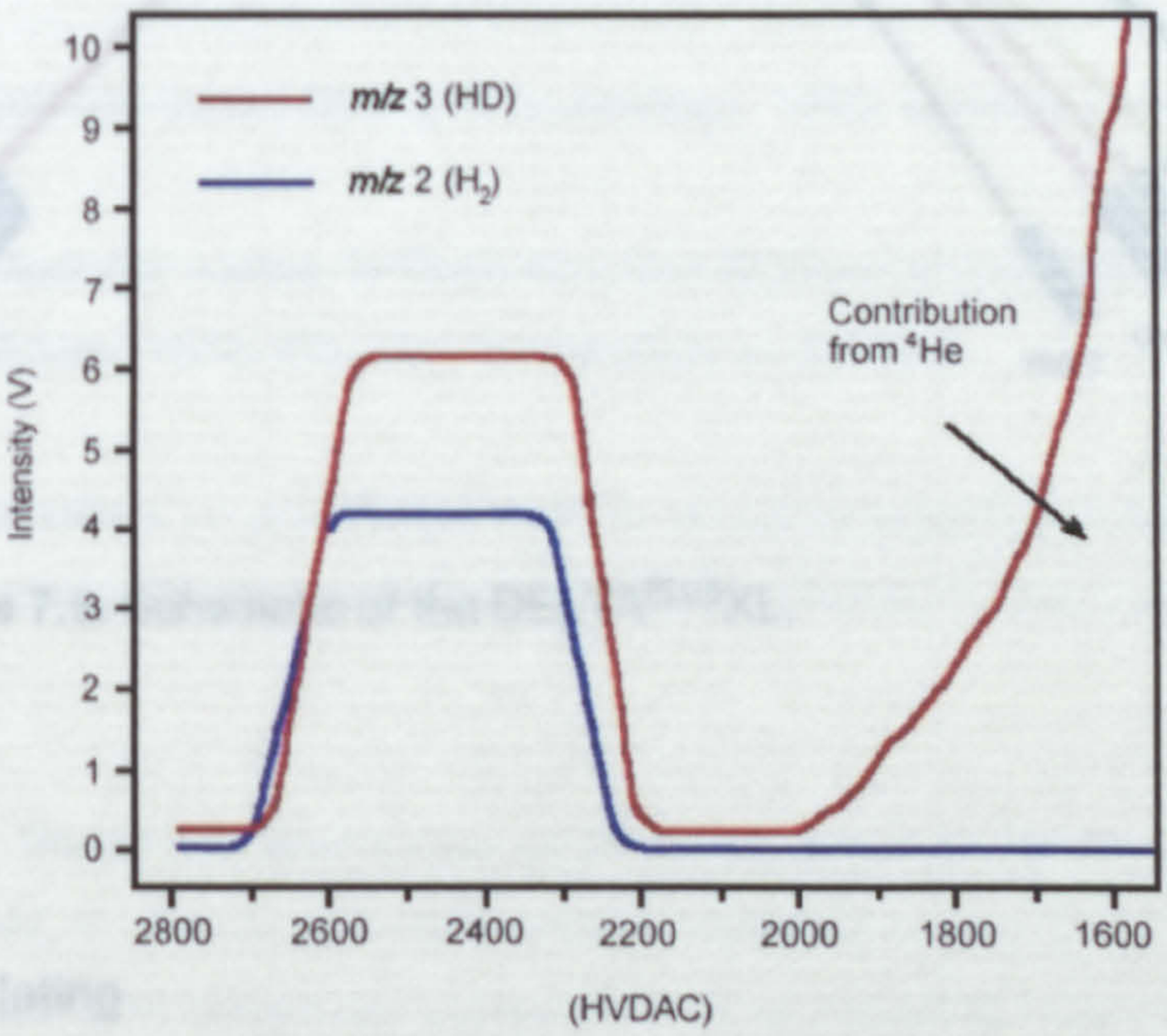

Figure 7.4. Contribution of $^{4}He^{+\cdot}$ ion to the *m/z* 3 signal.

As described by Hilkert et al. (1999), the IRMS has a wide simultaneous detection focal plane for m/z 2 and 3, and a gridless retardation lens with 100% transmission of the H/D-ion. The retardation lens is tolerant to beam size fluctuations, resulting in high stability and optical integrity of the ion signal. It gives complete suppression of the aforementioned $^{4}He^{+\cdot}$ ion. A further contribution to the *m/z* 3-signal originates from the H_3^+ ion. The correction factor is determined using H_2 gas pulses of different intensity. The basic requirement is that the H_3-factor is small, but most importantly stable. The isotope software automatically corrects for this contribution. The stability is not affected by the presence of the He carrier gas. The precision of the instrument in continuous flow mode (EA and GC) is specified at ±4‰.

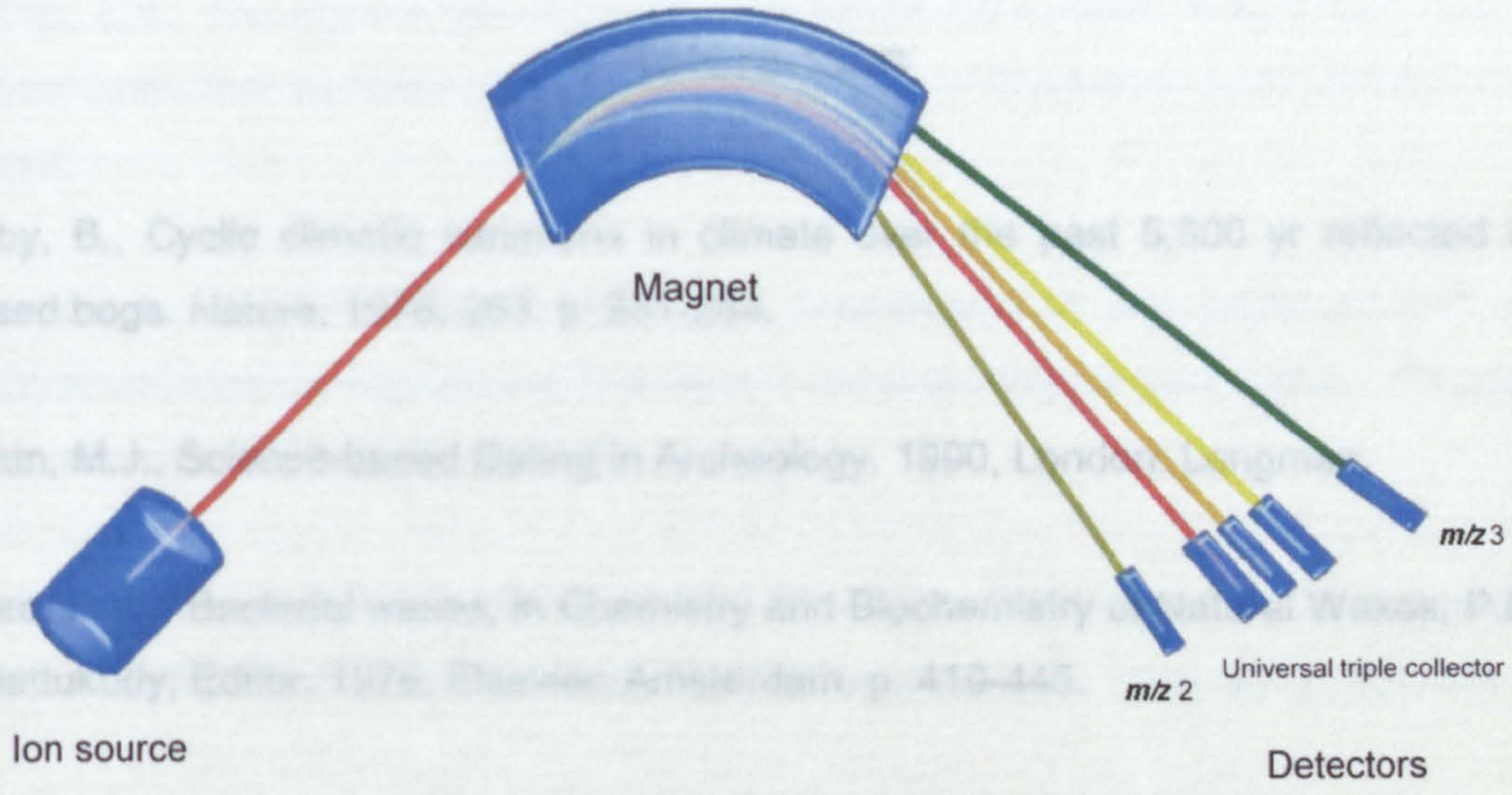

Figure 7.5. Schematic of the DELTA^{PLUS}XL.

7.6 Dating

7.6.1 ^{210}Pb dating

All samples submitted for ^{210}Pb dating were treated identically. Between 0.5 and 2.5 g were weighted off and then spiked with a known amount of Polonium 209. The samples were then treated with aqua regia to release all lead atoms. Supernatants were then evaporated and redissolved in 6M HCl (several times). After final dissolution a polished silver disc was introduced into the solution. After two days, it was removed and the activity collected on the silver disc measured with a gammaray detector. The slope of the linear trendline between depth and the natural logarithm of the ^{210}Pb gave the accumulation rate. The samples were processed and determinations made at the Geoscience Advisory Unit, Southampton oceanographic Centre.

7.6.2 ^{14}C dating

Bulk peat material (20 mg) was placed in solvent cleaned glass vials and submitted for pre-treatment and radiocarbon dating to the Oxford Radiocarbon accelerator.

8 References

Aaby, B., Cyclic climatic variations in climate over the past 5,500 yr reflected in raised bogs. Nature, 1976. 263: p. 281-284.

Aitkin, M.J., Science-based Dating in Archeology. 1990, London: Longman.

Albro, P.W., Bacterial waxes, in Chemistry and Biochemistry of Natural Waxes, P.E. Kolattukudy, Editor. 1976, Elsevier: Amsterdam. p. 419-445.

Allen, K.G., MacGee, J. and Wagenr, K.R., A new procedure to analyze free fatty acids application to 20-mg brain tissue samples. Journal of Chromatography, 1984. 309: p. 33-42.

Andersen, N., Paul, H.A., Bernasconi, S.M., McKenzie, J.A., Behrens, A., Schaeffer, P. and Albrecht, P., Large and rapid climate variability during the Messinian salinity crisis: Evidence from deuterium concentrations of individual biomarkers. Geology, 2001. 29(9): p. 799-802.

Appleby, P.G. and Oldfield, F., The calculation of ^{210}Pb data assuming a constant rate of supply of unsupported ^{210}Pb to the sediment. Catena, 1978. 5: p. 1-8.

Appleby, P.G., Shotyk, W. and Frankhauser, A., Lead-210 age dating of three peat cores in the Jura Mountains, Switzerland. Water, Air and Soil Pollution, 1997. 100: p. 223-231.

Aravena, R. and Warner, H., Oxygen-18 composition of *Sphagnum*, and microenvironmental water relations. The Bryologist, 1992. 95(4): p. 445-448.

Atkinson, T.C., Lawson, T.J., Smart, P.L., Harmon, R.S. and Hess, J.W., New data on speleothem deposition and palaeoclimate in Britain over the last forty thousand years. Journal of Quaternary Science, 1986. 1: p. 67-72.

Avsejs, L.A., The organic geochemistry and compound-specific radiocarbon dating of peat and other sedimentary materials, in School of Chemistry. 2001, Bristol, UK: Bristol.

Avsejs, L.A., Nott, C.J., Xie, S., Maddy, D., Chambers, F.M. and Evershed, R.P., 5-*n*-alkylresorcinols as biomarkers of sedges in an ombrotrophic peat section. Organic Geochemistry, 2002. 33: p. 861-867.

Baas, M., Pancost, P., van Geel, B. and Sinninghe Damsté, J.S., A comparative study of lipids in *Sphagnum* species. Organic Geochemistry, 2000. 31: p. 535-541.

Barber, K.E., Peat Stratigraphy and Climatic Change: a palaeoecological test of the theory of cyclic peat bog regeneration. 1981, Rotterdam: Balkema.

Barber, K.E., A large capacity Russian-pattern sediment sampler. Quaternary Newsletter, 1984. 44: p. 28-31.

Barber, K.E., Peatlands as scientific archives of past biodiversity. Biodiversity and Conservation, 1993. 2(474-489).

Barber, K.E., Chambers, F.M., Maddy, D., Stoneman, R. and Brew, J.S., A sensitive high-resolution record of late Holocene climatic change from a raised bog in Northern England. The Holocene, 1994. 4(2): p. 198-205.

Barber, K., Dumayne-Peaty, L., Hughes, P., Mauquoy, D. and Scaife, R., Replicability and variability of the recent macrofossil and proxi-climate record from raised bogs: field stratigraphy and macrofossil data from Bolton Fell Moss and Walton Moss, Cumbria , England. Journal of Quaternary Science, 1998. 13(6): p. 515-528.

Barber, K.E., Maddy, D., Rose, N., Stevenson, A.C., Stoneman, R. and Thompson, R., Replicated proxy-climate signals over the last 2,000 y from two distant UK peat bogs: new evidence for regional palaeoclimate teleconnections. Quaternary Science Reviews, 2000. 19(6): p. 481-487.

Barber, K.E., Chambers, F.M. and Maddy, D., Holocene palaeoclimates from peat stratigraphy: macrofossil proxyclimate records from three oceanic raised bogs in England and Ireland. Quaternary *Science Reviews*, 2003. 22(5-7): p. 521-539.

Bard, E., Raisbeck, G., Yiou, F. and Jouzel, J., Solar irradiance during the last 1,200 years based on cosmogenic nuclides. Tellus, 2000. B52(3): p. 985-992.

Bard, E., Raisbeck, G., Yiou, F. and Jouzel, J., Reconstructed solar irradiance data, . 2003, IGBP PAGES/World data center for paleoclimatology. Data Contribution series #2003-006. NOAA/HGDC Paleoclimatology Program, Boulder Co, USA.

Bell, M. and Walker, M.J.C., Late Quaternary Environmental Change: physical and human perspectives. 1992, London: Longman.

Bilke, S. and Mosandl, A., Measurements by gas chromatography/pyrolysis/mass spectrometry: fundamental conditions in $^{2}H/^{1}H$ isotope ratio analysis. Rapid Communications in Mass Spectrometry, 2002. 16: p. 468-472.

Blackford, J.J. and Chambers, F.M., Determining the degree of peat decomposition for peat-based palaeoclimatic studies. International Peat Journal, 1993. 5: p. 7-24.

Blackford, J.J. and Chambers, F.M., Proxy climate record for the last 1,000 years from Irish blanket peat and a possible link to solar variability. Earth and Planetary Science Letters, 1995. 133: p. 145-150.

Blackford, J., Palaeoclimatic records from peat bogs. Tree, 2000. 15(5): p. 193-198.
Blytt, A., Essays on the immigration of Norwegian flora during alternating rainy and dry periods. Cammermeyer, Kristiana, 1876.

Boon, J.J., Dupont, L. and De Leeuw, J.W., Characterization of peat bog profile by Curie-point pyrolysis-mass spectrometry combined with multivariant analysis and by pyrolysis gas chromatography-mass spectrometry, in Peat and Water, C.H. Fuchsman, Editor. 1986, Elsevier: London. p. 215-239.

Bradley, R.S., Paleoclimatology, reconstructing climates of the quaternary. second edition ed. International Geophysics Series, ed. R. Dmowska and J.R. Holton. Vol. 64. 1999, Burlington: Harcourt Academic Press.

Brassell, S.C., Eglington, G., Marlowe, I.T., Pflauman, U. and Sarnthien, M., Molecular stratigraphy: a new tool for climatic assessment. Nature, 1986. 320: p. 129-133.

Brenninkmeijer, C.A.M., van Geel, B. and Mook, W.G., Variations in the D/H and $^{18}O/^{16}O$ ratios in cellulose extracted from a peat bog core. Earth and Planetary Science Letters, 1982. 61: p. 283-290.

Bronk Ramsey, C., Radiocarbon calibration and analysis of Stratigraphy: the OxCal program. Radiocarbon, 1995. 37(2): p. 425-430.

Bronk Ramsey, C., Development of the Radiocarbon Program OxCal. Radiocarbon, 2001. 43(2A): p. 355-363.

Burgoyne, T.W. and Hayes, J.M., Quantitative production of H_2 by pyrolysis of gas chromatographic effluents. Journal of Analytical Chemistry, 1998. 70: p. 7136-5141.

Burk, R.L. and Stuiver, M., Oxygen isotope ratios in trees reflect mean annual temperature and humidity. Science, 1981. 211: p. 1417-1419.

Chappellaz, J., Barnola, J.M., Raynaud, D., Korotkevich, Y.S. and Lorius, C., Ice-core record of atmospheric methane over the past 160,000 years. Nature, 1990. 345: p. 127-131.

Charman, D.J., Hendon, D. and Packman, S., Multiproxy surface wetness records from replicate cores on an ombrotrophic mire: implications for Holocene palaeoclimate records. Journal of Quaternary Science, 1999. 14(451-463).

Chikaraishi, Y. and Naraoka, H., Compound-specific δD-$\delta^{13}C$ analysis of *n*-alkanes extracted from terrestrial and aquatic plants. Phytochemistry, 2003. 63: p. 361-371.

Ciucanu, I. and Kerek, F., Rapid and simultanious methylation of fatty and hydroxy fatty acids for gas-liquid chromatographic analysis. Journal of Chromatography, 1984. 284: p. 179-185.

Clymo, R.S. and Hayward, P.M., in Bryophyte Ecology, A.J.E. Smith, Editor. 1982, Chapmann and Hall. p. 229-289.

Clymo, R.S., Peat, in Mires: swamp, bog, fen and moor. Ecosystems of the world, A.I.P. Gore, Editor. 1983, Elsevier: Amsterdam. p. 159-224.

Clymo, R.S., The limits of peat bog growth. Physical Transactions of the Royal Society of London, 1984. B303: p. 605-654.

Clymo, R.S., Peat growth, in Quaternary Landscapes. 1991. p. 76-112.

Cook, E.R., D'Arrigo, R.D. and Mann, M.E., A well-verified, multiproxy reconstruction of the winter North Atlantic oscillation Index since A.D. 1,400. Journal of Climatology, 2002a. 15: p. 1754-1764.

Cook, E.R., D'Arrigo, R.D. and Mann, M.E., Well verified winter North Atlantic oscillation index reconstruction. 2002b, IGBP PAGES/World Data Center for Paleoclimatology. Data Contribution Series #2002-059. NOAA/NGDC Paleoclimatology Program, Boulder CO, USA.

Corrigan, D., Kloos, C., O'Connor, C.S. and Timoney, R.F., Alkanes from four species of *Sphagnum* Moss. Phytochemistry, 1973. 12: p. 213-214.

Corrigan, D., Kloos, C., O'Connor, C.S. and Timoney, R.F., Lipid components of *Sphagnum* mosses. Planta Medica, 1976. 29: p. 261-267.

Craft, C.B. and Richardson, C.J., Peat accretion and N, P, and organic C; accumulation in nutrient-enriched and unriched Everglades Peatlands. Ecological Applications, 1993. 3(3): p. 446-458.

Dansgaard, W., Stable isotopes in precipitation. Tellus, 1964. XVI(4): p. 436-468.

de Vries, H., Variations in concentration of radiocarbon with time and location on earth. Procl. Koninklijke Akademie van Wetenschappen, Amsterdam, 1958. B61: p. 94-102.

Dehmer, J., Petrology and organic geochemistry of peat samples from a raised bog in Kalimantan (Borneo). Organic Geochemistry, 1993. 20(3): p. 349-362.

Dehmer, J., Petrological and organic geochemical investigation of recent peats with known environments of deposition. International Journal of Coal Geology, 1995. 28: p. 111-138.

Dupont, L.M. and Mook, W.G., Palaeoclimate analysis of $^{2}H/^{1}H$ ratios in peat sequences with variable plant composition. Chemical Geology (isotope geoscience section), 1987. 66: p. 323-333.

Ehleringer, J.R. and Dawson, T.E., Water uptake by plants: perspectives from stable isotope composition. Plant, Cell and Environment, 1992. 15: p. 1073-1082.

Ehleringer, J.R. and Cerling, T.E., Photosynthetic pathways and climate, in Global biogeochemical cycles in the climate system, E.-D. Schulze, *et al.*, Editors. 2001, Academic Press: London. p. 267-278.

El-Daoushy, F., Tolonen, K. and Rosenberg, R., Lead-210 and moss-increment dating of two Finnish *Sphagnum* hummocks. Nature, 1982. 296: p. 429-431.

Epstein, S., Yapp, C.J. and Hall, J.H., The determination of the D/H ratio of non-exchangeable hydrogen in cellulose extracted from aquatic and land plants. Earth and Planetary Science Letters, 1976. 30: p. 241-251.

Epstein, S., Thompson, P. and Yapp, C.J., Oxygen and hydrogen isotopic ratios in plant cellulose. Science, 1977. 198: p. 1209-1215.

Epstein, S. and Krishnamurthy, R.V., Environmental information in the isotopic records in trees. Philosophical Transactions of the Royal Society, London, 1990. A330: p. 427-439.

Estep, M.F. and Hoering, T.C., Biogeochemistry of the stable hydrogen isotopes. Geochimica et Cosmochimica Acta, 1980. 44: p. 1197-1206.

Farrimond, P., Poynter, J.G. and Eglington, G., A molecular stratigraphic study of Peru Margin Sediments, Hole 686B, Leg 112., in Proceedings of the Ocean Drilling

Program, Scientific Results, E. Suess and R. von Huene, Editors. 1990, TX (Ocean Drilling Program): College Station.

Farrimond, P. and Flanagan, R.L., Lipid stratigraphy of a Flandrian peat bed (Northumberland, UK): comparison with the pollen record. The Holocene, 1995. 6: p. 69-74.

Farrimond, P., Taylor, A. and Telnaes, N., Biomarker maturity parameters: the role of generation and thermal degradation. Organic Geochemistry, 1998. 29: p. 1181-1197.

Ficken, K.J., Barber, K.E. and Eglington, G., Lipid biomarker, $\delta^{13}C$ and plant macrofossil stratigraphy of a Scottish montane peat bog over the last two millennia. Organic Geochemistry, 1998. 28(3/4): p. 217237.

Figge, R.A. and White, J.M.C., High-resolution Holocene and late glacial atmospheric CO_2 record: variability tied to changes in thermohaline circulation. Global Biochemical Cycle, 1995. 9(3): p. 391-403.

Fowler, A.J., Gillespie, R. and Hedges, R.E.M., Radiocarbon dating of sediments by accelerator mass spectrometry. Physics of the Earth and Planetary Interiors, 1986. 44: p. 15-20.

Friedli, H., Lötshcer, H., Oeschger, H. and Siegenthaler, U., Ice core record of the $^{13}C/^{12}C$ ratio of atmospheric CO_2 in the past two centuries. Nature, 1986. 324: p. 237-238.

Gascoyne, M., Palaeoclimate determination from cave calcite deposits. Quaternary Science Reviews, 1992. 11: p. 609-632.

Gignac, L.D. and Vitt, D., Habitat limitations of *Sphagnum* along climatic, chemical and physical gradients in mires of Western Canada. The Bryologist, 1990. 93(1): p. 7-22.

Gonfiantini, R., Standards for stable isotope measurements in natural compounds. Nature, 1978. 327: p. 524.

Hannon, G.E. and Gaillard, M.J., The plant macrofossil record of past lake level changes. Journal of Paleolimnology, 1997. 18: p. 15-28.

Heathcote, J.A. and Lloyd, J.W., Factors affecting the isotopic composition of daily rainfall at Driby, Lincolnshire. Journal of Climatology, 1986. 6: p. 97-106.

Hedberg, H.D., International Stratigraphic Guide. 1976, London & New York: John Wiley.

Hilkert, A.W., Douthitt, C.B., Schlüter, H.J. and Brand, W.A., Isotope ratio monitoring gas chromatography/mass spectrometry of D/H by high temperature conversion isotope ratio mass spectrometry. Rapid Communications in Mass Spectrometry, 1999. 13: p. 1226-1230.

Hong, Y.T., Jiang, H.B., Liu, T.S., Zhou, L.P., Beer, J., Li, H.D., Leng, X.T., Hong, B. and Qin, X.G., Response of climate to solar forcing recorded in a 6000-year $\delta^{18}O$ time-series of Chinese peat cellulose. The Holocene, 2000. 10(1): p. 1-7.

Hör, K., Ruff, C., Weckerle, B., König, T. and Schreier, P., Flavor authenticity studies by $^{2}H/^{1}H$ ratio determination using on-line gas chromatography pyrolysis isotope ratio mass spectrometry. Journal of Agricultural Food Chemistry, 2001. 49: p. 21-25.

Huang, Y., Eglington, G., Ineson, P., Latter, P.M., Bol, R. and Harkness, D., Absence of carbon isotope fractionation of individual *n*-alkanes in a 23-year field decomposition experiment with *Calluna vulgaris*. Organic Geochemistry, 1997. 26(7/8): p. 497-501.

Hughes, P.D.M., Mauquoy, D., Barber, K.E. and Langdon, P.G., Mire-development pathways and palaeoclimatic records from a full Holocene peat archive at Walton Moss, Cumbria, England. The Holocene, 2000. 10(4): p. 465-479.

Ingram, H. A. P., Soil layers in mires: function and terminology. Journal of Soil Science, 1978. 29: p. 224-227.

Ingram, M.J., Underhill, D.J. and Farmer, G., The use of documentary sources for the study of past climate. Climate and History, ed. T.M.L. Wigley, M.J. Ingram, and G. Farmer. 1981, London: Cambridge University Press. 180-213.

Ingram, H. A. P., Size and shape in raised mire ecosystems: a geophysical model. Nature, 1982. 297: p. 300-303.

Jones, P.D., Further composite rainfall records for the United Kingdom. Meteorological Magazine, 1983. 112: p. 19-27.

Jouzel, J., Petit, J.R. and Raynaud, D., Palaeoclimatic information from ice cores: the Vostok record. Transactions of the Royal Society of Edinburgh: Earth Sciences, *1990. 81: p. 349-355.*

Karunen, P., Mikola, H., Linko, R. and Euranto, E., Lipids in *Sphagnum* mosses of various ages. Canadian Journal of Botany, 1979. 53: p. 1335-1339.

Karunen, P. and Salin, M., Lipid composition of *Sphagnum fuscum* shoots of various ages. Finnish Chemistry, 1980. 7: p. 500-502.

Karunen, P. and Ekman, R., Senescence-related changes in the composition of free and esterified sterols and alcohols in *Sphagnum fuscum.* Zeitschrift für Pflanzenphysiologie, 1981. 104: p. 319-330.

Ketola, M., Luomala, E., Pihlaja, K. and Nyrönen, T., Composition of long-chain fatty compounds and sterols of four milled peat samples from Finnish peatlands. Fuel, 1987. 66: p. 600-606.

Kilian, M.R., van Geel, B. and van der Plicht, J., ^{14}C AMS wiggle matching of raised bog deposits and models of peat accumulation. Quaternary Science Review, 2000. 19: p. 1011-1033.

Killops, S.D. and Killops, J.K., An introduction to organic geochemistry. 1993, Harlow: Longman scientific and technical.

Kolattukudy, P.E., Croteau, R. and Buckner, J.S., Biochemistry of plant waxes, in Chemistry and biochemistry of plant waxes, P.E. Kolattukudy, Editor. 1976, Elsevier: *Amsterdam. p. 289-347.*

Kotarba, A., Lokas, E. and Wachniew, P., ^{210}Pb dating of young Holocene sediments in high-mountains lakes of the Tatra Mountains. Geochronometria, 2002. 21: p. 73-77.

Köller, C., Paläochemotaxonomie von Torfen Nordwestdeutschlands, . 2002, Oldenburg universität: Oldenburg.

Krishnamurthy, R.V. and Epstein, S., Glacial-interglacial excursion in the concentration of atmospheric CO_2: effect in the $^{13}C/^{12}C$ ratio of wood cellulose. Tellus, 1990. 42: p. 423-434.

Kuder, T. and Kruge, M.A., Preservation of biomolecules in sub-fossil plants from raised peat bogs - a potential palaeoenvironmental proxy. Organic Geochemistry, 1998. 29(5/7): p. 1355-1368.

Lamb, H.H., Climatic History and the Future. Climate: present, past and future. Vol. 2. 1977, London: Menthuen.

Langdon, P.G., Barber, K.E. and Hughes, P.D.M., A 7,500-year peat-based palaeoclimatic reconstruction and evidence for an 1,100 year cyclicity in bog surface wetness from Temple Hill Moss, Pentland Hills, Southeast Scotland. Quaternary Science Reviews, 2003. 22: p. 259-274.

Lean, J., Beer, J. and Bradley, R., Reconstruction of solar irradiance since 1,610: implications for climate change. Geophysical Research Letters, 1995. 22(23): p. 3195-3198.

Lean, J., Beer, J. and Bradley, R., Reconstructed solar irradiance data, . 1998, IGBP PAGES/World data center for paleoclimatology. Data Contribution series #1. NOAA/HGDC Paleoclimatology Program, Boulder Co, USA.

Lehtonen, K. and Ketola, M., Occurrence of long-chain acyclic methyl ketones in *Sphagnum* and *Carex* peats of various degrees of humification. Organic Geochemistry, 1990. 15: p. 275-280.

Lethonen, K., Ketola, M. and Glückert, G., Lipids in the surface water of the Karevansuo Virgin Bog, Southwestern Finland. Chemical Geology, 1991. 93: p. 313-323.

Lethonen, K. and Ketola, M., Solvent-extractable lipids of *Sphagnum*, *Carex*, *Bryales* and *Carex-Bryales* peats: content and compositional features vs. peat humification. Organic Geochemistry, 1993. 20(3): p. 363-380.

Leuenberger, M., Siegenthaler, U. and Langway, C.C., Carbon isotopic composition of atmospheric CO_2 during the last ice age from an antarctic ice core. Nature, 1992. 357: p. 488-490.

Linne von Berg, K.-H. (2001). Http://www.uni-koeln.de/math-nat-fak/botanik/lehre/nebenfach2001/moose/sphagnum/sphagnum3.jpg.

Lowe, J.J. and Walker, M.J.C., Reconstructing Quaternary environments. 1997, Harlow: Addison Wesley Longman limited.

Mackenzie, A.B., Logan, E.M., Cook, G.T. and Pulford, I.D., Distributions, inventories and isotopic composition of lead in ^{210}Pb-dated peat cores from contrasting biochemical environments: implications for lead mobility. The Science of the Total Environment, 1998. 223: p. 25-35.

Manley, G., Central England temperatures: monthly means 1,695-1,973. Quarterly Journal of the Royal Meteorological Society, 1974. 100: p. 389-405.

Marseli, A., Morelli, I., Bernardini, C. and Pacchiani, M., Triterpenes from mosses. IV constituents of some mosses. Phytochemistry, 1972. 11: p. 2003-2005.

Matthews, E. and Fung, I., Methane emissions fom natural wetlands: global distribution, area, and environmental characteristics of sources. Global Biochemical Cycles, 1987. 1: p. 61-86.

Mauqouy, D. and Barber, K., A replicated 3,000 yr proxy-climate record from Coom Rigg Moss and Felecia Moss, the Border Mires, Northern England. Journal of Quaternary Science, 1999. 14: p. 263-275.

Mauquoy, D., van Geel, B., Blauw, M. and van der Plicht, J., Evidence from Northwest European bogs shows Little Ice Age climatic changes driven by variations in solar activity. The Holocene, 2002a. 12(1): p. 1-6.

Mauquoy, D., Engelkes, T., Groot, M.H.M., Markesteijns, F., Oudejans, M.G., van der Plicht, J. and van Geel, B., High-resolution records of late Holocene climate change and carbon accumulation in two North-West European ombrotrophic peat bogs. Palaeogeography, Palaeoclimatology, Palaeoecology, 2002b. 186(3-4): p. 275-310.

Mauquoy, D. and Barber, K., Testing the sensitivity of the palaeoclimatic signal from ombrotrophic peat bogs in Northern England and the Scottish borders. Review of Palaeobotany and Palynology, 2002c. 119: p. 219-240.

McDermott, F., Mattey, D.P. and Hawkesworth, C., Centennial-scale Holocene climate variability revealed by a high-resolution speleothem $\delta^{18}O$ record from SW Ireland. Science, 2001. 294: p. 1328-1331.

McQueen, C., Field guide to the peat mosses of boreal North America. 1990, Hanover, Hn: University Press of New England.

Meier-Augustein, W., Stable isotope analysis of fatty acids by gas chromatography-isotope ratio mass spectrometry. Analytica Chimica Acta, 2002. 465: p. 63-79.

Ménot, G. and Burns, S., Carbon isotopes in ombrotrophic peat bog plants as climatic indicators: calibration from an altitude transect in Switzerland. Organic Geochemistry, 2001. 32: p. 233-245.

Ménot-Combes, G., Burns, S. and Leuenberger, M., Variations of $^{18}O/^{16}O$ in plants from temperate peat bogs (Switzerland): implications for palaeoclimate studies. Earth and Planetary Science Letters, 2002. 202: p. 419-434.

Moore, P.D. and Bellamy, D.J., Peatlands. 1974, London: Elek Science.

Neftel, A., Moor, E., Oeschger, H. and Stauffer, B., Evidence from polar ice cores for increase in atmospheric CO_2 in the past two centuries. Nature, 1985. 315: p. 45-47.

Nichols, D.S. and Brown, J.M., Evaporation from a *Sphagnum* moss surface. Journal of Hydrology, 1980. 48: p. 289-302.

Nott, C.J., Biomarkers in ombrotrophic mires as palaeoclimate indicators, in School of chemistry. 2000, Bristol, UK: Bristol.

Nott, C.J., Xie, S., Avsejs, L.A., Maddy, D., Chambers, F.M. and Evershed, R.P., *n*-alkane distributions in ombrotrophic mires as indicators of vegetation change related to climatic variation. Organic Geochemistry, 2000. 31: p. 231-235.

Oden, S., Die huminsauren. *Kolloidchemische Beihefte*, 1919. 11: p. 75.

Okland, R.H. and Ohlson, M., Age-depth relationships in Scandinavian surface peat: a quantative analysis. Oikos, 1998. 82: p. 29-36.

Ourisson, G., Albrecht, P. and Rohmer, M., The hopanoids-palaeochemistry and biochemistry of a group of natural products. Pure and Applied Chemistry, 1979. 51: p. 709-729.

Pancost, R.D., Freeman, K.H., Patzkowsky, E., Wavrek, D.A. and Collister, J.W., Molecular indicators of redox and marine photoautotroph composition in the late Middle Ordovician of Iowa, USA. Organic Geochemistry, 1998. 29(5-7): p. 1649-1662.

Pancost, R.D., van Geel, B., Baas, M. and Sinninghe Damsté, J.S., $\delta^{13}C$ values and radiocarbon dates of microbial biomarkers as tracers for carbon cycling in peat deposits. Geology, 2000. 28(7): p. 663-666.

Pancost, R.D., Baas, M., van Geel, B. and Sinninghe Damsté, J.S., Biomarkers as proxies for plant inputs to peats: an example from a sub-boreal ombrotrophic bog. Organic Geochemistry, 2002. 33: p. 675-690.

Pancost, R.D., Baas, M., van Geel, B. and Sinninghe Damsté, J.S., Response of an ombrotrophic peat to a regional climatic event revealed by macrofossil, molecular and isotopic data. The Holocene, 2003a.

Pancost, R.D. and Sinninghe Damsté, J.S., Carbon isotopic compositions of prokaryotic lipids as tracers of carbon cylcing in diverse settings. Chemical Geology, 2003b. 14134: p. 1-30.

Parker, D.E., Legg, T.P. and Folland, C.K., A new daily Central England temperature series. International Journal of Climatology, 1992. 12: p. 317-342.

Peters, K.E. and Moldowan, J.M., The Biomarker Guide. 1993, New Jersey: Prentice-Hall.

Pienitz, R., Smol, J.P. and Birks, H.J.B., Assessment of freshwater diatoms as quantitative indicators of past climate change in the Yukon and Northwest Territories, Canada. Journal Paleolimnology, 1995. 13: p. 21-49.

Preston, T., The measurement of stable isotope natural abundance variations. Plant, Cell and Environment, 1992. 15: p. 1091-1097.

Proctor, M.C.F., Raven, J.A. and Rice, S.K., Stable carbon isotope discrimination measurements in *Sphagnum* and other bryophytes: physiological and ecological implications. Journal of Bryology, 1992. 17: p. 193-202.

Quirk, M.M., Wardroper, A.M.K., Wheatley, R.E. and Maxwell, J.R., Extended hopanoids in peat environments. Chemical Geology, 1984. 42: p. 25-43.

Raven, J.A., Present and potential uses of the natural abundance of stable isotopes in plant science, with illustrations from the marine environment. Plant, Cell and Environment, 1992. 15: p. 1083-1091.

Reis-Kautt, M. and Albrecht, P., Hopane derived triterpenoids in soils. Chemical Geology, 1989. 76: p. 143-151.

Rinna, J., Güntner, U., Hinrichs, K.U., Mangelsdorf, K., van der Smissen, J.H. and Rullkötter, J., Temperature-related molecular proxies: degree of alkenone unsaturation and average chain lenght of *n*-alkanes. Paclim Conference *Proceedings, 1999: p.* 183-192.

Robbins, J.A., The Biogeochemistry of Lead in the Environment, , J.O. Nriagu, Editor. 1978, Elsevier: Amsterdam. p. 285-393.

Roberts, N., The Holocene: an Environmental History. 1998, Oxford: Blackwell.

Robin, G.d.Q., The climate record in polar ice sheets. 1983, Cambridge: Cambridge University Press.

Robinson, S.G., Maslin, M.A. and McCaven, I.N., Magnetic susceptibility variations in upper pleistocene deep-sea sediments of the N.E. Atlantic: implications for ice rafting and paleocirculation at the last glacial maximum. Paleoceanography, 1995. 10: p. 221-250.

Rohmer, M., Dastillung, M. and Ourisson, G., Hopanoids from C30 to C35 in recent muds- chemical markers for bacterial activity. Naturwissenschaften, 1980. 67: p. 456-458.

Rohmer, M., The discovery of a *mevalonate*-independent pathway for isoprenoid biosynthesis in bacteria, algea and higher plants. nat. Prod. Rep., 1999. 16: p. 565-574.

Ruff, C., Hör, K., Weckerle, B., Schreier, P. and König, T., $^{2}H/^{1}H$ ratio analysis of flavor compounds by on-line gas chromatography pyrolysis isotope ratio mass spectrometry (HRGC-P-IRMS): benzaldehyde. Journal of High Resolution Chromatography, 2000. 23(5): p. 357-359.

Salasoo, I., Alkane distribution in epicutilar wax of some evergreen *Ericaceae*. Canadian Journal of Botany, 1981. 59: p. 1189-1191.

Salasoo, I., Epicutilar wax alkanes of some heath plants in central Alaska. Biochemical system Ecology, 1986. 15: p. 105-107.

Salasoo, I., Epicutilar wax hydrocarbons of *Ericaeae* in Germany. Zeitschrift für naturforschung C: Biosciences, 1987a. 42: p. 499-501.

Salasoo, I., Alkane distribution in epicutilar wax of some heath plants in Norway. Biochem. Syst. ecol., 1987b. 15: p. 663-665.

Salasoo, I., Epicutilar wax hydrocarbons of *Ericaceae* in the Pacific Northwest of USA. Biochem. syst. Ecol., 1988. 16: p. 619-622.

Salasoo, I., Epicutilar wax alkanes of *Ericaceae* and *Empetrum* from alpine and sub-alpine heaths in Austria. Plant syst. ecol., 1989. 163: p. 71-79.

Sauer, P.E., Eglington, T.I., Hayes, J.M., Schimmelmann, A. and Sessions, A.L., Compound-specific D/H ratios of lipid biomarkers from sediments as a proxy for environmental and climatic conditions. Geochimica et Cosmochimica Acta, 2001. 65(2): p. 213-222.

Schiegl, W.G., Natural deuterium in biogenic materials. *Influence* of environment and geophysical applications, . 1970, University of South Africa: Pretoria.

Schiegl, W.A., Deuterium content of peat as paleoclimatic recorder. Nature, 1972: p. 512-513.

Schimmelmann, A., Lewan, M.D. and Wintsch, R.P., D/H isotope ratios of kerogen, bitumen, oil and water in hydrous pyrolysis of source rocks containing kerogen types I, II, IIS and III. Geochimica et Cosmochimica Acta, 1999. 63(22): p. 3751-3766.

Sessions, A.L., Burgoyne, T.W., Schimmelmann, A. and Hayes, J.M., Fractionation of hydrogen isotopes in lipid biosynthesis. Organic Geochemistry, 1999. 30: p. 1193-1200.

Sessions, A.L., Burgoyne, T.W. and Hayes, J.M., Correction of H_3^+ contributions in hydrogen isotope ratio monitoring mass spectrometry. Journal of Analytical Chemistry, 2001a. 73: p. 192-199.

Sessions, A.L., Burgoyne, T.W. and J.M., H., Determination of the H3 factor in hydrogen isotope ratio monitoring mass spectrometry. Journal of Analytical Chemistry, 2001b. 73: p. 200-207.

Sessions, A.L., Jahnke, L.J., Schimmelmann, A. and Hayes, J.M., Hydrogen isotope fractionation in lipids of the methane-oxidizing bacterium *Methylococcus capsulatus*. Geochimica et Cosmochimica Acta, 2002. 66(22): p. 3955-3969.

Sessions, A.L., Sylva, S.P., Summons, R.E. and Hayes, J.M., Isotopic exchange of carbon-bound hydrogen over geological timescales. Geochimica et Cosmochimica Acta, 2004. in press.

Sever, J.R., Lytle, T.F. and Haug, P., Lipid geochemistry of a Mississipi coastal bog environment. Contributions to Marine Science, 1972. 16: p. 149-161.

Shackleton, N.J. and Opdyke, N.D., Oxygen isotope and palaeomagnetic evidence for early Northern Hemisphere glaciation. Nature, 1977. 261: p. 547-550.

Shackleton, N.J. and Hall, M.A. Stable isotope history of the Pleistocene at ODP Site 677. in Proceedings of the ocean drilling program scientific results 111. 1990. College Station, Texas: Ocean drilling program.

Shackleton, N.J., Le, J., Mix, A. and Matthews, J.A., Carbon isotope records from Pacific surface waters and atmospheric carbon dioxide. Quaternary Science Reviews, 1992. 11: p. 387-400.

Shemesh, A. and Peteet, D., Oxygen isotopes in fresh water biogenic opal-Northeastern U.S. Alleröd-Younger Dryas temperature shift. Geophysical Research Letters, 1998. 25: p. 1935-1938.

Shore, J.S., Bartley, D.D. and Harkness, D.D., Problems encountered with ^{14}C dating of peat. Quaternary Science Reviews, 1995. 14: p. 373-383.

Smith, J.T., Appleby, P.G., Hilton, J. and Richardson, N., Inventories and fluxes of ^{210}Pb, ^{137}Cs and ^{241}Am determined from the soils of three small catchments in Cumbria, UK. Journal of the Environmental Radioactivity, 1997. 37(2): p. 127-142.

Speranza, A., van der Plicht, J. and van Geel, B., Improving time control of the Subboreal/Subatlantic transition in a Czech peat sequence by *^{14}C wiggle-matching*. Quaternary Science Reviews, 2000. 19: p. 1589-1604.

Speranza, A., van Geel, B. and van der Plicht, J., Evidence for solar forcing of climate change at ca. 850 cal BC from a Czech peat sequence. Global and Planetary Change, 2002. 35: p. 51-65.

Sternberg, L.d.S.L., 9. Oxygen and hydrogen isotope ratios in plant cellulose: Mechanisms and applications., in Stable Isotopes in Ecological Research. 1988, Springer-Verlag: Heidelberg. p. 124-141.

Stoneman, R.E., Holocene palaeoclimates from peat stratigraphy: extending and refining the model, . 1993, University of Southampton: Southampton.

Stuiver, M., Reimer, P.J., Bard, E., Beck, J.W., Burr, G.S., Hughen, K.A., Kromer, B., McCormac, G., van der Plicht, J. and Spurk, M., INTCAL98 radiocarbon age calibration, 24,000-0 cal BP. Radiocarbon, 1998. 40(3): p. 1041-1083.

Sukumar, R., Ramesh, R., Pant, R.K. and Rajagopalan, G., A $\delta^{13}C$ record of late quaternary change from tropical peats in Southern India. Nature, 1993. 364: p. 703-706.

Tabony, R.C., The homogenization and analysis of European rainfall records. Unpubliashed, available in Nataional Meteorological Library, Bracknell., 1980.

ten Haven, H.L. and Rullkötter, J., The diagenetic fate of taraxer-14-ene and oleane isomers. Geochimica et Cosmochimica Acta, 1988. 56: p. 2001-2024.

Tobias, H.J., Goodman, K.J., Blacken, C.E. and Brenna, J.T., High precision D/H measurements from hydrogen gas and water by continous-flow isotope ratio mass spectrometry. Journal of Analytical Chemistry, 1995. 67: p. 2486-2492.

Tobias, H.J. and Brenna, J.T., On-line pyrolysis as a limitless reduction source for high-precision isotopic analyis of organic derived hydrogen. Journal of Analytical Chemistry, 1997. 69: p. 3148-3152.

Urban, N.R., Eisenreich, S.J., Grigal, D.F. and Schurr, K.T., Mobility and diagenesis of Pb and ^{210}Pb in peat. Geochimica and Cosmochimica Acta, 1990. 54: p. 3329-3346.

van Breemen, N., How *Sphagnum* bogs down other plants. Tree, 1995. 10(7): p. 270-275.

van Geel, B. and Middeldorp, A.A., Vegetational history of Carbury Bog (Co. Kildare, Ireland) during the last 850 years and a test of the temperature indicator value of $^{2}H/^{1}H$ measurements of peat samples in relation to historical sources and meteorological data. New Phytology, 1988. 109: p. 377-392.

van Geel, B., Pals, J.P., van Reenen, G.B.A. and van Huissteden, J., The indicator value of fossil fungal remains, illustrated by the palaeoecological record of late Eemian/early Weichselian deposit in the Netherlands. Mededelingen Rijks Geologische Dienst, 1995. 52: p. 297-315.

van Geel, B., Buurman, J. and Waterbolk, H.T., Archeological and palaeoecological indications of an abrupt climate change in The Netherlands, and evidence for climatological teleconnections around 2650BP. Journal of Quaternary Science, 1996. 11: p. 451-460.

Webb, D. T. (2003). "Http://www.botany.hawai.edu/webb/BOT201/Mosses/Image115.gif." .

White, J.W.C., Cook, E.R., Lawrence, J.R. and Broecker, W.S., The D/H ratios of sap in trees: implications for water sources and tree ring D/H ratios. Geochimica et Cosmochimica Acta, 1985. 49: p. 237-246.

White, J.W.C., 10. Stable hydrogen isotope ratios in plants: a review of current theory and some potential applications, in Stable Isotopes in Ecological Research. 1988, Springer-Verlag: Heidelberg. p. 142-162.

White, J.W.C., Ciais, P., R.A., F., Kenny, R. and Markgraf, V., A high resolution record of atmospheric CO_2 content from carbon isotopes in peat. Nature, 1994. 367: p. 153-156.

Woodland, W.A., Charman, D.J. and Sims, P.C., Quantitative estimates of water tables and soil moisture in holocene peatlands from *testate amoebae*. The Holocene, 1998. 8: p. 261-273.

Xie, S., Nott, C.J., Avsejs, L.A., Volders, F., Maddy, D., Chambers, F.M., Gledhill, A., Carter, J.F. and Evershed, R.P., Palaeoclimate records in compound-specific δD values of a lipid biomarker in ombrotrophic peat. Organic Geochemistry, 2000. 31: p. 1053-1057.

Xie, S., Nott, C.J., Avsejs, L.A., Maddy, D., Chambers, F.M. and Evershed, R.P., Molecular and isotopic stratigraphy in an ombrotrophic mire for palaeoclimate reconstruction. Geological Chemica Acta, in press.

Yakir, D., Variations in the natural abundances of oxygen-18 and deuterium in plant carbohydrates. Plant, Cell and Environment, 1992. 15: p. 1005-1020.

Yapp, C.J. and Epstein, S., Climatic significance of the hydrogen isotope ratios in tree cellulose. Nature, 1982. 297: p. 636-639.

Ziegler, H., 8. Hydrogen isotope fractionation in plant tissues, in Stable Isotopes in Ecological Research. 1988, Springer-Verlag: Heidelberg. p. 105-123.

Appendix

Mass spectra of Figure 3.1

17β(H)-trisnorhopene

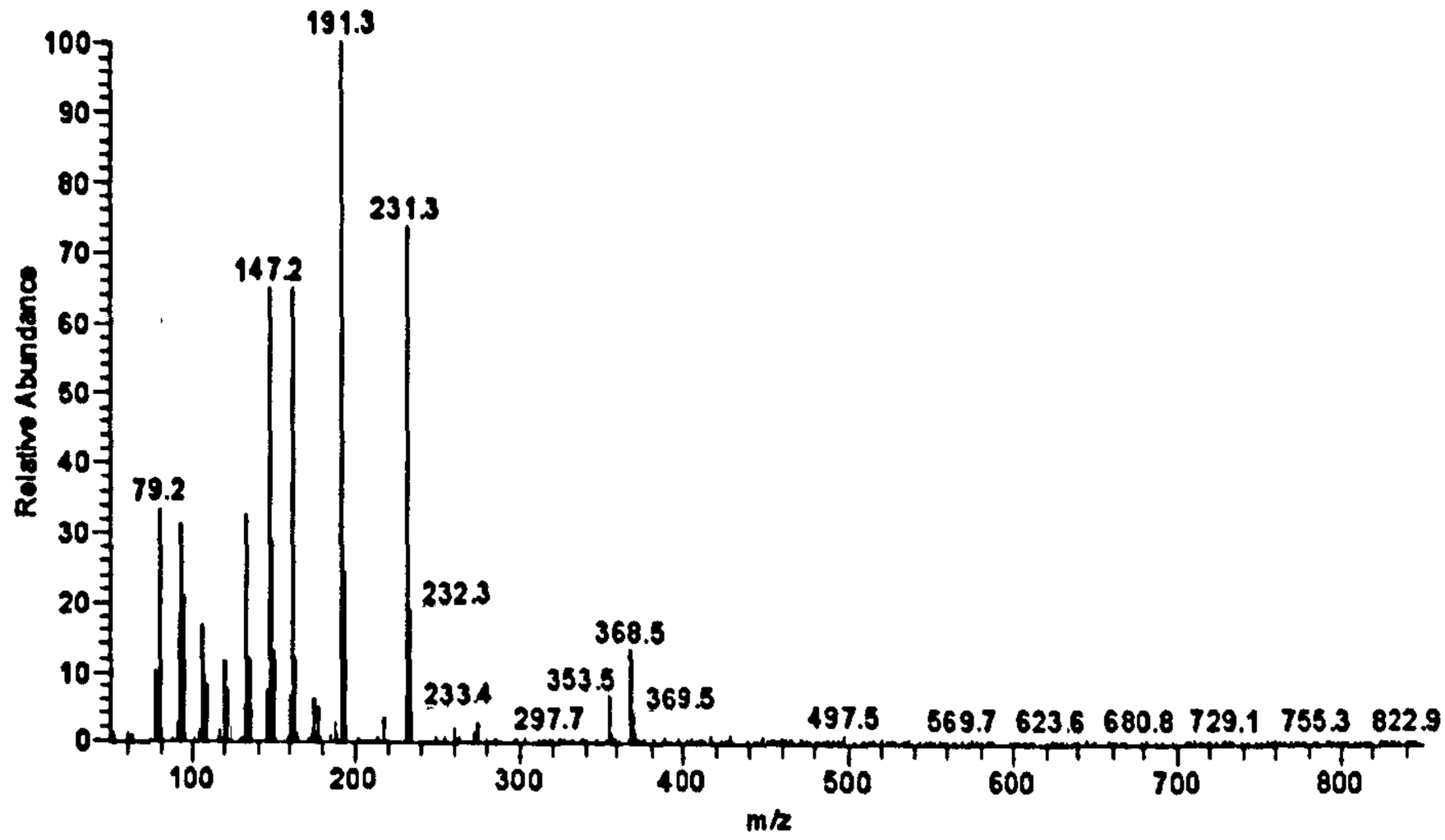

Taraxer-14-ene

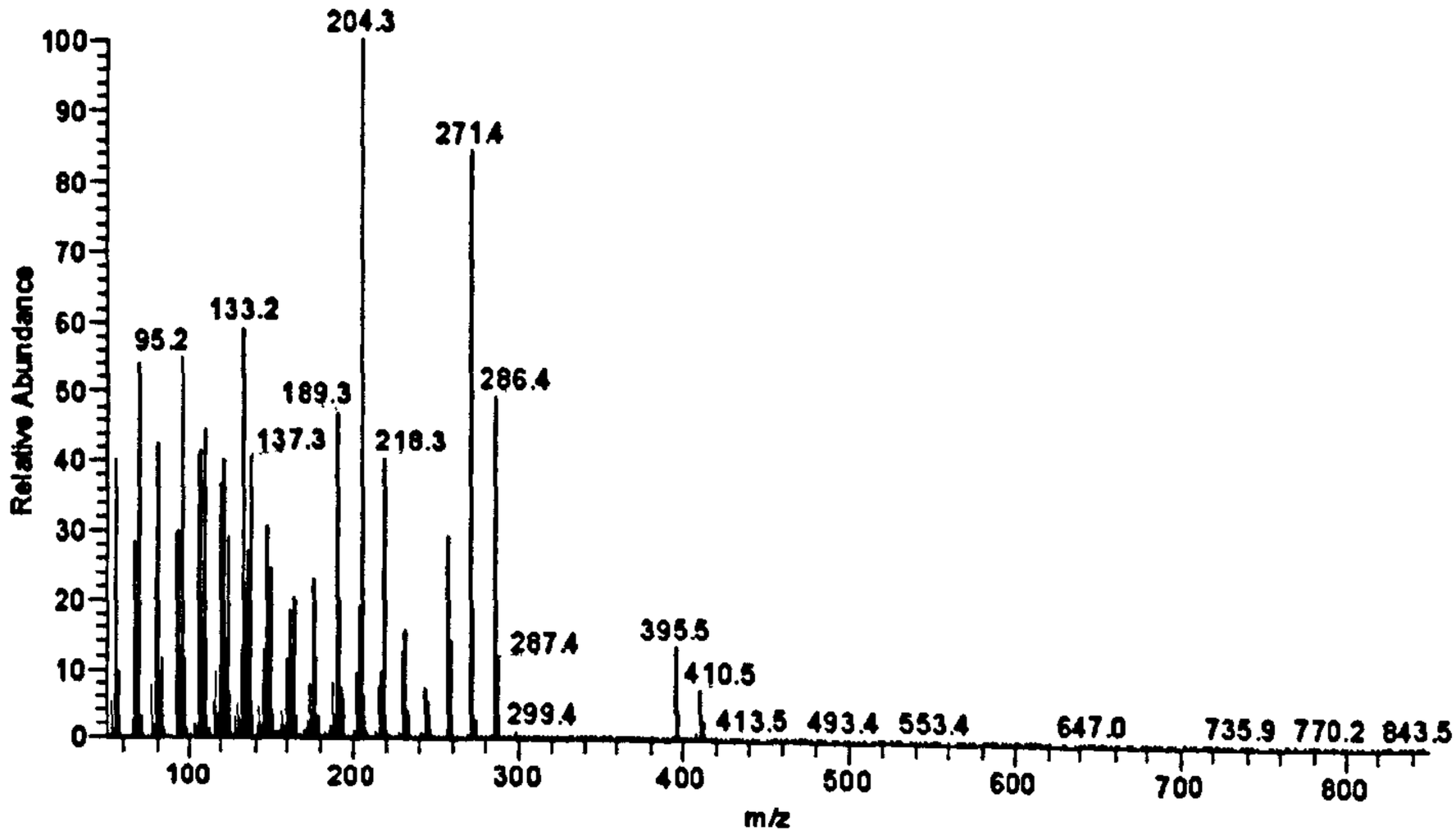

Olean-12-ene

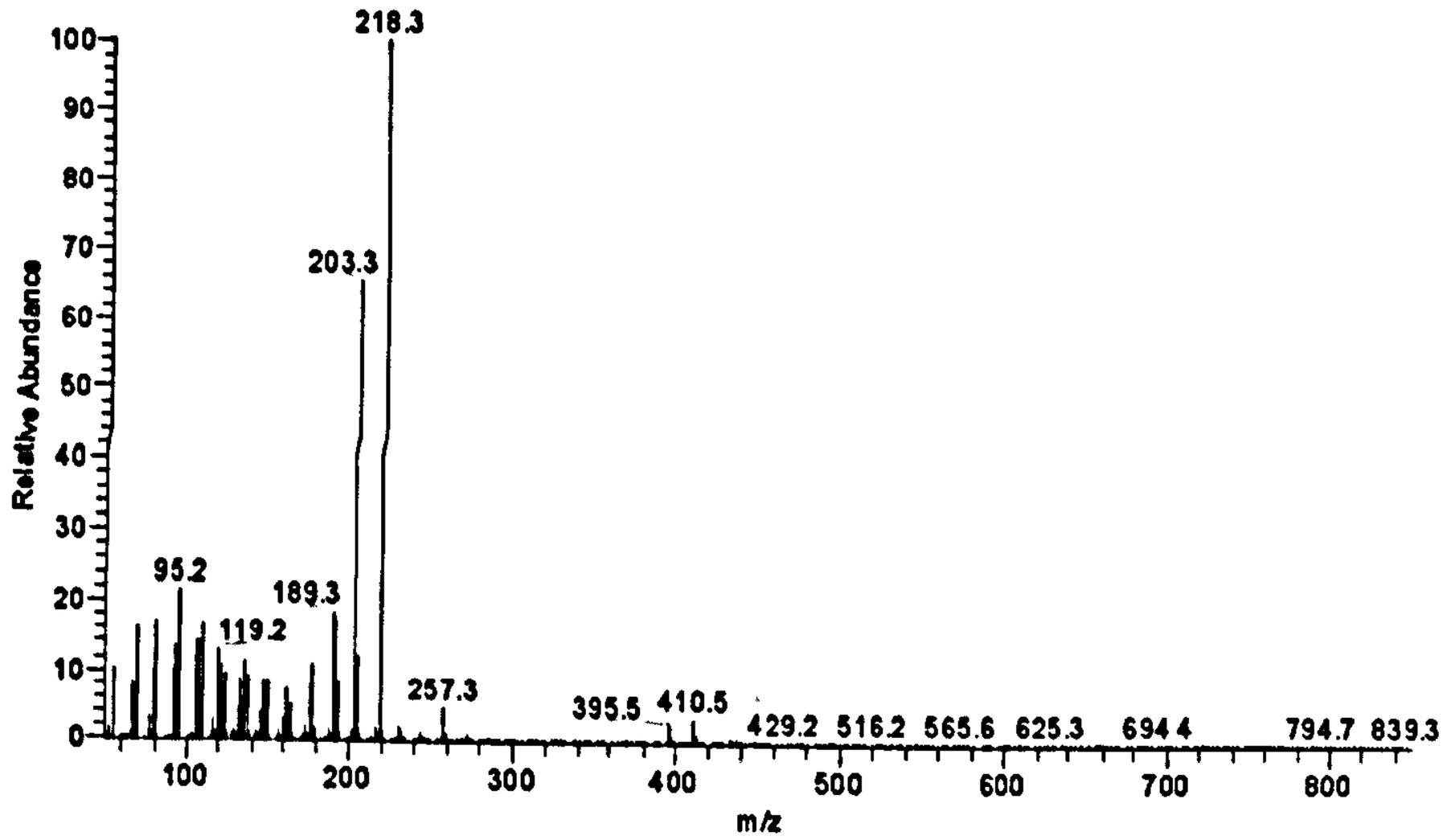

Urs-12-ene

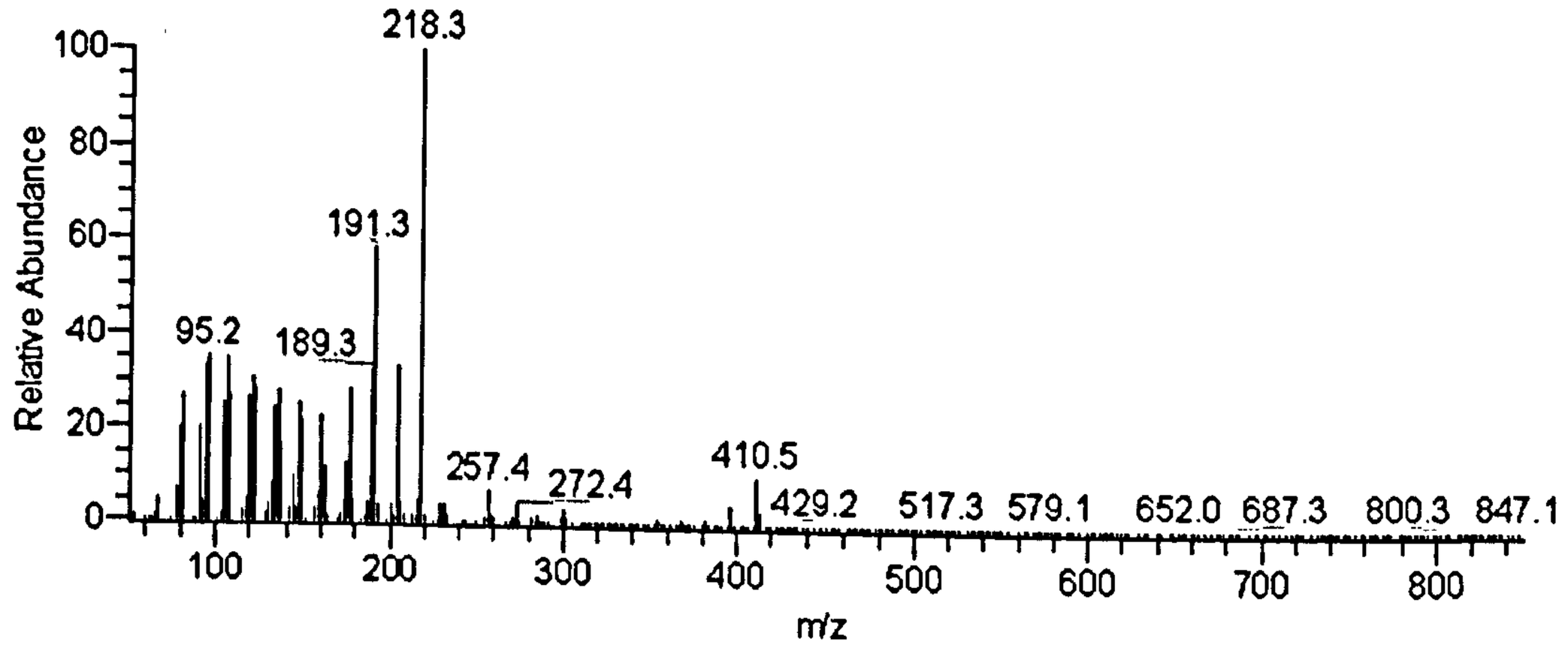

Taraxast-20-ene

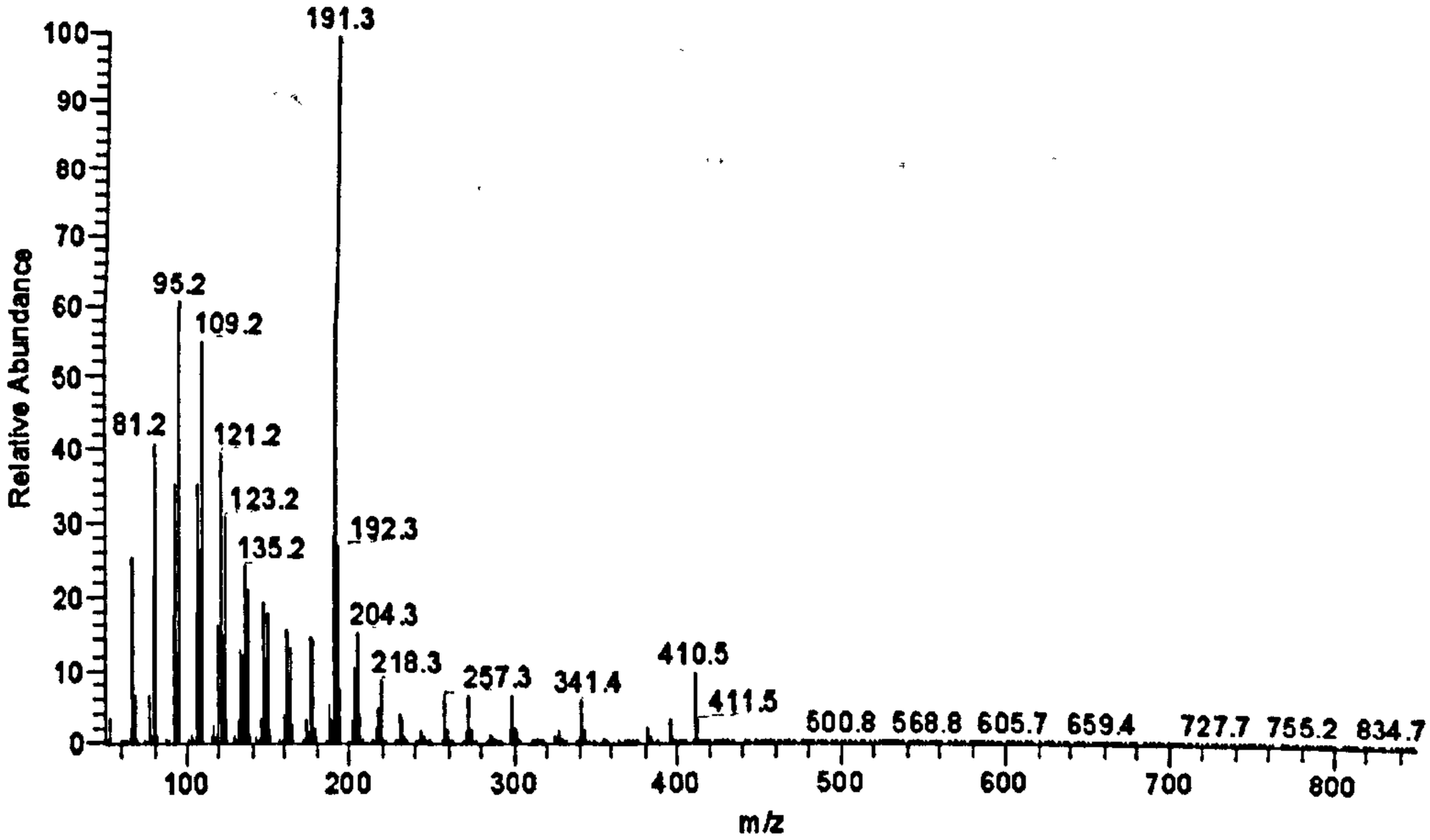

17α(H),21β(H)-homohopane

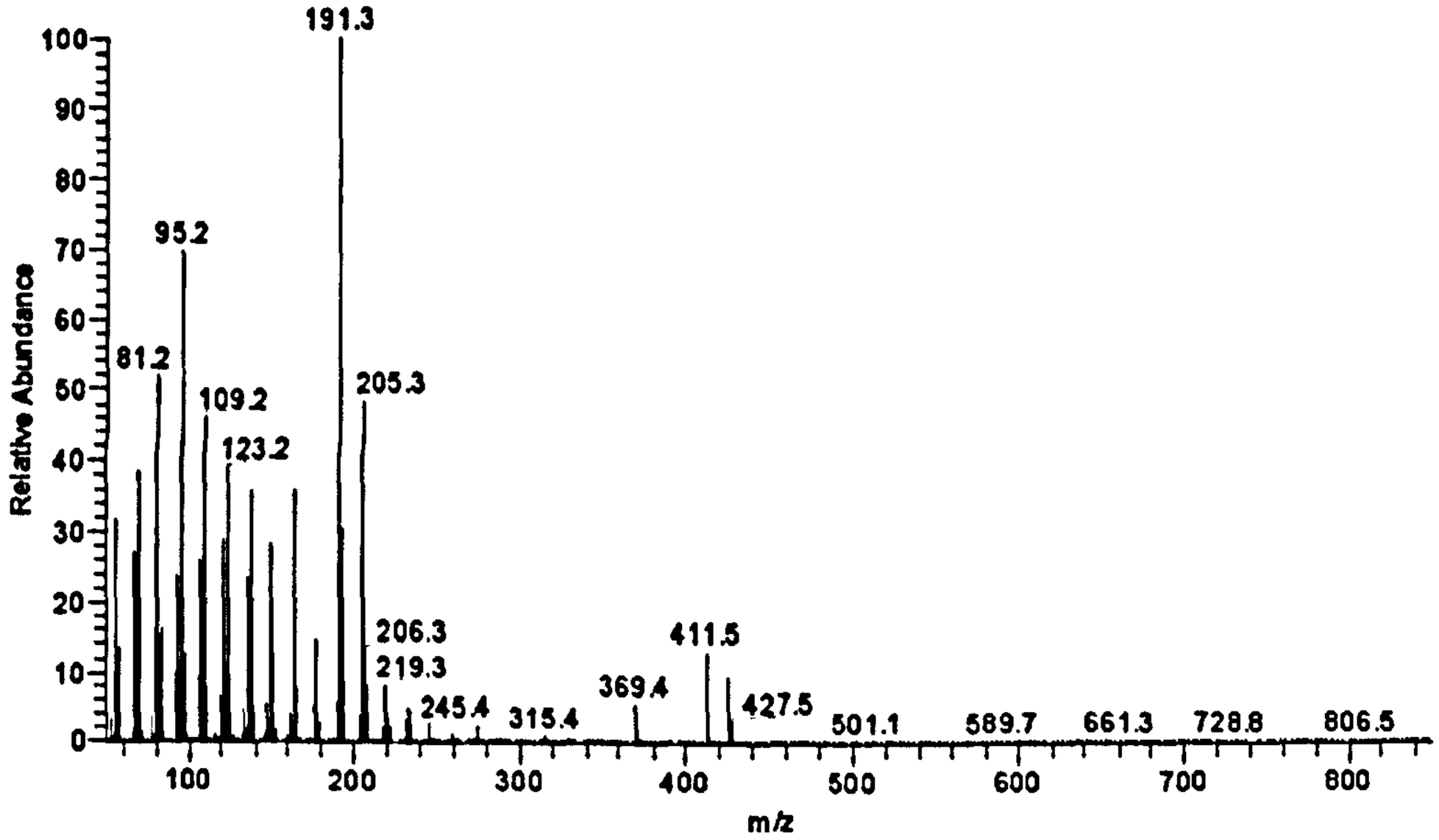

Diploptene

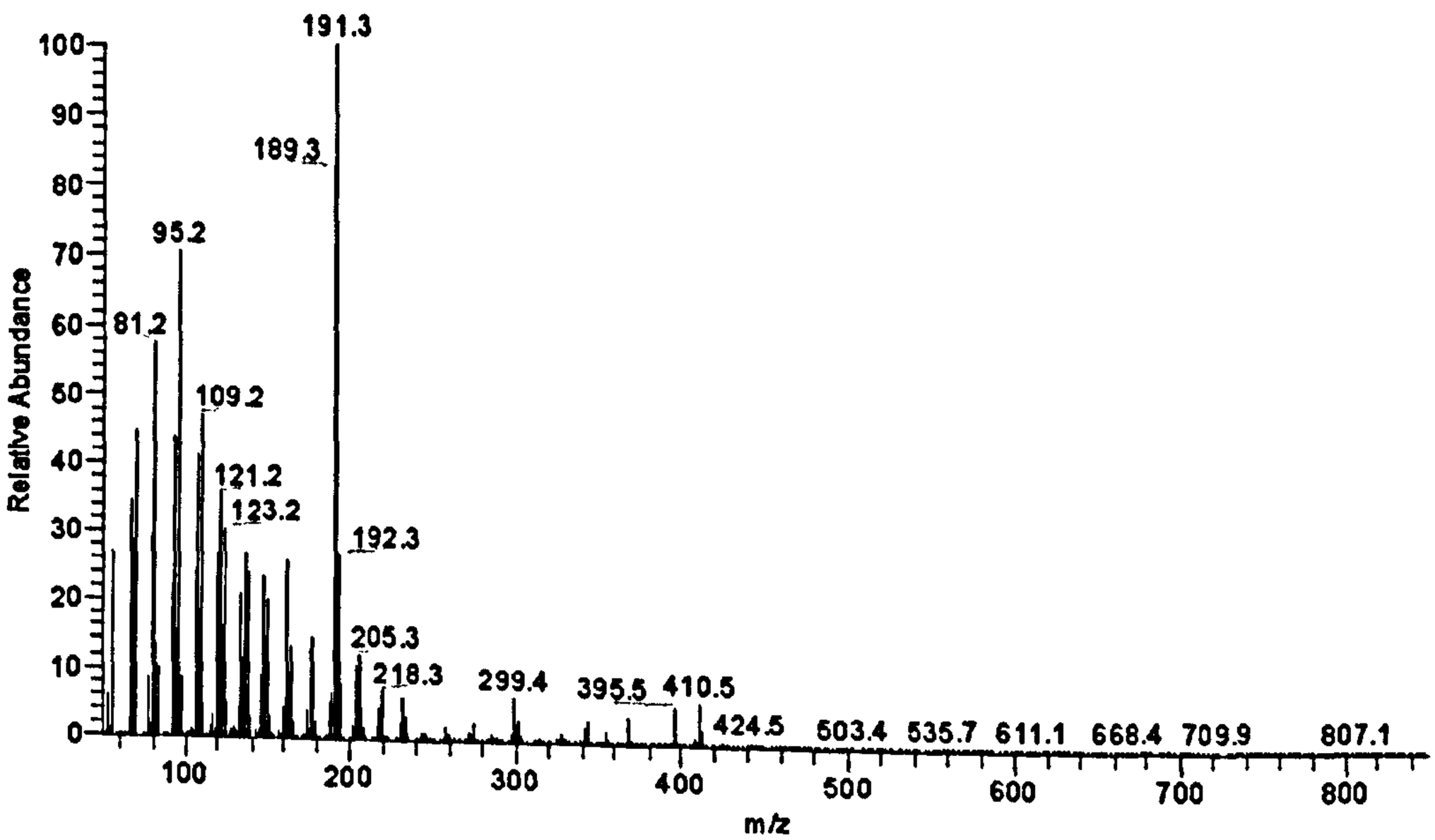

17β(H),21β(H)-homohopane